UNIVERSITY OF SOUTHAMPTON

FACULTY OF MEDICINE

Clinical and Experimental Sciences

'The Effect of Human Rhinovirus-16 Infection on MicroRNA, Tissue Barrier and Innate Immunity in Human Bronchial Epithelium from Healthy and Asthmatic Airways'

by

Natalie Jane Day

Thesis for the degree of Doctor of Philosophy

November 2016

Academic Thesis: Declaration Of Authorship

I, NATALIE JANE DAY declare that this thesis and the work presented in it are my own and has been generated by me as the result of my own original research.

'The Effect of Human Rhinovirus-16 Infection on MicroRNA, Tissue Barrier and Innate Immunity in Human Primary Bronchial Epithelium from Healthy and Asthmatic Airways'

I confirm that:

1. This work was done wholly or mainly while in candidature for a research degree at this University;
2. Where any part of this thesis has previously been submitted for a degree or any other qualification at this University or any other institution, this has been clearly stated;
3. Where I have consulted the published work of others, this is always clearly attributed;
4. Where I have quoted from the work of others, the source is always given. With the exception of such quotations, this thesis is entirely my own work;
5. I have acknowledged all main sources of help;
6. Where the thesis is based on work done by myself jointly with others, I have made clear exactly what was done by others and what I have contributed myself;
7. Either none of this work has been published before submission, or parts of this work have been published as: [please list references below]:

Signed: ……Natalie J Day……

Date: …23/05/2017……

ABSTRACT

THE EFFECT OF HUMAN RHNOVIRUS-16 INFECTION ON MICRORNA, TISSUE BARRIER AND INNATE IMMUNITY IN HUMAN BRONCHIAL EPITHELIUM FROM HEALTHY AND ASTHMATIC AIRWAYS

By Natalie Jane Day

Background: Rhinovirus (RV) is a common human respiratory pathogen. In healthy people RV infection causes the development of upper respiratory tract symptoms of limited duration, whilst in asthmatic patients the symptoms may be severe, prolonged and cause exacerbation of disease. Asthmatics were reported to have dysfunctional bronchial epithelial barrier with decreased junctional protein expression and impaired innate immune responses to infection, which may contribute to symptom exacerbation. MicroRNA (miR) are small RNAs that specifically bind to the 3' untranslated regions (3'UTRs) of target messenger RNAS (mRNA) and alter protein expression by influencing mRNA stability and translation. It was hypothesised that RV infection of human bronchial epithelial cells (HBEC) alters the expression of miRNA-23a, -200b, -200c and -429—miRs which are predicted to target mRNAs encoding proteins relevant to epithelial barrier integrity and innate immunity.

Hypotheses: HRV-16 infection of culture differentiated airway epithelia alters levels of miR-23a and the miR-200 family (miR-200b, -200c, -429).

MicroRNA responses will be different in healthy and asthmatic patients, potentially contributing to decreased epithelial integrity and impaired innate immune responses observed in asthmatics

Methods: Primary human bronchial epithelial cells from healthy and asthmatic donors were differentiated for 21 days at an air-liquid interface (ALI) before being infected with HRV-16. Supernatants and cells were harvested at 24, 48 and 72 hours. Cells were lysed for RNA extraction and levels of miRNAs and *in silico* predicted targets (Zinc finger E-box-binding homeobox 1 (ZEB1), TNF-α Inhibitory Protein 3 (TNFAIP3), E-cadherin and occludin) were assessed. Supernatants were tested for interferon (IFN)-λ protein release. Differentiated HBECs were treated for 72 hours with IFN-λ to assess the effect of HRV-16 induced antiviral mediators on expression of microRNAs and target mRNA/protein in intact epithelial barrier. Differentiating HBECs were treated for 21 days with IFN-λ to assess the effect of HRV-16 induced antiviral mediators on expression of miRNAs and target mRNA/protein in differentiating, 'repairing' barrier. Additional epithelial barrier characteristics were assessed in response to IFN-λ treatment through imunoflourescent staining, cell counts, fluorescein isothocynate (FITC) 4kD dextran

assays and transepithelial resistance (TER). Dual luciferase reporter assays were utilised to confirm miR-23a binding to predicted sequence target in 3'UTR of TNFAIP3.

Results: MiR-200b, -429 and -23a were significantly decreased in response to HRV-16—with a trend for greater reductions in asthmatic donors. Predicted miR-23a target TNFAIP3, predicted miR-429 target occludin and E-cadherin had significantly altered mRNA in response to HRV-16. There were no alterations to ZEB1. HRV-16 lead to significant inductions of IFN-λ mRNA and protein release. IFN-λ treatment of differentiated ALI cultures showed significant reductions of miR-23a and miR-429 in cultures from healthy donors with elevated TNFAIP3 and occludin mRNA and elevated ZEB1 protein expression. In cultures from asthmatic donors, miR-23a was significantly decreased in response to IFN-λ but there were no significant reductions in miR-429 with elevated TNFAIP3 expression and elevated ZEB1 protein expression. IFN-λ treatment decreased TER and changed cell morphology with less pronounced effects in asthmatic individuals. In differentiating ALI cultures, miR-23a and miR-429 were significantly decreased in healthy individuals, but no significant alterations were observed in asthmatics. ZEB1, E-cadherin, TNFAIP3 and occludin mRNA were significantly changed in response to IFN-λ in healthy donors with significant changes to E-cadherin and TNFAIP3 observed in asthmatic donors. Western blotting results were inconclusive. IFN-λ treatment decreased TER, increased FITC passage, decreased cell numbers and changed cell morphology with less pronounced effects in asthmatic individuals. Dual reporter luciferase assays confirmed miR-23a binding to predicted target sequence in 3'UTR of TNFAIP3/A20, which may affect NF-κB activation.

Conclusions: HRV-16 significantly reduces miR-200b, -429 and -23a which may account for alterations in epithelial barrier integrity and innate immune responses via microRNA targets ZEB1, E-cadherin, occludin and TNFAIP3/A20. IFN-λ protein, released in response to HRV-16, effects epithelial barrier properties in both intact and repairing barrier which may be mediated by significant reductions in miRNAs of interest and aforementioned targets. Asthmatic donors appear to be less responsive to IFN-λ which may underpin the impaired epithelial barrier and impaired innate immune responses to HRV-16 infection observed in these patients.

CONTENTS

TABLE OF FIGURES

TABLE OF TABLES

ACKNOWLEDGEMENTS

As with all PhDs, it is frankly impossible to have expected to have completed the process without a strong supporting cast helping me along the way—lending me their knowledge, skills, passion and belief along the way. Without their steady presence by my side, there would not be the 253 subsequent pages that you see here before you.

Firstly—and foremost—I have to express my sincerest gratitude to my supervisor, Dr. Jane Collins. Without her immense knowledge, motivation and patience (which I'm sure I tried, *a lot*) this research project would never have come together. Her guidance has been truly invaluable and the time and effort she's put in to helping further my scientific knowledge/skills is beyond comprehension. And, I am also horrendously thankful for all the emotional support that she has leant over the years whilst I've sobbed over western blots and had momentary imposter syndrome meltdowns. Without her, I very much doubt that I could've gone from the bumbling, emotionally-precarious MRes student of four years ago to the more robust, competent individual I am today.

Besides my supervisor, I would also like to thank my co-supervisor Dr. Tilman Sanchez-Elsner for allowing me to tap in to his extensive microRNA and cloning knowledge whenever questions arose—always doing so with an amazing anecdotal story and a smile to accompany it. I would also like to thank Dr Jens Madsen and Dr Lynne Bingle for taking the time to read this body of work and examining me on it and allowing me the opportunity to really earn my doctorate stripes.

As already mentioned, I was not alone in this endeavour and had many a scientist helping me along the way. Firstly, I must thank every member of the Epithelial Barrier and Inflammation group—past, present and future. Every single person involved in this team has played a role in bringing this story together and so my heartfelt gratitude is with them. However special thanks must be made to Dr Emily Wilkinson, Dr Richard Felwick and Dr Geraint Dingley. Emily for spending an alarming amount of time in the lab with me, imparting all her wisdom despite being in the last six months of her PhD; Richard for spending the past 3 years in the lab with me, sharing all the associated highs and lows of a PhD and helping make things less bleak on the bad days with incredibly dry-humour; and Geraint for all his knowledge on A20 he imparted whilst simultaneously scaring me

off western blotting for life and coining the 'Collins Group Curse' joke/not-so-joke which has followed us around long after his submission.

I must also give my sincerest thanks to members of the Brooke Lab—who unofficially adopted me over the years. Thanks to Dr Emily Swindle and Dr Maaike De Vieres who helped with many of the queries upon designing and setting up my first set of viral experiments. Thanks to Dr Matt Loxham who did some of the original work on microRNAs when he was part of the Epithelial Barrier and Inflammation group. Thanks must go to Professor Donna Davies whose thinking-frown is the thing of nightmares but has been terrific in posing new ideas and theories whenever faced with my data. Similarly, heartfelt thanks must go to the Junk RNA group for their help with all microRNA/cloning issues. Special thanks must go to Dr Rocio Martinez-Nunez who has been an incredible resource for troubleshooting and theoretical discussions throughout the years. And to Dr Hitasha Rupani who collected all the primary bronchial epithelial samples that made this project possible in the first place.

I must also thank many members of Level E for being incredible individuals to work alongside for this PhD. Thanks to the TB group members who shared our Tissue Culture lab—Patience Brace who never failed to put a smile on my face when we were both in at 7am/10pm for some ridiculous 12 hour experiment and Dr Liku Tereza who was never was offended by listening to Radio 1 all day and accompanied me through many sunless weekends.

Now to thank the people who, despite not working directly alongside me, went through the same journey. Firstly, thank you to my 'platonic life partner in crime' Callum, who has tried his best to keep me sane over the years and has spent far too many weekends sleeping on Southampton sofas and getting in to questionable shenanigans. Thank you to James and Alana who shared in the doctor-achieving-woes as they worked their way through med school (and succeeded) and were always there to tweet ridiculous things at 3am whenever we were stressed.

Thank you to my housemates Lyndsy, Kate and Ali who somehow managed to tolerate my quirks for three years and provided unshakable friendship and despite having their own PhD-woes were always there to pick me up out of mine and share many a mindless laugh over things that probably would terrify saner humans. Similarly, a thank you to the

rest of the Southampton PhD 2012 cohort for their friendship and support—especially Shabs who road-tripped, gigged and shared Surge Radio and LSPS duties with me and cooked us far too many meals after harsh weeks. I must also thank those in the Alternative and Indie Music society at the university—especially my fellow committee members of 2015/16 Dan, Joe and Sam—who whisked me away from the world of science and always shared my passion for music, vinyl and going out to Lennons and dancing until the early hours. I must also sincerely thank the crew at 7BitArcade who—when I started this PhD were complete strangers to me and yet have become some of my closest friends—especially Michael, Lindsay and Antony who, despite time-zones and hectic schedules have always been there with a gif just at the right time.

And I've saved the best to last… Thank you to the Day family—my Mum Angela (Mummehkins), Dad Steve (Papa Jenkins) and not-so-little brother Jonathan (Johnny D)—the three people who have stood by me through every single moment, listened to many teary/stressed phone-calls and never stopped believing in me, even when I had. Without them and their 'you can do it Thomas!' pep talks and endless off the wall humour, applying for this PhD and actually completing it would never have happened. This is, quite frankly, for you.

LIST OF ABBREVIATIONS

A20: Protein form of TNFAIP3

AGO: Argonaute protein

ALI: Air-Liquid Interface

AJ: Adherens Junction

ATF-2: Activating Transcription Factor-2

BAL: Bronchial Airway Lavage

BEBM: Bronchial Epithelial Basal Medium

BEGM: Bronchial Epithelial Growth Medium

bp: Base Pairs

cDNA: Complementary DNA

CDHR3: Cadherin-related family member 3

Ct: Cycle Threshold

CTNND2: Catenin, Cadherin Associated Protein Delta-2

CYLD: Cylindromatosis (turban tumor syndrome)

DAMP: Damage Associated Molecular Pattern

DMEM: Dulbeccos Modified Eagle's Medium

DNA: Deoxyribonucleic Acid

EGFR: Epithelial Growth Factor Receptor

dNTP: Deoxynuclotide Solution Mix

dsRNA: Double Strand RNA

EIF-3: Eukaryotic Initiation Factor-3

ELISA: Enzyme Linked Immunosorbent Assay

EMT: Epithelial to Mesenchymal Transition

EMTU: Epithelial Mesenchymal Trophic Unit

FADD: Fas Associated Death Domain

FBS: Fetal Bovine Serum

FITC: Fluorescein Isothocyanate

gDNA: Genomic DNA

GAPDH: Glyceraldehyde-3-phosphate Dehydrogenase

HBEC: Human Bronchial Epithelial Cell

HEPES: 4-(2-Hydroxyethyl)-1-piperazineethanesulfonic acid

HRP: Horseradish Peroxidase

HRV: Human Rhinovirus

HSP: Heat Shock Protein

ICAM-1: Intracellular Adhesion Molecule-1

ICS: Inhaled Corticosteroids

IFIT: Interferon-induced protein with tetratricopeptide repeats

IFN: Interferon

IFNAR1: Interferon-α/β receptor alpha chain

IFNAR2: Interferon-α/β receptor beta chain

IFNλR1: Interferon-λ receptor 1

IgG: Immunolglobulin-G

IL-1/8/13: Interleukin-1/8/13

IL10R2: Interleukin-10 Receptor beta chain

IP-10: Interferon-γ induced Protein 10

IPS-1: Interferon-β Promoter Stimulator-1

IRES: Internal Ribosomal Entry Subunit

IRF-3/7/9: Interferon Regulatory Factor 3/7/9

ISG: Interferon Stimulated Gene

ISG15: Interferon Stimulated Gene-15

ISGF3: Interferon Stimulated Gene Factor-3

ISP: Interferon Stimulated Protein

ISRE: Interferon Stimulated Response Element

JAK-1: Janus Kinase-1

JAM: Junctional Adhesion Molecule

kD: Kilodalton

LABA: Long Acting β-Agonist

LDLR: Low Density Lipoprotein Receptor

MDA-5: Melanoma Differentiaition Associated Protein-5

MEM: Minimum Essential Medium

MET: Mesenchymal to Epithelial Transition

MiR/MiRNA: MicroRNA

MOI: Multiplicity Of Infection

mRNA: Messenger RNA

MUT: Mutant

Mw: Molecular weight

Mx: Interferon-inducible GTP-binding Protein Mx

MyD88: Myeloid differentiation primary response gene 88

NAK: Numb Associated Kinase

NEAA: Non-Essential Amino Acids

NF-κB: Nuclear Factor-κB

2'-5' OAS: 2'-5' Oligoadenylate Synthase

OCLN: Occludin

PAMP: Pathogen Associated Molecular Pattern

PBEC: Primary Bronchial Epithelial Cells

Pen/Strep: Penicillin/Streptomycin

PKR: Protein Kinase R

PRR: Pattern Recognition Receptor

qPCR: Quantitative Polymerase Chain Reaction

RANTES: Regulated of Activation, Normal T-cell Expressed and Secreted

RDPR: RNA Dependent RNA Polymerase

RIG-1: Retinoic Acid Inducible Gene-1

RIP: Receptor Interacting Protein

RISC: RNA Induced Silencing Complex

RNA: Ribonucleic acid

RT-qPCR: Reverse Transcriptase Quantitative Polymerase Chain Reaction

RV: Rhinovirus

SD: Standard Deviation

SEM: Standard Error of Mean

SLPI: Secretory Leukocyte Peptidase Inhibitor

ssRNA: Single-stranded RNA

STAT-1/2: Signal Transduers and Activators of Transcription-1/2

TBK-1: TANK-binding Kinase 1

TCID50: Tissue Culture Infective Dose of 50%

TER: Transepithelilal Resistance

TGF-β: Transforming Growth Factor-β

TJ: Tight Junction

TLR: Toll Like Receptor

TNF-α: Tumour Necrosis Factor-α

TNFAIP3: TNF-α Inhibitory Protein 3 (A20)

TRAF: TNF Receptor Associated Factor

TRIF-1: TIR Domain Containing Adaptor Inducing Interferon-β-1

TYK1: Tyrosine Kinase-1

UTR: Untranslated Region

UV: Ultraviolet

UV-RV: Ultraviolet irradiated Human Rhinovirus-16

VEGF: Vascular Endothelial Growth Factor

VIPERIN: Virus Inhibitory Protein, Endoplasmic Reticulum Associated, Interferon Inducible

VPg: Viral Priming Protein

vRNA: Viral RNA

WHO: World Health Organisation

ZEB1/2: Zinc finger E-box-binding Homeobox 1/2.

ZO: Zonula Occludens

CHAPTER ONE: Introduction

Within the environment there are multiple different types of airborne particles that can pose a challenge to the human body and cause the activation of an immune response. Inhalation is one of the most common routes of entry for these particulates which is why it is essential that the airways have an efficient physical, biochemical and immunological barrier to minimise damage and prevent pathological changes occurring.

1.1: Asthma

Asthma is classified as a chronic inflammatory disease that affects the bronchial/conducting airways of the lung. It is one of the most common conditions within the population with 235 million people currently classified as asthmatic (Holgate, Arshad et al. 2010). In the UK alone there are 5.4 million individuals currently receiving treatment for asthma (1.1 million children and 4.3 million adults)(Holgate, Arshad et al. 2010, Asthma-UK 2015) with an average associated mortality of 0-5 people per 100,000 annually (Braman 2006, WHO 2007). Though the number of asthmatics in the UK is not increasing dramatically, current data suggests global prevalence is on the rise (Braman 2006). These combined statistics of prevalence and mortality, with ensuing economic cost and morbidities (Braman 2006, WHO 2007, Jackson and Johnston 2010) have led the World Health Organisation to describe asthma as a "global health burden" (Braman 2006, WHO 2007).

1.1.1: Characteristics of Asthma

Individuals diagnosed with asthma all present with sporadic episodes of reversible airway obstruction (Contoli, Caramori et al. 2005, Barnes 2008, Holgate 2010, Corren 2013). Beyond this, asthma is considered to be a very heterogeneous disease (Green, Brightling et al. 2007) in which patients present with a range of associated phenotypic changes such as: airway hyper-responsiveness, airway inflammation, and airway remodelling—which includes basement membrane and smooth muscle thickening as well as goblet cell hyperplasia (Barnes 1999, Barnes 2008, Holgate 2010). Typically asthma develops in childhood after the epithelium and/or immune cells of genetically predisposed individuals are exposed to a number of sensitising agents such as viruses, allergens or environmental stimuli (Davies and Holgate 2002, Murdoch and Lloyd 2010).

Following these exposure events, the epithelial-mesenchymal trophic unit (EMTU) becomes aberrantly 'reactivated' leading to an alteration in the microenvironment of the airway (Holgate, Davies et al. 2000, Davies 2009)(Figure 1.1). Microenvironment changes that underpin the development of an asthmatic phenotype include the skewing of the immune system towards a predominantly T_H2 response, increased inflammatory cytokine release leading to chronic inflammation development, and the activation of remodelling processes culminating in airway narrowing (Davies and Holgate 2002, Ngoc, Gold et al. 2005, Barnes 2008, Lambrecht and Hammad 2012). Once these remodelling events occur, they are irreversible leading to airway narrowing persistence throughout the individual's lifespan.

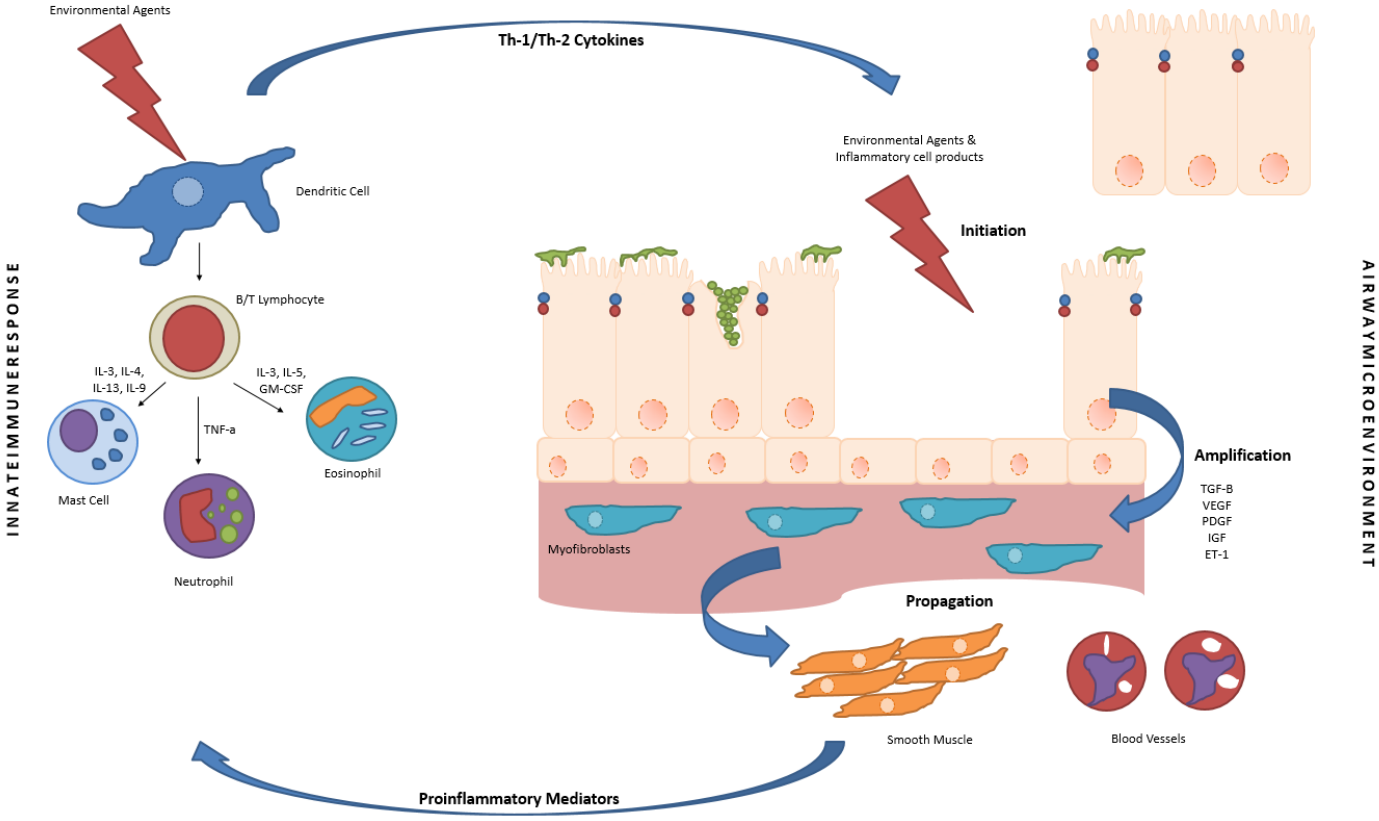

Figure 1.1: Diagrammatic representation of aberrant activation of EMTU in response to stimuli which underpins remodelling processes in asthma. Damage occurs at epithelial surface in response to environmental agents or inflammatory mediators. This response is amplified by release of various mediators (i.e TGF-β) which causes activation of remodelling processes. Remodelling leads to escalated inflammation which leads to escalated EMTU activation.

The heterogeneity witnessed within asthmatics has led to the development of asthma sub-classifications which are used to help increase the understanding of the disease (Green, Brightling et al. 2007, Corren 2013) as well as assist in finding relevant treatment options for patients according to clinical management guidelines (BTS 2014). The highest levels of classifications are based on the atopic status of the patient and the severity of symptoms. If a patient presents with exacerbation episodes that can be linked to the exposure to specific allergens (i.e. house dust mite, pollen) then they are classified as an allergic-asthmatic. If there is no apparent allergen association and the exacerbations are triggered by another environmental factor (i.e. exercise, cigarette smoke) they are considered a non-allergic asthmatic (Kim, DeKruyff et al. 2010). Allergic asthma is the most common form of asthma with >50% of all adult asthmatics classified as such (Corne, Smith et al. 1994, Pearce, Pekkanen et al. 1999, Holgate, Arshad et al. 2010). Once patients are separated via atopy, they are then categorised into mild, moderate and severe asthma based on symptom severity, persistence, exacerbation history and forced expiratory volume (FEV_1) (BTS 2014).

More recently there has been a push towards using further phenotype classifiers to further polarise asthmatics in a bid to find more effective treatment strategies (Corren 2013)—as not every treatment shows same efficacy in managing symptoms within the same disease subsets (Green, Brightling et al. 2007). One such phenotype classifier being used is the inflammatory subtype where categorisation is being defined according to levels of eosinophils and neutrophils within sputum/blood (Simpson, Scott et al. 2006, Green, Brightling et al. 2007). This has given rise to four new asthmatic subclassifiers:

- Eosinophilic asthma—those with elevated eosinophils
- Neutrophilic asthma—those with elevated neutrophils
- Mixed granulocytic asthma—those with elevated eosinophils and neutrophils
- Pauciganulocytic asthma—normal levels of both (Simpson, Scott et al. 2006)

1.1.2: Current Treatment Strategies

The stratification of asthma subsets has led to more comprehensive and effective asthma management treatments. These asthma treatments are unable to cure the disease and instead focus on making the asthma controllable and minimise symptom worsening. Inhaled corticosteroids (ICS) are one of the most commonly used therapeutic

management strategies and are often considered the most-effective way to reduce exacerbation risk in a large proportion of asthmatics (O'Byrne 2011). ICS work primarily by reducing eosinophilic inflammation within the airways which incidentally also leads to decreased airway hyper-responsiveness and decreased mucous secretion (Barnes 1998). In addition to ICSs, asthmatics are often prescribed inhaled β_2-agonists (O'Byrne 2011). These drugs work by increasing bronchodilation in airway smooth muscle to decrease airway narrowing. There are two classifications of β_2-agonists: short-acting agonists that are utilised for rapid symptom relief (3-5 minutes after inhalation) and long-acting agonists (LABAs) that are considered a 'maintenance drug' to allow for increased bronchodilation over 12 hours (Giembycz, Kaur et al. 2008). Whilst these traditional therapeutic approaches are very effective at managing many asthmatic subsets if the patients adhere to treatment, there are some asthmatic subsets—mainly those with severe asthma—that do not respond and thus still present with uncontrolled disease. These non-responsive patients (5-10% of total asthma sufferers) account for a large proportion of asthma-associated expenditure. Those with severe, uncontrolled disease may be put on therapies such as the anti-IgE monoclonal antibody treatment (omalizumab)(Holgate and Polosa 2006). Clinical management of asthma is a stepwise progression which follows guidelines from the British Thoracic Society (Figure 1.2)

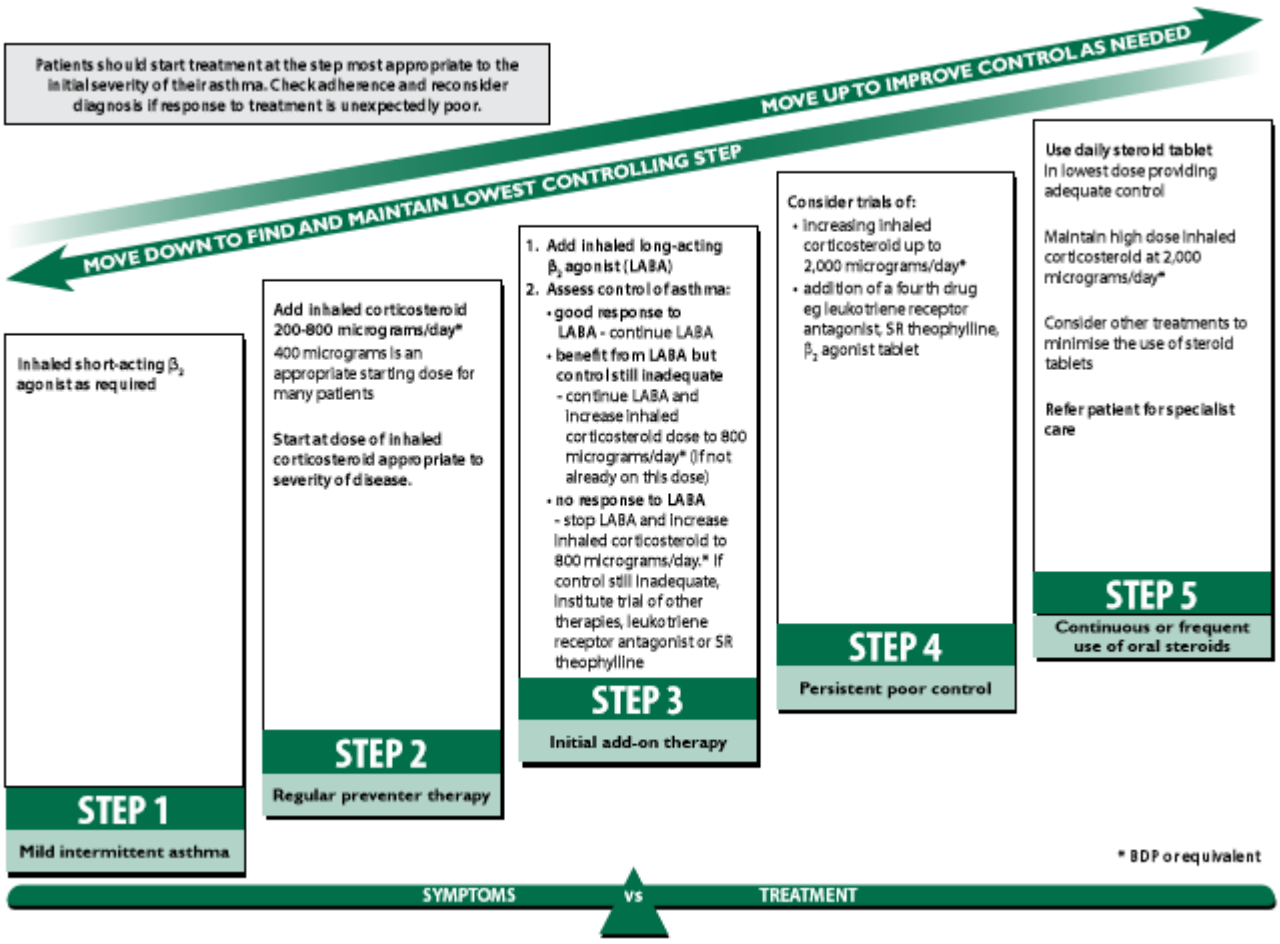

Figure 1.2: Stepwise clinical management of adult asthmatic patients as defined by the British Thoracic Association. Figure available from: https://www.brit-thoracic.org.uk/document-library/clinical-information/asthma/btssign-asthma-guideline-quick-reference-guide-2014/

1.1.3: Asthma Exacerbations

Along with the observed immunological and structural changes that characterise the disease, asthmatic individuals also experience short-term, reversible episodes of symptom worsening called asthma exacerbations—or colloquially, asthma attacks. During these exacerbation episodes, patients experience a rapid decline in their lung function caused by airway narrowing which is often accompanied by elevated inflammation and increased mucus production (Figure 1.3). Upon exacerbation episode resolution, lung function increases. In some cases, functionality returns to what had been observed prior to exacerbation whilst in other instances lung function never returns to the same level observed prior to exacerbation (Bai, Vonk et al. 2007, O'Byrne, Pedersen

et al. 2009). This means that with every asthma exacerbation episode, patients may experience a more long-term decrease in their lung function, which ultimately has a negative impact on patient quality of life and disease progression (Figure 1.4).

As these exacerbation episodes may have a detrimental effect on asthma sufferers, it is essential that we try to minimise these incidents. In children up to 85% of exacerbation episodes can be linked to respiratory viral infections (Wark, Johnston et al. 2005, Jackson and Johnston 2010). Atmar et al identified that, in a cohort of 148 asthmatics admitted to hospital due to an exacerbation episode, 55% were linked to a respiratory viral infection (Atmar, Guy et al. 1998). It has been shown in several studies that Human Rhinovirus (HRV) is one of the most predominant virus types present in asthmatic exacerbation episodes, with RT-PCR studies identifying it in >60% of cases (Wark, Johnston et al. 2005, Jackson and Johnston 2010, Inoue and Shimojo 2013). There have also been several cohort studies that have shown a close associated between HRV infection, wheezing and the development of asthma (Grunberg and Sterk 1999, Contoli, Caramori et al. 2005, Inoue and Shimojo 2013) as well as studies that have temporally linked HRV infection and asthma exacerbation (Johnston, Pattemore et al. 1996). As HRV is highly communicable and highly prevalent within the population, it is considered a significant risk to those with asthma.

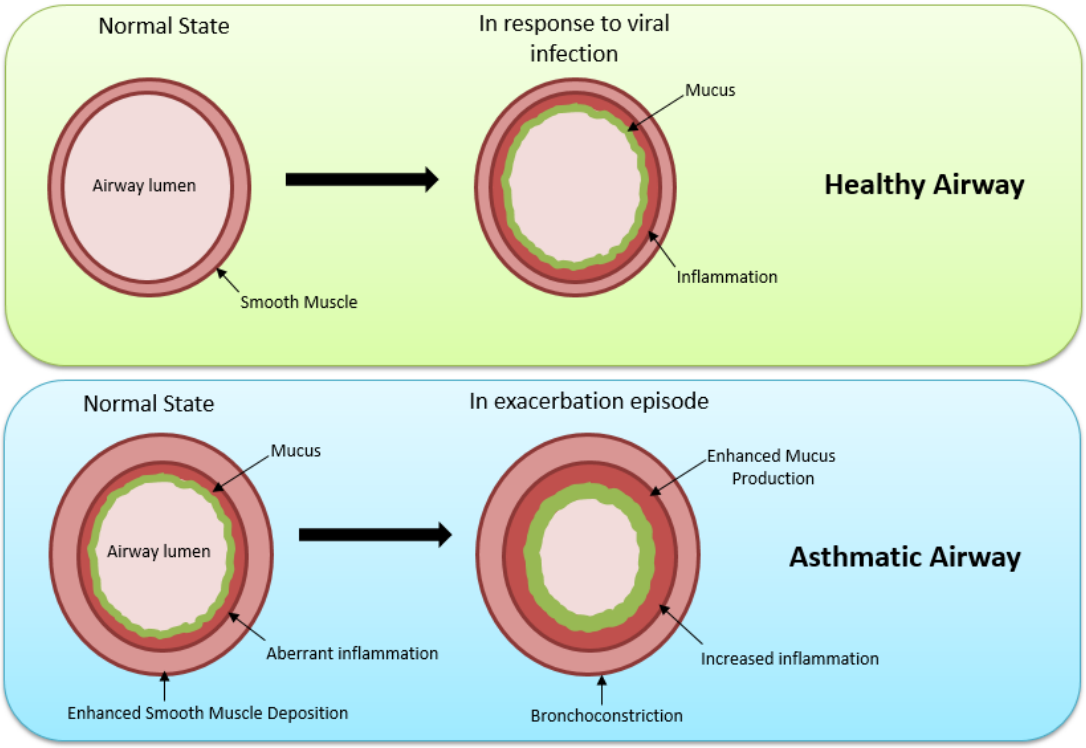

Figure 1.3: Diagrammatic representation of healthy airway in 'normal' state and in response to viral infection compared to asthmatic airway in 'normal' state and in exacerbation episode (which may, or may not, be linked to viral infection). Asthmatic individuals present with a narrower airway lumen at 'normal' state with enhanced smooth muscle deposition, inflammation and mucus production. In exacerbation episodes these airway lumen is further narrowed by bronchoconstriction, increased inflammation and elevated mucus production

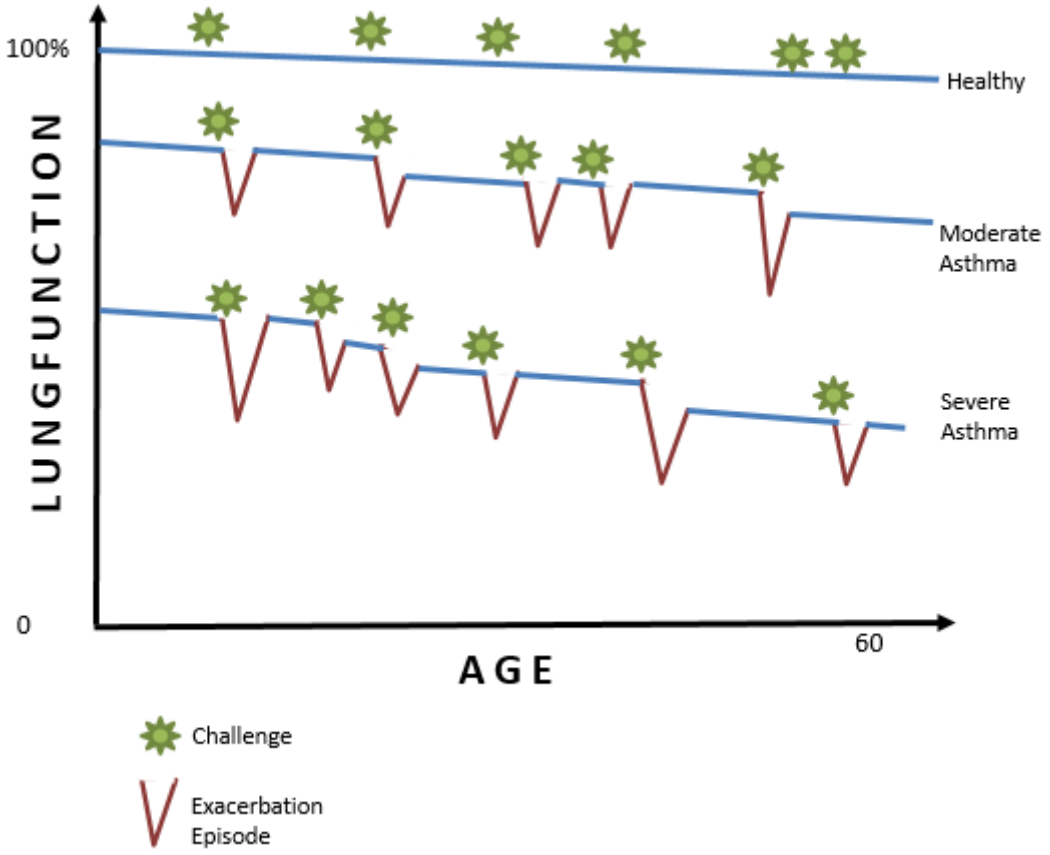

Figure 1.4: Diagrammatic representation of lung function between birth and age 60 in healthy, moderate asthmatic and severe asthmatic individuals. Healthy individuals have a gradual decline in lung function linked to ageing processes. Individuals with have decreased lung function to begin. These individuals experience short-term rapid declines in lung function (exacerbations) which are linked to environmental challenges. Lung function may return to level prior to exacerbation after resolution or this may increase lung function decline.

1.2: Human Rhinoviruses

Human Rhinoviruses are a considerable global health burden with 500 million cases per annum in the USA and an associated expenditure of $40 billion. HRV infections typically lead to mild upper respiratory tract symptoms (i.e. congestion and sore throat) for 3-7 days in healthy individuals (Grunberg and Sterk 1999, Gavala, Bertics et al. 2011, Kim and Gern 2012). For 'at risk' individuals—typically defined as the elderly/young, immunocompromised or those with underlying respiratory pathologies—HRV infections cause more severe symptoms that persist for greater lengths of time (10-14 days)(Grunberg and Sterk 1999, Arden and Mackay 2009, Kim and Gern 2012) and, in some instances, can exhibit lower respiratory tract symptoms caused by viral colonisation of lower respiratory tract epithelium (Papadopoulos, Bates et al. 2000, Costa, Bergallo et al. 2009).

Rhinoviruses are small, non-enveloped, positive, single stranded RNA viruses (+ssRNA) that belong to the *Picornaviridae* family of *Enteroviruses*. Based on phylogenetic sequencing, HRV is subclassified into three strains: A, B and C (Grunberg and Sterk 1999, Savolainen, Blomqvist et al. 2003, Fuchs and Blaas 2010, Jacobs, Lamson et al. 2013). Cross-neutralisation assays have identified 75 distinct HRV-A and 25 HRV-B serotypes. Due to the difficulties surrounding the culturing of HRV-C, it has been problematic to identify distinct serotypes belonging to this family. It has therefore been suggested that serotype identification and strain classification should be based on genetic sequencing of the key HRV protein VP1 (McIntyre, Knowles et al. 2013). The HRV-A, -B and -C strains are further subclassified in to major and minor HRV strains—which are determined by the receptors that the virus utilises for viral attachment and subsequent entry in to cells. Major HRV strains (i.e HRV-16) utilise intercellular adhesion molecule-1 (ICAM-1) whilst minor HRV strains (i.e HRV-23) utilise low-density lipoprotein receptors (LDLR)(Hofer, Gruenberger et al. 1994). HRV-C is reported to utilise the putative cadherin-like adhesion molecule, CDHR3, as a receptor for entry in to cells (Bochkov, Watters et al. 2015) and a mutation in CDHR3 has been linked to increased exacerbation rates in childhood asthma (Bonnelykke, Sleiman et al. 2014)

1.2.1: HRV-16

One serotype belonging to the HRV-A family is HRV-16. HRV-16 has a genome of 7124bp (excluding its' poly(A) tail) which is translated in a continuous manner. The subsequent protein is processed into 11 distinct viral proteins by viral proteases which are encoded within the HRV-16 genome (Table 1.1)(Lee, Wang et al. 1995).

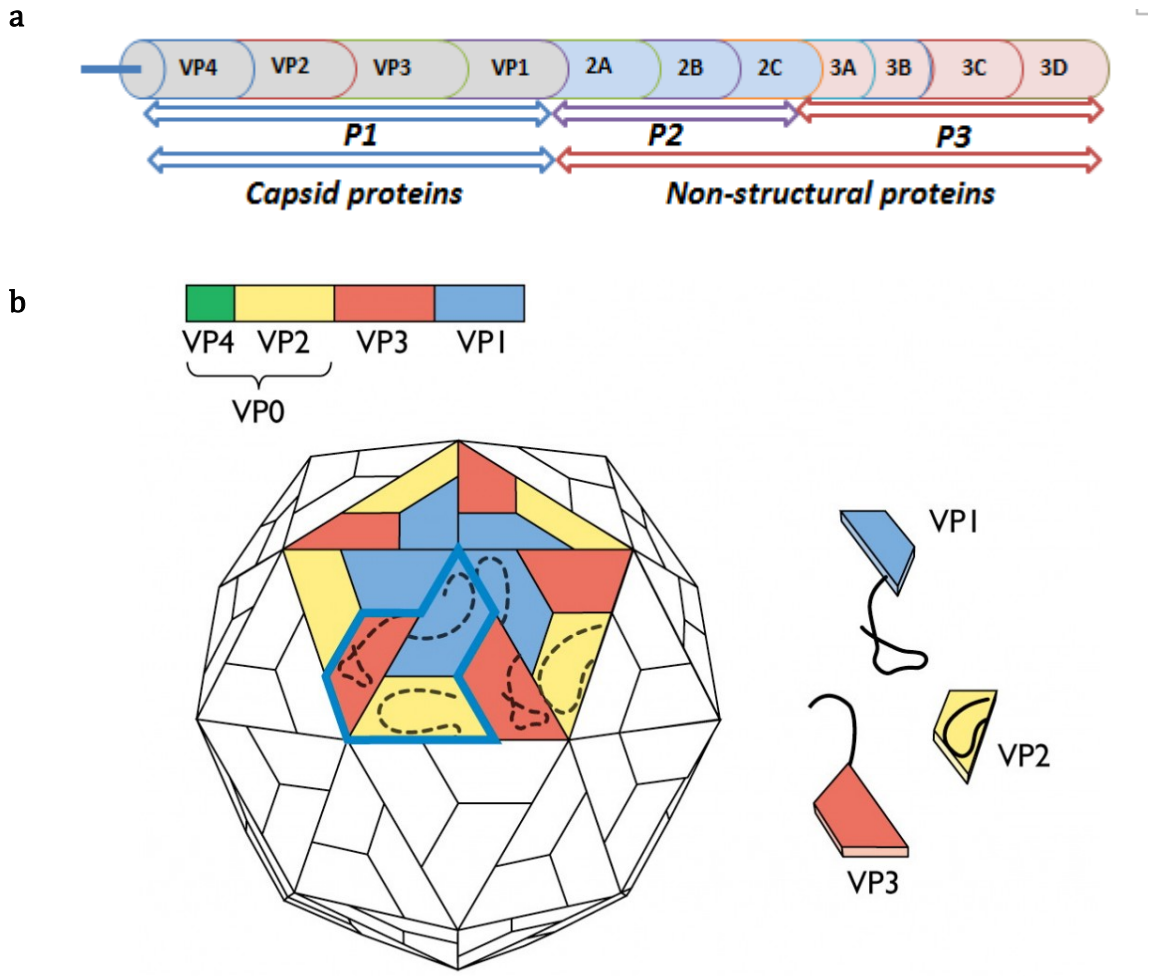

Figure 1.5: Diagrammatic representation of HRV-16 genome (a) and ichosahedral shape of intact viral structure (b). Figure B taken from: http://www.twiv.tv/virus-structure/

Genomic Region	Viral Protein Encoded
VP1-VP4	Four individual capsid proteins
2A	Viral Protease
3B	Viral priming protein (VPg)
3C	Viral Protease
3D	RNA-dependent RNA Polymerase (RDPR)

Table 1.1: Genomic region of HRV-16 and viral protein region encodes for

VP1-4 are the structural proteins encoded for in the HRV-16 genome. These viral proteins are the capsid proteins, which are first assembled into protomer units before 60 protomers are subsequently assembled to create the icosahedral capsid structure that surrounds the ssRNA genome. VP1, VP2 and VP3 are on the exterior surface of the capsid and give rise to the viral antigenicity through variations in these structures—especially VP1(McIntyre, Knowles et al. 2013). VP4 in on the internal surface of the structure and tethers the ssRNA genome to the capsid. The remaining proteins are non-structural and play roles in genome replication and virion assembly (Savolainen, Blomqvist et al. 2003, Arden and Mackay 2009, Jacobs, Lamson et al. 2013)(Figure 1.5).

1.2.2: HRV-16 Lifecycle

HRV-16 is communicated throughout the population through the inhalation of HRV particles. As HRV-16 belongs to the major receptor group of rhinoviruses, it binds ICAM-1 receptors, which are displayed on airway epithelial cells. This binding is mediated specifically via the VP1 capsid protein interacting with immunoglobulin-like domain 1 on the extracellular surface of ICAM-1. This interaction causes the activation of clathrin-mediated pinocytosis/endocytosis of the receptor-virus into the cytosol of the epithelial cell. Whilst in the endosome, the capsid proteins undergo a conformational change which is mediated both by the VP1-ICAM-1 interaction and additionally through the low pH within the endosome. These conformational changes lead to the opening of holes in the capsid, leading to VP4 exposure and release, which leads to ssRNA release. In addition to VP4 exposure, the conformational changes expose the VP1 N-terminal sequences,0. which are amphipathic and bind to the endosome membrane. Attachment of VP1 N-terminus to the endosomal membrane allows for the ssRNA genome to be released in to

the cytoplasm (Fuchs and Blaas 2010, Fuchs and Blaas 2012, Jacobs, Lamson et al. 2013). The binding and internalisation of rhinovirus particles can take as little as 15 minutes after the initial inhalation event (Lessler, Reich et al. 2009).

Once the ssRNA genome is in the cytoplasm, there are two routes in which ribosomal attachment is mediated. The first is via the VPg, which upon uridylation (VPg-pUpU), causes ribosome association to the 5' end of the ssRNA and initiates translation (Takegami, Kuhn et al. 1983). Secondly the leader structure in the 5' end can assume a complex structure mediated by base-pairing to create the internal ribosome entry site (IRES) to which the ribosomes associate which negates the need for uridylation, an AUG start codon or 5' end binding of ribosomes (E.K Wagner 2008). Upon ribosomal association, the continuous translation event initiates to give rise to the polyprotein. This replication event occurs 5-10 hours post-infection (serotype dependent)(Koliais and Dimmock 1973). Following completion of replication events, the polyprotein is processed in to the separate proteins and assembled in to viral progeny, which are then 'released' from the infected cell. Typically completion of HRV lifecycle occurs >20 hours from the initial infection event (Lessler, Reich et al. 2009)(Figure 1.6).

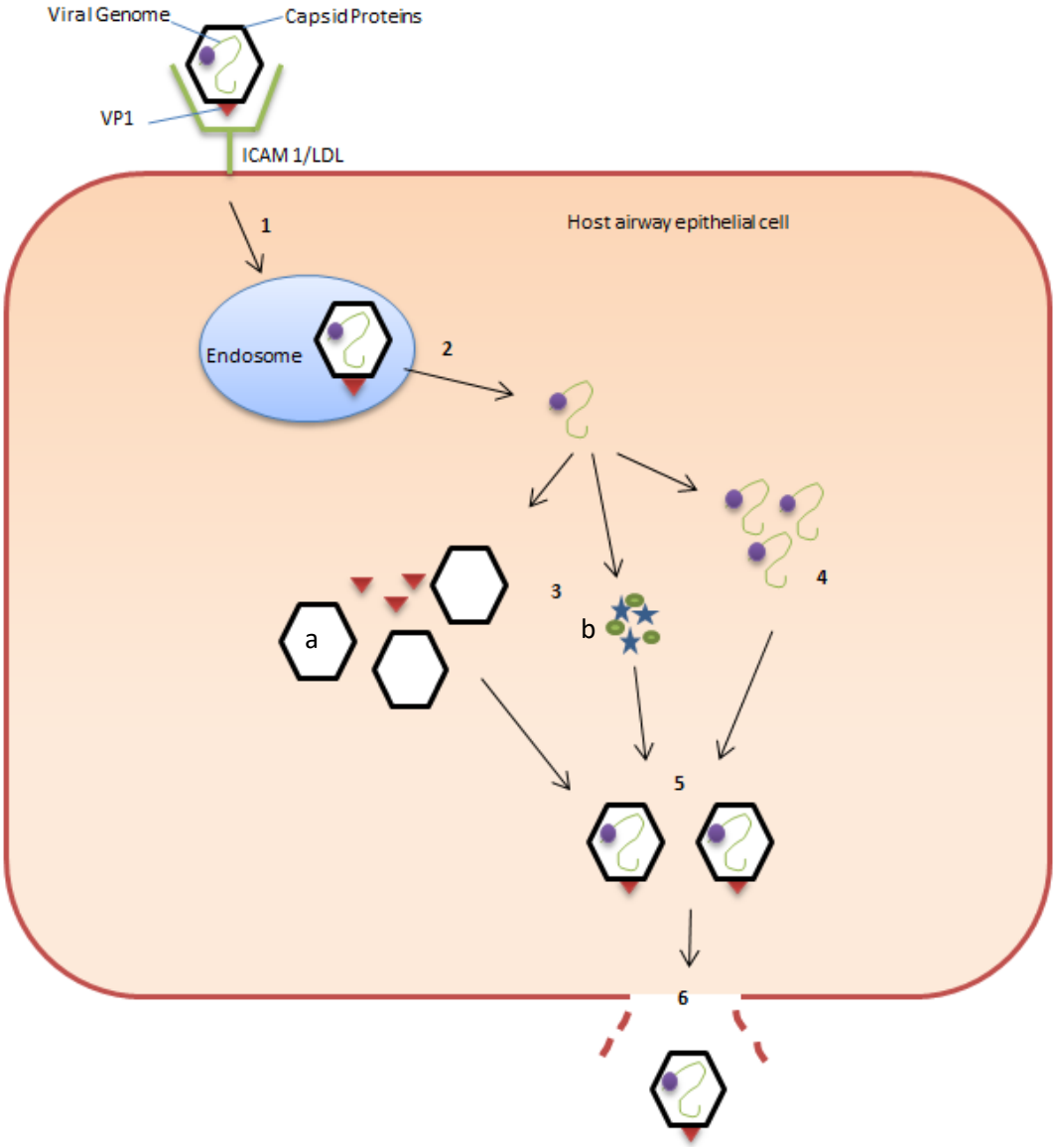

Figure 1.6: Diagrammatic representation of HRV-16 lifecycle. (1) HRV-16 binds to ICAM-1 via VP1 to trigger clathrin-mediated endocytosis. (2) Endosomal pH drops leading to viral uncoating and ssRNA exposure. (3) Translation of structural (a) and non-structural proteins such as RDPR (*illustrated as blue stars*) and viral proteases (*illustrated as green blobs*)(b). (4) Replication of ssRNA. (5) Assembly of components into infective viral

1.3: Airway Epithelium Defence Mechanisms

1.3.1: Structure of Airway Epithelium

The bronchial airway epithelium is a pseudostratified layer composed of 3 main morphological groups of epithelial cells: basal, secretory and ciliated. Each cell type plays their own specific role in epithelial maintenance and defence to ensure long-term tissue health (Knight and Holgate 2003).

Basal cells are the lowest layer of the pseudostratified epithelium and are in contact with the basal lamina, neighbouring basal cells and ciliated/secretory cells (Evans, Van Winkle et al. 2001). Basal cells are suggested to function as progenitor cells in epithelial barrier maintenance and repair as they are pluripotent and have been shown to be able to reconstitute a full pseudostratified epithelial layer (Crystal, Randell et al. 2008). Basal cells are also suggested to function in inflammatory processes within the layer due their cytokine secretory properties (Knight and Holgate 2003) and their suggested interaction with inflammatory cells during their migration into the pseudostratified layer (Evans, Van Winkle et al. 2001).

There are two secretory cells within the airway epithelium: Club cells and goblet cells. Club cells produce and secrete bronchial surfactant which acts to stabilise the airways and also assist in bronchoalveolar transport (Knight and Holgate 2003). Goblet cells make up a greater proportion of the secretory cells within the pseudostratified epithelium with an estimated 6800 cell/mm^2 present (Knight and Holgate 2003). They produce and secrete a number of lipids and glycoproteins—the pivotal of which is mucous. Mucous is a high-molecular weight (Mw) glycoprotein (mucin) which primarily functions to trap inhaled particulate matter (including pathogenic material) and prevent it from damaging the epithelial layer and increase its' ease of removal by ciliated cells (Rogers 1994).

Columnar ciliated epithelial cells are the most abundant cell type in the airway epithelium—accounting for >50% of the total number in the pseudostratified layer. Each cell has ~300 cilia which are utilised to clear particulate containing mucous from the airway through 'sweeping' the mucous-particulate bolus back up the airway to the throat where it can be removed via swallowing/coughing in a process known as mucocilary clearance. Ciliated epithelia are integral to epithelial defence and maintenance as they

function to create a physical and immunological barrier against inhaled particulates (Knight and Holgate 2003, Vareille, Kieninger et al. 2011).

1.3.2: Airway Defence via the Physical Barrier

The first line of airway epithelial defence is provided by the physical barrier which comes in two forms. The first physical barrier is provided by the goblet and ciliated cells working in tandem to provide the mucocilary clearance system. As briefly touched upon above, the goblet cells produce large amounts of mucin type glycoproteins, which is stored within the cells in granules. Upon detection of secretion stimuli these granules are rapidly secreted from the goblet cells in vast quantities which result in covering the epithelial layer in a layer of the highly 'sticky' mucous. This 'sticky' property of the mucous means that inhaled pathogens and particles often become trapped in the mucous, preventing it from causing damage to the epithelial cells below. The brush-like movement of the ciliated epithelial cells causes the formation of a mucous bolus, which is then subsequently pushed back up the bronchus wherein it can be physically removed (Rogers 1994, Knight and Holgate 2003, Vareille, Kieninger et al. 2011).

If the particulate/pathogenic material is not removed from the epithelial surface by the mucocilary clearance system, the second physical barrier is exceedingly important to limit pathogen entry and prevent subsequent epithelial injury and airway inflammation. This second defence mechanism is the tight intercellular junctions between the neighbouring ciliated epithelial cells, which provide the epithelial layer with a tight and cohesive barrier (Nawijn, Hackett et al. 2011, Vareille, Kieninger et al. 2011, Ganesan, Comstock et al. 2013). It is also suggested that this barrier extends further than the top layers of the pseudostratified epithelium, with less well defined junctions between ciliated cells and the basal cells beneath (Evans, Van Winkle et al. 2001) and potential processes directly linking the ciliated epithelium to the basal lamina (Figure 1.7).

Intercellular junctions of the pseudostratified epithelium are localised to the apicolateral borders of cells. They come in three classifications: tight junctions (TJs), adherens junctions (AJs) and desmosomes which have different biological functions—but all must be present and maintained to ensure epithelial barrier integrity.

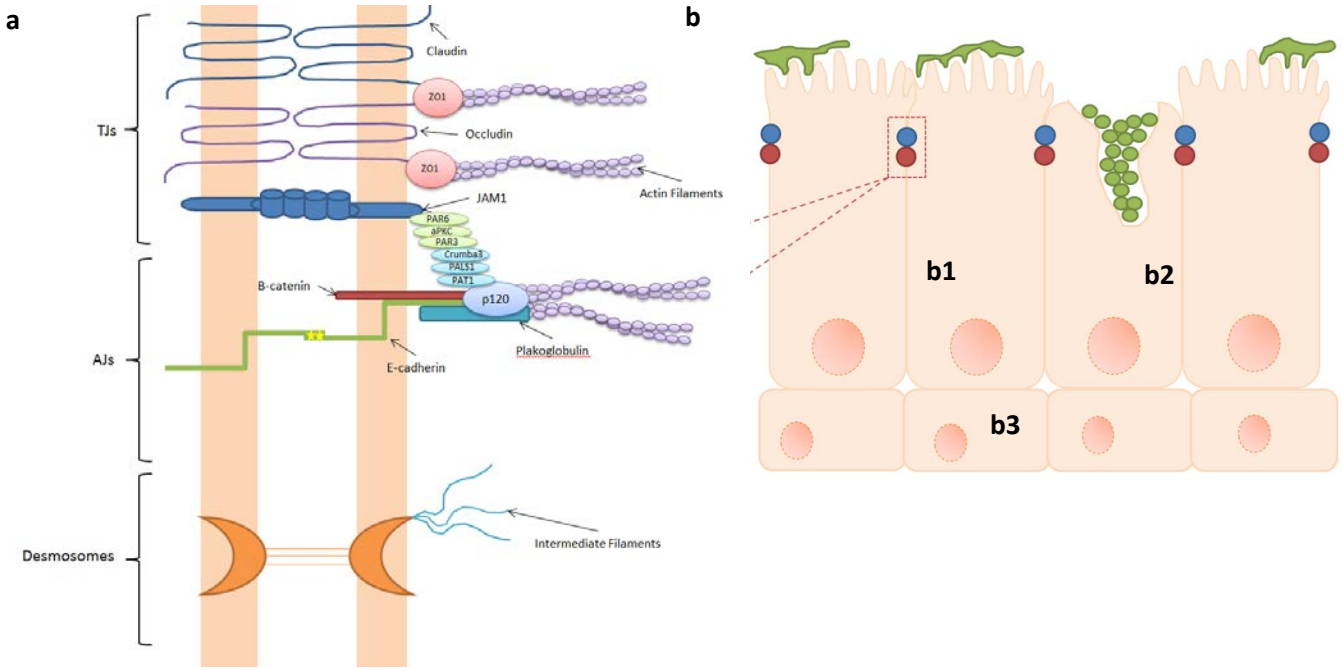

Figure 1.7: Diagrammatic representation of bronchial epithelium . (a) schematic representation of the intercellular junctions of the TJs, AJs and demosomes between neighbouring cells and (b) pseudostratified architecture of the epithelium showing (b1) ciliated columnar epithelium, (b2) secretory goblet cells and (b3) basal epithelial cells

1.3.2.a: Tight Junctions

Tight junctions (TJs) are involved in regulation of the ionic and macromolecular paracellular permeability in addition to playing a role in determining cellular polarity (Anderson and Van Itallie 1995). Tight junctions are made up of >40 separate proteins (Anderson and Van Itallie 1995, Tsukita and Furuse 2000, Schneeberger and Lynch 2004) which interact to create the complex and stable architecture of the junction. Despite the number of proteins and diversity, they can be classified into transmembrane proteins, scaffolding proteins and linker proteins. Each of these subclassifications has their own unique biological function in the maintenance of TJ integrity (Van Itallie and Anderson 2014) and together they create the 'continuous, circumferential, belt-like structure' of the junction.

Transmembrane TJ proteins are primarily claudin(s), occludin and JAM-A and are described as the integral TJ proteins (Tsukita and Furuse 2000, Schneeberger and Lynch 2004, Hartsock and Nelson 2008, Anderson and Van Itallie 2009, Van Itallie and Anderson 2014).

Claudin(s) are a family of >25 related small (20-25kDa) tetraspan transmembrane proteins which organise in transmembrane fibrils that 'link' neighbouring ciliated cells together via homophilic/heterophilic transcellular interactions and cause the assembly of the TJ. Claudins in turn then link to the scaffolding proteins zonular occludens (ZO) via their PDZ domain in the intercellular space to complete the archetctural backbone of the TJ (Tsukita and Furuse 2000, Schneeberger and Lynch 2004, Anderson and Van Itallie 2009, Van Itallie and Anderson 2014).

Unlike claudins, occludin is not involved in TJ assembly but is thought to be involved in the regulation of TJ stability and disassembly. Occludin is a 60kDa tetraspan transmembrane protein, which interacts transcellularly via homophilic interaction, first described in 1993 (Furuse, Hirase et al. 1993). As with claudins, the intercellular C-terminus of occludin interacts with scaffold proteins ZO-1/2/3 (Anderson and Van Itallie 1995, Schneeberger and Lynch 2004, Van Itallie and Anderson 2014). Occludin itself is highly phosphorylated on its serine/threonine residues when associated with the TJs. Upon dephosphorylation of Ser/Thr residues and enhanced phosphorylation of tyrosine residues, occludin is seen to disassociate with the TJ (Rao 2009) and instead become cytoplasmically localised (Schneeberger and Lynch 2004). The loss of occludin from TJs leads to a loss of junctional integrity, as demonstrated by low TER measurements in cellular cultures with low occludin in TJs and higher TER in response to high levels of occludin in TJs (Schneeberger and Lynch 2004).

Junctional Adhesion Molecule 1/A (JAM-1/A) is a 43kDa glycosylated protein belonging to the Immunoglobulin-G (IgG) family first described in 1998 (Martin-Padura, Lostaglio et al. 1998, Schneeberger and Lynch 2004). It is implicated in regulation of cellular polarity through its' interactions with proteins of the cell polarity complex and is the main protein involved in the TJs proposed cell polarity function (Anderson and Van Itallie 1995, Bazzoni 2003). It has two extracellular Ig-like loops in addition to one transmembrane domain and an intracellular domain. The transmembrane domain of JAM-1/A is

responsible for creation of homophilic interactions with neighbouring JAM-1/A molecules whilst the intracellular domain once more has a PDZ binding domain which interacts with the ZO scaffold proteins (Anderson and Van Itallie 1995, Schneeberger and Lynch 2004, Van Itallie and Anderson 2014).

Scaffolding proteins of the TJs are mainly the zonula occludens (ZO 1-3) (Stevenson, Siliciano et al. 1986) and the cingulin and cingulin-like proteins (Anderson and Van Itallie 1995). Zonula occludens belong to the membrane associated guanylate kinase (MAGUK) family of proteins and are very similar in structure with 3 N-terminal PDZ domains, a Src-homology 3 domain and a guanylate kinase homology domain. The ZOs associate with PDZ domains of the TJ transmembrane proteins just beneath the TJ contact points. The ZOs can then hetero/homophilically interact with one another to create a scaffolding plaque, which subsequently can bind to proteins of the cytoskeleton, such as actin or other actin binding proteins (Anderson and Van Itallie 1995, Schneeberger and Lynch 2004, Anderson and Van Itallie 2009, Van Itallie and Anderson 2014). In addition to their cytoskeletal links, ZOs also cause associations between TJs and associated AJs. Zonula occludens proteins may additionally have signalling properties as they have been shown to be localised to the nucleus in some instances (Matter and Balda 2003, Schneeberger and Lynch 2004). Cingulin is a peripheral membrane protein that contains a coil-coiled domain and binds directly to ZOs. As with the ZOs, it plays a role in TJ structure and is proposed to play a role in signalling. As it extends further from the TJ than the ZOs it is suggested to connect the TJs to cytoskeletal elements that the ZOs cannot 'reach' (Anderson and Van Itallie 1995, Schneeberger and Lynch 2004, Van Itallie and Anderson 2014).

There are many linker proteins, which are associated with the transmembrane and scaffolding proteins in the TJs. The linker proteins have been implicated in maintaining junctional integrity as well as being involved in regulating cell polarity through mediation of the ZOs/cingulin interactions with the cytoskeleton. Linker proteins include partitioning defective protein-3 (PAR-3), atypical protein kinase C (aPKC) and Crumbs3 (Schneeberger and Lynch 2004) .

1.3.2.b: Adherens Junctions

Adherens Junctions (AJs) are part of the apico-lateral junctional complex with TJs and help to further adhesive contacts between cells as well as playing roles in cell polarity, transcriptional regulation, intracellular signalling and TJ formation and stabilisation (Kemler 1992, Ivanov, Philippova et al. 2001, Vareille, Kieninger et al. 2011). As such, AJs, are often described as the 'key junction' as TJ formation is linked to E-cadherin association in AJs (Hardyman, Wilkinson et al. 2013). As with the TJs, AJs are made up of multiple interacting proteins the majority of which either belong to the catenin or cadherin family of proteins (Meng and Takeichi 2009).

Cadherins are a family of cell-surface proteins which are Ca^{2+} dependent cell adhesion molecules that homophilically interact with one another to provide very strong adhesive contacts between cells and within tissues (Kemler 1992, Hartsock and Nelson 2008). There are multiple members of the cadherin family—including E-, N-, P- and R-cadherin (Meng and Takeichi 2009). E-cadherin is a type I cadherin transmembrane glycoprotein of 120kDa first described in 1985 (Boller, Vestweber et al. 1985). It has one transmembrane region, composed of five extracellular cadherin repeat domains (EC), which are responsible for mediating the homophilic interactions in a Ca^{2+} dependent manner (Meng and Takeichi 2009). Of these EC domains, it has recently been elucidated that it is EC1 that plays an essential role in mediating contact and initiating the adhesion event (Shapiro, Fannon et al. 1995, Perez and Nelson 2004, Shapiro and Weis 2009). The cytoplasmic region of E-cadherin is responsible for contacts with AJ-associated catenins (Ozawa, Ringwald et al. 1990) which stabilise E-cadherin and connect the AJs to the cytoskeleton (Meng and Takeichi 2009). Additionally these catenin binding domains are responsible for cytoplasmic interactions between laterally clustered E-cadherins to enhance AJ strength which is referred to as AJ 'maturation' (Hartsock and Nelson 2008).

There are four core catenin proteins involved in maintenance of AJ stability, cell polarity and transcriptional regulation: p120-catenin, β-catenin, α-catenin (Kemler and Ozawa 1989, Hartsock and Nelson 2008, Meng and Takeichi 2009) and γ-catenin (plakoglobulin)(Tian, Liu et al. 2011). In addition to AJ stability, catenins have been shown to be key intracellular signalling molecules linking extracellular 'cues' to the nucleus (Klezovitch and Vasioukhin 2015). p120-catenin binds to a conserved peptide on the cytoplasmic juxamembrane domain of E-cadherin (Reynolds, Daniel et al. 1996, Meng

and Takeichi 2009) which prevents its' subsequent internalisation thus increasing E-cadherin concentrations at AJs—directly influencing strength of adhesive contacts between cells (Reynolds 2007, Hartsock and Nelson 2008). p120-catenin also plays a role in cellular motility through inhibition of RhoA activity (Meng and Takeichi 2009) and also being able to modulate the NF-κB proinflammatory response by downregulating toll-like receptor (TLR) 4 signalling through suppression of myeloid differentiation primary response gene 88 (MyD88) adaptor binding (Wang, Malik et al. 2011). β-catenin binds to the C-terminal cytoplasmic domain of E-cadherin, an interaction that is strengthened by phosphorylation of specific serine residues on β-catenin. As with p120-catenin, β-catenin serves to stabilise E-cadherin at the AJ to promote junctional stability. β-catenin additionally plays a role in a number of signalling pathways including Wnt-signalling to effect cell adhesion and morphogenesis events (Hartsock and Nelson 2008, Tian, Liu et al. 2011). α- catenin binds to β-catenin via its' β-catenin binding domain and is thought to link the E-cadherin-β-catenin complex to the actin cytoskeleton though this cannot be confirmed via *in vitro* experiments (Hartsock and Nelson 2008).

1.3.2.c: Desmosomes

Desmosomes are punctate junctions that play a role in providing adhesive contact between neighbouring epithelial cells. They are abundant in skin and additionally in cardiac muscle and the dura mater of the meninges (Holthofer et al., 2007), tissues where strong tissue cohesion has to be maintained. They are composed of the transmembrane desmosomal cadherins (desmocollins and desmogleins) and intracellular desmosome adhesion molecules which link the desmosome 'plaque' to the intermediate filaments of the cytoskeleton (Huber 2003, Garrod and Chidgey 2008). The desmosomal cadherins of neighbouring cells homo/hetrophilically interact via their extracellular domains in a Ca^{2+} dependent manner due to the molecular conformation being stabilised by binding to calcium ions (Shapiro et al., 1996) Calcium independent desmosomal adhesion has also been described which is thought to convey junctional stability in tissues where cohesive strength is vital such as in the skin barrier—Ca^{2+} independence is thought to lead to 'hyper adhesion' of the desmosomes (Garrod and Chidgey 2008). Both desmoglein and desmocollin family members have intracellular domains which interact with desmosome adhesion molecules such as plakoglobin and plakophilins 1-3 (Huber 2003). These adhesion molecules cluster together and with the addition of the desmosomal plakin

family of proteins (such as plectin and perilakin (Huber 2003)) form the desmosome plaques which link to intermediate filaments (Garrod and Chidgey 2008).

1.3.3: Impairment of Physical Barrier in Asthma

There are several structural changes observed in asthmatic airway such as enhanced collagen I, III and V deposition in the subepithelial layers, smooth muscle thickening and several types of cellular hyperplasia. Within these remodelling events, it is observed that there are several changes that can occur which impact upon the structure of the pseudostratified epithelium. In addition to large structural changes, individuals with asthma often present with an impaired physical barrier in their airway epithelium—which is a key feature of asthma pathogenesis.

Epithelial desquamation has been noted in biopsies from individuals with fatal asthma-related complications. Epithelial desquamation is the denuding of the bronchial epithelium, which can vary in severity resulting in an epithelial layer that has regions of intact epithelium, areas with columnar cell loss and regions with complete cellular loss exposing the basal lamina. In addition to the denuding events, desquamation leads to other epithelial changes such as enhanced expression of heat shock protein-70 (Hsp-70) (effecting cell stress and effecting apoptosis) and enhanced expression of epithelial growth factor receptor (EGFR) (effecting cell proliferation and differentiation) which may underpin some of the other airway remodelling events characteristic of asthma (Holgate 2007). Despite evidence to suggest that this is a pathological change witnessed in asthma, there is also conflicting evidence to suggest that some desquamation events are an artefact of bronchial sampling (Ordonez and Fahy 2001).

In addition to cellular desquamation, there is also an alteration in the proportion of different cell types in the pseudostratified layer in asthmatics. Those with mild and moderate disease present with a higher proportion of goblet cells—indicating goblet cell hyperplasia. In addition to higher numbers of goblet cells, asthmatics have differential mucin gene expression (higher MUC5AC expression), elevated levels of mucous stored within goblet cells, and higher levels of mucous secretion than healthy individuals (Ordonez, Khashayar et al. 2001). There is emerging evidence to suggest that this goblet cell hyperplasia is not only restricted to the upper airways, but additionally there are

increased goblet cells in lower airway epithelial layers, where they previously were not expressed (Holgate 2007).

In addition to these larger changes in pseudostratified epithelium composition, asthmatics also present with significant changes to their 'intact' columnar epithelium,which negatively impacts epithelial barrier integrity within these individuals. This is demonstrated by decreased transepithelial resistance and increased macromolecular permeability of asthmatic primary bronchial epithelial cells (PBECs) *in vitro* (Xiao, Puddicombe et al. 2011). Asthmatics have impaired TJ formation and have lower TJ numbers within the pseudostratified epithelium. Additionally within their remaining TJs, they have decreased expression of key TJ-associated proteins such as ZO-1 and occludin (de Boer, Sharma et al. 2008, Yeo and Jang 2010, Xiao, Puddicombe et al. 2011). Similarly in the AJs, there was decreased expression of E-cadherin and α-cateninin in atopic individuals with stable diease (de Boer, Sharma et al. 2008). Loss of E-cadherin and p120 catenin in columnar epithelium in severe asthmatics was also reported (Hardyman et al., 2013). Epithelium from allergic and non-allergic asthma patients has showed a 30-40% decrease in desmosomal length (Shahana, Bjornsson et al. 2005) which may contribute to increased shedding and barrier fragility recorded in disease.

1.3.4: Airway Defence via the Biochemical Barrier

Whilst the airway epithelium is structurally organised to minimise pathogenic penetration, there is an additional, non-specific microbial clearance mechanism utilised. Respiratory secretions show a number of different antimicrobial agents (Table 1.2) which act to provide a full protective repertoire for the airway. The precise composition of the antimicrobial secretions are variable according to secretion origin and inflammatory state of the lung (Ganz 2002, Vareille, Kieninger et al. 2011, Ganesan, Comstock et al. 2013). In addition to these antimicrobial agents, nitric oxide (NO) has been detected in bronchial airway lavage (BAL) and this is proposed to play a role in this biochemical barrier, though the precise mechanism of action is yet to be elucidated (Ganz 2002).

Antimicrobial Agent	Proposed Role in System
Lysozyme	Enzymatic activity against peptidoglycan cell-walls in bacteria
Lactoferrin	Inhibition of microbial respiration
Defensins	Enzymatic activity against microbial cell walls
Secretory Leukoprotease Inhibitor (SLPI)	Inihibtion of proteolytic enzymes

Table 1.2: Antimicrobial agents and their theorised role in biochemical defence in the lungs

1.4: Innate Immune Responses in Airway Epithelium

If the above mechanisms fail to prevent HRV-16 entry and binding to ICAM-1 the innate immune system responds. This innate response includes inducing a proinflammatory and antiviral state within the cells with the aim to eradicate the infected cells and limit pathogenic spread (Schleimer, Kato et al. 2007). In more severe infections the activation of the innate immune response acts as a primer for the activation of the adaptive immune response if necessary (Schleimer, Kato et al. 2007).

During the replication of the HRV-16 genome a double-stranded RNA (dsRNA) replicatory intermediate is formed. dsRNA is detected by the intracellular pattern recognition receptors (PRRs) which includes the Toll Like Receptor-3 (TLR-3), Melanoma Differentiation-Associated gene-5 (MDA-5) and Retinoic acid Inducible Gene-1 (RIG-I)(Tosi 2005, Parker and Prince 2011). Recognition of the pathogenic pattern by these receptors leads to the activation of immune signalling cascades which culminates in:

- Activation of nuclear factor-κB (NF-κB) and subsequent proinflammatory state adoption (Tosi 2005)
- Production of type I and III interferons (IFNs) and subsequent antiviral state adoption (Takaoka and Yanai 2006)
- Activation of FAS Associated Death Domains (FADD)/caspases and subsequent cellular apoptosis (Georas and Rezaee 2014)

Specifically each outcome is generated through the activation of the pathway through the PRR activation and recruitment of the adaptor proteins, which initiate the associated signalling cascade. TLR-3 activation leads to the recruitment of the TIR Domain Containing Adaptor Inducing Interferon-β-1 (TRIF) adaptor protein, which culminates with the activation of the interferon-regulatory factor-3 (IRF-3). IRF-3 is one of a family of IRF's activated to increase expression of IFNs, which enhances the antiviral state within cells (Goodbourn, Didcock et al. 2000, Levy and Garcia-Sastre 2001, Durbin, Kotenko et al. 2013). MDA-5 and RIG-I activation causes the recruitment of IPS-1 adaptor protein. IPS-1 can activate signalling cascades that activates IRF-7—once again involved in IFN expression and antiviral state adoption—and the transcription factor Nuclear Factor-κB (NF-κB)(Kumar, Takada et al. 2004). TLR-3 is also capable of activating NF-κB through activation of TNF Receptor Associated Factor 6 (TRAF6) by the TRIF adaptor protein. NF-κB activation leads to multiple cellular outcomes, one of which is the activation of the proinflammatory immune response, which acts to remove viral particles (Subauste, Jacoby et al. 1995, Bochkov, Hanson et al. 2010). IPS-1 additionally can activate the FAS associated death domain (FADD) which leads to the activation of subsequent caspase signalling which culminates in cellular apoptosis—limiting pathogenic replication by removing infected cells from the system completely (Festjens, Vanden Berghe et al. 2007)(Figure 1.8).

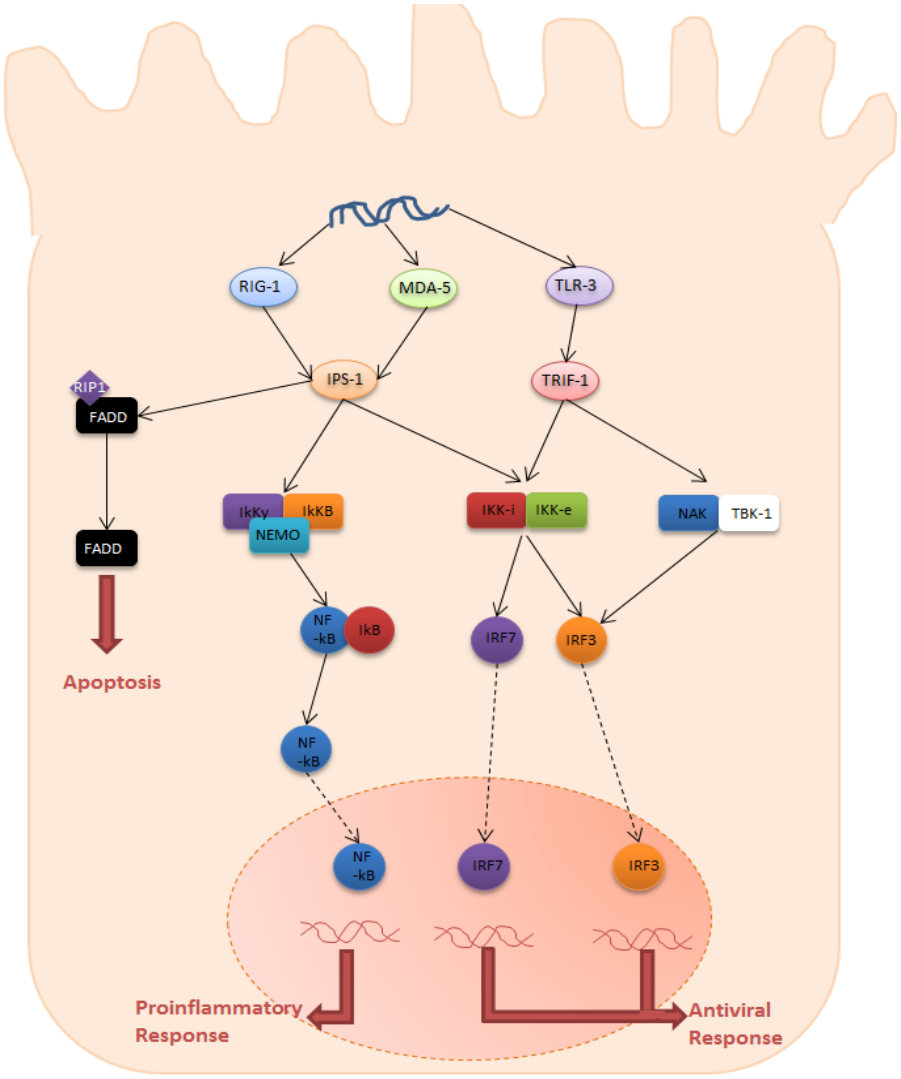

Figure 1.8: Diagrammatic representation of bronchial epithelium showing the signalling pathways involved with pathogen recognition and subsequent innate immune responses of defence launched in response to pathogen detection

1.4.1: Proinflammatory Immune Response

The proinflammatory response mainly serves to remove viral particles from the airway epithelium to minimise infection spread through the release of proinflammatory mediators. These mediators have two main mechanisms of action:

- Chemotactic mediators: these are able to chemoattract and subsequently activate cells belonging to the innate/adaptive immune response (Bals and Hiemstra

2004). These include β-defensins, interleukin-8 (IL-8) and RANTES (Subauste, Jacoby et al. 1995, Dotzauer and Kraemer 2012).

- Inflammatory mediators: these act to limit pathogen movement, trigger inflammation events (swelling, fever) and initiate wound healing (Bals and Hiemstra 2004). These include IL-1α/β, Tumour Necrosis Factor-α (TNF-α) and the proinflammatory interferon, IFN-γ (Subauste, Jacoby et al. 1995, Dotzauer and Kraemer 2012).

1.4.1.a: Nuclear Factor-κB

NF-κB is the transcription factor primarily responsible for mediating the transcription of proinflammatory mediators and hence triggering the subsequent proinflammatory response within the system. NF-κB has additionally been implicated to play a role in other immune responses including elevation of antigenic processing and presentation, modulation of adhesive properties of cells and contribution to production of the type I IFNs (Caamano and Hunter 2002, Kumar, Takada et al. 2004).

There are 5 related members of the NF-κB family: p50, p52, RelA (p60), c-Rel and RelB. All five members have sequence homology of 300 amino acid (aa) residues, which makes up their Rel homology domain at the N-terminal. The Rel homology domain is responsible for NF-κB dimerisation (both heterodimeric and homodimeric) to give rise to the functional NF-κB transcriptional unit. Only RelA, RelB and c-Rel have transcriptional activating domains in their C-terminal and hence can activate transcription. The transcription activating domain is absent in p50 and p52 and thus these can only activate transcription upon heterodimerisation with RelA/RelB/c-Rel (Caamano and Hunter 2002, Kumar, Takada et al. 2004, Oeckinghaus and Ghosh 2009).

Activation of NF-κB is tightly controlled to ensure there is no aberrant activation of the proinflammatory response. Aberrant activation of NF-κB and proinflammatory responses have been noted in many chronic diseases including irritable bowel disease (IBD) and asthma (Tak and Firestein 2001, Lawrence 2009). To ensure regulation, NF-κB is sequestered in to the cytoplasm in an inactive state through covalent association with regulatory inhibitor of Kappa-B (IκB). In the canonical NF-κB pathway (activated by IPS-1 adaptor protein signalling), upon viral sensing the NF-κB signalsome—containing IκB Kinase (IκK-α and IκK-β subunits) and IκKγ (NEMO)—becomes activated. The

signalsome phosphorylates IκB on $-NH_2$ serine residues, which allows for NF-κB disassociation and targets IκB for proteosomal degradation. Free NF-κB units are then able to dimerise and translocate to the nucleus to initiate transcription (Caamano and Hunter 2002, Kumar, Takada et al. 2004, Lawrence 2009, Oeckinghaus and Ghosh 2009)(Figure 1.9).

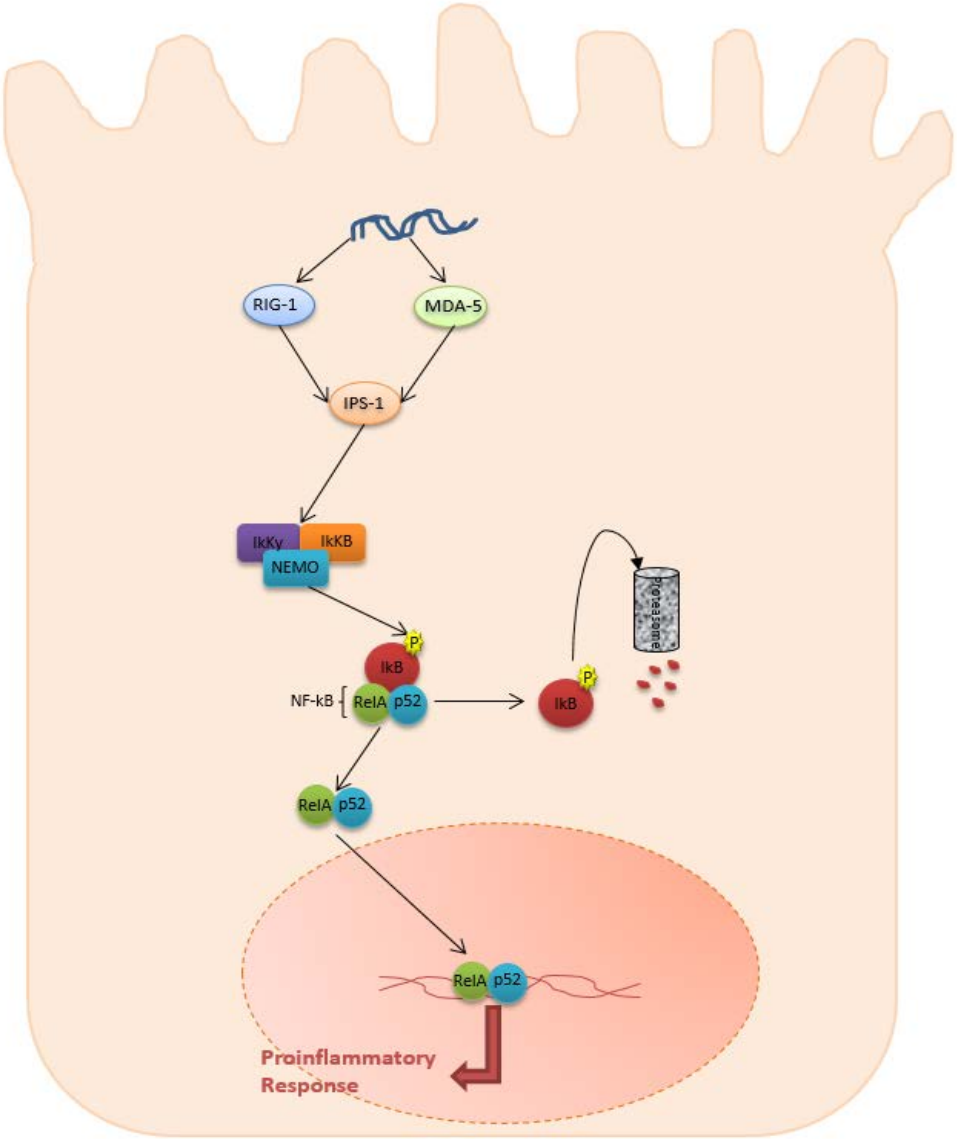

Figure 1.9: Diagrammatic representation of bronchial epithelium showing the activation of NF-κB via canonical IPS-1 pathway. IPS-1 is activated through MDA-5 and RIG-1 sensing of dsRNA replicatory intermediates from virus. This activates the NF-κB signalsome which subsequently phosphorylates regulatory IkB units on NH_2 residues. Phosphorylated IkB disassociates from NF-κB and is degraded. NF-κB translocates to the nucleus and initiates transcription of a number of genes including those involved in mediating the proinflammatory response.

1.4.1.b: Negative Regulation of NF-κB

NF-κB activation is tightly regulated through a number of different mechanisms by a wide variety of proteins to ensure that NF-κB signalling—and subsequent proinflammatory signalling—is only a short-term stimuli. These proteins can generally be classified into one of three groups: proteins that inhibit signalling to IκK signalsome, proteins that inhibit activation of the IκK signalsome or proteins that inhibit NF-κB transcription (Ruland 2011).

Inhibition of signalling to the IκK signalsome tends to be carried out by dominant-negative adaptors. These proteins, including MyD88s, are able to interfere with signalling from PRRs such as the TLRs inhibiting the recruitment of the adaptor proteins and thus terminating any downstream activation of NF-κB (Ruland 2011). In addition there are proteins, including Cylindromatosis (turban tumor syndrome) (CYLD), which are able to terminate activation of the adaptor proteins and inhibit further signal transduction (Kovalenko, Chable-Bessia et al. 2003, Ruland 2011). In the aforementioned example this is TRAF6.

Proteins that inhibit the IκK signalsome activity are often proteins with the capacity to deubquitinate their targets (Ruland 2011). In addition to a role in inhibiting signalling to the IκK signalsome, CYLD also is able to deubiqutinate IκK-γ, preventing disassociation from NF-κB and proteasome degradation of the protein (Kovalenko, Chable-Bessia et al. 2003). TNF-α induced protein-3 (TNFAIP3)/A20 is a crucial negative regulator of NF-κB activation via an inhibitory feedback loop (Parvatiyar and Harhaj 2011) which involves the addition and removal of ubiquitin.

The final classification of NF-κB regulatory proteins are those that directly affect NF-κB mediated signalling. Within the nucleus, there are multiple proteins such as E3 SUMO-protein ligase (PIAS-1) and non-degraded IκK-γ which can interfere with the ability of NF-κB to bind to deoxyribonucleic acid (DNA). Additionally the COMM domain containing protein 1 (COMMD1)-suppressor of cytokine signalling 1 (SOCS1)-Cullin-2 E3 ubquitin ligase complex can ubiqutinate NF-κB dimers within the nucleus, causing their disassociation from DNA and targeting them for proteasomal degradation (Ruland 2011)(Figure 1.10).

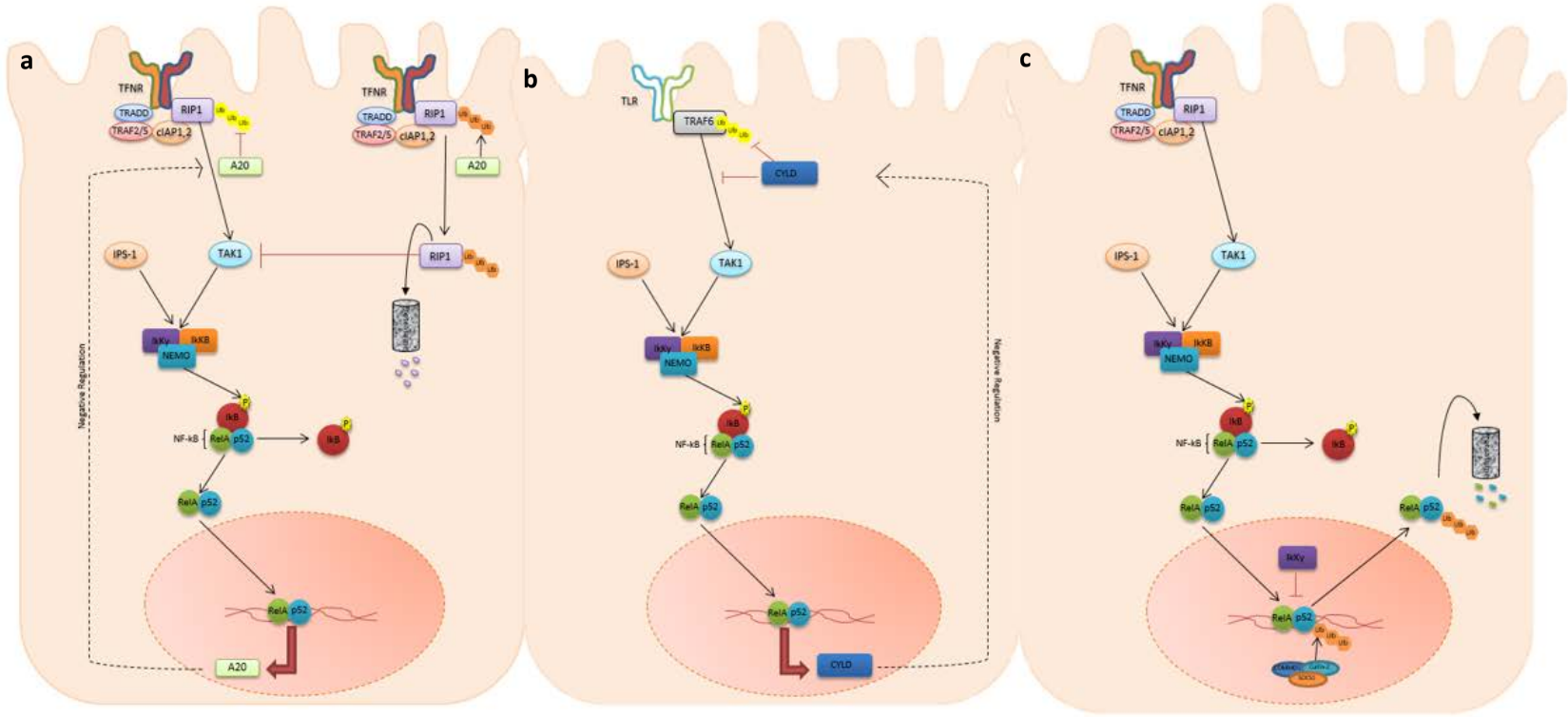

Figure 1.10: Diagrammatic representation of bronchial epithelium showing the negative regulation of NF-κB via a number of different mechanisms. (a) TNFAIP3/A20 utilises a dual ubiquitin editing function to increase RIP-1 degradation, preventing TAK1 activating the NF-κB signalsome. (b)CYLD functions to prevent activation of NF-κB signalsome by preventing TLR adaptor protein TRAF6 from becoming activated. (c) Non-degraded IKKγ prevents NF-κB binding to DNA. COMMD1-SOCS1-Cullin-2 ubiqutinates NF-κB causing translocation from within the nucleus and allows for proteosomal degradation

1.4.2: Antiviral State Adoption

It is the activation of the IRF family of transcription factors that leads to the expression of the type I and III interferons (IFNs). It is the expression and release of these IFNs which allow cells to become less infection permissible and adopt an 'antiviral state' (Goodbourn, Didcock et al. 2000, Levy and Garcia-Sastre 2001, Durbin, Kotenko et al. 2013). The antiviral state is established by the release of expressed IFNs from infected cells and signalling in paracrine manner to neighbouring uninfected cells. Released IFNs additionally act in an autocrine manner to establish a positive feedback loop to enhance IFN release. IFN-induced signalling culminates with the expression of interferon stimulated genes (ISGs) which can modulate a number of cellular processes that contribute to the neighbours of infected cells adopting an antiviral state (Sadler and Williams 2008).

The antiviral response initiated by infected cells in the airway epithelium is highly efficient at limiting rhinovirus infection in neighbouring epithelial cells. It is noted that *in vitro* infection of PBECs with HRV-16 at a multiplicity of infection (MOI) = 10, only 5% of the cells across the culture become infected (Chen, Hamati et al. 2006). It is also noted that pre-treatment of PBECs *in vitro* with as little of 0.1ng/ml exogenous IFN causes a significant decrease in HRV-1A replication during infection (Becker, Durrani et al. 2013).

1.4.2.a: Type I Interferons

The type I IFN family contains 13 IFN-α subsets, IFN-β, IFN-ε, IFN-κ and IFN-ω—all of which belong to the class II family of α-helical cytokines. Of these IFNs, IFN-α and –β are the most widely accepted to play a role in the response to HRV-16 infection (Goodbourn, Didcock et al. 2000).

During infection, IFN-β is the first of the type I IFNs to be transcribed through the association of NF-κB, IRF-3 and c-Jun/activating transcription factor 2 (ATF-2) to transcriptional start sites within the DNA. Upon viral detection within the cell, PRRs TLR-3, RIG-I and MDA-5 are activated and this causes the recruitment and activation of their adaptor proteins TRIF-1 and IPS-1 respectively. Activated TRIF-1 allows for binding and activation of IKK-ι/IKK-ε and/or TANK-binding kinase 1 (TBK1)/NF-κB activating kinase (NAK), which subsequently phosphorylates IRF-3—causing its activation. Phosphorylated IRF-3 will bind to the IFN-β promoter; though alone it is not sufficient to

cause transcription and instead requires the co-localisation of phosphorylated AFT-2 and activated NF-κB (Yoneyama, Suhara et al. 1998, Goodbourn, Didcock et al. 2000, Levy and Garcia-Sastre 2001, Takaoka and Yanai 2006). When all three transcriptional molecules are bound to DNA, IFN-β transcription and subsequent translation is initiated. IFN-β is then released from the infected cell, acting in a paracrine manner across neighbouring cells and also in an autocrine feedback loop to further enhance IFN-β from the infected cell, in addition to triggering secondary IFN-α expression.

When type I IFNs are released, they bind to the IFN-α receptor 1 subunit (IFNAR1), which dimerises with IFNAR2 to form the activated IFNAR. The receptor dimerisation on the cellular surface leads to the activation of intracellular tyrosine kinase-1 (TYK1) (anchored to IFNAR2) and Janus kinase 1 (JAK1) (anchored to IFNAR1) via transphosphorylation. Activation of these JAK signalling molecules allows for the phosphorylation of the subsequent signal transducer and activator of transcription 1/2 (STAT1/2) signalling molecules, which can then heterodimerise with one another. STAT1-STAT2 heterodimer translocates to the nucleus and associates with IRF-9/p48 to form the complete interferon stimulation gene factor 3 (ISGF3) which binds to interferon stimulated response elements in the DNA and causes the transcription of ISGs (Yoneyama, Suhara et al. 1998, Levy and Garcia-Sastre 2001, Takaoka and Yanai 2006, de Weerd, Samarajiwa et al. 2007).

Amongst the many ISGs that are upregulated first by IFN-β signalling, IRF-7 is the most fundamental. It is the expression of IRF-7, which is responsible for binding to, and promoting the expression of, IFN-α within the system. IFN-α will reinforce the action of the IFN-β and utilise the same signalling cascades to further upregulate ISGs (Sato, Suemori et al. 2000)(Figure 1.11).

1.4.2.b: Type III Interferons

Until the early 2000's, it was widely accepted that there were only two families of IFNs (type I—as above—and type II—IFN-γ). However, evidence suggested there was a third family of IFNs, which played a similar functional role to the type I IFNs but were distinct from this family (Donnelly and Kotenko 2010). This third family—the type III IFNs—now has four members identified: IFN-λ1, IFN-λ2, IFN-λ3 and IFN-λ4. IFN-λ4 is a more recent

addition to the family and is only present in individuals who have a frameshift mutation in the IFNL4-ΔG gene (O'Brien, Prokunina-Olsson et al. 2014).

Activation of IFN-λ transcription is not well characterised though it is known that IFN-λ promoters in the DNA have binding sites for both NF-κB and IRFs (Uze and Monneron 2007). It has been proposed that, unlike the type I IFN family, the type III IFNs do not require coordinated binding of NF-κB and IRFs, but instead these transcription factors bind and activate IFN-λ expression independently which may indicate that the type III IFNs respond to wider pathogenic stimuli than their type I counterparts (Ank, West et al. 2006). As with the type I IFNs, released IFN-λs are proposed to initiate paracrine signalling in neighbouring uninfected cells and are involved in autocrine signalling (Dickensheets, Sheikh et al. 2013).

Released IFN-λ binds to IFN-λR1 (unique receptor) and IL10R2 (shared with the IL-10 cytokine family) which causes receptor dimerisation. As with type I IFN signalling, this causes activation of Tyk2 (on IFN-λR1) and JAK1 (on IL10R2) via transphosphorylation. This again results in the activation of the downstream STAT pathway culminating in the activation of ISGF3 to cause ISG transcription. It has also been shown that dimerised IFN-λ receptor can directly interact with proteins involved in ISGF3 and ISGF3 modulation such as IRF-9 and PI3K (Goodbourn, Didcock et al. 2000, Uze and Monneron 2007, Iversen and Paludan 2010)(Figure 1.11).

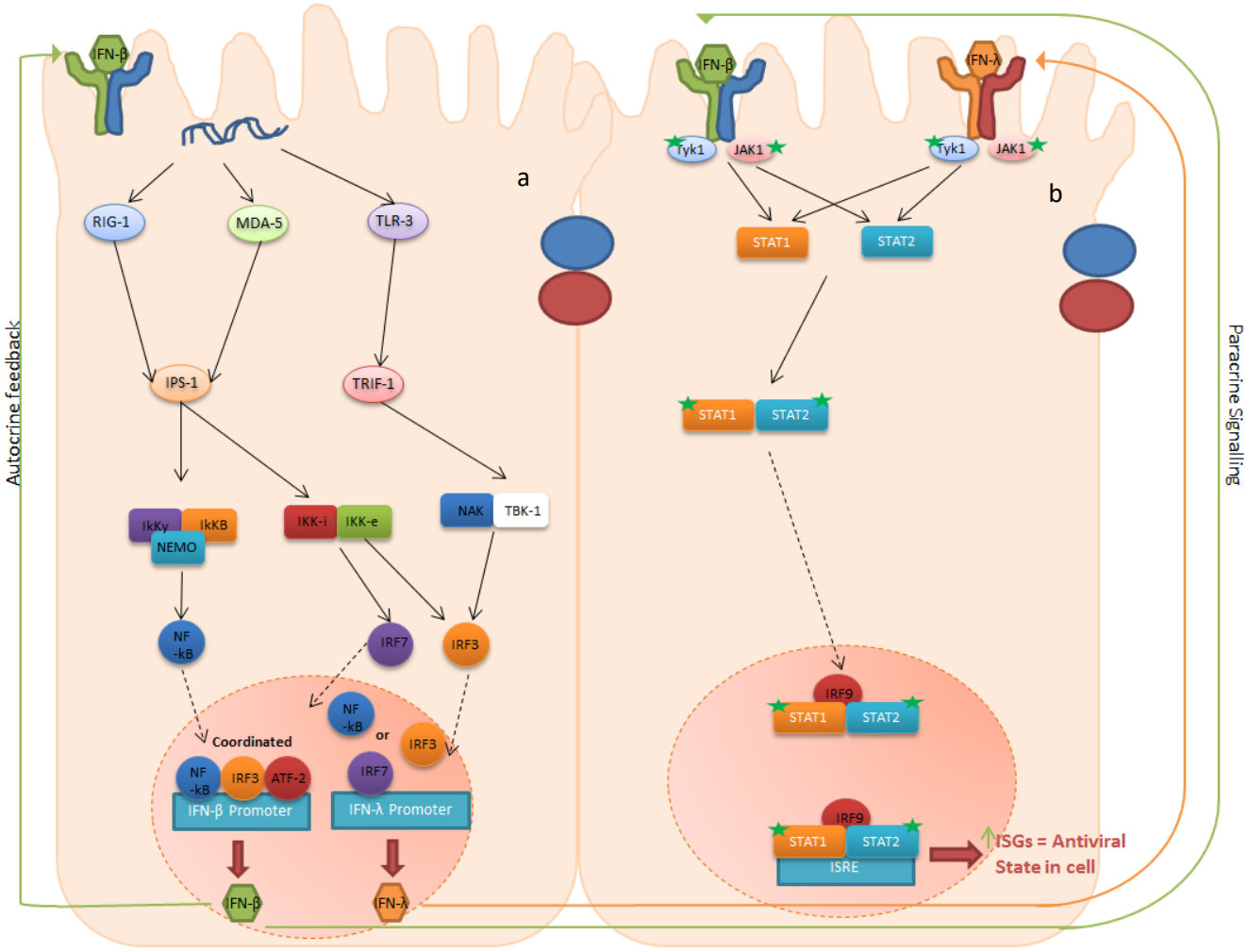

Figure 1.11: Diagrammatic representation of signalling pathways involved in interferon production in infected bronchial epithelium (a) and subsequent response to interferon exposure in non-infected neighbouring cells (b).

1.4.2.c: Interferon Stimulated Genes

The activation of ISGF3 by either type I or type III IFNs cause the transcription of ISGs which results in the production of interferon-stimulated proteins (ISPs) which are the primary effectors of the IFN response. There are over 300 genes activated in this IFN response (Sadler and Williams 2008) which span a variety of cellular networks including: intracellular signalling, immune modulation, host defence, inflammatory response, apoptosis, transcription, adhesion, and cytoskeletal regulation (de Veer, Holko et al. 2001). Of these networks, ISGs involved in intracellular signalling and host defence are the most highly induced (de Veer, Holko et al. 2001). The overarching role of the ISGs is to make the cells less permissive to viral infection by reducing their capacity to enable viral replication, assembly and release (Figure 1.12).

The interferon-induced proteins with tetratricopeptide repeats (IFIT) gene family has been shown to be upregulated both in response to *in vitro* HRV-16 infection of PBECs (Chen, Hamati et al. 2006) and in response to exogenous IFN-β treatment (Rusinova 2013)(Table 1.3). This family have a multitude of antiviral effects including inhibition of translation via inactivation of eIF3 (IFIT2), inhibition of cell proliferation via inactivation of COP9 signalsome subunit 5 (CSN5/IFIT4) and alteration of cytoskeletal elements (IFIT2). In addition to these cellular effects, IFIT family members are able to act as PRR, as they bind to unmodified 5'triphosphorylated RNA, a replicatory intermediate in some viral lifecycles, such as influenza A. This binding causes a decrease in viral RNA (vRNA) through an unidentified mechanism (Levy and Garcia-Sastre 2001, Fensterl and Sen 2011, Diamond and Farzan 2013).

IFIT gene	*Upregulation during HRV-16 infection*	*Upregulation in response to exogenous IFN-β 12 hours post-treatment*
IFIT1 (ISG56)	21.47	442.7
IFIT2 (ISG54)	4.11	102.5
IFIT4 (ISG60)	4.36	160.7
IFIT5 (ISG58)	No data available.	7.7

Table 1.3: Relative IFIT mRNA upregulation from baseline expression in response to viral infection (HRV-16) and 12 hours exogenous IFN-β treatment in HBECs

Virus inhibitory protein, endoplasmic reticulum associated, IFN-inducible (Viperin/RSAD2) is another protein strongly induced in response to HRV-16 infected (11.51 fold induction)(Chen, Hamati et al. 2006) and exogenous IFN-β treatment (245.1 fold induction)(Rusinova 2013). Viperin is a member of the S-adenosyl-L-methionine – dependent methyltransferase (SAM)-dependent radical enzyme family and plays a role in inhibiting viral replication and release. The mechanism of action is yet to be elucidated. It is suggested that viperin may act to inhibit lipid raft formation, hence inhibiting viral budding and additionally distort the endoplasmic reticulum, leading to inhibition of viral protein transportation. As viperin is able to bind to IRF-7, it is suggested that it may play a role in a positive feedback mechanism to elevate and enhance IFN production (Levy and Garcia-Sastre 2001, Sadler and Williams 2008, Fitzgerald 2011, Mattijssen and Pruijn 2012).

MxA and MxB GTPases are also highly induced in response to exogenous IFN (9.94 fold induction)(Rusinova 2013) and HRV-16 infection (9.01 fold induction)(Chen, Hamati et al. 2006). Though the precise mechanism of Mx protein action is not understood, it is postulated that Mx proteins can recognise fully assembled nucleocapsids and prevent their movement to viral replication sites, thus impeding viral replication. In addition to immobilisation, Mx proteins are thought to cause degradation of the nucleocapsids and other viral proteins to reduce viral load in the infected epithelial cells (Haller, Staeheli et al. 2007, Haller, Stertz et al. 2007, Sadler and Williams 2008).

2'-5'-oligoadenylate synthetases (OAS) are a family of four isozymes which are all induced in response to exogenous IFN-β and HRV-16 infection (Table 1.4)(Chen, Hamati et al. 2006, Rusinova 2013). When these isozymes are active they allow for the expression of the 2'-5'-oligoadenylates which bind and activate RNase L. RNase L completely halts translation in the cell through indiscriminate cleavage of RNA within the cell (Levy and Garcia-Sastre 2001, Sadler and Williams 2008).

OAS gene	*Upregulation during HRV-16 infection*	*Upregulation in response to exogenous IFN-β 12 hours post-treatment*
OAS1	4.88	73.8
OAS2	6.05	43.9
OAS3	6.19	20.37
OASL	2.61	67.9

Table 1.4: Relative OAS mRNA upregulation from baseline expression in response to viral infection (HRV-16) and 12 hours exogenous IFN-β treatment in HBECs

Like OAS, RNA-activated protein kinase (PKR) is another protein that completely inhibits protein synthesis within the cell. Upon IFN stimulation, inactive PKR is translated and this becomes active after an autophosphorylation event triggered by PRK binding to dsRNA replicatory intermediates. Catalytically active PKR will phosphorylate eIF-2a causing inhibition of translation (Levy and Garcia-Sastre 2001, Sadler and Williams 2008).

Interferon stimulated gene of 15kDa (ISG15) is another protein involved in antiviral state adoption and is 14 fold upregulated during HRV-16 infection. ISG15 is a homologue of ubiquitin and unlike the previously discussed ISGs, it does not impact viral replication but instead plays a role in immune signalling alteration. ISG15 is able to ISGylate (covalent addition of ISG15 to proteins, similar to ubiquitination) 158 predicted protein targets enhancing protein stability and their subsequent activity (Zaheer, Wiehler et al. 2014).

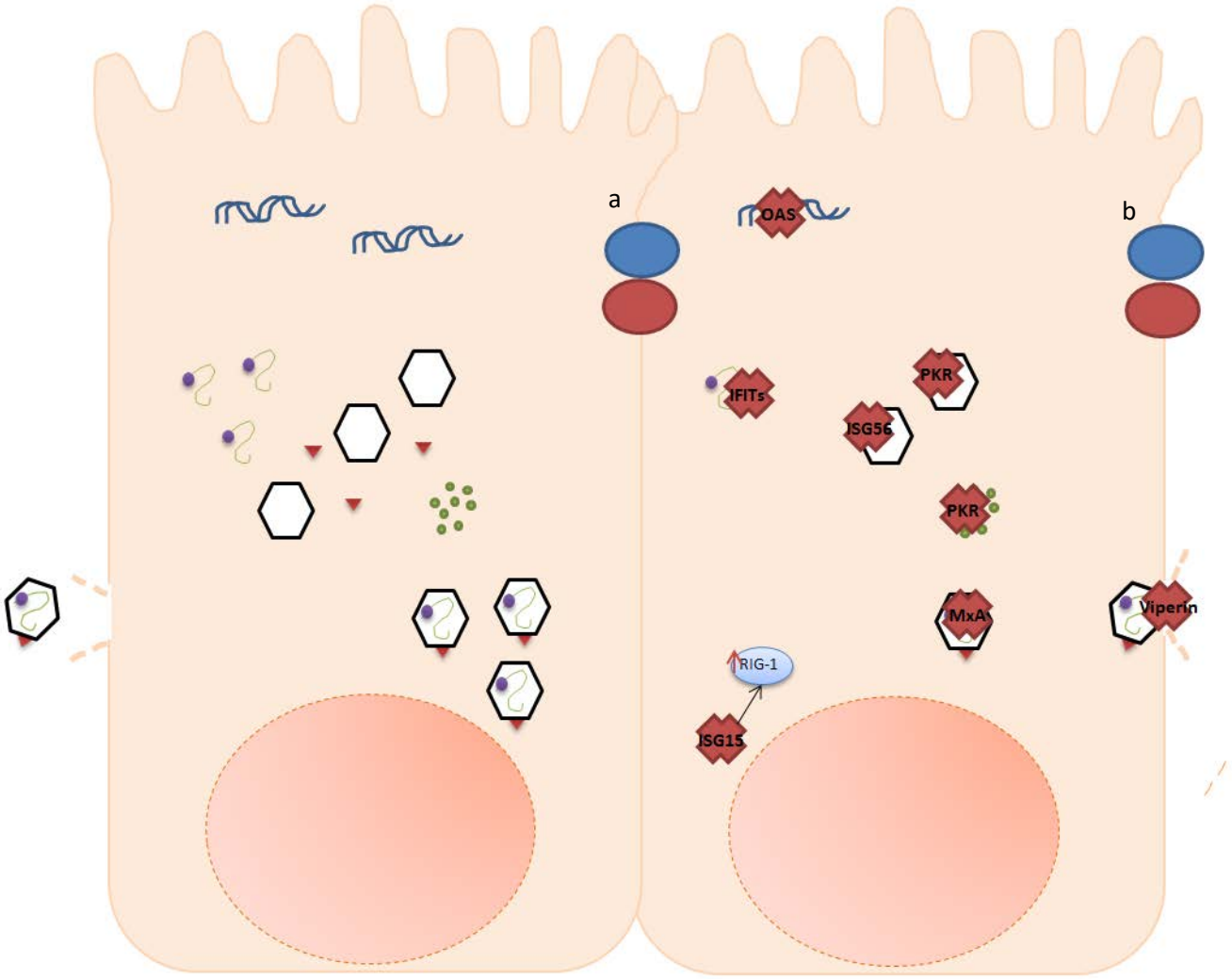

Figure 1.12: Diagrammatic representation of HRV-16 infected cell (a) with key steps of viral replication lifecycle and diagram of where ISGs involved in the antiviral response interfere with the viral replication (b).

1.4.3: Impairment of Innate Immune Response in Asthma

It is accepted that certain individuals with asthma have an impaired/abnormal innate immune response to viral infection. These aberrant responses are suggested to contribute to increased symptom severity and infection duration the response to HRV infection.

1.4.3.a: Proinflammatory Immune Response Impairment

There are a number of cytokines and chemokines that have been shown to be dysregulated in asthmatic individuals. These dysregulated immune modulators skew that airway towards a more proinflammatory state—underpinning a key pathogenic change of the disease.

IL-13 is shown to be overexpressed in sputum and biopsies from asthmatic individuals (Saha, Berry et al. 2008),especially those who suffer from allergic asthma (Wills-Karp 2004). IL-13 contributes to causing airway inflammation through recruitment of inflammatory cells, including eosinophils and monocytes, into the airway spaces and plays a key role in airway hyper-responsiveness. In addition, the over-expression of IL-13 contributes to mucous hyperplasia and subepithelial fibrosis—contributing to airway remodelling (Wills-Karp 2004). IL-4 is closely associated with IL-13 in promoting the allergic asthma phenotype (Wills-Karp 2004). IL-4 is responsible for enhancing *in vivo* production of IgE (Finkelman, Katona et al. 1988) and IgG1 (Snapper, Finkelman et al. 1988) which both play a role in airway hyper-responsiveness.

IL-6 is significantly elevated in bronchoalveolar lavage from symptomatic asthmatic individuals when compared to asymptomatic asthmatics (Broide, Lotz et al. 1992). Elevated IL-6 in asthmatics has been correlated to decreased FEV_1, indicating IL-6 overexpression has a negative impact on lung function (Rincon and Irvin 2012). IL-8 is also significantly induced in BAL from asthmatic patients, which is associated with enhanced neutrophil recruitment to the airway, contributing to enhanced inflammation in the region (Ordonez, Shaughnessy et al. 2000).

1.4.3.b: Interferon Immune Response Impairment

There is great debate as to the role the type I and III IFNs play in asthma pathogenesis. In one of the first papers examining IFNs in asthma, it was shown that asthmatic patients had markedly higher HRV-16 viral loads (>50 fold) when compared to healthy

individuals and this correlated with a significantly decreased level of IFN-β release (Wark, Johnston et al. 2005). Subsequent studies of the type I IFNs have shown in some incidences, asthmatics have markedly decreased IFN-β and IFN-α in bronchial airway lavage (BAL) samples, when infected with HRV-16 at both 8 ($p=*<0.001$) and 24 ($p=*<0.05$) hours (Sykes, Edwards et al. 2012). However, this same research group, when looking at a well-controlled asthma cohort, could not detect any significant differences in IFN-β production in response to HRV-16 and HRV-1B infection when compared to healthy controls. In addition, they could not detect any IFN-α in either group (Sykes, Macintyre et al. 2014).

Similarly IFN-λ has been shown to be impaired in some studies, whilst not in others. In BAL samples from asthmatics there was significantly less IFN-λ release ($p=*<0.05$) when compared to healthy patients when infected with HRV-16 (Contoli, Message et al. 2006). This additionally correlated with significantly less IFN-λ mRNA in PBECs from asthmatics compared to healthy individuals in response to HRV-16 infection (Contoli, Message et al. 2006). Conversely IFN-λ2/3 mRNA levels in sputum from asthmatics was higher and IFN-λ1 levels similar, compared to healthy individuals in one study (Bullens, Decraene et al. 2008). Another study also showed that IFN-λ levels were elevated in a HRV-associated wheezing paediatric cohort, which correlated with worsening of symptoms (Miller, Hernandez et al. 2012). There is also evidence to suggest that in some asthmatics, IFN-λ release is not impaired. In one study of healthy and well-controlled asthmatics, there were no significant difference in IFN-λ release (Sykes, Macintyre et al. 2014).

1.5: MicroRNAs

MicroRNAs (miRNAs/miR) are a species of single stranded RNA molecules that are between ~21-25 nucleotides in length (Doench and Sharp 2004). They are considered to act during the post-transcriptional, pre-translational phase within cells, to lead to differential protein expression. Whilst in many cases this differential protein expression serves a functional role, microRNAs have been shown to also be altered in a number of human pathologies including cancer (Jansson and Lund 2012).

There is emerging evidence that miRNAs play a role in epithelial barrier maintenance (Gregory, Bert et al. 2008), innate immune responses and viral responses within the system (Vaz, Mer et al. 2011). There is also evidence to suggest that microRNAs are

differentially expressed in individuals with asthma (Wu, Wang et al. 2014). Together this evidence may suggest that microRNAs could underpin key processes involved in epithelial barrier defence against HRV-16 infections. Additionally it may suggest that these microRNA mechanisms are different between healthy and asthmatic patients, which could impact the difficulties asthmatic individuals experience in response to rhinovirus infections.

1.5.1: Biosynthesis of microRNAs

MicroRNAs themselves are encoded within the genome, typically in intergenic regions, though many are found in introns and some in exons of non-coding protein transcripts, with a tendency to be found clustered close together (Winter, Jung et al. 2009). They are transcribed by RNA polymerase II (Pol II) from the DNA template, forming the pri-miRNA structure. Pri-miRNAs contain both the 3' (denoted as 3p) and 5' (denoted as 5p) version of the miRNA in a stem loop structure with both leading/lagging strands which contain the guanine cap and poly A tail to protect the structure from degradation. The pri-miRNA is then processed in the nucleus by the Drosha and DiGeorge syndrome chromosomal (or critical) region 8 (DGCR8) containing processing complex. Processing removes the leading/lagging strands to give the remaining hairpin pre-miRNA (Doench and Sharp 2004, Winter, Jung et al. 2009, Krol, Loedige et al. 2010, Wahid, Shehzad et al. 2010, Tran and Hutvagner 2013, Moreno-Moya, Vilella et al. 2014).

Pre-miRNAs are exported from the nucleus via exportin-5 wherein an unknown helicase and dicer process the pre-miR to remove the hairpin loop structure and give rise to the mature miRNA-miRNA* duplex. This duplex contains both the 3p and 5p version of the microRNAs in their processed form, ready to be incorporated in to the RNA induced silencing complex (RISC) to exert their biological effect (Doench and Sharp 2004, Krol, Loedige et al. 2010, Moreno-Moya, Vilella et al. 2014). It is often found that one of the miRNAs in this duplex (denoted by the *) is incorporated less into RISC and hence less biologically relevant (Ameres and Zamore 2013). Mature miRNA is incorporated in to RISC in association with argonaute 1-4 (AGO1-4) proteins, leading to the functional miRNA silencing unit, whilst the mature miRNA* is often degraded (Figure)(Doench and Sharp 2004, Krol, Loedige et al. 2010, Tran and Hutvagner 2013, Moreno-Moya, Vilella et al. 2014)(Figure 1.13).

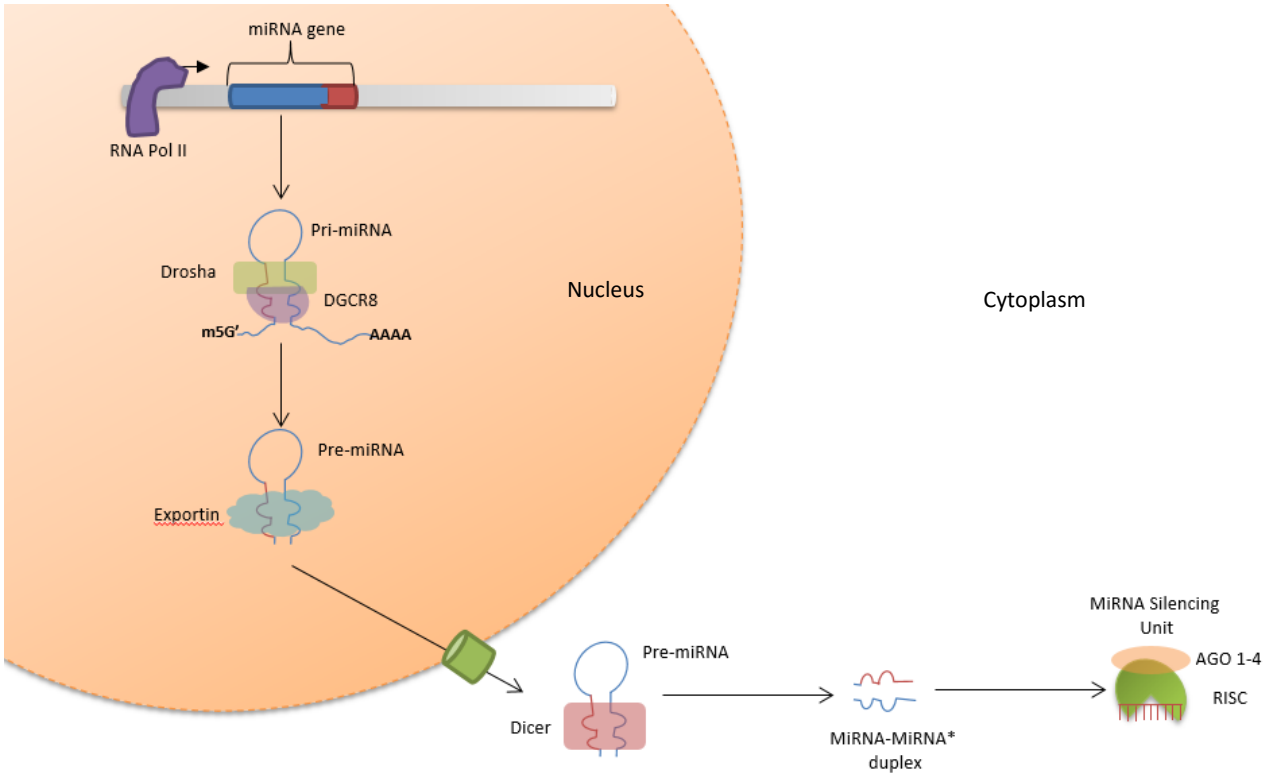

Figure 1.13: Diagrammatic representation of canonical microRNA biogenesis. RNA Pol II transcribes miRNA gene to produce pri-miRNA. Drosha and DGCR8 process pri-miRNA to remove leading/lagging strand and form pre-miRNA. Exportin-5 association allows for pre-miRNA to be exported from the nucleus in to the cytoplasm where Dicer cleaves the hairpin loop to form mature miRNA-miRNA* duplex. One of these mature microRNAs associates with AGO-14 and RISC to form functional miRNA silencing unit.

1.5.2: MicroRNA mechanism of action

Once mature microRNAs are incorporated in to the functional microRNA silencing unit, they exert their post-transcriptional effect. MicroRNAs are able to target specific mRNAs through their seed-sequence, a 7-8 nucleotide sequence in the microRNA which is 100% complementary to a sequence in the 3' untranslated region (UTR) of the target mRNA. Seed sequences direct the mature miR:mRNA targeting event and then the remaining miRNA sequence complementarity to the 3'UTR of the mRNA, determines whether the target is subjected to translational repression or degradation (Doench and Sharp 2004, Valencia-Sanchez, Liu et al. 2006, Krol, Loedige et al. 2010). Current evidence suggests that translational repression events are more common than mRNA degradation (Valencia-Sanchez, Liu et al. 2006, Wilczynska and Bushell 2015)(Figure 1.14).

Translational repression via microRNAs can cause an alteration to the level of the target protein without impacting upon the mRNA level (Doench and Sharp 2004). It is thought that this is achieved through three distinct repressive events. The first is inhibition of the initiation event through microRNAs interfering with the ability of eIF4F complex to associate with the poly(A)-binding protein (PABPC), thus preventing the mRNA from forming the circular structure required for translational events. The second is inhibition of elongation, which is either through inhibition of ribosomal subunit movement along the mRNA or increasing ribosomal disassociation from the mRNA. The third event is through co-translational degradation of the protein (Eulalio, Huntzinger et al. 2008), however the protease involved in this mechanism is not yet known. It is believed that these repressive events are initiated when there is limited downstream complementarity between the 3'UTR of the mRNA and the rest of the microRNA sequence (Doench and Sharp 2004, Valencia-Sanchez, Liu et al. 2006).

MRNA degradation causes an alteration of both the protein and mRNA level of the microRNA target (Krol, Loedige et al. 2010). There are several mechanisms by which the miRNAs facilitate the degradation of the mRNA—though generally it is considered that the miRNAs allow for AGO1-4 proteins in the RISC to catalyse mRNA degradation (Ameres and Zamore 2013). MiRNAs have been shown to assist in decapping and deadenylating the target mRNA through recruiting the likes of probable histone binding protein Caf1 (CAF1), C-C chemokine receptor type 4 (CCR4) and mRNA decapping protein 2 (DCP2) (Eulalio, Huntzinger et al. 2008) which effects mRNA stability,

enhancing its' AGO-mediated degradation. It is believed that mRNA degradation events are initiated when there are higher levels of complementarity between the miRNA and its' target mRNA's 3'UTR (Doench and Sharp 2004, Wahid, Shehzad et al. 2010).

Current studies have begun to highlight the complexities of miRNA targeting events. Each microRNA has the capacity to bind to the 3'UTRs of (and thus the regulate expression of) multiple mRNAs (Wilczynska and Bushell 2015). It has been shown that in some contexts, one miRNA may regulate multiple targets of one pathway (Judson, Greve et al. 2013). In other contexts one mRNA is regulated by multiple microRNAs (Wu, Huang et al. 2010). In addition to this there is evidence to suggest that the same miRNA can have different modulatory effects according to: Cell type, developmental stages and extracellular signalling (Avraham and Yarden 2012). It has also been shown that isoforms of miRNAs exist which adds further specificity—and complexity—to miRNA-mediated mRNA alteration (Ameres and Zamore 2013).

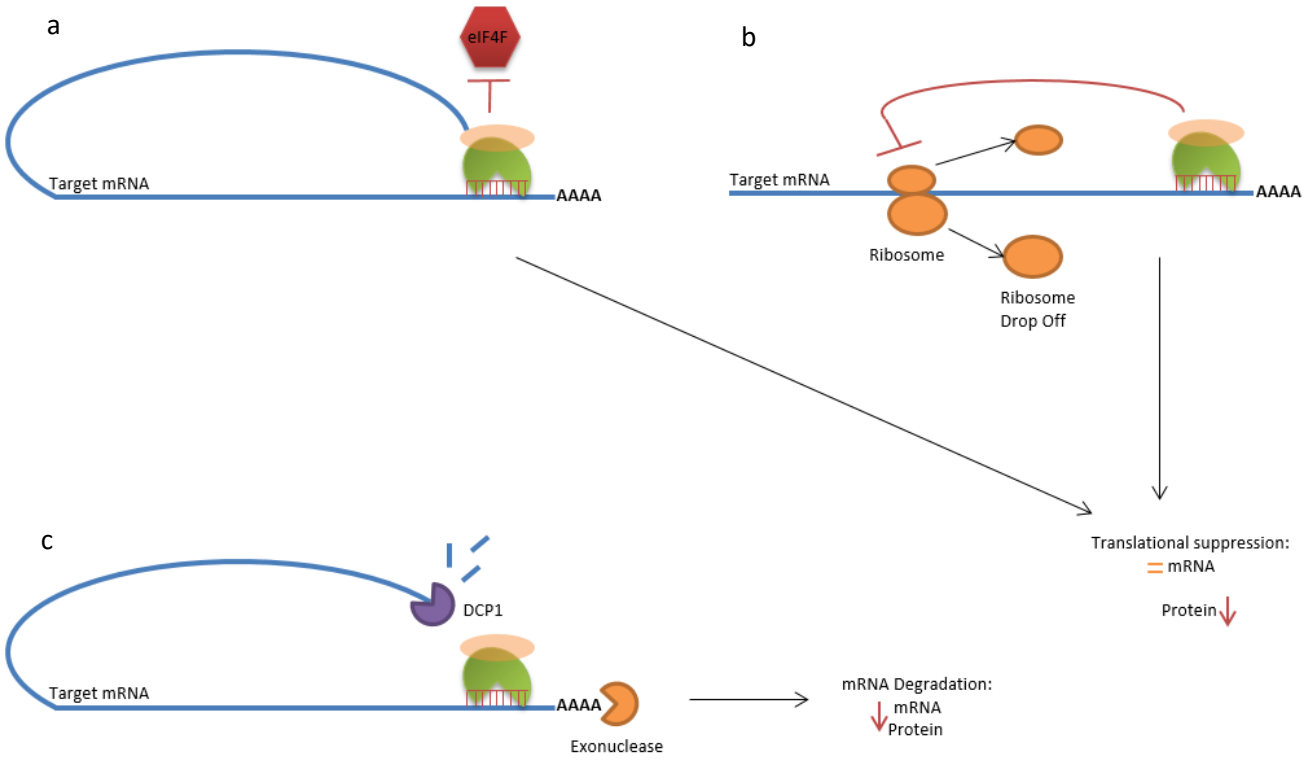

Figure 1.14: Diagrammatic representation of microRNA functionality. MicroRNAs may either cause: translational suppression through inhibiting initiation (a) or increasing ribosomal drop-off (b) or mRNA degradation through the recruitment of exonucleases and proteins such as DCP1 (c)

1.5.3: MicroRNAs in Epithelial Barrier Defence

Previous studies have implicated a number of microRNAs that play a role in epithelial barrier defence within cells. In intestinal epithelium, miR-122a has been shown to regulate the expression of the tight junction protein occludin, which in turn correlated with changes in epithelial barrier permeability (Ye, Guo et al. 2011). In a colitis mouse model, overexpression of miR-146b led to improvement of the epithelial barrier (Nata, Fujiya et al. 2013). Levels of miR-212 have been shown to be upregulated in colonic cells exposed to ethanol, which in turn led to decreased expression of ZO-1 within the TJs which disrupted TJ formation and destabilised the epithelial barrier and increased permeability (Tang, Banan et al. 2008).

When expression of members of the miR-200 family (miR-200a, -200b, -200c, -429 and -141) were downregulated, it was found that the level of E-cadherin protein in AJs was also reduced. This, in turn, increased AJ breakdown and enhanced epithelial-to-mesenchymal transition (EMT) within the cells (Paterson, Kolesnikoff et al. 2008). It was shown that some members of this miRNA family bind to the 3'UTR of the transcriptional repressors of E-cadherin, Zinc finger E-box-binding Homeobox 1/2 (ZEB1/2), to cause mRNA degradation and suggesting a mechanism of action for this family's impact upon epithelial barrier integrity (Gregory, Bert et al. 2008). In the Epithelial Barrier and Inflammation group at Southampton University, a study on a colonic cell line showed a link between decreased levels of miR-200b, -200c and -429 and barrier dysregulation in response to TNF-α treatment (*Loxham, Collins, unpublished*). It has additionally been shown that miR-429 is dysregulated in several malignant cancer phenotypes which is suggested to be linked to another miR-429 predicted target δ-catenin 2 (CTNND2) which is also able to disrupt E-cadherin expression in AJs (Lu 2010).

1.5.4: MicroRNAs in Innate Immunity

Previous studies have implicated a number of microRNAs that can impact upon the innate immune response. Several miRNAs have been implicated in modulation of the proinflammatory innate response via modulation of the NF-κB signalling cascade (Ma, Becker Buscaglia et al. 2011, Vaz, Mer et al. 2011). MiR-155 upregulation in *Helicobacter pylori* infection was correlated to elevated NF-κB levels (Xiao, Liu et al. 2009). It has been shown that miR-155 can target IKKε and potentially IKKβ, which limits NF-κB activation (Ma, Becker Buscaglia et al. 2011). MiR-391a is suggested to be one of the most potent

microRNAs in NF-κB activation through downregulating expression of NF-κB repressing factor (NKRF)(Ma, Becker Buscaglia et al. 2011). Upregulation of miR-181b via a STAT3 positive feedback loop leads to the inhibition of expression of the NF-κB negative regulator CYLD. Decreased expression of CYLD led to increased NF-κB activation. Within the Epithelial Barrier and Inflammation group, miR-23a was elevated in response to TNF-α and Transforming Growth Factor-β (TGF-β) treatment in renal epithelial cells, which correlated with altered NF-κB activation (*Dingley, Collins, unpublished*). effect.

1.5.5: MicroRNAs in Viral Infection

MiRNAs have been implicated to play a role in virus infection both to the advantage of the host and, in some instances, to the advantage of the virus itself.

Computational analysis has shown a number of microRNA binding sites naturally occurring within viral genomes—suggesting that viral lifecycle could be influenced by human miRNAs (Watanabe, Kishi et al. 2007). Of viruses profiled, it has been suggested that +ssRNA viruses are most likely to be regulated by endogenous miRNAs and within this group, the *picornaviridae* family had the largest number of predicted/potential miRNA binding sites (Watanabe, Kishi et al. 2007). The miR-23 family has been confirmed to bind to porcine reproductive and respiratory syndrome virus (PRRSV) RNA and impair PRRSV replication and decrease viral load. In the same instance miR-23a/b increased activation of IRF-3/7 which lead to elevation of IFNs and ISGs (Zhang, Guo et al. 2014). MiR-128 and miR-155 have both been shown to directly bind to the genome of HRV-1B and are able to inhibit viral replication—and inhibition of these microRNAs increases viral replication in BEAS-2B cells (Bondanese, Francisco-Garcia et al. 2014).

Recent evidence also suggests that there are ~200 virally encoded miRNAs—most of which are found in DNA viruses, specifically those belonging to the herpesvirus family (Watanabe, Kishi et al. 2007, Skalsky and Cullen 2010). These virally encoded miRNAs either share homology with human miRNAs—such as miR-11 from herpes simplex virus (HSV) and miR-155—or novel miRNAs which have seed sequences in the 3'UTRs of human mRNAsas well as in the viral genome itself (Skalsky and Cullen 2010). The role of viral microRNAs is not yet fully elucidated but it is suggested that the virus utilises the microRNAs to enhance viral replication, 'hijack' cellular processes and they may also play a role in viral evasion (Watanabe, Kishi et al. 2007, Skalsky and Cullen 2010, Skalsky, Olson et al. 2014).

In addition to viral miRNAs conveying a potential advantage in viral evasion/replication, it is noted that several human miRNAs also have this effect. MiR-23a has been shown to facilitate replication of HSV-1—with miR-23a overexpression corresponding to higher plaque formation—due to miR-23a's suppressive effect on IRF-1 expression (Ru, Sun et al. 2014). Influenza A infection has been shown to upregulate expression of miR-146a/b which enhanced viral replication potentially through innate immune response modulation via the miR-146a/b predicted targets mitogen activated protein kinase 3 (MAPK3) and interleukin-1 receptor associated kinase-1 (IRAK1) (Buggele, Johnson et al. 2012).

1.5.6: MicroRNAs in Asthma

MicroRNA dysregulation and changes are widely accepted to occur in a range of pathologies—including asthma. Solberg et al. were one of the first groups to show a large number of miRNAs were differentially expressed in steroid-naïve asthmatics (217), steroid-receiving asthmatics (200) and a healthy control group (Solberg, Ostrin et al. 2012). Subsequently more miRNA changes have been reported—including differential microRNA expression between asthmatic subclassifications (Maes, Cobos et al. 2016)—and as such it seems highly likely that miRNA alterations may play a role in all pathological changes associated with the disease.

MiR-155 has been shown to be downregulated in airway epithelium from asthmatic donors and leads to the dysregulation of the proinflammatory cytokine IL-6 (Martinez-Nunez, Bondanese et al. 2014). Similarly, miR-155 deficient mice were shown to develop an aberrant inflammatory response to environmental challenge in their lungs—responding in an 'asthma like' manner (Rodriguez, Vigorito et al. 2007). In ovalbumin-induced asthma models in mice, miR-126 was markedly increased in airway tissue of chronically challenged animals which was also linked to decreased eosinophilia in the region (Collison, Herbert et al. 2011). MiR-21 dysregulation is also observed in allergic asthma—leading to decreased expression of its' target IL-12 which ultimately impacts upon T_H-cell polarisation (Lu, Munitz et al. 2009).

1.6: Hypothesis

It is hypothesised that upon infection with HRV-16, culture differentiated airway epithelia from healthy and asthmatic patients will show altered levels of miR-23a and the

miR-200 family (miR-200b, -200c, -429). It is hypothesised that there will be a difference between the microRNA responses in the healthy and asthmatic patients.

1.7: Aims and Objectives

Aim 1: To identify potential targets of miR-23a, -200b, -200c and -429 which may play a role in maintaining epithelial barrier integrity and in modulating innate immune responses.

Objectives 1:

- To use bioinformatic prediction software to identify potential microRNA targets for investigation.
- To assess validity of bioinformatic predictions with regards to likelihood of miRNA:mRNA binding and targeting events.

Aim 2: To assess the effect of HRV-16 infection on levels of miR-23a, -200b, -200c and -429 in air-liquid interface (ALI) cultures and submerged monolayer cultures from healthy and asthmatic patients.

Objectives 2:

- To confirm productive HRV-16 infection of ALI and monolayer cultures via vRNA quantification by RT-mediated qPCR and $TCID_{50}$ assays.
- To confirm immunological response of ALI and monolayer cultures to HRV-16 infection via quantifying IFN mRNA induction (RT-qPCR) and release (IFN ELISA assays)
- To quantify expression of miR-23a, -200b, -200c and -429 in response to HRV-16 infection via RT-mediated qPCR.
- To quantify mRNA expression of predicted microRNA targets in response to HRV-16 infection via RT-mediated qPCR.

Aim 3: To assess effect of the antiviral mediator IFN-λ on miR-23a, -200b, -200c and -429 in ALI cultures from healthy and asthmatic donors.

Objectives 3:

- To quantify expression of microRNAs of interest in response to IFN-λ treatment during: (a) 0-3 days of differentiation, (b) over 21 days of differentiation and (c) 72 hours after 21 days of differentiation via RT-qPCR.
- To quantify mRNA and protein expression of predicted microRNA targets in response to IFN-λ treatment of (b) and (c) via RT-qPCR (mRNA) and western blotting (protein).
- To assess epithelial barrier integrity in response to IFN-λ treatment via transepithelial resistance, FITC 4kD-Dextrans and confocal-imaged immunofluorescent staining.

Aim 4: To confirm microRNA targeting and binding to predicted 3'UTRs via dual luciferase reporter assays.

Objectives 4:

- To isolate pre-miRNAs and 3'UTRs of interest from genomic DNA via PCR.
- To create pcDNA 3.1 pre-miRNA and pRL-TK 3'UTR expression constructs for use in dual luciferase reporter assays,
- To co-transfect pcDNA 3.1 pre-miRNA construct and pRL-TK 3'UTR constructs in to a cell-line to assess luciferase translation to confirm miR:mRNA binding.

CHAPTER TWO: Methodology

2.1: Cell Culture

2.1.1: Collection of Primary Bronchial Epithelial Cells (PBECs)

Bronchial epithelial cells were collected from healthy or asthmatic volunteers as part of the study: '*Investigation of the pathophysiological mechanisms in airway diseases such as asthma and COPD*' (REC ref: 05/Q1702/165)were approved by Southampton and South West Hampshire Research Ethics Committees (A). Patient characteristics of cells utilised throughout this thesis are listed in Appendix A.

Cells were either derived from bronchoscopy brushes or from lobectomy tissues which were then processed accordingly:

Bronchoscopy brushes: 2x bronchial brushings were collected from the volunteer and stored in 10ml PBS (Lonza, Switzerland) in a universal tube for transport from the Biomedical Research Unit to the laboratory. 20ml of MEM++ (PAA Laboratories, UK)(Table 2.1) was added before centrifugation at 1300G for 7 minutes at room temperature. Supernatant was carefully decanted and pellet was resuspended in 4ml BEGM++ (Lonza)(Table 2.2). Resuspended cells were added to a T25 coated with 25µl 2.5mg/ml Collagen I Bovine Protein (Life Technologies (Thermo Fisher Scientific), USA) and incubated at 37^{o}C/5% CO_2 until 70% confluency was reached with media changes every 1-2 days during the growth period.

	Volume (ml) per 500ml MEM (PAA Laboratories, UK)
FBS (Sigma-Aldrich)	50
100x Non-Essential Amino Acids (Thermo Fisher Scientific)	5
10,000 units/ml Pen/ 100,000µg/ml Strep (Sigma-Aldrich)	5

Table 2.1: MEM++ Media Constituents

	Volume (µl) per 50ml BEBM (Lonza)
Bovine Pituitary Extract (Lonza)	200
Epithelial Growth Factor (Lonza)	50
Insulin(Lonza)	50
Hydrocortisone (Lonza)	50
Transferrin (Lonza)	50
Epinephrine (Lonza)	50
Triiodothyronine (Lonza)	50
1µl/ml of BEGM of Retinoic Acid (Appendix B) were added to the BEGM growth media to give BEGM+ and either 1µl/ml of GA-1000 (Lonza, Switzerland) of 1µl/ml of Pen/Strep (Sigma-Aldrich, USA) was added to give complete BEGM++ just prior to addition to cells. Complete BEGM++ was only stored and utilised for 14 days after formulation as additives were suggested to be unstable if left for longer periods of time.	

Table 2.2: BEGM++ Growth Media constituents

Lobectomy tissues: tissue deemed healthy from lung resections was stored in 50ml PBS (Lonza) for transport from theatre to the laboratory. Tissue was cut along the length of the bronchus and washed x5 in 10ml of Hams-F12:DMEM (Table 2.3)(Lonza, Switzerland). Tissue was then incubated overnight at 4^{o}C with 25ml Hams-F12:DMEM containing 1mg/ml natural protease (Sigma-Aldrich, USA). Following overnight incubation, tissue was placed into a petri-dish containing Hams-F12:DMEM and bronchus cut was opened. Hams-F12:DMEM containing 1mg/ml natural protease that was used for the overnight incubation was utilised for rinsing of bronchus using a long nosed pipette to remove maximal bronchial epithelial cells. Media used for rinse was then transferred to universal tube and 1ml FBS (Sigma-Aldrich) was added to inhibit protease activity. Cells were then centrifuged at 1300G for 7 minutes at 4^{o}C. Cell supernatant was decanted and cells were resuspended in 5-10ml BEGM++ (Table 2.2) for a further centrifugation at conditions specified above. Supernatant was once again decanted and cells were resuspended in an appropriate volume of BEGM++ (Table 2.2) to give an appropriate seeding density of cells. 4ml of cell suspension was added to each well of a 6-well plate that had been pre-coated with 17µl 2.5mg/ml Collagen I Bovine Protein (Life Technologies (Thermo Fisher Scientific)). Cells were then incubated at 37^{o}C/5% CO_2

until 70% confluency was reached with media changes every 1-2 days during the growth period.

	Volume (ml)
DMEM (Lonza)	5
Hams-F12 (Lonza)	5

Table 2.3: Hams-F12:DMEM media constituents

Once cells had reached 70% confluency they were either utilised for experiments or transferred to 2ml BEGM Freeze Media (Lonza)(Table 2.4) for long-term storage in liquid-N_2.

	Volume (ml) per 7ml BEGM (without RA/GA-1000/Pen/Strep)(Lonza)
DMSO (Sigma-Aldrich)	1
FBS (Sigma-Aldrich)	2

Table 2.4: PBEC Freeze media constituents

2.1.2: Growth of Submerged Monolayer Cultures

25ml of pre-warmed BEGM++ (Table 2.2) was added to a T75 that had been coated with 160µl 2.5mg/ml Collagen I Bovine Protein (Life Technologies (Thermo Fisher Scientific)). Processed PBECs (processed as Section 2.1) were added to the flask and incubated at 37^{o}C/5% CO_2 until 70% confluent with media changes every 1-2 days.

PBECs were washed (x3) with PBS (Lonza) before 650µl of Trypsin-EDTA (Sigma-Aldrich,) was added and flask was incubated at 37^{o}C/5% CO_2 until all the cells had lifted from the plastic. 10ml of MEM++ (Table 2.1)(PAA Laboratories) was added to halt trypsinisation and cells were centrifuged at 1300G for 7 minutes at 4^{o}C. Supernatant was decanted and cells were resuspended in 1ml BEGM++ for counting before being resuspended in an appropriate volume of BEGM++ (Table 2.2) to give a final seeding density of 40,000 cells/ml.

3.8cm^2 (surface area), 12-well plates were coated with 50µl of 2.5mg/ml Collagen I Bovine Protein (Life Technologies (Thermo Fisher Scientific)). 40,000 cells were seeded

in each well before incubation at 37°C/5% CO_2. Media was changed on a daily basis until cells were 60% confluent, wherein they were used for experiments.

2.1.3: Growth of Air-Liquid Interface (ALI) Cultures

25ml of pre-warmed BEGM++ (Table 2.2) was added to a T75 that had been coated with 160µl 2.5mg/ml Collagen I Bovine Protein (Life Technologies (Thermo Fisher Scientific)). Processed PBECs (processed as Section 2.1.1) were added to the flask and incubated at 37°C/5% CO_2 until 80% confluent (~3-5 days) with media changes every 1-2 days.

1.12cm^2 (surface area) 0.4µm (pore-size) transwell inserts (Corning, USA) were pre-coated with 50µl of 0.5mg/ml Collagen I Bovine Protein (Life Technologies (Thermo Fisher Scientific)) and added to 24-well plate. 500µl of BEGM++ (Table 2.2) was added to the basal compartment and plates were incubated at 37°C/5% CO_2 for a minimum of 30 minutes to warm transwells/media.

PBECs were washed (x3) with PBS (Lonza) before 650µl of Trypsin-EDTA (Sigma-Aldrich) was added and flask was incubated at 37°C/5% CO_2 until all the cells had lifted from the plastic. 10ml of MEM++ (Table 2.1)(PAA Laboratories) was added to halt trypsinisation and cells were centrifuged at 1300G for 7 minutes at 4°C. Supernatant was decanted and cells were resuspended in 1ml BEGM++ for counting before being resuspended in an appropriate volume of BEGM++ (Table 2.2) to give a final seeding density of 70,000 cells/200µl. 200µl cells were added to the apical compartments of transwells and plates were incubated at 37°C/5% CO_2 leaving the cultures to grow submerged (with a daily media change) until cells reached 95% confluency (~24-48 hours).

At 95% confluency the cells were taken to air-liquid interface. BEGM++ was removed from both the basal and apical compartments and replaced with 300µl 1x ALI media (Table 2.5)(Lonza). Cells were left to differentiate for 21 days at 37°C/5% CO_2 with media changed on a daily basis.

(a) BEGM for ALI	**Volume (µl) per 50ml BEBM (Lonza)**
Bovine Pituitary Extract (Lonza)	400
Epithelial Growth Factor (Lonza)	100
Insulin (Lonza)	100
Hydrocortisone (Lonza)	100
Transferrin (Lonza)	100
Epinephrine (Lonza)	100
Triiodothyronine (Lonza)	100
1.5mg/ml BSA (Life Technologies)	100

(b) DMEM for ALI	**Volume (ml) per 50ml DMEM (Lonza, Switzerland)**
100x Non-Essential Amino Acids (Life Technologies (Thermo Fisher Scientific)	0.5
10,000 units/ml Pen/ 100,000µg/ml Strep (Sigma-Aldrich)	0.5
100x Sodium Pyruvate (Life Technologies (Thermo Fisher Scientific)	0.5
100x L-glutamine (Life Technologies (Thermo Fisher Scientific)	0.5

(c) 1x ALI media	**Volume (ml)**
BEGM for ALI	25
DMEM for ALI	25

Table 2.5: 1x ALI media constituents. Media in (a) and (b) are composed first before (c).

2.1.3a: Transepithelial Resistance

Transepithelial Resistance (TER) measurement was utilised to assess the ionic permeability of ALI cultures. During air-liquid interface differentiation, TER measurements were taken at days 7, 14 and 21 to assess barrier formation and ensure that the cultures were growing as expected. Basolateral 1x ALI media was removed and replaced with 300µl of fresh 1x ALI media. 100µl of TER media (Table 2.6)(Lonza) was added to the apical surface. Filters were then reincubated for 1 hour at 37^{o}C/5% CO_2 to allow the cultures to normalise before TER was read.

	Volume (ml)
DMEM for ALI (Table 2.5b)	5
BEBM (Lonza)	5

Table 2.6: TER media constituents

basolateral (longer electrode) compartments and voltage was measured by EVOM II Voltage Metre (World Precision Instruments).

After completion of the readings, TER media was removed from the apical compartments and cells were reincubated at 37°C/5% CO_2

2.2: Viral Preparation

2.2.1: HRV-16 Viral Amplification

H1 HeLa cells (ATCC, USA) were added to a T25 flask containing 8ml of pre-warmed MEM++ (Appendix B)(PAA Laboratories). Cells were incubated at 37°C/5% CO_2 with daily media changes until 40% confluency was reached. MEM++ was then removed and HeLa cells were washed (x3) with Infection Media (Table 2.7)(PAA Laboratories) and 0.5ml of Infection Media was added to T25 before cells were reincubated at 37°C/5% CO_2 for 15 minutes.

1ml of a previously prepared HRV-16 stock with a titre of $1.17x10^7$ viral particles/ml (prepared by Dr Emily Wilkinson) was added to H1 HeLas in T25. Flask was placed on a rocker at room temperature for 1 hour to allow for viral adherence to ICAM-1. Post-shaking a further 0.5ml of Infection Media was added to T25 (total volume= 2ml) and placed in incubator at 33°C/5% CO_2 for 12-24 hours until >75% of cells appeared lysed. T25 flask was then freeze-thawed at -80°C/room temperature (x3) before virus-containing supernatant was decanted and spun at 1300G for 7 minutes at 4°C.

This infection cycle was repeated in T75s and T175s containing 60% confluent H1 HeLas under the conditions outlined above until appropriate stock volumes were generated (Infection Media and virus-containing supernatant ratios listed in Table 2.8). Once ample stock had been generated, the virus-containing supernatant was filtered through a 0.22μm filter to remove cellular debris. This stock was then aliquotted and stored in liquid-N_2.

	Volume (ml) per 100ml MEM (PAA Laboratories, UK)
1M HEPES Buffer (Sigma-Aldrich)	1.6
7.5% $NaHCO_3$ (Sigma-Aldrich)	1
Tryptose Phosphate Broth (Sigma-Aldrich)	4
30mM $MgCl_2$	1
100x Non-Essential Amino Acids (Life Technologies (Thermo Fisher Scientific))	1
FBS (Sigma-Aldrich)	2
10,000 units/ml Pen/ 100,000µg/ml Strep (Sigma-Aldrich)	1

Table 2.7: Infection media constituents

Flask Size (for amplification)	**(a) Volume of Infection Media (prior to rocking)**	**(b) Volume of virus-containing supernatant (prior to rocking)**	**Volume of Infection Media (after rocking)**
T75 (First amplification)	1ml	1ml	2ml
T75 (successive amplifications)	Equal volume to (b)	All	Equal volume to (a) + (b)
T175	Equal volume to (b)	All	Equal volume to (a) + (b)

Table 2.8: Conditions for viral amplification

2.2.2: Infective Viral Particle Quantification via Tissue Culture Infective Dose 50% (TCID50)

H1 HeLa cells were grown in MEM++ (Table 2.1)(PAA Laboratories) until 80% confluent. Cells were then trypsinised as previously described and resuspended in an appropriate volume of Infection Media (Table 2.7)(PAA Laboratories) to give a final seeding density of $1.6x10^4$ cells/100µl. 100µl H1 HeLas/well were plated on a 96-well plate and incubated at $37^oC/5\%$ CO_2 for 15-20 minutes whilst viral dilutions were made up.

250µl of newly generated HRV-16 stock was serially diluted in Infection Media to give viral concentrations of 10^{-1} to 10^{-8}. 100µl of each dilution was added to each well of $1.6x10^4$ H1 HeLa cells in the 96-well plate. Plates were incubated in the dark at 37°C/5% CO_2 for 5 days.

After 5 days plates were removed from incubation and 50µl of crystal violet solution (Table 2.9) was added to each well. Plates were left to stain in the dark for 30 minutes. Following this plates were washed (x3) with H_2O and tapped dry. TCID50 was calculated via the Spearman-Karber formula (Formula 1). An average of 3 TCID50s were used to calculate the final infectious viral particle titre of HRV-16 stock ($3.75x10^7$ infectious particle/ml).

$$TCID50 = l - [d(s - 0.5)]$$

$$Where\ l = log10\ highest\ concentration$$
$$d = log10\ of\ difference\ between\ subsequent\ dilutions$$
$$s = \frac{number\ of\ white\ wells}{number\ of\ wells\ per\ row}$$

Formula 1: Spearman-Karber Formula for TCID50 of HRV-16

	Volume (ml)
1x PBS (Lonza)	450
Formaldyhyde (Sigma Aldrich)	5
Ethanol (Sigma Aldrich)	5
	Weight (g)
Crystal Violet (Sigma Aldrich)	0.65

Table 2.9: 0.1% w/v Crystal Violet Solution

2.2.3: Viral Genome Equivalent Quantification

vRNA was extracted from 500ul of viral stock using '*Total RNA Purification*' protocol as outlined in QIAGEN's RNeasy Kit handbook (QIAGEN, Germany). Viral genome equivalent quantification was then assessed using a Reverse Transcriptase mediated quantitive PCR (RT-qPCR) against a commercially available known standard of HRV-16 (Primer Design, UK).

2.5µl of undiluted HRV-16 RNA was used in a Reverse Transcription reaction performed on DNA Engine Tetrad 2 Thermal Cycler (BioRad). Table x and x show the constituents and conditions of the RT-reaction. 2.5µl of the resultant cDNA was utilised in the quantitive PCR (qPCR) performed on 7900HT Fast Realtime PCR System (Applied Biosystems). Table 2.10-2.13 show the constituents and conditions of this PCR reaction. Aside from quantification against a known standard, the HRV-16 cDNA was checked for HRV-1B cross-contamination (Primer Design).

	1x Reaction Volume (µl)
10x RT Buffer (Life Technologies, (Thermo Fisher Scientific), USA)	1.0
100nM dNTP's (Life Technologies, (Thermo Fisher Scientific), USA)	0.4
Random Hexamers (Life Technologies, (Thermo Fisher Scientific), USA)	1.0
50 units/µl Multiscribe (Life Technologies, (Thermo Fisher Scientific), USA)	0.5
20 units/µl RNase Inhibitor(Life Technologies, (Thermo Fisher Scientific), USA)	0.5
RNA	2.5
H_2O	1.6

Table 2.10: Reverse transcription mastermix for HRV-16 quantification

	Temperature (°C)	**Duration (h:m:s)**
Incubation	25	0:30:00
RT (Cycle 1)	37	1:30:00
RT (Cycle 2)	37	0:59:30
Inactivation	85	0:05:00

Table 2.11: Reverse transcription conditions for HRV-16 quantification

	1x Reaction Volume (µl)
2x PCR Mastermix (Life Technologies, (Thermo Fisher Scientific), USA)	5
HRV-1B or HRV-16 Primers (Primer Design, UK)	0.5
RNase Free H_2O	2
cDNA	2.5

Table 2.12: PCR mastermix for HRV-16 quantification

	Temperature (°C)	**Duration (h:m:s)**
Incubation	50	0:02:00
Enzymatic Activation	95	0:10:00
Denaturing (40 Cycles)	95	0:00:15
Annealing/Extension (40 Cycles)	60	0:01:00
Disassociation	95/60/95	0:00:15 (each)

Table 2.13: qPCR conditions for HRV-16 quantification

2.2.4: UV Irradiation of HRV-16 Stock

500µl/well of HRV-16 stock was added to a 12-well plate. This plate was placed in a plastic container with ice ready for UV-irradiation. UV-box was run for 2 minutes prior to addition of HRV-16 containing plate to ensure bulbs were pre-warmed and maximum energy could be applied from the beginning of exposure. HRV-16 plate was then added, removing lid from both the plate and the plastic ice containing container. UV-box was then set to apply 1200J/1 hour to fully irradiate virus.

Following irradiation, a TCID50 assay was carried out to assess infectivity of UV-RV control. H1 HeLa death only occurred at 10^{-1}—likely to be caused by the high numbers of DAMPs found in the irradiated viral stock.

2.3: Viral Infection of PBECs

2.3.1: Viral Infection of Monolayer Cultures

Once monolayers reached 70% confluency BEGM++ culture medium was removed and cells were incubated at 37°C/5% CO_2 for 16-18 hours in Starvation Media (Lonza)(Table 2.14).

	Volume (µl) per 50ml BEBM (Lonza, Switzerland)
500x Insulin-Transferrin-Selenium (Lonza, Switzerland)	100
1.5mg/ml BSA	500

Table 2.14: Starvation media constituents

To infect the cells, 1ml of HRV-16/UV-RV at MOI 2 and MOI 5 (Formula 2) in Starvation Media was added to each well. Cells were placed on a rocker for 1 hour at room temperature before being washed (x3) with HBSS (Lonza). 1ml fresh Starvation Media was then added and cells were incubated for at 37°C/5% CO_2 with RNA and supernatant harvesting 4 hour intervals until 12 hours and 24 hour intervals until hours 72 hours.

$$Volume\ of\ Virus = \frac{(Number\ of cells)xMOI}{TCID50}$$

Formula 2: Volume of virus required to infect cultures

2.3.2: Viral Infection of ALI Cultures

ALI cultures were differentiated as per normal over the first 21 days. On day 22, 1x ALI media (Table 2.5)(Lonza) was removed from basal compartment and replaced with 300µl of Starvation Medium (Lonza)(Table 2.14) and the cells were incubated for 18-24 hours. Following starvation TER was carried out as in Section 2.1.3a. Following TER, media was removed from both apical and basal surfaces and replaced with 300µl Starvation Media in the basal compartment and 200µl of HRV-16/UV-RV at MOI 1 (Formula 2) in Infection Media apically. Cells were left to infect at 37^{o}C/5% CO_2 for 6 hours. Basal media was removed and replaced with 300µl of infection media. Apical media was also removed with transwells being washed (x3) with HBSS (Lonza) before 200µl of fresh Infection Media was added to the apical surface. Cells were incubated at 37^{o}C/5% CO_2 with cell-free supernatants and RNA harvested at each 24 hour interval until 72 hours post-infection.

2.3.3: Cell-free Supernatant Harvesting

Supernatants were removed from cell surface using a long nosed pipette and supernatants from repeated conditions were pooled. Supernatants were spun at 7000RPM for 5 minutes at 4^{o}C to pellet any shed cells. Supernatants were then aliquotted and stored at -20^{o}C for future use. Any cellular debris was added back into wells for RNA harvesting.

2.3.4: RNA Harvesting

600µl of QIAzol Lysis Reagent (QIAGEN) was added to each well/filter and left to stand for 2-3 minutes at room temperature. Cells were then further lysed physically using a 'rubber policeman'. RNA lysates in QIAzol were stored at -80^{o}C until total RNA could be extracted using the Qiagen miRNeasy kit (QIAGEN) following the '*Extracting total RNA from human/animal cells*' protocol in the handbook with the following modifications:

- 20µl of Chloroform added per 100µl of QIAzol (120µl)
- Elution volume of 50µl H_2O
- Prior to final RNA elution step, columns left to stand for 2-3 minutes

2.4: Interferon Treatment of ALI Cultures

2.4.1: IFN Treatment During 21 Day Differentiation

Cells were grown and seeded on transwells as outlined in Section 2.1.3. Once cells were seeded on filters, they were grown as a submerged culture until 95% confluency was obtained. Once cultures reached this confluency an air-liquid interface was established via removal of apical media and 1x ALI media (Table 2.5) being utilised opposed to BEGM++. Cells were incubated at 37°C/5% CO_2 at this air-liquid interface for 24 hours prior to IFN treatment.

For IFN treatment, 1x ALI media was removed and replaced with 300µl basolateral 1x ALI media which either contained no interferon (untreated) or 1ng/ml of IFN-λ1 (Peprotech, USA)(IFN-λ treated). Cells were subsequently left to differentiate at 37°C/5% CO_2 for 21 days with daily media and IFN-treatment carried out.

TER of these cultures were measured every other day. Supernatants, RNA and protein were harvested at day 7, 14 and 21. FITC 4kD Dextran and cell count measurements were additionally taken at day 7, 14 and 21.

2.4.1a: FITC 4kD Dextran

FITC 4kD Dextran (Sigma-Aldrich) measurement was used to assess the macromolecular permeability of ALI cultures in response to IFN treatments.

1 hour prior to beginning the experiment, basolateral 1x ALI media was removed and replaced with 900µl TER media (Table 2.6)(Lonza, Switzerland). 250µl of TER media was added apically before cells were incubated for 1 hour at 37°C/5% CO_2

FITC 4kD Dextran was diluted in TER media and 100µl was added apically to each filter to give a final total of 2mg/ml of FITC 4kD Dextran. Filters were reincubated for 3 hours at 37°C/5% CO_2. After incubation 100µl of apical media (in duplicate) was removed and 100µl of basolateral media (in triplicate) were added to a black 96-well plate (Corning) and measured on a microplate reader with excitation of 490nm and emission readings at 520nm.

2.4.1b: Cell Counting

FITC 4kD Dextran was removed from filters and filters were washed three times with 300µl of PBS (Lonza) to fully remove FITC molecules. 150µl of Trypsin-EDTA (Sigma-Aldrich) was added apically to each filter and cells were incubated at 37°C/5% CO_2 until cells detached (between ~3-7 minutes).

850µl of MEM++ (Table 2.1) was added to each filter to halt trypsinisation. 2µl of DNAse was added to each filter to prevent cellular aggregation. Cells were spun at 700RPM for 5 minutes at 4°C. Supernatant was decanted and cells were resuspended in a further 1ml MEM++ (Table 2.1). 20µl of the cell suspension was removed and counted on a haemocytometer.

2.4.1c: Cell-free Supernatant Harvesting

Cell free supernatant was harvested as described in Section 2.3.3

2.4.1d: RNA Harvesting

RNA was harvested as described in Section 2.3.4

2.4.1e: Protein Harvesting

Protease Inhibitor Cocktail (Sigma-Aldrich) was added to Sample Buffer (Table 2.15)and heated at 95°C for 5 minutes. 100µl of heated Sample Buffer was added to each transwell filter and physical lysis was carried out. Lysates from filters of the same condition were pooled in a 1.5ml eppendorf tube before lysates were heated at 95°C for 5 minutes. Samples were allowed to cool to room temperature and then spun at 13,200RPM for 5 minutes. Lysates were then aliquotted for use in Western Blotting.

	Volume (ml)
ddH_2O	9.0
0.5M Tris (pH 6.8)	3.0
Glycerol (Sigma-Aldrich)	2.4
10% SDS (Thermo Fisher Scientific)	9.6
1M DTT (Sigma-Aldrich)	24µl

Table 2.15: Sample Buffer

2.4.2: IFN Treatment Post 21 Day Differentiation

Cells were cultured for 21 days at Air Liquid Interface as described in Section 2.1.3. After 21 days cells were treated with IFN-λ.

1x ALI media was removed from the basolateral compartment and replaced with 300µl of 1x ALI media which either contained no interferon (untreated) or 0.5ng/ml of IFN-λ1 (Peprotech)(IFN-λ1 treated), Cells were reincubated at 37°C/5% CO_2 for three days with daily media/IFN-treatment being carried out.

TER of the cultures were measured at 24, 48 and 72 hours post-treatments. RNA, protein and supernatants were also harvested at these three time points using the methodologies described in Sections 2.3.3 (cell-free supernatant), 2.3.4 (RNA) and 2.4.1e (protein).

2.5: Quantification of MicroRNA

MicroRNA Quantification was conducted using specific microRNA RT-qPCR assays designed by Life Technologies (Life Technologies (Thermo Fisher Scientific)).

RT reactions for each microRNA were carried out using 1µl of 10ng/µl of extracted RNA for replication alongside a small, specific stem loop primer of the microRNAs of choice (Figure 2.1) performed on DNA Engine Tetrad 2 Thermal Cycler (BioRad). In this reaction the stem-loop primer annealed to the mature microRNA in a highly specific manner (95-100% specificity to target miRNA) and 3' to 5' cDNA was synthesised. The resulting cDNA product had one strand which contains the original 22-25nt mature miRNA and a synthesised copy strand which had a 22-25nt region complementary to the mature miRNA as well as the stem loop primer structure of approximately 40nt (Figure 2.1)(Table 2.16-17).

0.7µl of the resultant cDNA was utilised in the qPCR reaction (Table 2.18-19) performed on 7900HT Fast Realtime PCR System (Applied Biosystems). During the denaturation phase of qPCR the stem loop structure of the cDNA was removed (the mechanism of which has not been disclosed by the manufacturer) leading to the formation of a 60nt mature microRNA product for the qPCR primers to anneal and amplify from. The forward primer was specific for the naturally occurring mature microRNA and amplified from this cDNA template strand. The reverse primer was specific for the RT-extended microRNA region and amplified from this strand. Further reaction specificity was provided by

TaqMan probes which anneal specifically at the cusp between the artificial 40nt sequence from the RT reaction and the mature microRNA.

MicroRNAs-23a, 200b, 200c and 429 were analysed utilising this RT-qPCR assay. RNU-44 and miR-1275 were utilised as internal controls for normalisation of the data to allow the utilisation of the Comparative Ct method (ΔΔCt) of analysis. RNU-44 is a small, highly-stable, nuclear non-coding RNA that is expressed at equal abundance across all tissue/cell types and is therefore commonly used as a microRNA normaliser. Previous microarray data obtained in the laboratory (Loxham, Collins- Unpublished) indicates that miR-1275 is expressed at high levels and shows a high stability in a number of cells which made it a good candidate for a control microRNA.

RT-qPCR data was extracted by SDS 2.3 (Applied Biosystems) with threshold values set to 0.1Ct for analysis. Data was analysed using ΔΔCt method.

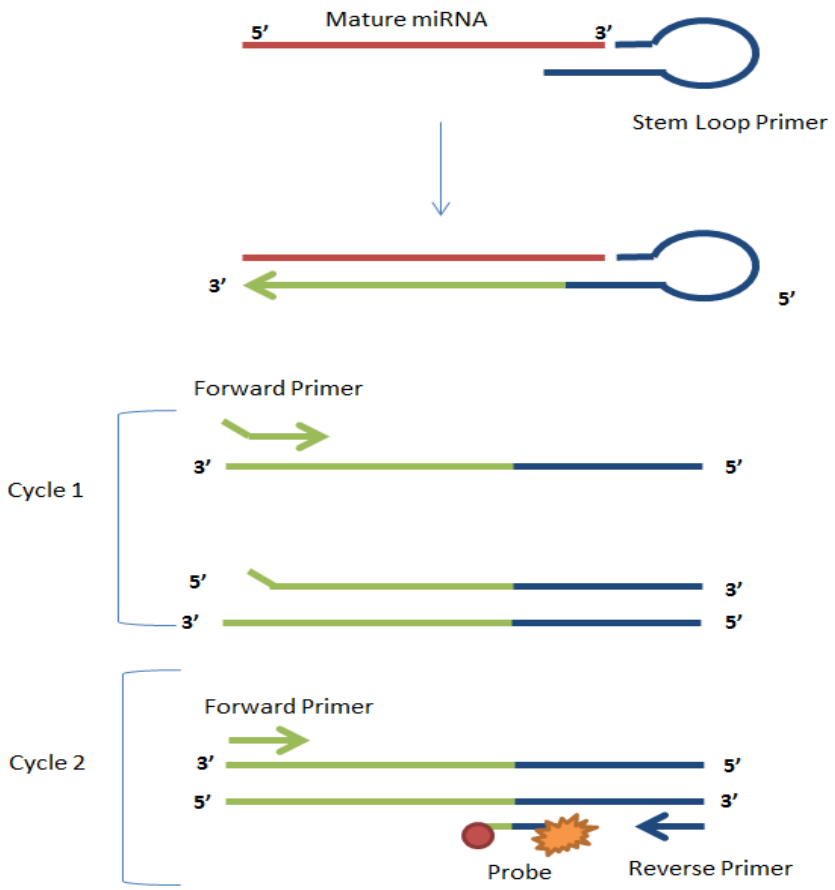

Figure 2.1: Diagrammatic representation microRNA RT-qPCR reaction process

	1x Reaction Volume (µl)
10x RT Buffer (Life Technologies, (Thermo Fisher Scientific), USA)	0.75
100nM dNTP's (Life Technologies, (Thermo Fisher Scientific), USA)	0.08
5x Primers (Life Technologies, (Thermo Fisher Scientific), USA)	1.5
50 units/µl Multiscribe (Life Technologies, (Thermo Fisher Scientific), USA)	0.5
20 units/µl RNase Inhibitor(Life Technologies, (Thermo Fisher Scientific), USA)	0.1
10ng/µl RNA	1.0
H_2O	3.575

Table 2.16: Reverse transcription mastermix for microRNA quantification

	Temperature (°C)	**Duration (h:m:s)**
Incubation	16	0:30:00
RT (Cycle 1)	42	0:30:00
Inactivation	85	0:05:00

Table 2.17: Reverse transcription conditions for microRNA quantification

	1x Reaction Volume (µl)
2x PCR Mastermix (Life Technologies, (Thermo Fisher Scientific), USA)	5
Primers (Life Technologies (Thermo Fisher Scientific), USA)	0.5
RNase Free H_2O	3.8
cDNA	0.7

Table 2.18: PCR mastermix for microRNA quantification

	Temperature (°C)	Duration (h:m:s)
Incubation	50	0:02:00
Enzymatic Activation	95	0:10:00
Denaturing (40 Cycles)	95	0:00:15
Annealing/Extension (40 Cycles)	60	0:01:00
Disassociation	95/60/95	0:00:15 (each)

Table 2.19: PCR conditions for microRNA quantification

2.6: Quantification of mRNA

Extracted RNA samples were diluted in dH_2O to a final concentration of 30.3ng/µl. 6.6µl of this RNA was utilised in the RT-PCR as the template for the random hexamers to amplify from (Table 2.20-21). RT-PCR performed on DNA Engine Tetrad 2 Thermal Cycler (BioRad).

Resultant cDNA was diluted 1:10 with dH_2O and utilised in a Taqman qPCR for relative mRNA expression against primers specific for the gene of interest. This was performed on 7900HT Fast Realtime PCR System (Applied Biosystems). GAPDH was selected as the 'housekeeping' internal control as its' expression remains fairly constant within cells derived from the same patient (Table 2.22-24).

RT-qPCR data was extracted by SDS 2.3 (Applied Biosystems) with threshold values set to 0.2Ct for analysis. Data was analysed using ΔΔCt method.

	1x Reaction Volume (µl)
10x RT Buffer (Life Technologies, (Thermo Fisher Scientific), USA)	1.0
100nM dNTP's (Life Technologies, (Thermo Fisher Scientific), USA)	0.4
Random Hexamers (Life Technologies, (Thermo Fisher Scientific), USA)	1.0
50 units/µl Multiscribe (Life Technologies, (Thermo Fisher Scientific), USA)	0.5
20 units/µl RNase Inhibitor(Life Technologies, (Thermo Fisher Scientific), USA)	0.5
30.3ng/µl RNA	6.6

Table 2.20: Reverse transcription mastermix for mRNA quantification

	Temperature (°C)	**Duration (h:m:s)**
Incubation	25	0:30:00
RT (Cycle 1)	37	1:30:00
RT (Cycle 2)	37	0:59:30
Inactivation	85	0:05:00

Table 2.21: Reverse transcription conditions for mRNA quantification

	1x Reaction Volume (µl)
2x PCR Mastermix (Life Technologies, (Thermo Fisher Scientific), USA)	5
HRV-1B or HRV-16 Primers (Primer Design, UK)	0.5
RNase Free H_2O	2
cDNA	2.5

Table 2.22: PCR mastermix for mRNA quantification

	Temperature (°C)	Duration (h:m:s)
Incubation	50	0:02:00
Enzymatic Activation	95	0:10:00
Denaturing (40 Cycles)	95	0:00:15
Annealing/Extension (40 Cycles)	60	0:01:00
Disassociation	95/60/95	0:00:15 (each)

Table 2.23: PCR conditions for mRNA quantification

2.7: Protein Quantification

2.7.1: Protein Quantification in Cell-free Supernatants via ELISA

Antibody mediated Enzyme Linked Immunosorbent Assays (ELISA) were utilised to quantify protein levels of IFN-λ1 released in response to HRV-16 infection of PBEC monolayers and ALI cultures. A 96-well plate is firstly coated with a capture antibody which is specific to the target protein. Upon addition of supernatant, the capture antibody will bind any of its' target and upon washing, all proteins bar the one of interest can be removed. A HRP-linked detection antibody is then added which will bind to antibody-antigen. Addition of the stop solution allows quantification of the protein of interest via a blue to yellow colour change, caused by the oxidisation reaction of 3,3',5',5'-Tetramethylbenzidine.

IFN-λ1 ELISA (R&D Systems, USA): Mouse, anti-human IFN-λ1 capture antibody was diluted to a working concentration of 4.0µg/ml in PBS (Lonza, Switzerland) and plate was coated with 100µl/well of capture antibody. Plate was left to coat overnight at room temperature on a rocker. Plate was washed (x3) with 0.05% Tween-20 in PBS (wash buffer). 300µl/well of reagent diluent (R&D Systems, USA) was added and left at room temperature for 1 hour to fully block plates. Plates were washed (x3) with wash buffer. A 7 point standard curve (4,000 pg/ml to 62.5 pg/ml) of recombinant human IFN-λ1 was made up in reagent diluent. 100µl of standard curve/undiluted supernatant was added to wells and the plate was left to incubate on a rocker at room temperature for 2 hours. Plates were once again washed (x3) with wash buffer before 100µl/well working

concentration (400ng/ml) of mouse, anti-human IFN-λ1 detection antibody was added. Plates were incubated for a further 2 hours on a rocker at room temperature. Plates were washed (x3) with wash buffer before 100µl/well of Streptavidin-HRP (diluted to 1:200 working concentration with reagent diluent) added. Plates were incubated for 20 minutes in the dark at room temperature. Plates were washed (x3) with wash buffer and 100µl/well of substrate solution (R&D Systems, USA)(1:1 mixture of H_2O_2 and tetramethylbenzidine) was added before a further 20 minute incubation in the dark was conducted. 50µl of stop solution (2N H_2SO_4) was added (R&D Systems, USA) and plates were tapped gently to mix before being read.

All plate readings were carried out using a Dynatech MR7000 plate reader set at 450nm wavelength with 570nm corrections applied.

2.7.2: Protein Quantification in Cells via Western Blotting

2.7.2a: Bicinichonic Acid (BCA) Assay

A BCA assay was first carried out to determine the concentration of the protein in the cell lysates utilising a colourmetric detection method. The peptide bonds in the protein reduce Cu^{2+} ions from the Copper II Sulphate Pentahydrate in the BCA Protein Assay Reagents to Cu^{+}. Bicinichonic acid in the BCA Protein Assay Reagent will then chelate with the Cu^{+} ions to form the purple colouration which is then measured.

A 7 point standard curve of a known concentration of Bovine Serum Albumin from 2mg/ml was made up in H_2O and 20µl was added to a 96-well clear plate in duplicate. Unknown protein samples were thawed on ice before being diluted 1:5 and 1:10 with H_2O to ensure protein concentration would fall on standard curve. 20µl of each unknown sample was added to the 96-well plate in duplicate and plate was placed on ice until the working BCA reagent was made up. Working BCA Reagent was made through the addition of 50 parts of Pierce BCA Protein Assay Reagent A (Life Technologies (Thermo Scientific), USA) to 1 part of Pierce BCA Protein Assay Reagent B (Life Technologies (Thermo Scientific), USA). 200µl of Working BCA Reagent was added to each well before the plate was gently agitated to mix the solutions and then incubated at 37^{o}C for 30 minutes. After incubation, the plate was read on a Dynatech MR7000 plate reader set at 570nm wavelength and protein concentration was determined.

2.7.2b: Polyacrylamide gel electrophoresis (PAGE)

Protein samples were thawed on ice before being diluted further in sample buffer to give a final concentration of 16µg of protein across all samples. Protein samples were then heated at 95°C for 3 minutes to fully redissolve SDS and denature proteins in the sample. 5µl of Bromophenol Blue was added to 50µl DTT (Sigma-Aldrich, USA) and 1µl per 10µl protein sample was added to the sample. Protein sample was pulse spun before loading on to a 7.5%/10% Stain Free Mini-Protean TGX Gel (BioRad, UK) alongside a high molecular weight ladder (Thermofisher Scientific, USA). PAGE was peformed at 120V in Running Buffer (Table 2.24) for 1 hour and 30 minutes to ensure full resolution of all proteins within the sample.

	1x 1L ddH_2O
0.025M Tris Base (w/v) (Thermo Fisher Scientific, USA)	3.03g
0.192M Glycine (Thermo Fisher Scientific, USA)	14.41g
0.1% SDS (Thermo Fisher Scientific, USA)	1.00g

Table 2.24: 1x Running Buffer for western blot (pH 8.3)

2.7.2c: Transferring the Gel

Gels were transferred to a membrane utilising the semi-dry, fast transfer set-up developed by BioRad (BioRad UK).

Already assembled PDVF Mini-Transfer kits (BioRad, UK) were removed from 4°C and assembled directly in to the Trans-Blot Turbo Transfer system's cassette (BioRad, UK). Components labelled 'bottom' (3x pre-soaked filter papers, activated PDVF-membrane) were placed on the anode of the cassette before addition of the gel and 'top' components (3x pre-soaked filter papers) were added towards the cathode. This completed the Mini-Transfer Kit assembly.

The cassette was then sealed and placed into the Trans-Blot Turbo Transfer system's base unit and run on pre-defined BioRad parameters based on Mw of target proteins:

- Mid-Mw Proteins (e.g. OCLN): 25V, 1.3A, 7 minutes

- High Mw Proteins (e.g. ZEB1): 25V, 1.3A, 10 minutes
  (N.B: Times noted here for 1x Mini Gel Transfer)

Following the blotting procedure, the sandwich was disassembled and the membrane was dried at room temperature on blotting paper for 1 hour. The membrane was then sealed in a pocket and stored at 4^{o}C until ready to be probed.

2.7.2d: Detecting Protein

Protein ladders were cut away from the membrane and sealed in a separate pouch for use to quantify proteins after detection. The remaining lanes of the membrane were sealed into a pouch containing Blocking Buffer (Table 2.25) and placed on a rocker at room temperature for 1 hour.

	1x
ECL Blocking Powder (GE Healthcare)	1.6g
Wash Buffer (Table 2.27)	Make up to 80ml

Table 2.25: 1x Blocking Buffer for western blot

	1x
0.137M NaCl (w/v) (Thermo Fisher Scientific)	8.01g
0.020M Tris (Thermo Fisher Scientific)	2.42g

Table 2.26: 1x TBS for western blot

	Volume for 1x
TBS	1.0l
Tween-20	1.0ml

Table 2.27: 1x Wash Buffer for western blot

The membrane was washed for five minutes in Wash Buffer (Table 2.27) three times before a final 15 minute prolonged wash. The membrane was transferred to a pouch containing primary antibody, which was diluted in Blocking Buffer as in Table 2.25 and placed on a rocker at room temperature overnight.

Following incubation with primary antibody, the membrane was washed as before (3x 5 minutes; 1x 15 minutes) before being incubated on a rocker for 1 hour with its'

corresponding HRP-linked secondary antibody diluted in Blocking Buffer (Table 2.28). The membrane was then immediately developed through addition of a 1:1 ratio of Developing Solution A and Developing Solution B (GE Healthcare, UK) which was then imaged through Chemiluminescence on a ChemiDoc Imaging system (BioRad, UK).

Primary Antibody	**Dilution**	**Secondary Antibody**	**Dilution**
Anti-ZEB1 Rabbit mAb (Cell Signalling Technologies)	1:1000	HRP-linked anti-Rabbit from Donkey (GE Healthcare, UK)	1:2000
Anti-A20 Rabbit pAb (Cell Signalling Technologies)	1:1500	HRP-linked anti-Rabbit from Donkey (GE Healthcare, UK)	1:2000
Anti-Occludin mAb (Invitrogen)	1:500	HRP-linked anti-Rabbit from Donkey (GE Healthcare, UK)	1:2000
Anti-E-cadherin mAb (Invitrogen)	1:1000	HRP-linked anti-Rabbit from Donkey (GE Healthcare, UK)	1:2000
Anti-Actin HRP-linked mAb (Abcam)	1:5000	N/A	

Table 2.28: Primary and secondary antibodies and dilution for western blotting

If the membrane was to be probed again for another protein, the membrane was stripped through addition of Stripping Buffer (Table 2.26) and incubation at 55^{o}C for 25 minutes. The membrane was then allowed to cool to room temperature for 5 minutes before being washed (3x 5 minutes; 1x 15 minutes) in Wash Buffer (Table 2.29). The membrane was then blocked and probed as before.

	1x 99.3ml ddH_2O
Tris-HCl (Thermo Fisher Scientific)	0.985g
SDS (Thermo Fisher Scientific)	2.00g
B-Mercaptoethanol (Sigma-Aldrich)	Addition of 0.7ml to Stripping Buffer just before use

Table 2.29: 1x Stripping Buffer for western blot

2.8: Staining and Confocal Microscopy

2.8.2a: Cell Fixation

Prior to staining, cells on transwell filters were fixed. The organic solvent methodology utilised here both provides a 'fix' to structural integrity through cellular dehydration caused by addition of ice-cold Methanol and makes cells permeable to staining antibodies through addition of ice-cold Acetone. In addition the organic solvent methodology leads to precipitation of proteins associated with cell architecture.

Transwells were placed in to a new 24-well plate before being gently washed on both basolateral and apical surfaces (x3) using 4^{o}C PBS. Following washes, 700µl of ice-cold 1:1 Acetone:Methanol was added to the basolateral compartment and a further 200µl added apically. Transwells were then incubated at -20^{o}C for 20 minutes to ensure complete cellular dehydration and protein precipitation of specimens. Following incubation, both apical and basolateral fixative was removed from Transwells and samples were once again washed on both surfaces (x3) with 4^{o}C PBS. This process was repeated x3. Transwells were then stored at 4^{o}C, submerged in PBS for 24 hours prior to staining.

2.8.2b: Filter Preparation

Following 24 hour storage, Transwells were removed from 4^{o}C and allowed to warm to room temperature. Transwells were processed one at a time to ensure cells did not dry out or become damaged during filter preparation procedure.

Basolateral PBS was removed using a pasture pipette before removal of apical PBS—with great care being taken not to touch/damage the cells. The Transwell was then removed from the plate and inverted. Using a sharp scalpel, the filters were cut away from the plastic support. Removed filters were then placed carefully on to a microscope slide and if necessary were carefully flattened. Using a hydrophobic pen, a ring was marked around

the filter to ensure subsequent material 'domed' over the target sample. PBS was added to each filter to ensure they stayed moist whilst other filters were prepared.

2.8.2c: Staining

After all filters were prepared, PBS was removed from cells. Each cell was blocked for 30 minutes in the dark with 100µl 5% Goat-Serum (Invitrogen, UK) and 1% BSA (Invitrogen, UK) in PBS. After blocking, 100µl of primary antibody diluted in 1% BSA (in PBS) was added to each filter in concentrations outlined in Table x. Filters were incubated for 2 hours in the dark. Filters were then washed for 5 minutes in PBS three times before addition of 100µl of secondary antibody diluted in 1% BSA in PBS as in Table 2.30. Filters were incubated for 1 hour in the dark before another PBS wash step to fully remove secondary antibody from the filters. A 1:500 dilution of 1mg/ml DAPI (Sigma-Aldrich) was used as the nuclear counterstain and added to filters for 15 minutes incubation in the dark. Filters were once again washed (x3) with PBS to remove excess DAPI before Mowiol mountant was added to the filter and coverslip was affixed. Slides were stored at 4^{o}C in the dark until ready to photograph/image on a Leica SP8 Confocal microscope in the Biomedical Imaging Unit at Southampton General Hospital.

Primary Antibody	Dilution	Secondary Antibody	Dilution
Anti-Occludin mouse mAb (Invitrogen)	1:250	Anti-mouse Alexafluor-488 from Goat	1:1000
Anti-E-cadherin mouse mAb (Invitrogen)	1:100	Anti-mouse Alexafluor-488 from Goat	1:1000

Table 2.30: Primary and secondary antibodies and dilution for immunofluorescent staining

2.9: Statistical Analysis

Data collected was subjected to statistical analysis utilising GraphPad Prism (Version 6.2) software. All data sets were assessed using paired statistical analysis to compare untreated (control) conditions against treated conditions to allow examination of whether the observed difference was large enough to suggest a response to applied stimulus. This, however, made the presumption that untreated and treated samples

behaved identically at baseline. Wilcoxon signed rank tests were utilised where possible (>n=4) as data was liable not to be normally distributed due to inter-patient variability. Paired t-tests were used in situations where <n=4 thus could not be assessed using non-parametric statistical analyses.

CHAPTER THREE: *In silico* prediction of miRNA binding sites in 3'UTRs of putative mRNA targets

3.1: Introduction

The epithelial barrier and innate immune responses are both altered in response to RV infection(Tosi 2005, Takaoka and Yanai 2006, Sajjan, Wang et al. 2008). In addition to paracellular/ionic barrier effects, HRV infection cause higher levels of proinflammatory cytokine release—such as IL-6, IL-8 and IL-13—and significant elevation of type I and III IFN release. From the current literature, it could be possible that alterations of microRNA in response to infection could be responsible for these changes in the airway epithelium (see introduction in Chapter 1). In addition to this, it has been well characterised that individuals with asthma present with an impaired epithelial barrier prior to infection (de Boer, Sharma et al. 2008, Yeo and Jang 2010, Xiao, Puddicombe et al. 2011) as well as impaired innate immune responses to virus (Wark, Johnston et al. 2005, Contoli, Message et al. 2006, Bullens, Decraene et al. 2008)—which could be attributed to differential miRNA responses/expression and thus explain why viral infection in these individuals is more problematic than experienced in healthy cohorts.

Previous studies in the group had confirmed that TNF-α ± TGF-β induced barrier dysregulation, in colonic and renal epithelia, correlated with differential expression of a number of microRNAs, including the miR-200 family (miR-200b, -200c and -429) (Dingley, Collins - personal communication). It was therefore decided to focus on these microRNAs for successive investigation. MicroRNAs are ssRNA molecules of 21-25 nucleotides in length that act postrancriptionally to influence protein expression utilising specific ~7-8 nucleotide seed-sequences which allow them to target—and potentially bind to—several different 3'UTRs (Doench and Sharp 2004, Krol, Loedige et al. 2010) to promote mRNA degradation or reduce the rate of protein translation (Eulalio, Huntzinger et al. 2008). Currently there were multiple online resources for prediction of microRNA targets including (but not limited to): TargetScan.org, miRBase.org and microRNA.org. Utilising these prediction tools, the microRNA of interests were to be investigated to highlight whether there were potential biologically relevant seed-sequences in mRNAs

that could contribute to the innate immune responses and epithelial barrier changes observed in response to viral infection.

3.2: Hypothesis, Aims and Objectives

It is hypothesised that miR-23a and the miR-200 family (miR-200b, -200c, -429) have predicted mRNA targets that are involved in regulation of the innate immune response and maintenance of epithelial barrier integrity.

Aim: To identify a number of mRNAs that are implicated in epithelial barrier and innate immune responses and have a predicted seed sequence for the specific miRNA's in their 3'UTR.

Objective(s):

- To use a range of online bioinformatic prediction tools (miRBase, TargetScan and MicroRNA.org) to identify potential mRNA targets of miR-23a, -200b, -200c and -429.
- Assess efficacy of bioinformatic predictions will be assessed to identify mRNAs of interest for further experimental validation.

3.3: *In Silico* prediction Methodology

As briefly mentioned above (Section 3.2) there are multiple online resources for the identification of potential microRNA binding sites in the 3'UTR of mRNA. Each database emphasises different miRNA characteristics to further assess the likelihood of microRNA targeting, binding and eventual effect. TargetScan.org primarily emphasises seed sequence complementarity alongside sequence conservation throughout vertebrates—with the assumption that conserved sequences are more likely to be physiologically relevant. MiRBase.org emphasises structural observations of 3'UTR/mRNA and compares against previously published data to assess potential binding. MicroRNA.org is one of the more comprehensive databases as it utilises a miRanda algorithm to attribute a miSVR score (Betel, Wilson et al. 2008). This miSVR score is a numerical value assigned to rank efficacy of prediction based on combined inputs from: Literature data, miRNA conservation within vertebrates, expression profiles (in human, rat and mice tissues/cells), seed complementarity, downstream complementarity and free energy (Peterson, Thompson et al. 2014).

As the microRNA.org is the only prediction software to utilise this miRanda algorithm, it was determined to be the most preferential prediction tool. This is because the generated mirSVR score more comprehensively reflects the likelihood of binding due to the variety of characteristics it is developed off (Betel, Wilson et al. 2008) whilst also remaining user friendly. It is known that the seed sequence determines miRNA binding to the 3'UTR, but stability of this binding and subsequent miRNA-induced effect is reliant on whether the binding is stable. Binding stability is determined by further sequence complementarity between miRNA and 3'UTR, accessibility of seed/mRNA for binding (effected by conformational shape) and free energy— characteristics that are not considered by other *in silico* prediction tools. The miRanda algorithm has been programmed to take these multiple factors in to account and thus has been shown to identify miRNA binding sites that are non-canonical and non-conserved but pull-down assays have identified miRNA:mRNA binding (Betel, Koppal et al. 2010). With this knowledge, microRNA.org was utilised as the primary prediction software for this *in silico* investigation. Additional cross-referencing with TargetScan.org and miRBase.org was carried out to compare databases and further corroborate sites (Peterson, Thompson et al. 2014).

3.4: Results

MirSVR scores generated by the miRanda algorithm suggests the predicted log-fold downregulation of the target in response to microRNA binding. The closer a mirSVR score is to 0—the more likely the microRNA:mRNA binding has no meaningful physiological downregulation, which is suggested to indicate no *in vivo* binding. Conversely the closer to -2.0 a mirSVR score is the more probable the miR:mRNA binding has physiological impact *in vivo* (Betel, Koppal et al. 2010).

Total culminative mirSVR scores are also shown in the microRNA.org database on the initial miRNA search page. These culminative scores add mirSVR scores of each binding site together (for microRNAs with multiple binding sites in a 3'UTR) to assign a numerical value of meaningful physiological downregulation of binding microRNAs in total. This culminative mirSVR score assumes all binding sites are bound to simultaneously.

3.4.1: miR-200b

The highest mirSVR scores in MiR-200b are predicted in ZEB2 (-6.73) and ZEB1 (-5.40) 3'UTRs. This high mirSVR score indicates that it is increasingly likely that the miRNA has

an effect on ZEB1/2 expression (Peterson, Thompson et al. 2014). These zinc-finger E-box binding homeobox proteins are transcription factors that have previously been implicated in the regulation of EMT via repression of E-cadherin transcription (Bolos, Peinado et al. 2003). MiR-200b has 6 predicted binding sites in the 3'UTR of ZEB2—all of which are thought to be highly conserved throughout vertebrates. These binding sites have varying upstream bp complementarity and hence have different binding stabilities. The most stable predicted of these miR-200b:ZEB2 binding sites has a 7bp complementarity and presents with an individual mirSVR score of -1.2704. There are 5 predicted binding sites for miR-200b in the 3'UTR of ZEB1 on microRNA.org and cross-comparison with TargetScan.org confirms that all five of these sites are conserved amongst vertebrates thus likely to have physiological consequences. The strongest of these has 7bp complementarity and has a mirSVR score of -1.3201. MiR-200b may also modulate TJ stability as there is a predicted miRNA binding site in the 3'UTR of occludin (Schneeberger and Lynch 2004, Anderson and Van Itallie 2009, Van Itallie and Anderson 2014). This predicted site has a mirSVR score of -1.041 with a 5bp complementarity between the microRNA and 3'UTR suggesting stable binding properties and in addition, TargetScan identifies conservation of this site throughout vertebrates. MiR-200b may also be able to modulate innate immune responses due to a predicted seed-sequence on the 3'UTR of TNFAIP3/A20—a negative regulator of NF-κB activation (Parvatiyar and Harhaj 2011). Cross-comparison with TargetScan.org shows that this predicted site is not well conserved throughout all vertebrates. In microRNA.org, the predicted site has 6bp of additional complementarity upstream from the seed sequence suggesting fairly stable binding but the higher mirSVR score of -0.1820 suggests that it has less 'favourable' characteristics to facilitate miRNA:mRNA binding and subsequent effect—thus it may be less physiologically relevant. MiR-200b also has a seed sequence in the 3'UTR of some key antiviral proteins such as Viperin (RSAD2)(Levy and Garcia-Sastre 2001). There is a 9bp complementarity between miR-200b:RSAD2 3'UTR which suggests a stable binding, but the low mirSVR score (-0.3632) predicts a low physiological effect which is further supported by the lack of microRNA binding site conservation throughout vertebrate families (Figure 3.1).

3' aguaguAAU-GGUCCGUCAUAAu 5' hsa-miR-200b ||| |: ||||||| 354:5' auuguuUUAUCUUAUCAGUAUUa 3' ZEB1	mirSVR score: -1.2158 PhastCons score: 0.6164
3' aguaguaaugguccGUCAUAAu 5' hsa-miR-200b ||||||| 449:5' ugcuaaauccgcuuCAGUAUUu 3' ZEB1	mirSVR score: -1.1860 PhastCons score: 0.7176
3' aguaGUAAUGGUCCGUCAUAAu 5' hsa-miR-200b |||| |: ||||||| 881:5' gugcCAUUUCU---CAGUAUUu 3' ZEB1	mirSVR score: -0.7855 PhastCons score: 0.7703
3' agUAGUAAUGGUCCGUCAUAAu 5' hsa-miR-200b ||: ||||| ||||||| 1229:5' ugAUUUUUACCUAUCAGUAUUa 3' ZEB1	mirSVR score: -1.3201 PhastCons score: 0.7906
3' aguAGUAAUGGUCCGUCAUAAu 5' hsa-miR-200b ||| ||| ||||||||| 1300:5' ucuUCA-AACCUGGCAGUAUUa 3' ZEB1	mirSVR score: -0.8914 PhastCons score: 0.8099
3' aguAGUAAUGGUCCGUCAUAAu 5' hsa-miR-200b |:|||| :| |||||| 1847:5' uacUUAUUA-UAAAAAGUAUUu 3' TNFAIP3	mirSVR score: -0.1820 PhastCons score: 0.7007
3' aguAGUAAUGGUCCGUCAUAAu 5' hsa-miR-200b |:| |:|| ||||||| 126:5' gcuUUAACAUCA-UCAGUAUUg 3' OCLN	mirSVR score: -1.0410 PhastCons score: 0.5867
3' aguAGUAA--UG-GUCCGUCAUAAu 5' hsa-miR-200b ||||| || || ||||||| 483:5' uguUCAUUUGACAGAGUCAGUAUUu 3' RSAD2	mirSVR score: -0.3632 PhastCons score: 0.5214

Figure 3.1: ***In silico*** **miR-200b binding predictions for ZEB1, TNFAIP3/A20, occludin (OCLN) and viperin (RSAD2)**

3.4.2: miR-200c

As with miR-200b, miR-200c's highest mirSVR scores belong to ZEB2 and ZEB1 with -6.73 and -5.39 respectively, suggesting that miR-200c is highly likely to alter epithelial barrier characteristics via ZEB modulation of EMT processes (Bolos, Peinado et al. 2003). The strongest of the miR-200c:ZEB2 binding sites has 6bp of complementarity in addition to the seed sequence giving a mirSVR score of -1.3148. Within the ZEB1 3'UTR there are 6 predicted miR-200c binding sites, the strongest of which has 7bp of complementarity between the 3'UTR and microRNA and has a mirSVR score of -1.3135. As with miR-200b, miR-200c seed sequences are highly conserved amongst vertebrate families. MiR-200c may also effect TJs through modulating occludin expression (Schneeberger and Lynch 2004, Anderson and Van Itallie 2009, Van Itallie and Anderson 2014) as it too has a seed sequence in the 3'UTR of occludin. MiR-200c:OCLN 3'UTR has a 6bp complementarity in addition to the seed sequence and a predicted mirSVR of -1.0410 which once again indicates a fairly strong binding capability and its' conservation throughout vertebrate species further supports physiological relevance. MiR-200c has a predicted binding site in the 3'UTR of TNFAIP3/A20—however this binding has no additional base-pairing/complementarity suggesting a weak binding stability and with a low mirSVR score (-0.1820) and no conservation through vertebrate families which once again suggests limited physiological effects (Figure 3.2).

Figure 3.2: *In silico* miR-200c binding predictions for ZEB1, TNFAIP3/A20 and occludin (OCLN)

3.4.3: miR-429

MiR-429 belongs to the miR-200 family and targets many of the same 3'UTR mRNAs targets discussed above. MiR-429's highest mirSVR scores once again belong to ZEB2 (-6.72) and ZEB1 (-5.43). There are 7 predicted binding sites in the 3'UTR of ZEB2 for miR-429 which are well conserved in vertebrates, the strongest of which has 4bp of further binding complementarity and a mirSVR score of -1.3143. MiR-429 had 5 predicted binding sites in the 3'UTR of ZEB1 with the strongest mirSVR score being -1.3196 with a further 7bp of complementarity between miRNA and 3'UTR. MiR-429 also has a highly-conserved predicted binding site in the 3'UTR of occludin and out of the three members of the miR-200 family, it has the strongest mirSVR score (-1.0383) and the highest microRNA:3'UTR complementarity (8bp). As with the other microRNAs belonging to the miR-200 family, miR-429 has a predicted binding site in the 3'UTR of TNFAIP3/A20 and thus may play a role in regulating the activation and activity of NF-κB (Parvatiyar and Harhaj 2011). MiR-429:3'UTR TNFAIP3/A20 has a mirSVR score of -0.1837 with 6bp of further complementarity between the microRNA and mRNA. Together this suggests miR-429 is likely to have a larger role in TNFAIP3/A20 expression in the physiological system when compared to miR-200b/c (Figure 3.3).

Figure 3.3: ***In silico*** **miR-429 binding predictions for ZEB1, TNFAIP3/A20 and occludin (OCLN)**

3.4.4: miR-23a

MiR-23a's highest mirSVR scores belong to ZNF138 (-8.40) and ZNF730 (-4.66). Both of these are zinc-finger containing proteins which play a role in transcriptional regulation and are thought to play a role in cellular proliferation and differentiation. With regards to predicted mRNA targets that may impact upon epithelial barrier and innate immune responses miR-23a has a highly-conserved predicted binding site in the 3'UTR of ZEB1 (-1.0347 mirSVR score with 3bp of additional complementarity) and additionally has a seed-sequence in the 3'UTR of E-cadherin mRNA itself (-1.1446 mirSVR score with no further complementarity beyond seed-sequence—and no conservation amongst vertebrates) thus potentially closely regulating AJs (Vareille, Kieninger et al. 2011). MiR-23a potentially plays a much larger role in regulation of the innate immune response due to its' predicted target sites in: IRF-2 (a competitive inhibitor of IRF-1 (Harada, Fujita et al. 1989), hence modulating IFN-α/β transcription and release —-1.21 mirSVR score and 2bp complementarity, conserved), JAK1 (a key downstream molecule of the IFN-induced signalling cascade (Yoneyama, Suhara et al. 1998, Levy and Garcia-Sastre 2001)—a -0.6278 mirSVR score and 5bp complementarity, non-conserved) and STAT2 (another key downstream molecule of the IFN-induced signalling cascade (Yoneyama, Suhara et al. 1998, Levy and Garcia-Sastre 2001)—with -0.3942 mirSVR score and 9bp complementarity, non-conserved). In addition to these targets, miR-23a also has a predicted target in the 3'UTR of NF-κB regulator, TNFAIP3/A20 (Parvatiyar and Harhaj 2011). This site has a mirSVR score of -1.2941 and 4bp of further complementarity between the 3'UTR and miRNA but as in the miR-200 family, this predicted site is not well-conserved throughout vertebrate families (Figure 3.4).

Figure 3.4: ***In silico*** **miR-23a binding predictions for ZEB1, TNFAIP3/A20, E-cadherin (CDH1), IRF2, JAK2 and STAT2**

3.5: Discussion

MiR-200b, -200c, -429 and -23a were chosen as specific candidate microRNAs due to previous evidence obtained by the Epithelial Barrier and Inflammation Group to suggest that expression is increased in both colonic and kidney epithelial cells in response to epithelial-barrier modulating stimuli (TNF-α/TGF-β). To determine whether these microRNA changes could impact upon the integrity of the epithelial barrier and contribute to modulation of the innate immune response during RV infection, bioinformatically predicted mRNA targets were examined.

The miR-200 family have numerous highly stable, highly conserved predicted binding sites in the 3'UTR of ZEB1 and ZEB2. Given the mirSVR scores assigned to the miRNA:mRNA binding, it is exceedingly likely these interactions are stable (Betel, Wilson et al. 2008) and therefore may act to reduce protein levels by promoting mRNA target degradation or reducing the level of protein translation (Eulalio, Huntzinger et al. 2008). As previously mentioned, ZEB1 and ZEB2 are zinc-finger E-box binding transcription factors that have been implicated in EMT regulation through transcriptional repression of E-cadherin (Bolos, Peinado et al. 2003). E-cadherin is one of the core Ca^{2+} dependent glycoproteins in the AJs of epithelial cells and is a key protein in maintaining epithelial barrier integrity (Vareille, Kieninger et al. 2011, Hardyman, Wilkinson et al. 2013). It has been shown that decreased E-cadherin expression is associated with triggering EMT (Cano, Perez-Moreno et al. 2000) and thus promoting junctional disassembly. It can therefore be suggested that the increase in colonic epithelial barrier permeability in response to TNF-α previously observed in the Epithelial Barrier and Inflammation group could be linked to decreased miR-429 expression, leading to elevated ZEB-1/2 mediated repression of E-cadherin transcription. This suggestion is further supported by data published by Bracken et al. and Gregory et al. who have confirmed that miR-200 family members miR-200b and miR-429 do bind to the predicted seed-sequences in the 3'UTR of ZEB1 and ZEB2 and altering these microRNAs impacts upon E-cadherin expression (Bracken, Gregory et al. 2008, Gregory, Bert et al. 2008).

MiR-23a also has a highly conserved, stable predicted binding site of the 3'UTR of ZEB1 and thus may also play a role in regulating the expression of E-cadherin via ZEB1 mediated transcriptional repression as described above. Unlike the miR-200 family, this

miRNA:mRNA targeting event has yet to be confirmed and thus only remains a postulation.

The miR-200 family also has a predicted binding site on the 3'UTR of protein numb homologue (NUMB)—though the lack of upstream complementarity between the miRNAs and 3'UTR suggests a weak/unstable binding. NUMB is considered to be a repressor of E-cadherin expression and thus plays a role in AJ integrity and epithelial barrier maintenance (Gulino, Di Marcotullio et al. 2010, Sato, Watanabe et al. 2011). NUMB interacts with the c-terminus of p120-catenin and causes its' disassociation from transmembranous E-cadherin which, in turn, allows adaptor protein complex-2 (AP2) access to the dilucine motif of E-cadherin and triggers clathrin-mediated endocytosis (Sato, Watanabe et al. 2011, Ding, Ma et al. 2015). This, in turn, would lead to disassembly of the AJ which would correlate with increased epithelial barrier permeability.

In addition to modulating E-cadherin expression indirectly via ZEB1, miR-23a also has a predicted seed-sequence in the 3'UTR of E-cadherin. Analysis of upstream sequence homology suggests that binding strength/stability between microRNA and target is not particularly strong—opposing against mirSVR scores which suggests a relatively strong physiological effect. Upon examination of why this mirSVR score is so high despite a lack of complementarity, a previous publication from Cao et al. was found that confirmed miR-23a targeting E-cadherin and thus is liable to have been taken in to account by the miRanda algorithm to develop the mirSVR score. However, this publication from Cao et al. does not sufficiently validate miR-23a binding to the 3'UTR of E-cadherin using reporter assays, instead using miR-23a knock outs to correlate microRNA and protein expression (Cao, Seike et al. 2012). Thus at this stage it can still only be postulated that miR-23a can bind to the 3'UTR of E-cadherin mRNA and effect protein level to potentially effect epithelial barrier integrity.

These data, alongside the known disruption short-term disruption to transepithelial resistance and decreased E-cadherin protein expression during viral infection *in vitro* (Yeo and Jang 2010), suggest that the miR-200 family and miR-23a may decrease for in response to HRV infection. This decrease in miR-200b, -200c, -429 and to a less certain extent -23a theoretically should allow for enhanced expression of ZEB1/2 which, in turn,

will repress E-cadherin transcription leading to decreased protein leading to destabilisation of AJs.

MiR-200 family members may additionally be able to affect the epithelial barrier through modulation of occludin protein expression. MiR-200b, -200c and -429 have one predicted stable binding site in the 3'UTR of occludin which presents with a mirSVR score that suggests a potential feasible interaction and repressive event occurring. As discussed in Chapter 1, Section 1.3.2.a, occludin is a key tetraspan transmembrane that is localised to the TJs in the airway epithelium and a loss of occludin is associated with decreased TJ integrity as demonstrated by decreased TER measurements (Schneeberger and Lynch 2004). Once again, it could be suggested that the observations from the Epithelial Barrier and Inflammation group regarding the correlated altered miR-429 expression and altered epithelial barrier integrity in response to TNF-α/TGF-β treatment may be in due to occludin expression. This suggestion is further supported by recent data published by Yu et al. who confirmed that miR-429 targets and binds to the 3'UTR of occludin and can downregulate subsequent protein expression which can increase intestinal epithelial barrier dysfunction (Yu, Lu et al. 2016).

These data alongside the known increased permeability of the airway epithelium *in vitro* when infected with HRV and correlated decreased occludin protein expression (Sajjan, Wang et al. 2008, Yeo and Jang 2010) suggests that the miR-200 family may be elevated in response to viral infection. The increase in miR-200b, -200c and -429 levels should theoretically cause increased mRNA degradation/repression of occludin—leading to decreased protein levels and thus causing TJ disruption and epithelial barrier dysregulation.

MiR-23a may also effect occludin expression indirectly through its' predicted binding to the 3'UTR of TNFAIP3 (Kolodziej, Lodolce et al. 2011). At the same time this miR-23a:TNFAIP3 3'UTR targeting/binding may also have consequences for the proinflammatory state of cells. As previously mentioned, TNFAIP3/A20 is a critical negative regulator of NF-κB activation—which works in an inhibitory feedback loop (Parvatiyar and Harhaj 2011). Upon NF-κB activation, TNFAIP3/A20 is expressed. A20 has an ubiquitin editing activity which subsequently allows for deubiquitination of protective K63-linked polyubiquitated chains on TRAF-6 (Shembade and Harhaj 2010)

and receptor interacting protein 1 (RIP-1) (Wertz, Newton et al. 2015). Loss of these residues lead to destabilisation of TRAF-6 which prevents IκK signalsome activation and hence decreases NF-κB activation. In addition to this, A20 also has an E3-ubiquitin ligase domain which adds K48 polyubiquitin chains enhancing recognition and degradation of TRAF-6 and RIP-1 by the proteasome to further decrease NF-κB activity thus effecting inflammation within the cell (Ruland 2011, Wertz, Newton et al. 2015). It is this ubiquitin editing property of A20 which potentially plays a role in maintenance of epithelial barrier integrity through deubiquitination of polyubiqutinated occludin—causing increased retention of occludin to TJs. Unlike previous postulated miRNA:mRNA interactions, there is currently no experimental validation of this predicted binding.

In addition to the miR-200 family having direct effects on occludin expression via the predicted binding to occludin 3'UTR, the family may additionally effect occludin expression through stable predicted binding sites on the 3'UTR of TNFAIP3/A20. This proposed TNFAIP3/A20 expression modulation may also impact the proinflammatory state of cells via the negative regulation of NF-κB activation. As with miR-23a, this predicted binding has yet to be experimentally validated in any system.

These data alongside the known short-term increase NF-κB dependent proinflammatory cytokines (such as IL-6) during rhinovirus infection (Zhu, Tang et al. 1996), suggest that miR-23a and the miR-200 family may decrease in response to HRV. The decrease in these microRNAs should lead to elevation of TNFAIP3/A20—causing decreased NF-κB activation (via TNFAIP3/A20 negative regulation). As a consequence of this, occludin stability within TJs may elevate as seen in intestinal epithelium in Kolodziej et al. (Kolodziej, Lodolce et al. 2011), though this directly contradicts previous evidence that suggests occludin protein expression decreases in bronchial airway epithelial cells in response to HRV-16 infection (Yeo and Jang 2010).

The predicted targets of miR-23a, -200b, -200c and -429 identified here bioinformatically suggest mechanisms of how changes in these microRNAs may have contributed to altered epithelial barrier integrity as observed in previous data obtained by the Epithelial Barrier and Inflammation group. In addition, these predicted targets also highlight how NF-κB activation—and subsequent innate immune responses—can be effected by alterations to the microRNAs of interest. It is already known that both healthy and asthmatic human

bronchial epithelial cells have weakened epithelial barrier integrity (Sajjan, Wang et al. 2008) and immunologically respond to HRV-16 infection (Subauste, Jacoby et al. 1995)—thus leading to the postulation that these microRNAs of interest may play a role in this viral response through modulating expression of predicted targets ZEB1, E-cadherin, occludin and TNFAIP3/A20.

CHAPTER FOUR: Studies to Confirm the effect of MicroRNA Binding to Predicted 3'untranlated mRNA Target Sequences

4.1: Introduction

In silico prediction softwares have highlighted a number of potential miR-23a and miR-200 family mRNA targets which are implicated in epithelial barrier maintenance/repair (ZEB1, E-cadherin and occludin) and innate immune regulation (TNFAIP3). Although these bioinformatic tools have been shown to have a high level of accuracy in predicting miRNA:mRNA binding *in vivo*, each specific site has to be experimentally confirmed.

One of the most widely utilised methodologies for confirming miRNA:mRNA effects on protein expression utilises a Dual-Luciferase reporter assay (Jin, Chen et al. 2013). This approach allows for assessment of luciferase and its subsequent activity in a standardised enzymatic assay. Mammalian Luciferase expression constructs can be modified by inserting a segment of the 3'UTR of the target mRNA, carrying a complementary miRNA seed sequence at the 3' end of the luciferase open reading frame. The luciferase reporter is cotransfected along with an expression construct containing the pre-miRNA/miRNA mimic and transfection efficiency control into a cell line The effect of the presence of the 3' UTR and miRNA binding site, on the activity of the reporter in the presence and absence of miRNA is enzymatically assessed. To further confirm specificity of miRNA targeting event, seed target sequence mutants are also utilised to test the effect on luciferase activity (Jin, Chen et al. 2013).

To determine whether miR-23a and miR-429 are targeting the 3'UTR of the predicted mRNAs and thus suggesting that any observed alterations of mRNA/protein in experimental conditions may be linked to microRNA alterations, these Luciferase reporter assays will be utilised.

4.2: Hypothesis, Aims and Objectives

It is hypothesised that miR-23a utilises the *in silico* seed binding sequence in the 3'UTR of TNFAIP3/A20 to reduce expression of a 5' coding region. It is additionally

hypothesised that miR-429 binds to the bioinformatically predicted seed binding sequence in the 3'UTR of occludin.

Aim: To confirm in plasmid cotransfection experiments that miR-23a and miR-429 cause a reduction in luciferase activity via predicted complementary miRNA seed sequences in the 3'UTR of target mRNAs.

Objective(s):

- To isolate and amplify pre-miR-23a and pre-miR-429 sequences from genomic DNA and clone these into the pcDNA 3.1 expression vector.
- To use PCR with genomic DNA to isolate sequences of the 3'UTRs of TNFAIP3 and occludin mRNA that include the predicted miRNA-23a and -429 binding sites clone these into pRL-TK luciferase vector.
- To co-transfect these constructs in to H1 HeLa cells to carry out Dual Luciferase reporter assays to test effect on expression.

43: Results

4.3.1: Assessment of MiR-23a binding to TNFAIP3/A20 3'UTR in luciferase expression reporter assays

Pre-MiR-23a and 3'UTR TNFAIP3/A20 constructs were designed and created by Geraint Dingley and Rocio Martinez-Nunez using cloning strategies outlined in Section 4.3.2/3

(Figure 4.1). Richard Felwick optimised and performed the transfection in to a H1 HeLa cell-line and carried out Dual Luciferase reporter assays illustrated here.

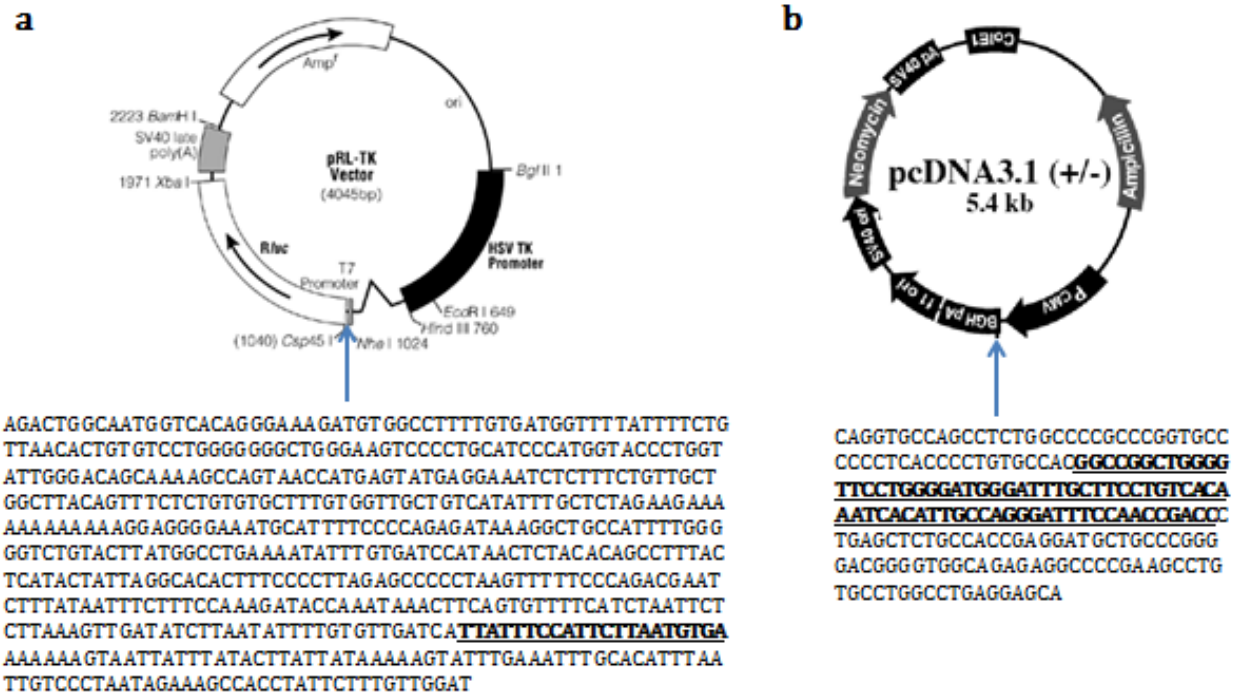

Figure 4.1: TNFAIP3/A20 3'UTR pRL-TK reporter vector and pre-miR-23a pcDNA 3.1 expression vector utilised in dual luciferase reporter assays for in vitro binding studies. (a) pRL-TK vector with 594bp of TNFAIP3/A20 3'UTR containing miR-23a predicted binding site (bold) was cloned in between position 1971 and 1978 (b) pcDNA 3.1 vector with 196bp fragment containing pre-miR-23a (bold) cloned. Constructs designed and created by Dr Geraint Dingley and Dr Rocio Martinez-Nunez

Relative luciferase activity was significantly decreased when pRL-TK-TNFAIP3/A20 3'UTR wild type (A20) was co-transfected with pcDNA 3.1 expressing pre-miR-23a (23a) when compared to a pcDNA 3.1 empty (without pre-miR) vector (-). Relative luciferase activity was unchanged between pRL-TK-TNFAIP3/A20 3'UTR seed target mutant (A20mut) was co-transfected with pcDNA 3.1 expressing pre-miR-23a (23a) and pcDNA 3.1 empty vector. Controls with pRL-TK empty (no 3'UTR insert) and pRL-TK empty with pcDNA 3.1 expressing pre-miR-23a showed no significant changes in relative luciferase activity from normalising conditions (Figure 4.2).

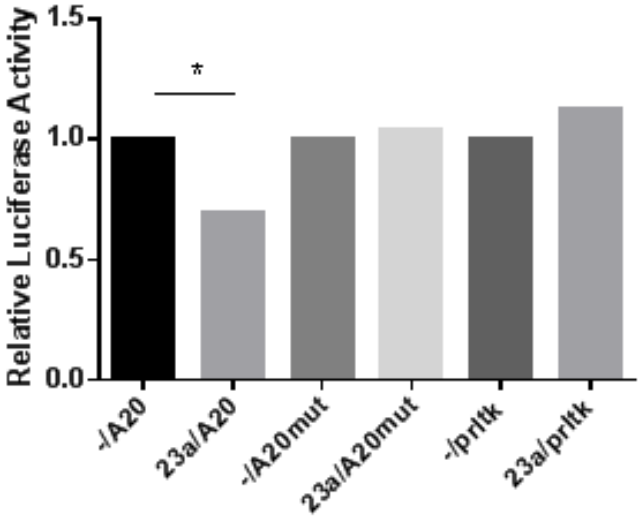

Figure 4.2: Co-transfection of pcDNA 3.1 pre-miR-23a (23a) and pRL-TK containing wild type TNFAIP3/A20 fragment (A20) or mutant fragment (A20mut) in H1 HeLa cells. Samples were normalised to empty pcDNA 3.1/pRL-TK wild type TNFAIP3/A20 to give a relative luciferase activity.

4.3.2: Pre-MiR-429 pcDNA 3.1 Vector Construction

Stem-loop pre-miR-429 sequence was obtained from MiRBase.org and cross-checked with miR-429 sequence in NCBI RefSeq. To ensure full isolation of pre-miR-429 from genomic material and enhance cloning efficiency, small portions of upstream and downstream sequence (from RefSeq) were included in design of product for vector insertion.

Primers were designed to include HindIII-Xba1 restriction sites on forward and KpnI-MluI restriction sites on reverse to allow for a restriction digest and insertion in to the pcDNA 3.1 vector between the HindIII and KpnI polylinker sites. The internal Xba1 and Mlu1 sites were included at this stage to allow for further subcloning into other vectors if required. Primers were additionally designed to meet >40% GC content and a melting

temperature >50°C with no secondary structures and no identified binding elsewhere within the human genome (Figure 4.3).

Figure 4.3: Strategy for isolation of pre-miR-429 from genomic DNA and subsequent cloning in to pcDNA 3.1 expression vector. Green indicates miR-429 seed element with yellow showing remaining sequence of mature miR-429.

Gel electrophoresis confirmed amplification of two ~160bp products which was the expected size of the miR-429 PCR product (Figure 4.5). DNA was extracted from agarose gel digested and ligated in to pcR-2.1 TOPO TA cloning vector and transformed into transformation competent E. coli. E. coli were plated on Amp(+) LB agar selection plates and successful colonies were picked and sent for sequencing (Source Bioscience, Cambridge).

Of the 7 colonies sent for sequencing, 3 colonies were positively aligned to the designed pre-miR-429 product of 164bp using NCBI Blast. These colonies also showed correct + sense orientation and contained HindIII-KpnI restriction sites for cloning into pcDNA 3.1. This would facilitate the formation of pcDNA 3.1 pre-miR-429 expression vector for Dual Luciferase reporter assays.

4.3.3: Occludin 3'UTR pRL-TK Vector Construction

Sequence of 3'UTR of occludin was obtained from NCBI RefSeq. Utilising microRNA.org, predicted binding site for miR-429 binding was identified between position 126-146 with the seed target sequence at position 139-146. To ensure full isolation of predicted binding site and to increase efficiency of fragment uptake in to pRL-TK vector—fragment was designed to be 400-800bp size.

Primers were designed to include a forward XbaI restriction site to allow cloning into the pRL-TK vector at position 1971 and a reverse Not1 restriction site to clone into pRL-TK at position 1978. As with pre-miRs, primers were designed with melting temperatures >50^{o}C and >50% GC content and cross-referenced to ensure no secondary structures and no identified genomic sequence specificity to reduce mispriming events (Figure 4.4).

Gel electrophoresis confirmed the amplification of products ~560bp which was the expected size of 3'UTR fragment of occludin (Figure 4.5b). This DNA product was then excised from the gel and cloned in to a TOPO TA cloning vector and positive colonies were selected via Amp+ LB agar. There were minimal colonies on LB agar plates and of these 3 were sent for sequencing (Source Bioscience Cambridge). Of these colonies, none were positive for the 562bp 3'UTR occludin insert. Publication of data from Yu et al. negated repetition of the experiment (Yu, Lu et al. 2016).

3'UTR of OCLN (562bp fragment):

GGCTGATGCCAAGTTGTTTGAGAAATTAAGTATCTGACATCTCTGCAATCTTCTCAGAAG
GCAAATGACTTTGGACCATAACCCCGGAAGCCAAACCTCTGTGAGCATCACAAAGTTTTG
GTTGCTTTAACATCATCAGTATTGAAGCATTTTATAAATCGCTTTTGATAATCAACTGGG
CTGAACACTCCAATTAAGGATTTTATGCTTTAAACATTGGTTCTTGTATTAAGAATGAAA
TACTGTTTGAGGTTTTTAAGCCTTAAAGGAAGGTTCTGGTGTGAACTAAACTTTCACACC
CCAGACGATGTCTTCATACCTACATGTATTTGTTTGCATAGGTGATCTCATTTAATCCTC
TCAACCACCTTTCAGATAACTGTTATTTATAATCACTTTTTTCCACATAAGGAAACTGGG
TTCCTGCAATGAAGTCTCTGAAGTGAAACTGCTTGTTTCCTAGCACACACTTTTGGTTAA
GTCTGTTTTATGACTTCATTAATAATAAATTCCCTGGCCTTTCATATTTTAGCTACTATA
TATGTGATGATCTACCAGCCTCC

OCLN Forward:

GGCTGATGCCAAGTTGTTTG

Forward cloning site is Xba1 into Xba1 in the pRL-TK vector at position 1971

TCTAGA – Xba1

TCTAGAGGCTGATGCCAAGTTGTTTG MT 61.61 50% GC

OCLN Reverse:

GGAGGCTGGTAGATCATCACA

Reverse cloning site is Not1 into Not1 in the pRL-TK vector at position 1978

GCGGCCGC- Not1

GCGGCCGCGGAGGCTGGTAGATCATCACA MT 60.09 52.38% GC

Figure 4.4: Strategy for isolation of 562bp fragment of occludin 3'UTR from genomic DNA and subsequent cloning in to pcDNA 3.1 expression vector. Green indicates miR-429 seed target sequence.

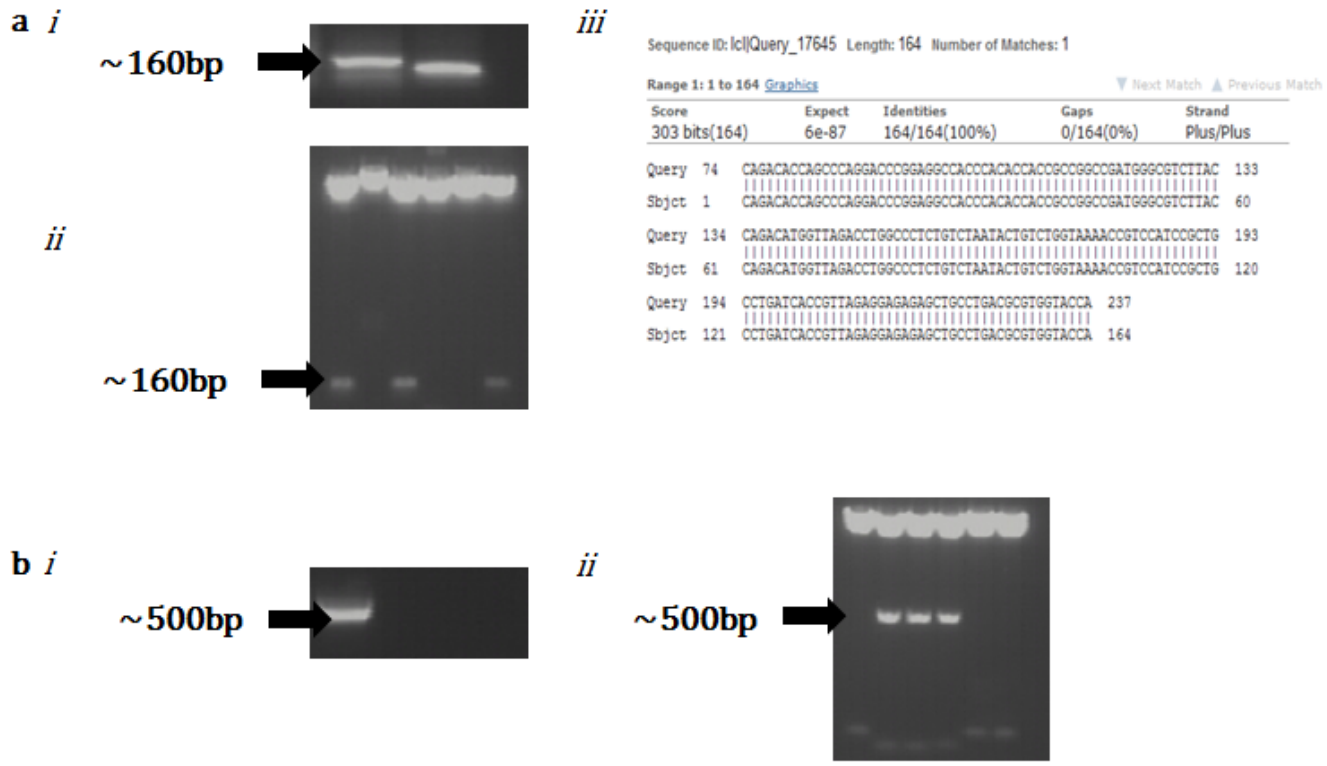

Figure 4.5: PCR products from genomic isolation for pre-miR-429 (a) and occludin (b). Product was isolated from gDNA (i) and inserted in to a TOPO vector. + colonies were digested (ii). Insert + colonies were sequenced (iii)

4.4: Discussion

In Chapter 3, bioinformatic prediction tools were utilised to identify miR-23a and miR-429 seed target sequences within the 3'UTRs of mRNAs associated with epithelial barrier integrity/regulation and innate immune responses—as both of these characteristics are impaired in asthmatics. However without *in vitro* confirmation of microRNA binding to the 3'UTR of the mRNA, changes in miRNAs could only be correlated to effects on predicted targets. This is because *in silico* prediction tools are an exhaustive list of all potential targets and likelihood of binding—but do not assure *in vitro/in vivo* binding (Betel, Wilson et al. 2008, Betel, Koppal et al. 2010, Peterson, Thompson et al. 2014). Utilising *in vitro* reporter assays, predicted miRNA:mRNA binding events could be explored to confirm existence (Jin, Chen et al. 2013) and confirm that the microRNAs exert an effect upon *in silico* predicted targets: ZEB1, TNFAIP3/A20, occludin and E-cadherin.

The dual luciferase reporter assays utilised here confirm that miR-23a binds to the identified seed target sequence in the 3'UTR of TNFAIP3/A20 *in vitro* and thus may modulate target expression. In wild type constructs, cotransfection of a miR-23a expression vector and TNFAIP3/A20 3'UTR reporter significantly reduced the relative luciferase activity when compared to a non-miRNA expressing vector control. The decrease in relative luciferase activity indicates reduction in translation of the Renilla luciferase reporter—thus indicating miRNA binding. This binding was confirmed to be specific through the use of the TNFAIP3/A20 3'UTR seed-target mutant constructs in which cotransfection of the miR-23a expression vector did not reduce relative luciferase activity. The lack of change indicates a miRNA seed sequence directed, specific binding occurring in the wild-type—thus indicating that miR-23a does modulate the translation of TNFAIP3/A20 as bioinformatic predictions suggested.

TNFAIP3/A20 has previously been shown to have a negative regulatory effect on NF-κB activation (Parvatiyar and Harhaj 2011). As miR-23a was shown to effect the expression of TNFAIP3/A20, it theoretically may also modulate NF-κB activation and subsequently influence innate immune responses. This could be further investigated in future through the utilisation of

Though miR-429 was successfully isolated and cloned in to a pcDNA 3.1 expression vector, elucidation of optimal conditions for *in vitro* binding assays for miR-429:3'UTR TNFAIP3/A20 in H1 HeLa cells was not achieved. Without the *in vitro* data to confirm a specific, targeted binding between the microRNA and the seed sequence in the 3'UTR of TNFAIP3/A20, the observed correlation between decreased miR-429 expression and elevated TNFAIP3/A20 mRNA and protein expression remain correlated, opposed to causational.

Difficulties also occurred in cloning and expressing the 3'UTR occludin fragment in a TOPO TA vector—thus a pRL-TK reporter construct was not created. To increase the likelihood of successful fragment insertion in to the TOPO cloning vector, ratio of insert to vector could be altered, along with reaction conditions such as enhanced salt or increased reaction duration. However, recent data from Yu et al. negated the need for further investigation as this paper confirmed that *in silico* predictions were correct. MiR-429:3'UTR occludin binding does occur *in vitro* and that this interaction is seed-sequence dependent (Yu, Lu et al. 2016). Confirmation of this binding suggests that the previous observations of significant increases in occludin mRNA are highly likely to be caused, in part, by the significant reduction of miR-429 expression in response to HRV-16/IFN-λ,

As previously discussed, Korpal et al. have confirmed miR-429 binding to seed sequences within the 3'UTR of ZEB1 and ZEB2 via *in vitro* dual luciferase reporter assays as utilised above (Korpal, Lee et al. 2008). In addition to confirmation of miRNA:mRNA binding, Korpal et al. showed that overexpression of miR-429 lead to decreased ZEB1/2 expression which, in turn, correlated with increased E-cadherin expression and inhibited EMT processes (Korpal, Lee et al. 2008). These data suggest that the observed elevation in ZEB1 mRNA and protein levels could be a direct consequence of decreased miR-429 expression—in addition to other miR-200 family members (Gregory, Bert et al. 2008)—which ultimately may cause reduction in E-cadherin expression.

Bioinformatic predictions also highlighted that miR-23a seed sequences were also present in the 3'UTR of ZEB1 and E-cadherin. Currently these remain as *in silico* predictions as there is no published data to confirm miRNA binding to the 3'UTRs of these targets. Cao et al. have previously shown that overexpression of miR-23a is correlated to decreased E-cadherin expression and enhanced EMT which may suggest that miR-23a

does indeed regulate E-cadherin expression (Cao, Seike et al. 2012). Cho et al. have previously shown that overexpression of miR-23a does not affect ZEB1 mRNA expression whilst overexpression of ZEB1 causes increased miR-23a expression in what may be a negative feedback loop (Cho, Gelinas et al. 2011). It is, however, difficult to draw conclusions from this publication as levels of ZEB1 protein in response to miR-23a overexpression were not evaluated.

Together this experimental data and data from the literature confirm that:

- MiR-23a targets, and binds to, TNFAIP3/A20 3'UTR modulating expression which subsequently may alter NF-κB activation—potentially impacting upon innate immune responses.
- MiR-429 targets, and binds to, occludin 3'UTR modulating expression altering which may alter TJ properties—potentially impacting upon epithelial barrier integrity.
- MiR-429 targets, and binds to, ZEB1 3'UTR modulating expression, which may alter AJ properties—potentially impacting upon epithelial barrier integrity.

CHAPTER FIVE (Part I): MicroRNA Changes in Response to HRV-16 Infection in Primary Bronchial Epithelial Monolayer Cultures

5.1: Introduction (I)

As discussed in Chapter 3, changes in miR-23a and miR-200 family were correlated with altered epithelial barrier integrity in response to exogenous TNF-α/TGF-β treatment in colonic epithelial cell lines and primary renal epithelium (Loxham, Felwick, Dingley, Collins—personal communication). Bioinformatic analysis of these microRNAs identified a number of stable binding sites in the 3'UTRs of targets that may play a role in epithelial barrier (occludin, ZEB1 and E-cadherin)(Bolos, Peinado et al. 2003, Vareille, Kieninger et al. 2011) and innate immune response regulation (TNFAIP3/A20)(Parvatiyar and Harhaj 2011). Together this suggested that exogenous cytokine treatment might affect epithelial barrier and innate immune responses through altering miRNA expression, culminating in altered expression of the aforementioned targets.

It has been well documented that epithelial cells in the respiratory tract respond to HRV infection through initiating an innate immune response (Subauste, Jacoby et al. 1995, Kelly and Busse 2008, Bochkov, Hanson et al. 2010). This immune response induces a proinflammatory and antiviral state within the cells to enhance viral particle removal and limit infection spread (Schleimer, Kato et al. 2007). Many of the proinflammatory mediators released in response to HRV infection (i.e. IL-6) are expressed in response to the activation of the transcription factor NF-κB (Caamano and Hunter 2002). Whilst this proinflammatory state is advantageous for pathogenic clearance, it has to be carefully regulated as aberrant inflammation can lead to a number of physiological issues (Lawrence 2009). To ensure that the NF-κB mediated proinflammatory response is only a short-lived stimulus, activation is negatively regulated by a number of proteins including A20 (Ruland 2011). It is noted that in *in vitro* HRV infections, proinflammatory mediators are 'short lived'—suggesting inactivation of NF-κB through negative feedback mechanisms and making regulation of A20 expression of interest in this context. The analysis in Chapter 3 leads to the following:

5.2: Hypothesis, Aims and Objectives (I)

Hypothesis: HRV-16 infection of cultured airway epithelium causes changes in the levels of miR-429 and -23a.

Aim: To identify if selected microRNAs change in response to HRV-16 infection in HBECs grown as submerged monolayer cultures and subsequently identify if bioinformatically predicted mRNA target expression is correlated to differential miRNA expression.

Objective(s):

- To infect a submerged monolayer culture of airway epithelium with HRV-16 and characterise infection through assessing viral genome equivalent nucleic acid (via RT-qPCR) and infectious viral particle release (via TCID50) patterns.
- To confirm monolayer cultures respond to HRV-16 infection in a physiologically relevant manner through assessment of IFN-β/λ mRNA induction (via RT-qPCR).
- To assess changes in miR-429 and miR-23a levels in response to HRV-16 infection (via RT-qPCR).

5.3: Methods

Initially it was decided to test the miRNA response in primary bronchial cells grown as monolayers in 24 well plates. This option was explored because it is more rapid to produce cultures ready for infection. Also it was done to test the possibility that airway epithelia in monolayer culture may be more susceptible to infection by HRV16, as shown in basal cells from differentiated cultures (Jakiela, Brockman-Schneider et al. 2008).

HBECs from healthy donors were grown as a submerged monolayer culture for 3-5 days in 24-well plates. Cells were infected with HRV-16 at a predetermined MOI (Section 4.3.1) for 48-72 hours with samples taken at 4, 8, 12, 24, 48 and 72 hours post-infection. HRV-16 infection was confirmed using RT-mediated qPCR to determine viral genome equivalent values and TCID50 to assess infectious progeny production and release. IFN-β and IFN-λ mRNA induction was assessed using RT-mediated qPCR to ensure *in vitro* cultures responded to HRV-16 infection in a manner which has been observed *in vivo*.

5.4: Results (I)

5.4.1: Optimisation of HRV-16 MOI on Monolayers

Quantification of viral genome equivalent material confirmed that there was a lower level of intact, measurable genomic material in the UV-irradiated controls compared to HRV-16 infected cells. Levels of UV-RV material did not alter during experimental progression—indicating the UV-RV controls are replication incompetent. As expected, the higher the MOI, the higher the level of HRV-16 genomic material present. MOI=1 has a steady level of genomic material throughout the time course with no pronounced peak; MOI=2 has highest genomic material after 12 hours post-infection, indicating viral replication; MOI=5 has highest genomic material at 8 hours post-infection with subsequent decline over the time course (Figure 4.1).

TCID50 confirmed infectious viral particle release in all cultures infected with HRV-16, regardless of MOI. Infectious viral particle release was below assay detection for UV-RV (data not shown), further supporting the use of UV-RV as a control. Infectious progeny release was correlated to higher MOIs, aligning with genomic material measurements, however infectious particle release differences between MOIs were less pronounced (Figure 5.1).

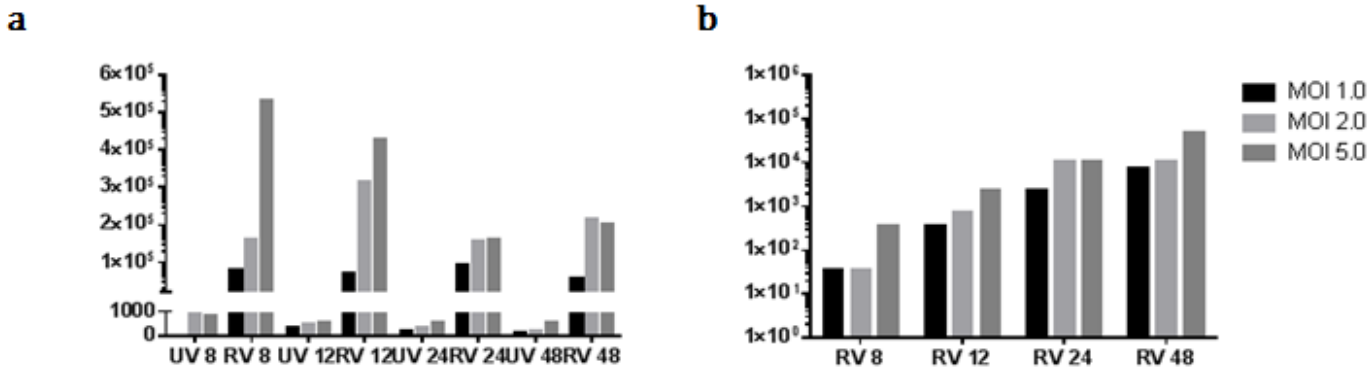

Figure 5.1: HRV-16 infection characteristics from monolayer cultures from 8-48 hours post infection with MOI=1, 2 or 5. (a) vRNA/genome equivalent quantification obtained via RT-mediated qPCR; (b) infectious particle release obtained via TCID50. n=1

IFN-β mRNA was induced in response to both UV-RV and HRV-16 infection in monolayers and peaked at 48 hours post-infection in all cultures. As previously observed, higher infection multiplicities correlated to stronger induction of expression. IFN-β mRNA induction in MOI=1 was erratic, with higher levels of mRNA expression occurring in response to UV-RV controls at both 12 and 24 hours post-infection. MOI=2 showed consistent higher IFN-β mRNA induction in response to replicatory competent virus with the most pronounced effect occurring at 48 hours. MOI=5 also showed higher mRNA induction in response to HRV-16 compared to UV-RV at all time points except 24 hours—in which UV-RV response was slightly elevated (Figure 5.2).

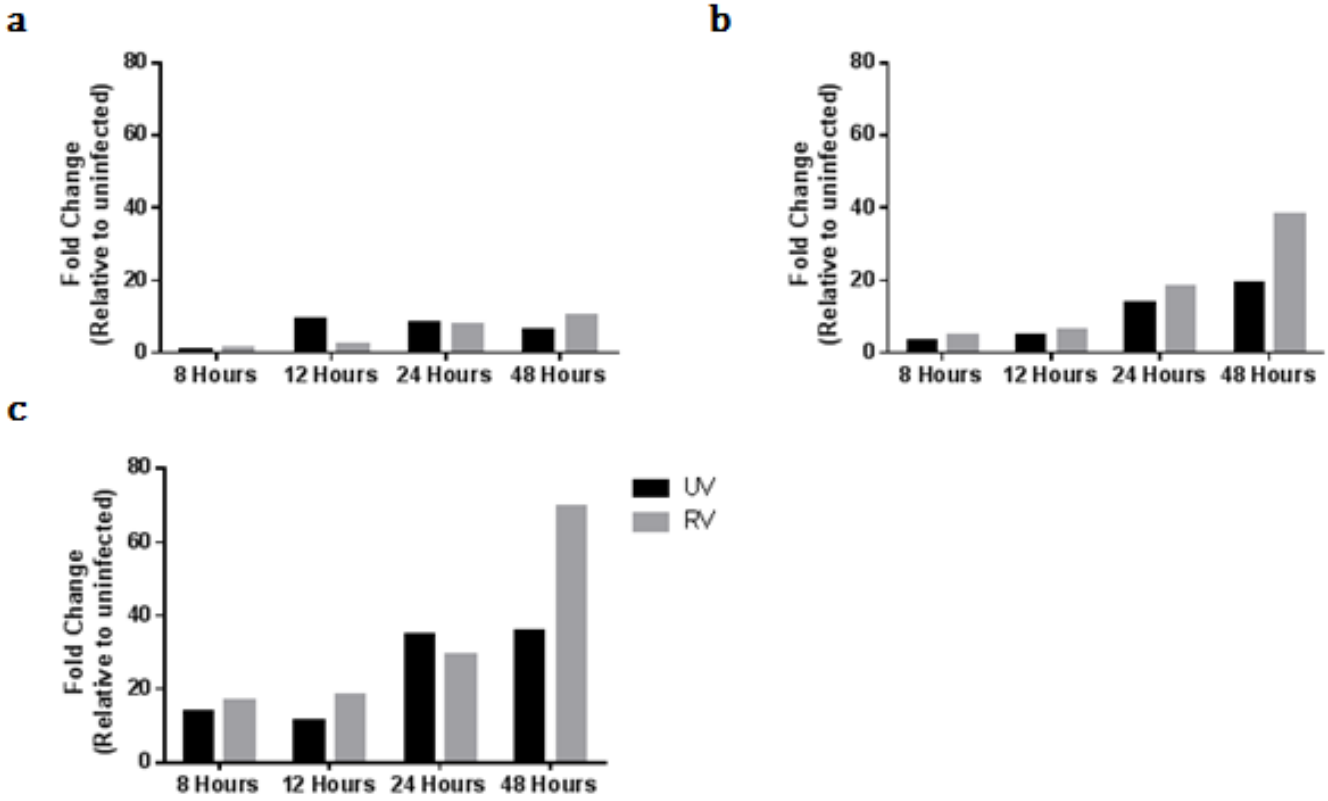

Figure 5.2: RT-qPCR quantification of IFN-β mRNA in response to UV-RV (UV) and HRV-16 (RV) at MOI=1 (a), 2 (b) and 5 (c) 8-48 hours post-infection in monolayer cultures from healthy donors. Samples were normalised to uninfected to give relative fold-change. Graphs represent n=1.

IFN-λ mRNA was also induced in response to HRV-16 and UV-RV in monolayers and as with IFN-β, peak induction was observed at 48 hours in all infection multiplicities. Whilst MOI=5 showed higher levels of mRNA induction in response to infection, MOI=1 and MOI=2 had similar mRNA inductions in response to infection. As observed in IFN-β cultures, MOI=1 lead to more erratic mRNA expression with levels below detection at 8 hours and with a higher expression in response to UV-RV control at 12 hours. MOI=2 and MOI=5 both showed higher levels of IFN-λ mRNA expression in response to replicatory competent virus than UV-RV control (Figure 5.3).

Due to the variable induction of IFN mRNAs in response to UV-RV and HRV-16 observed in MOI=1, this MOI was discounted for use in subsequent experimental series. MOI=2 and MOI=5 gave more consistent IFN mRNA induction and thus were chosen as more suitable candidates for monolayer infections. As infectious particle release was not largely different between the two cultures, it was decided to use the lower of the infection multiplicities (MOI=2).

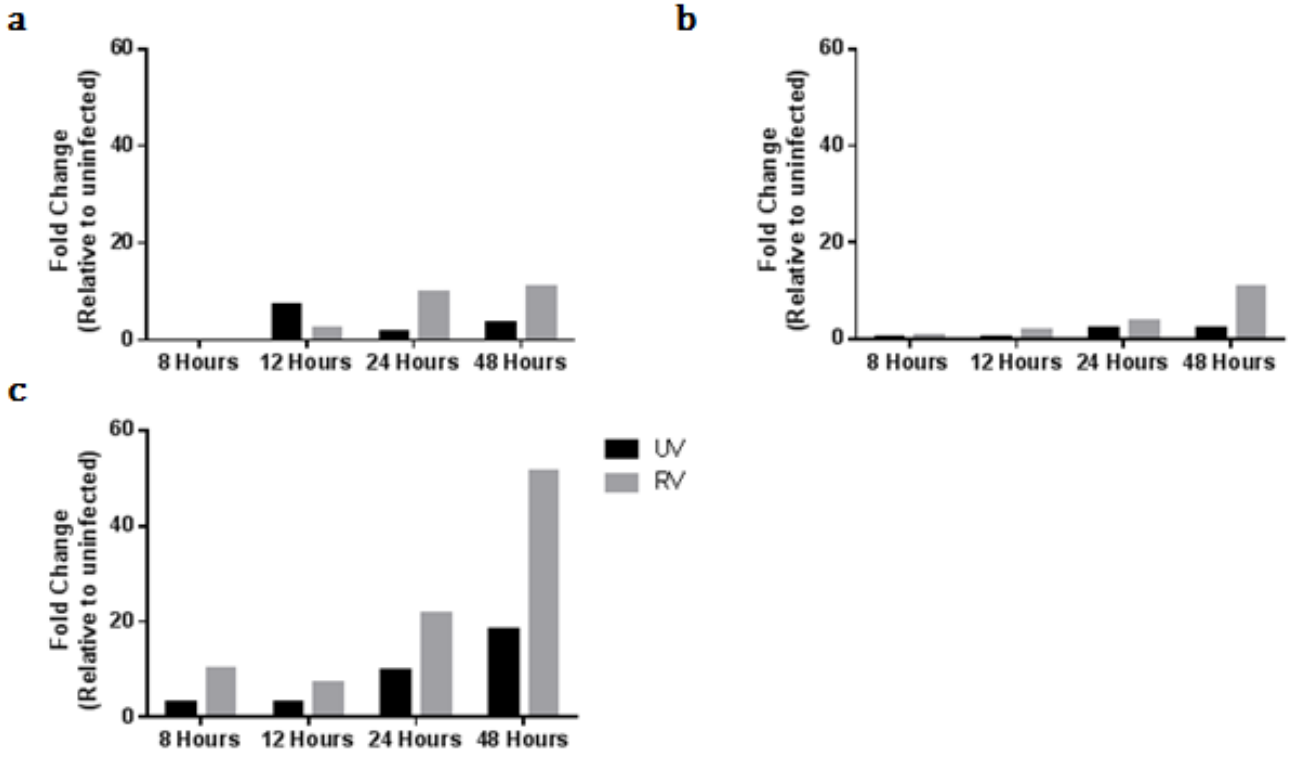

Figure 5.3: RT-qPCR quantification of IFN-λ1 mRNA in response to UV-RV (UV) and HRV-16 (RV) at MOI=1 (a), 2 (b) and 5 (c) 8-48 hours post-infection in monolayer cultures from healthy donors. Samples were normalised to uninfected to give relative fold-change. Graphs represent n=1.

5.4.2: Characterisation of HRV-16 Infection in Monolayer Cultures

Quantification of viral genome equivalent material showed significantly higher (p=0.0313) copy numbers in HRV-16 samples when compared to the UV-RV control. Copy numbers were highest at 8 hours post-infection, with a declining number over subsequent time points. TCID50 confirmed infective viral particle release from monolayers when infected with the replicatory competent HRV-16—but not the UV-irradiated viral control. Peak infective viral particle release was 36 hours after highest genome equivalent material was detected, at 48 hours post-infection (Figure 5.4).

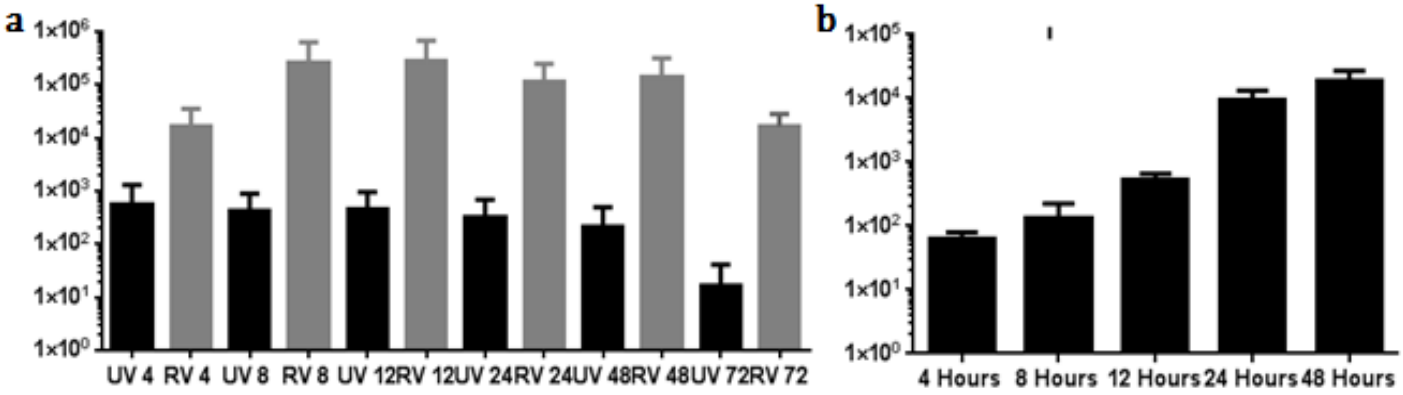

Figure 5.4: HRV-16 infection characteristics from monolayer cultures from 4-72 hours post infection with MOI=2. (a) vRNA/genome equivalent quantification obtained via RT-mediated qPCR; (b) infectious particle release obtained via TCID50. Graphs represent n=5 (except 72 hours where n=3), Error bars= SD.

IFN-β mRNA expression was elevated in response both to UV-RV and HRV-16—though there was a greater induction in response to replicatory competent virus compared to the control which approached significance at 4 hours post-infection (p=0.0625) and was significantly different at 12 hours (p=0.046). IFN-β mRNA induction was highest at 48 hours post-infection—correlating with peak infective particle release data obtained from TCID50 (Figure 5.5a).

IFN-λ1 mRNA expression was also elevated in response to HRV-16 and UV-RV—with higher expression induction in HRV-16 compared to the UV-irradiated control which was significant at 24 (p=0.0313) and 48 hours (p=0.0156) and . MRNA induction was highest

at 48 hours post-infection, this aligned with the highest infectious particle release from these cultures. (Figure 5.5b).

Of all IFNs measured, IFN-λ1 mRNA was the most strongly induced in response to HRV-16 within monolayer cultures. Relative to uninfected controls, IFN- λ1 was elevated 33.1 fold at 24 hours (peak), whilst IFN-β mRNA had ~10 fold elevation in expression at its' peak (24 hours) and IFN-λ2/3 mRNA expression was ~19 fold elevated at 72 hours post-infection (peak).

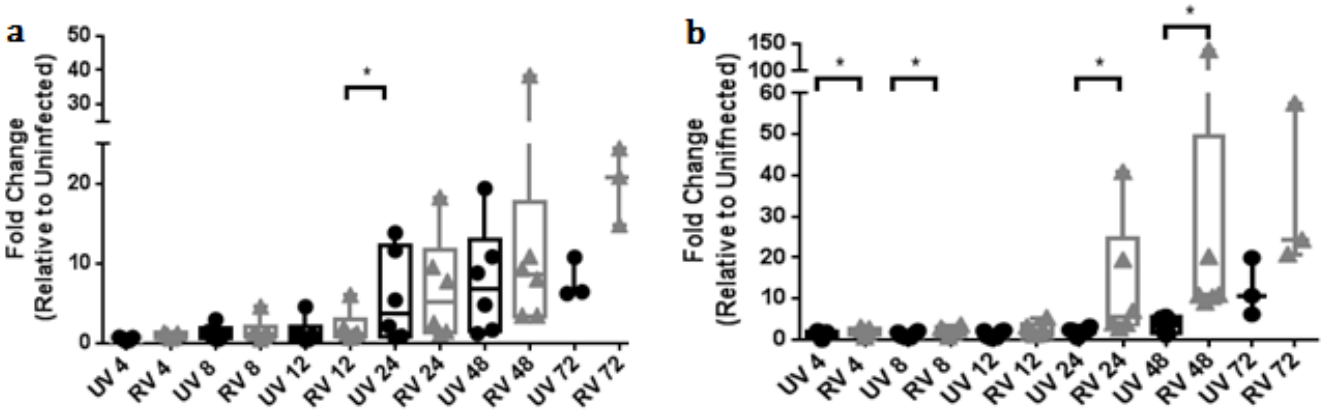

Figure 5.5: RT-qPCR quantification of IFN-β (a) and IFN-λ (b) mRNA in response to UV-RV (UV) and HRV-16 (RV) 4-72 hours post-infection in monolayer cultures from healthy donors. Samples were normalised to uninfected to give relative fold-change. Graphs represent n=5 (except 72 hours where n=3), p=*≤0.05calculated via Wilcoxon matched pairs, signed rank test. Expressed as interquartile range and median.

IFN-λ1 protein release in the supernatant was quantified via ELISA as with ALI supernatants (Figure 5.6). Only n=3 samples had IFN-λ1 protein release that was above the 62.5pg/ml detection limit of the assay. Levels of protein were elevated in response to HRV-16 compared to UV-RV at 8, 12 and 24 hours after initial infection—though this was not significant (p=0.0625). Protein release was highest at 12 hours with a mean of ~300pg/ml from n=3 supernatants, however this did not correlate with data obtained from mRNA quantification (Figure 5.6).

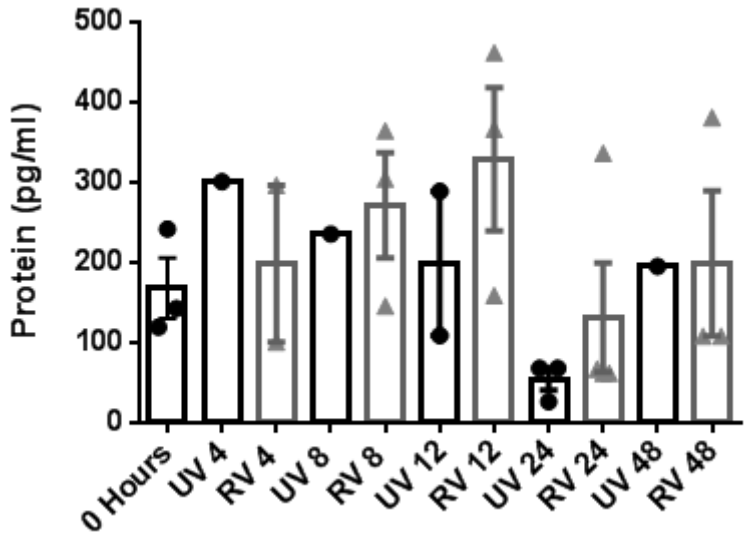

Figure 5.6: ELISA quantification of IFN-λ protein in supernatants from HRV-16 infected monolayer cultures from healthy donors. Graphs represent n=3 (except 72 hours where n=2 (a) of 3 (b), p*= <0.05 calculated via Wilcoxon matched pairs, signed rank test. Error bars= SEM.

5.4.3: MicroRNA Responses during HRV-16 Infection in Monolayer Cultures

MiR-23a levels were not changed in response to HRV-16 at 4, 8 and 24 hours post-infection in the monolayer cultures. There were slight decreases in response to replicatory virus at 12 and 48 hours—though this was not significant. MiR-23a was most greatly reduced in response to HRV-16 at 48 hours with a ~29% decrease; whilst levels were decreased by ~20% at 12 hours (Figure 5.7a).

MiR-429 levels were elevated in HRV-16 compared to UV-RV controls between 4-12 hours—but this was not significant. Levels were most greatly elevated at 12 hours where there was a ~59% increase in miR-429 in response to replication competent virus. Levels of miR-429 were similar in response to UV-RV and HRV-16 at 24 and 48 hours (Figure 5.7b).

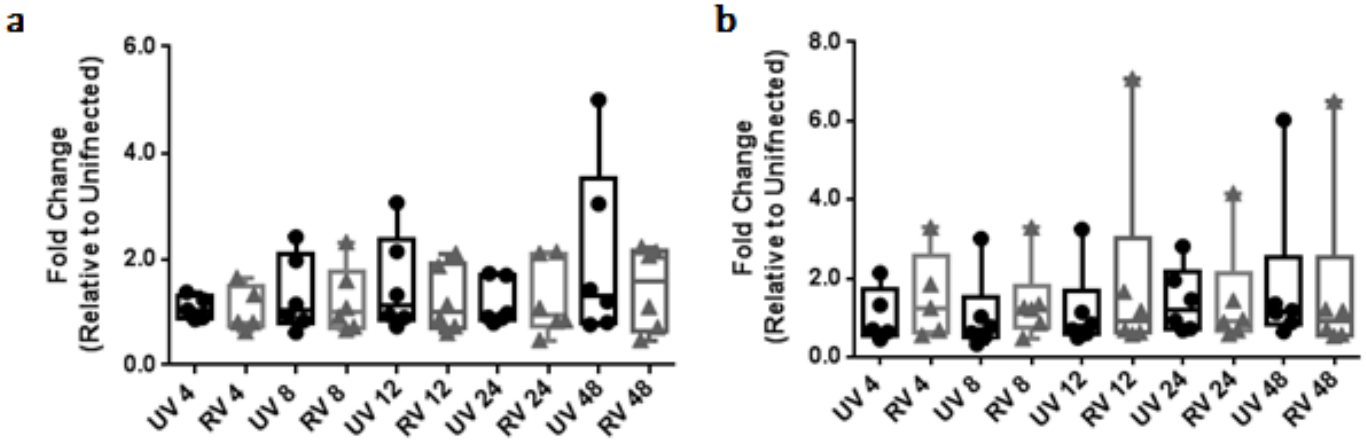

Figure 5.7: RT-qPCR quantification of miR-23a (a) and miR-429 (b) in response to UV-RV (UV) and HRV-16 (RV) 24-72 hours post-infection in monolayer cultures from healthy donors. Samples were normalised to UV-24 to give relative fold-change. Graphs represent n=5, p=*≤0.05calculated via Wilcoxon matched pairs, signed rank test. Expressed as median and interquartile range

5.4.4: Predicted Target mRNA Responses during HRV-16 Infection in Monolayer Cultures

As there were no significant changes to the microRNAs of interest in response to HRV-16 infection, changes in the mRNA level of the predicted microRNA targets ZEB1, E-cadherin, occludin and TNFAIP3/A20 were not assessed.

5.5: Discussion (I)

This study tested the hypothesis that the microRNAs miR-23a and the miR-200 family are altered in response to HRV16 infection in monolayer cultures of primary bronchial epithelia.

Prior to characterising changes in the miRNAs of interest in response to HRV-16 infection in HBEC monolayers, infection had to be confirmed. Monolayer cultures were permissible the infection both by replicatory competent (HRV-16) and replicatory incompetent (UV-RV) virus as shown by genome quantification results obtained via RT-qPCR. In monolayers, genomic material was highest at 8 hours post-infection aligning with *in vivo* data which suggests viral replication occurs between 5-8 hours post infection. TCID50 confirmed that whilst monolayers were permissible to infection, only HRV-16 infected samples had infectious progeny formation and release from cultures—which peaked at

48 hours. *In vivo* data suggests infectious particle release begins 18-24 hours after viral inhalation and usually resolves after 72 hours, thus the HRV infection characteristics obtained from the monolayers does appear to mirror *in vivo* (Corne, Marshall et al. 2002, Lessler, Reich et al. 2009).

In addition to ensuring monolayers were permissible to infection and replication competent, cellular responses were measured to ensure the model responded to infection in a manner similar to *in vivo*. As IFNs are important innate immune response mediators that have previously been shown to be strongly induced in response to HRV infection in airways (Wark, Johnston et al. 2005, Kotla, Peng et al. 2008) it was decided to quantify levels of the type I IFN—IFN-β—and the type III IFN—IFN-λ—expressed in monolayer cultures in response to HRV-16 infection. IFN-β and IFN-λ mRNA was induced in response to both UV-RV and HRV-16 infection—with precise induction levels varying between each patient. IFN upregulation has been shown in response to both formation of the dsRNA replicatory intermediate and PAMP recognition (Tosi 2005, Parker and Prince 2011)—though it has not previously been determined whether there are any differences in the interferon repertoire stimulated in response to dsRNA or PAMPs and whether all IFNs are stimulated to the same extent. This data suggests that this is not perhaps the case and that the IFN families have distinct responses to HRV-16 in HBECs. IFN-λ mRNA was significantly higher in response to HRV-16 compared to UV-RV from 8 hours—much earlier than IFN-β mRNA (48 hours). 8 hours is the time in which peak vRNA was detected, suggesting that IFN-λ mRNA upregulation is more strongly induced in response to viral replication than IFN-β. IFN-β mRNA is more strongly induced in response to UV-RV compared to IFN-λ—suggesting that IFN-β is likely to be induced in response to the 'sensing' of PAMPs opposed to dsRNA replicatory intermediates.

Comparison of induction of the two IFN families indicated that IFN-λ was most strongly induced in response to HRV-16 when compared to uninfected controls. This may be linked to the specificity of IFN-λ effect regulated by the localisation of IFN-λR1 primarily to epithelial cells (Sommereyns, Paul et al. 2008, Mordstein, Neugebauer et al. 2010, de Weerd and Nguyen 2012). Further analysis of the CT values of the IFN mRNAs indicated that whilst fold-change of IFN-λ mRNA is higher than IFN-β, IFN-β mRNA is more abundant than IFN-λ. IFN-β receptors are expressed on more cell types than IFN-λ—including being expressed on innate immune cells (de Weerd and Nguyen 2012)—thus it

is likely that the effect of upregulating IFN-β has a wider impact upon a vast number of cell types, whilst IFN-λ upregulation mainly effects epithelial surfaces (Sommereyns, Paul et al. 2008, Mordstein, Neugebauer et al. 2010, de Weerd and Nguyen 2012). In combination this suggests that the two IFN families play differential functional roles in response to HRV-16—IFN-β is likely to play a broad spectrum antiviral role, affecting both the epithelium and the myeloid innate immune cells whilst IFN-λ is a much more specific response to viral replication which primarily effects IFN-λR1 bearing epithelial cells—perhaps to modulate/maintain epithelial barrier integrity during infection.

After confirming that HRV-16 infection and associated-immune response occurred in the *in vitro* monolayer model, miR-23a and miR-429 levels were quantified to determine whether they altered in response to these stimuli. Neither miR-23a nor miR-429 were significantly changed at any point of the experiment duration. MiR-23a was slightly decreased in response to HRV-16 infection vs UV-RV at 12 and 48 hours with the remaining time points showing similar levels of miRNA between the two groups. MiR-429 was slightly elevated at 4, 8, 12 hours post-infection in HRV-16 compared to UV-RV controls, with similar miRNA levels between the groups at 24 and 48 hours. Due to the lack of significant alterations in microRNA levels in response to HRV-16 infection in monolayer cultures, it was decided to not quantify mRNA levels of the *in silico* predicted targets.

Whilst the infection and immune characteristics of the monolayers indicated that it was an appropriate *in vivo* model—further consideration of the model highlighted several potential limitations. Monolayers are, as the name suggests, a model which has a single cell layer of cells which is architecturally dissimilar than *in vivo* where bronchial epithelial cells are arranged in a pseudostratified layer (Stem Cell Technologies (a) 2013, Stem Cell Technologies (b) 2013). Loss of the pseudostratified architecture means cells in the monolayers have differential adhesive contacts—both apically and laterally—when compared to *in vivo* or cells grown as part of a more physiological relevant model (Prytherch, Job et al. 2011). As this particular experiment focusses on potential miR-mediated effects on the epithelial barrier, having an epithelial barrier that does not closely reflect *in vivo* limits the usefulness of the model.

In addition to this, growing submerged monolayer cultures of HBECs is suggested to allow for cellular division but not cellular differentiation (Stem Cell Technologies (a) 2013, Stem Cell Technologies (b) 2013). Phase contrast observation of monolayer cultures showed very low abundance of ciliated epithelial cells, suggesting a lack of differentiation in this culturing methodology (data not shown, ((Stem Cell Technologies (a) 2013, Stem Cell Technologies (b) 2013)). To determine the extent of cellular differentiation in monolayers, mRNA expression of ciliated and goblet cell markers could be carried out. *In vivo*, the airway epithelium is highly differentiated giving rise to a polarised cell population (Knight and Holgate 2003). As with the lack of pseudostratification, this lack of different cell populations in monolayers suggests that results obtained from the model may not be physiologically relevant (Prytherch, Job et al. 2011, Inc 2013). It has previously been shown that some respiratory viruses—such as RSV—can only infect specific cellular populations both *in vivo* and *in vitro* (Zhang, Peeples et al. 2002). HRV has been shown to infect both ciliated and non-ciliated epithelial cells (de Arruda, Mifflin et al. 1991, Jakiela, Brockman-Schneider et al. 2008), however it is primarily ciliated epithelial cells that are shed in response to HRV infection (Turner, Hendley et al. 1982). As this experimental design is analysing the potential miRNA responses to HRV-16 infection, the lack of ciliated epithelial cells in monolayers limits the usefulness of the model.

With these model limitations in mind, the lack of significant miRNA alterations in response to viral infection is more likely to be a consequence of a non-physiologically reflective experimental design. Examination of other HBEC culturing methodologies suggests that air-liquid interface (ALI) is currently one of the closest physiologically reflective *in vitro* models as cells differentiated at ALI for 21+ days are shown to have a pseudostratified architecture with highly differentiated and polarised cells (Stewart, Torr et al. 2012). As such, it was decided to retest the hypothesis in ALI cultures.

CHAPTER FIVE (Part II): MicroRNA Changes in Response to HRV-16 Infection in Primary Bronchial Epithelial ALI Cultures

5.6: Introduction (II)

Whilst the previous experimental series in Part I confirmed that HBEC monolayers were permissive to HRV16 infection and supported viral replication and release, the cultures did not show significant changes in the target microRNAs. This could mean that either these microRNAs are not altered in HRV-16 infection both *in vivo* and *in vitro*—thus are not responsible for alterations in NF-κB activation or epithelial barrier—or that the specific *in vitro* model does not respond and does not accurately reflect an *in vivo* response.

Consideration of the monolayer model highlighted several reasons in which it may have given a false negative and may not be as accurately reflective of *in vivo* which included: lack of cellular differentiation, lack of pseudostratified architecture and a lack of apical adhesive contacts. As such, it was decided to repeat this experiment utilising a model that is more closely reflective of the upper respiratory tract *in vivo*—culturing and differentiating the cells at an ALI.

HBEC cells that are grown and differentiated at ALI culture for 21+ have been suggested to be one of the most physiologically relevant *in vitro* cell culture models for airway experimentation (Fulcher, Gabriel et al. 2005). This model is currently widely used in experimental settings. Differentiating HBEC cells on semi-porous Transwell supports in the presence of ALI media with pre-determined concentrations of additives and a high concentration of retinoic acid—has been shown to allow cells to differentiate towards a mucociliary phenotype with the presence of basal, ciliated and goblet cells in culture (Stewart, Torr et al. 2012). The presence of different cellular populations is more reflective of *in vivo* and, as discussed in Chapter 4- Part I, Section 4.4, allowed for HRV-16 to infect both ciliated and non-ciliated epithelial cell populations to a similar proportion that would occur physiologically. Additionally the presence of the mucociliary phenotype of the culture allowed for recapitulation of the complete physical barrier with

mucous production/protection and cilia-mediated clearance as seen *in vivo (*Knight and Holgate 2003)—once again ensuring experimental HRV-16 infection is more physiologically relevant.

Aside from allowing for cellular differentiation/polarity, ALI cultures have been shown to have a pseudostratified architecture which resembles the *in vivo* structure (Fulcher, Gabriel et al. 2005). It has also been observed that ALI cultured cells form an epithelial barrier from ~7 days of differentiation as determined by increasing TER readings (Wark, Johnston et al. 2005). Characterisation of epithelial barrier properties in ALI cultures cells indicated that these cells are not only capable of forming epithelial junctions, but also junctional proteins are as *in vivo* (Wark, Johnston et al. 2005). Given that a large proportion of this study was to determine whether HRV-16-mediated epithelial barrier change was regulated by miRNAs—it was of upmost importance that the *in vitro* barrier was as physiologically reflective as possible.

It has also been additionally suggested that HBEC cells differentiated at ALI culture have differential gene expression than non-differentiated cells (Fulcher, Gabriel et al. 2005). As miRNAs are a method of post-transcriptional, pre-translational regulation it was important the model was as close to *in vivo* gene expression as possible.

In addition to changing the HBEC culturing model to one that was more physiologically relevant, it was decided to also observe miRNA changes in response to virus in ALI cultures from asthmatic donors and compare this to healthy cohort responses. This was because it has been well documented that asthmatic individuals have decreased epithelial barrier integrity with lower TER readings and increased macromolecular permeability (Xiao, Puddicombe et al. 2011), decreased numbers of TJs within their pseudostratified layers, decreased levels of ZO-1 and Occludin expression within intact TJs, decreased levels of E-cadherin and α-catenin within AJs, and decreased desmosome length (Shahana, Bjornsson et al. 2005, de Boer, Sharma et al. 2008, Yeo and Jang 2010). Asthmatic individuals additionally have been shown to have altered innate immune responses—with altered levels of proinflammatory cytokines such as IL-6 and IL-8. Studies have additionally suggested that type I and III IFNs are impaired in some asthma cohorts—with significantly reduced IFN-β production in BAL samples from asthmatics at 8 and 24 hours in response to HRV-16 infection and similarly a significantly reduced level of IFN-

λ in BAL and HBECs in response to infection (Wark, Johnston et al. 2005, Contoli, Message et al. 2006, Sykes, Edwards et al. 2012, Sykes, Macintyre et al. 2014).

5.7: Hypothesis, Aims and Objectives (II)

Hypothesis: HRV-16 infection of ALI differentiated airway epithelium causes changes in the levels of miR-23a, -200b, -200c and -429.

Differential miRNA responses will occur in ALI cultures derived from asthmatic patients compared to healthy patients.

Messenger RNA for predicted miRNA targets, TNFAIP3/A20, ZEB1, occludin and E-cadherin are co-expressed—and modulated—in ALI differentiated airway epithelium. *Aim:* To assay selected microRNAs in response to HRV-16 infection in HBECs grown at ALI culture from both healthy and asthmatic donors. To subsequently identify if bioinformatically predicted mRNA target expression are coexpressed or change relative to assayed miRNA expression.

Objective(s):

- To infect ALI culture of differentiated airway epithelium with HRV-16 and characterise infection through assessing genome equivalent nucleic acid (via RT-qPCR) and viral particle release (via TCID50) patterns.
- To confirm ALI cultures are infected with HRV-16 by measurement of physiologically relevant induction of IFN-β/λ mRNA (via RT-qPCR).
- To assess changes in miR-23a/-200b/-200c/429 levels in response to HRV-16 infection (via RT-qPCR).
- To assess levels of mRNA for predicted miR targets, TNFAIP3/A20, ZEB1, occludin and E-cadherin (via RT-qPCR).

5.8: Methods (II)

Primary human bronchial epithelial cells from healthy and asthmatic donors were differentiated at air-liquid interface for 21 days to allow for the development of a cellular culture that most closely mimicked the pseudostratified epithelial layers observed *in vivo*. Cells were then infected with HRV-16 at a MOI of 1 and cultured for a further 72 hours, with washings at 24 hourly intervals to mimic *in vivo* mucocilary clearance.

ALI culture infection was confirmed through quantification of viral genome equivalent via RT-qPCR. Viral replication was measured via infectious particle release assessed by TCID50. In addition, IFN-β and IFN-λ responses were quantified via RT-qPCR and ELISA to assess mRNA induction and protein release to ensure cultured epithelial cells responded to HRV-16 infection in a manner comparable to *in vivo* Rhinovirus infections.

5.9: Results (II)

5.9.1: Characterisation of HRV-16 Infection in ALI Cultures

Viral genome equivalents were significantly higher in HRV-16 compared to UV irradiated HRV-16 (UV-RV) at 24 and 48 hours in healthy cultures ($p=0.0313$) and at 24, 48 and 72 hours in asthmatics ($p=0.0313$). Viral genome equivalent levels were highest at 24-hours post-inoculation which decreased over subsequent time points. There was no observable difference in levels of viral genome material between the healthy or asthmatic groups (Figure 5.8a).

Data obtained on infectious particle release correlated with genome equivalent data. Infectious particles were only detectable in cultures infected with HRV-16 and not UV-RV; confirming the validity of UV-RV as a non-replicative control. Infectious viral particle was highest at 24 hours post-infection in both patient groups—with lower levels at 48/72 hours. As with the PCR data, there were no observable differences in the responses observed in the healthy or asthmatic patients (Figure 5.8b).

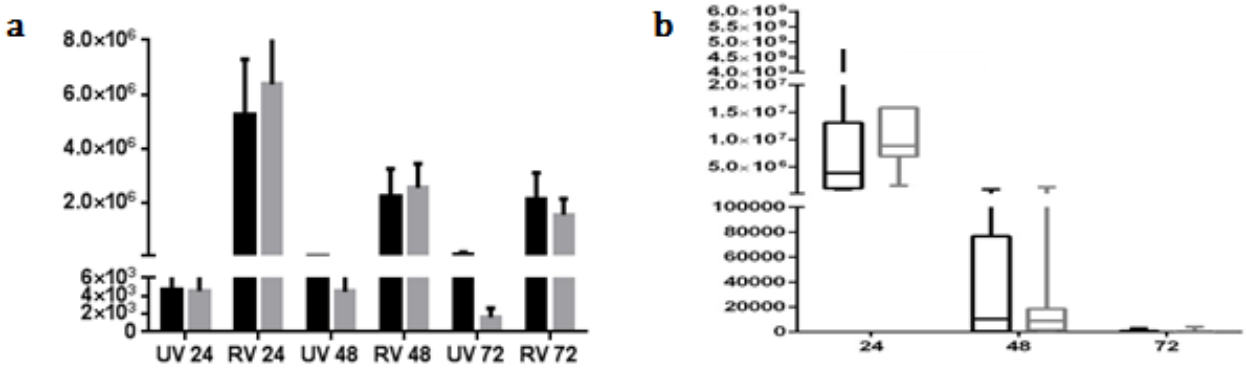

Figure 5.8: HRV-16 infection characteristics from ALI cultures from healthy and asthmatic donors from 24-72 hours post infection with MOI=1. (a) vRNA/genome equivalent quantification obtained via RT-mediated qPCR; (b) infectious particle release obtained via TCID50. Graphs represent n=6, p=*≤0.05calculated via Wilcoxon matched pairs, signed rank test. Expressed as median and interquartile range with 95% confidence intervals shown. *Data provided by Emily Wilkinson.*

To ensure cultures were responding to HRV-16 infection, IFN-β and IFN-λ1 mRNA expression were measured via RT-mediated qPCR and expressed as fold change over UV controls (Figure 5.9). IFN-β mRNA was significantly higher in response to HRV-16 compared to UV-irradiated controls at 24 (p=0.0156) and 48 hours (p=0.0313) in both healthy and asthmatic cultures (Figure 5.9a-b). IFN-β mRNA induction was highest at 24 hours—18.5 fold higher compared to UV-RV controls in healthy and 25.7 fold higher in asthmatics—with decreasing levels at 48 and 72 hours. IFN-λ1 mRNA was significantly higher in response to HRV-16 compared to UV-RV at 24 (p=0.0156), 48 (p=0.0156) and 72 hours (p=0.0313) in both healthy and asthmatic individuals (Figure 5.9c-d). IFN-λ1 mRNA induction peaked at 24 hours as observed with IFN-β mRNA. Comparison of the IFN mRNA induction between healthy and asthmatic individuals confirmed no significant differences between the responses, however asthmatic individuals showed a wide spread in the data with high mRNA induction in response to viral infection in some donor cultures.

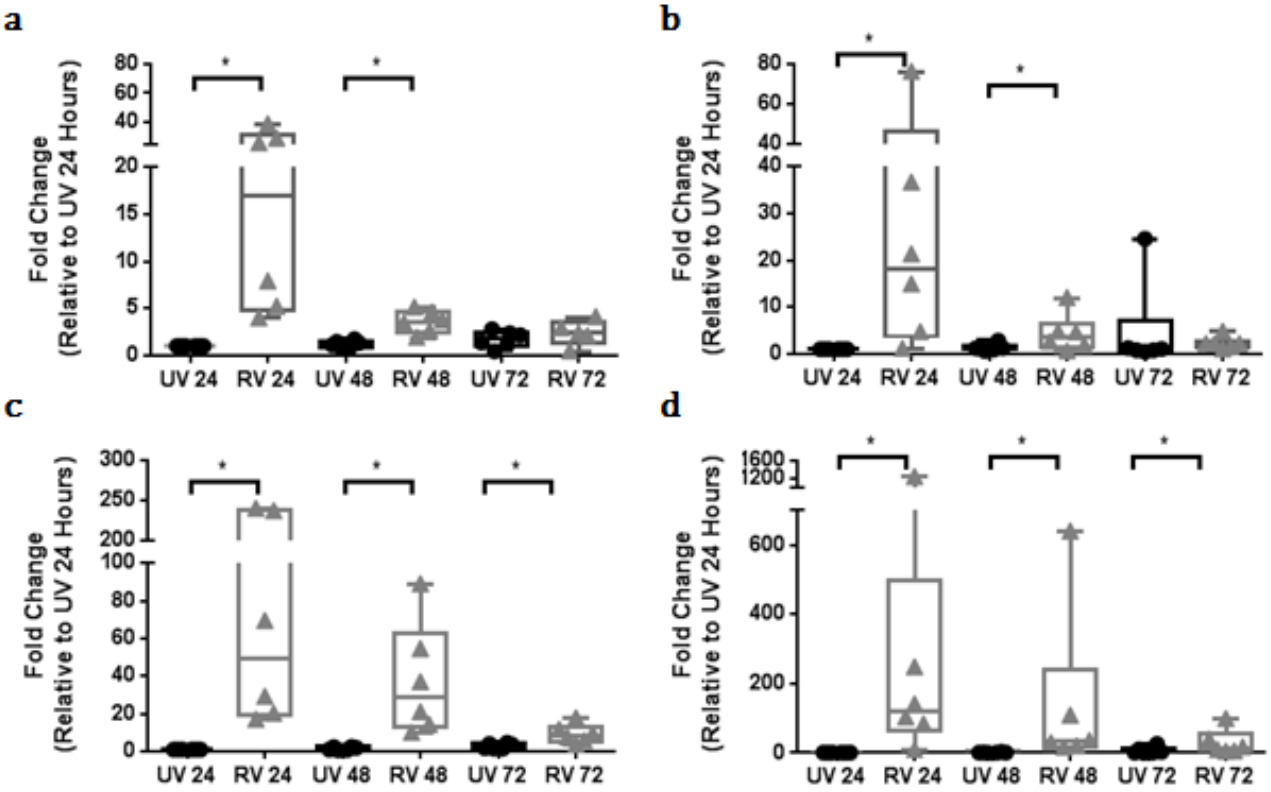

Figure 5.9: RT-qPCR quantification of IFN-β (a-b) and IFN-λ1 (c-d) mRNA in response to UV-RV (UV) and HRV-16 (RV) 24-72 hours post-infection in ALI cultures from healthy (a, c) and asthmatic (b, d) donors. Samples were normalised to UV-24 to give relative fold-change. Graphs represent n=6, p=*≤0.05calculated via Wilcoxon matched pairs, signed rank test. Expressed as median and interquartile range with minimum/maximum shown

5.9.2: MicroRNA Responses during HRV-16 Infection in ALI Cultures

After confirming that the ALI cultures were HRV-16 infection permissive, replication competent and had anticipated IFN responses similar to those *in vivo*, microRNA levels were assessed using RT-mediated qPCR assays designed by Life Technologies (Chapter 2, Section 2.5)(Figure 4.10).

MiR-23a was significantly decreased in response to rhinovirus infection compared to UV-RV controls at 48 and 72 hours in both healthy (p= 0.0313—48; p=0.05—72)(Figure 5.10a) and asthmatic (p=0.0496—48; p= 0.0313—72) cultures (Figure 5.10b). In healthy cultures, miR-23a was decreased ~60% subsequent to infection at 48 hours and decreased by ~70% after 72 hours. In asthmatic cultures, miR-23a was decreased ~68%

subsequent to infection at 48 hours and decreased by ~76% by 72 hours. There was no significant difference in the miR-23a decrease between healthy and asthmatic ALIs—though there appeared to be a trend for the microRNA to decrease more in response to virus in the asthmatic group.

MiR-200b was significantly decreased in response to HRV-16 at 48 and 72 hours ($p=0.0313$) in healthy cultures (Figure 5.10c) and at 48 hours in asthmatics ($p=0.0313$)(Figure 5.10d). In healthy cultures this significant decrease equated to ~32% in response to virus at 48 hours and ~17% at 72 hours. In asthmatic ALI cultures, this percentage decrease was lower at 24 hours ~28% at 48 hours and although there was a greater percentage decrease at 72 hours in response to virus ~35%, this was not statistically significant.

Though miR-200c belongs to the same microRNA family as miR-200b/429, it did not decrease significantly in response to HRV-16 in any experimental condition (Figure 5.10e-f). In ALI cultures from healthy patients, miR-200c was slightly decreased in response to virus at 24 and 48 hours but was slightly elevated by 72 hours post-inoculation. In asthmatic cultures, miR-200c was slightly elevated in response to virus at 24 hours but was at comparable levels at both 48 and 72 hours after infection.

MiR-429 was significantly decreased in response to virus compared to the UV-RV control in both healthy and asthmatics. In healthy ALIs, miR-429 was significantly decreased at 24 ($p=0.0313$), 48 ($p=0.0313$) and 72 ($p=0.0313$) hours (Figure 5.10g). In asthmatic cultures, miR-429 was significantly decreased at 48 and 72 hours ($p=0.0313$)(Figure 5.10h). In the healthy cohort, there was a decrease to ~78% in miR-429 in response to virus at 24 hours which further decreased to ~52% and 60% at 48 and 72 hours respectively. MiR-429 was decreased to ~70% in HRV-16 compared to UV-RV at 48 hours and this reduced further to a ~61% reduction by 72 hours in asthmatic ALIs.

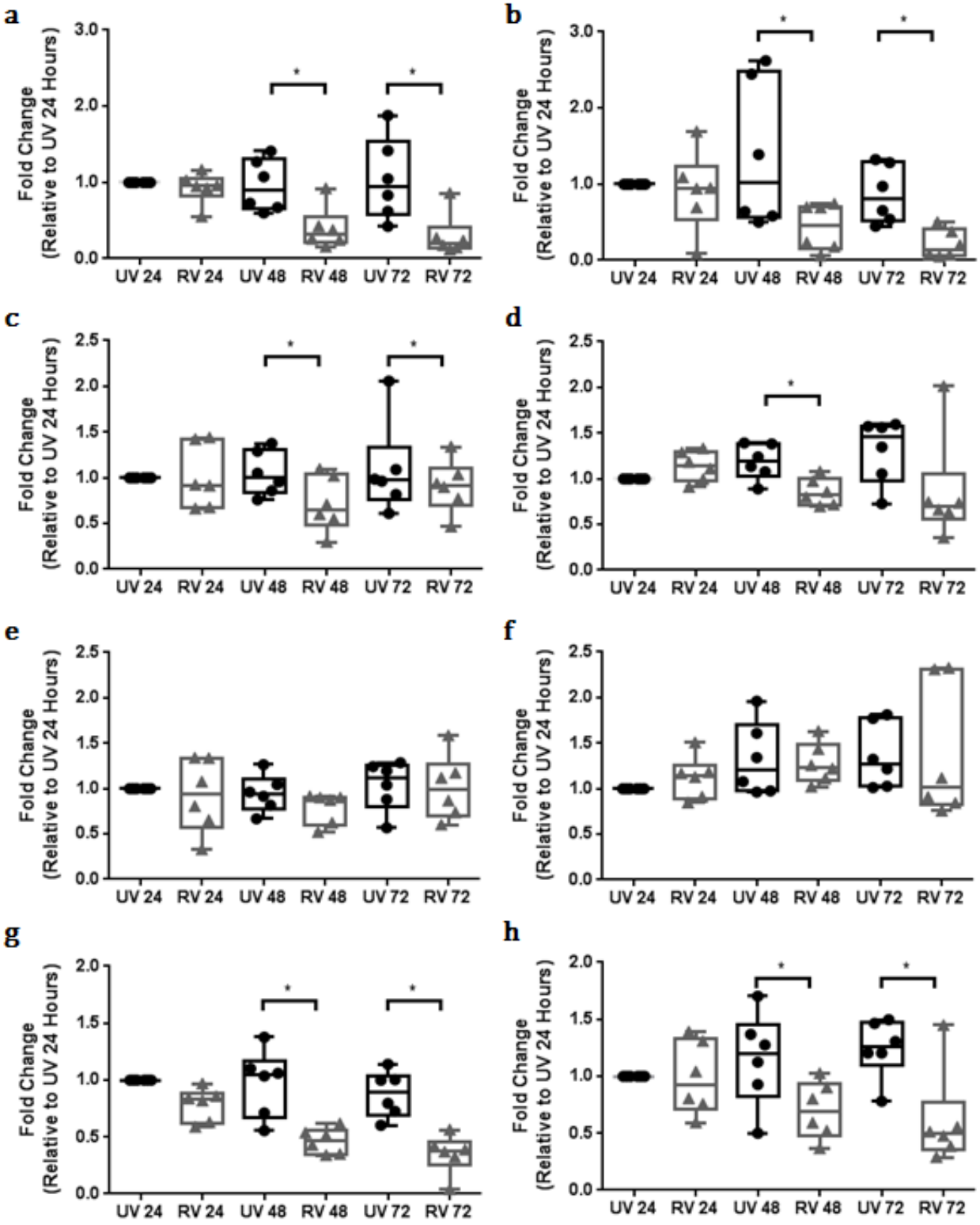

Figure 5.10: RT-qPCR quantification of miR-23a (a-b); miR-200b (c-d); miR-200c (e-f) and miR-429 in response to UV-RV (UV) and HRV-16 (RV) 24-72 hours post-infection in ALI cultures from healthy (a, c, e, g) and asthmatic (b, d, f, h) donors. Samples were normalised to UV-24 to give relative fold-change. Graphs represent n=6, p=*≤0.05calculated via Wilcoxon matched pairs, signed rank test. Expressed as median and interquartile range with minimum/maximum shown

5.9.3: Predicted Target mRNA Responses during HRV-16 Infection in ALI Cultures

Bioinformatic predictions had highlighted several targets of miR-23a, -200b, -200c and -429 that could be involved in modulating the epithelial barrier and innate immune responses during HRV-16 infection. MicroRNAs are known to be able to modify the post-transcription, pre-translation events by either causing mRNA degradation or translational suppression (Chapter 1, Section 1.5.2)—as such it was decided to quantify mRNA levels of ZEB1 (miR-23a, -200b, -200c, -429 target), E-Cadherin (miR-23a target), TNFAIP3 (miR-23a, -200b, -429 target) and Occludin (miR-200b, -200c, -429 target) to check they were coexpressed and elucidate whether these microRNAs might exert an effect on mRNA degradation (Figure 5.11).

In healthy ALI cultures, ZEB1 levels were almost identical between HRV-16 and UV-RV at 24 hours. At 48 hours, there were no statistically significant changes in levels of ZEB1mRNA. Asthmatic cultures also showed no statistically significant changes in mRNA levels across time points post infection by HRV16 (Figure 5.11a-b).

In ALI cultures derived from healthy patients, E-Cadherin mRNA was significantly decreased in response to virus at 24 hours ($p=0.0313$) in healthy cultures. At 48 and 72 hours, E-cadherin mRNA levels were not significantly altered in response to HRV-16 when compared to the UV-RV control. E-cadherin mRNA was not significantly changed in response to virus at any time point in asthmatic ALI cultures (Figure 5.11c-d).

Healthy ALI cultures showed higher levels of TNFAIP3 mRNA in response to HRV-16 when compared to UV-irradiated control throughout all of the observed time-points. This increase was not statistically significant, although at 72 hours it was nearing significance with $p=0.0781$ observed. TNFAIP3 mRNA levels were significantly elevated in response to virus at 48 hours ($p=0.0313$) in asthmatics, with a trend of higher mRNA level also present at 24 hours though this was not significant ($p=0.072$)(Figure 5.11e-f).

Occludin mRNA levels were significantly increased in response to HRV-16 compared to UV-RV in both the healthy and asthmatic cultures. Healthy ALI cultures showed a significant increase in occludin mRNA at 48 hours ($p=0.0313$). In the asthmatic cohort, occludin mRNA was significantly increased at 48 ($p=0.0469$) and 72 ($p=0.0313$) hours

in response to infection. Additionally there was a trend for mRNA elevation at 24 hours ($p=0.0781$) in response to virus (Figure 5.11g-h).

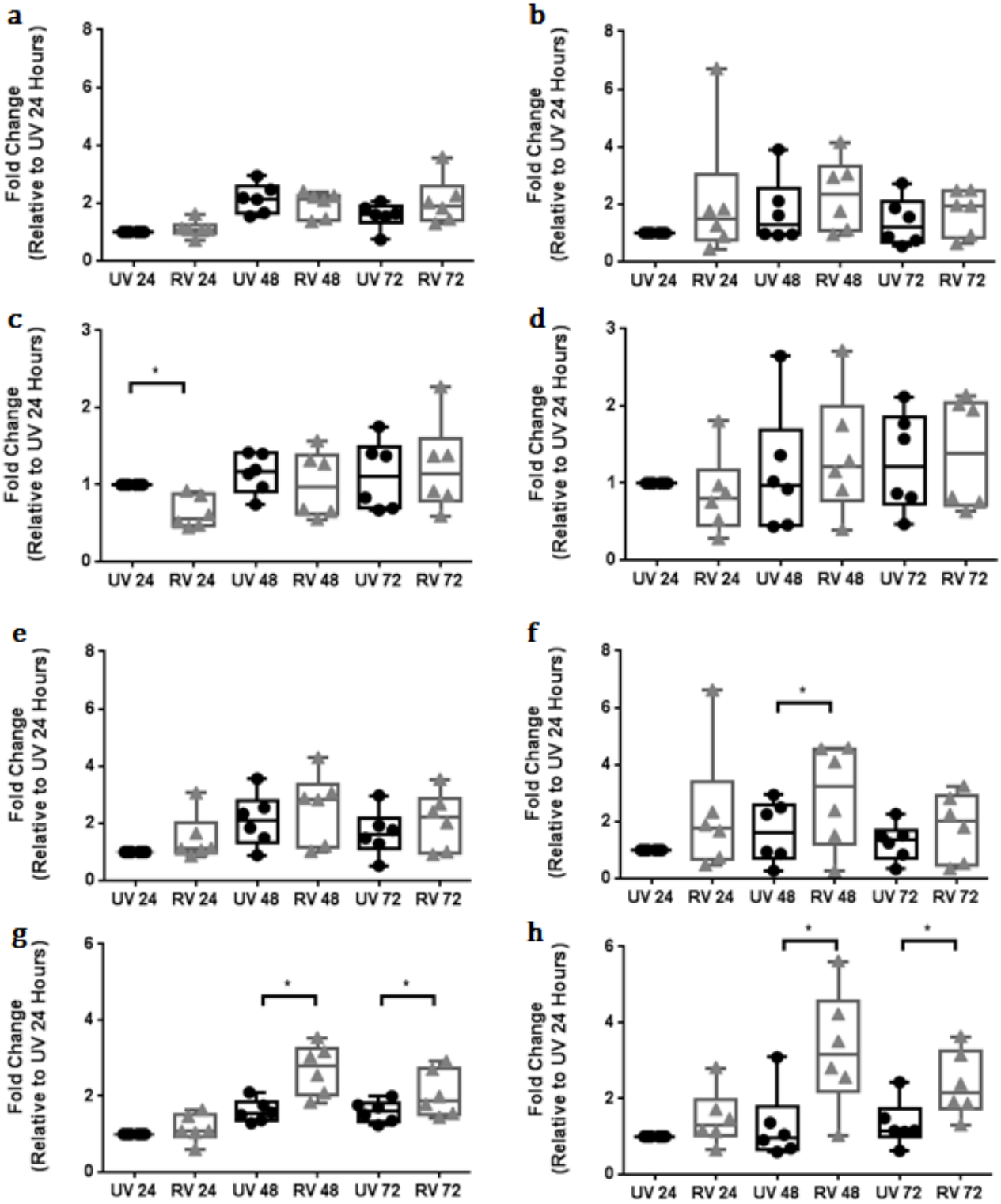

Figure 5.11: RT-qPCR quantification of ZEB1 (a-b); E-cadherin (c-d); TNFAIP3 (e-f) and occludin mRNA in response to UV-RV (UV) and HRV-16 (RV) 24-72 hours post-infection in ALI cultures from healthy (a, c, e, g) and asthmatic (b, d, f, h) donors. Samples were normalised to UV-24 to give relative fold-change. Graphs represent n=6, p=*≤0.05 calculated via Wilcoxon matched pairs, signed rank test. Expressed as median and interquartile range with minimum/maximum shown

5.10: Discussion (II)

In this part of my study I have tested the hypothesis that infection of ALI differentiated cultures of primary bronchial epithelial cells with HRV16, results in changes in expression of miRNA-23a, and 200 family members. In addition I have sought to establish that specific mRNAs for putative targets of these miRNAs, namely ZEB1, E-cadherin, TNFAIP3 and occludin, are coexpressed in the same infected airway epithelial cells.

Primary differentiated ALI cultures of bronchial human airway cells are widely considered to be the most physiologically relevant model of airway epithelium (Pezzulo, Starner et al. 2011, Stewart, Torr et al. 2012). Cells cultured at ALI for 21 days are shown to be highly differentiated and architecturally resemble the pseudostratified layer observed *in vivo* (Berube, Prytherch et al. 2010). In viral infection, it is the columnar epithelial cells of this layer that are the primary site for viral invasion, replication and release—protecting the lower levels of more-infective basal cells from pathogenic materials. To accompany the viral infection, it is seen that these cells are highly efficient at launching an innate immune response to minimise infection and increase pathogen clearance via cellular apoptosis and shedding (Bossios, Psarras et al. 2005).

The ALI cultures used in this experimental series were shown to support HRV-16 infection, replication and viral release by RT-mediated qPCR and TCID50 assays (Figure 5.8). Infection by UV-irradiated virus (therefore replication incompetent) and HRV-16 was shown by genome quantification. Levels of viral RNA were significantly lower in UV infected cultures and did not change over the 72 hour infection period, confirming an absence of replication. HRV-16 infected cultures had much higher levels of vRNA—with no significant differences in genomic material in cultures from healthy or asthmatic donors—which decreased over the 72 hour experiment. Typically it is suggested that rhinovirus infections have a duration of 3-5 days *in vivo* (Lessler, Reich et al. 2009), which aligns with the decline observed here in the ALI cultures suggesting a gradual clearance of the infection. TCID50s confirmed that whilst cells were permissible to uptake of both UV-RV and HRV-16 particles, UV-RV infection did not permit the production or release of infective progeny, whilst HRV-16 led to a significantly higher level of infective progeny being released in to supernatant to propagate further infection. Infective progeny release was highest at 24 hours after infection—aligning with the time of the highest viral copy number and aligning with clinical observations of rhinovirus progeny typically being

observed from 18-24 hours post-initial exposure (Lessler, Reich et al. 2009). Contradictory to Wark et al., there were no significant differences in the viral loads between cultures derived from healthy and asthmatic donors (Wark, Johnston et al. 2005).

To further confirm that ALI cultures responded to HRV-16 infection in a similar manner to that seen *in vivo*, IFN mRNA quantification was carried out. In previous HRV-16 studies, both IFN-β and IFN-λ have been confirmed to be induced in response to viral infection both *in vivo* and *in vitro* (Wark, Johnston et al. 2005, Kotla, Peng et al. 2008, Sykes, Edwards et al. 2012, Becker, Durrani et al. 2013, Gaajetaan, Geelen et al. 2013). Both types of interferon mRNA was significantly elevated in response to HRV-16 compared to UV-RV at all time points in both healthy and asthmatic individuals. As with viral load, there were no significant differences in the IFN mRNA response to virus in the healthy or asthmatic cohorts once again contradicting previously published data (Sykes, Edwards et al. 2012)(Figure 5.9).

As mentioned above, there were no significant differences in the response to virus in ALI cultures from asthmatic and healthy patients—which contradicts Wark et al. (Wark, Johnston et al. 2005) and Sykes, Edwards et al. (Sykes, Edwards et al. 2012) However as discussed in Chapter 1, Section 1.4.3.b, IFN release impairment is a highly contentious issue and a variety of studies—such as Sykes, Macintyre et al. (Sykes, Macintyre et al. 2014)—have been unable to find significant differences between the two patient groups. It is likely, looking at recent understandings of asthma classification and stratification (Corren 2013) that some subsets of asthma present with higher viral loads and impaired type I IFN release, whilst other patients do not. When looking at the 'spread' of the asthmatic IFN-β mRNA response it appears that there are two different clusters of responses, two patients having a lower response (<5-fold mRNA induction at 24 hours) with 4 patients having a higher response (>5-fold mRNA induction at 24 hours) suggesting two different subclassifications of asthma in this cohort—highlighting the need for larger n-numbers, or better clinical classifications, in this study.

MiR-200b, -200c, -429 and 23a were chosen as candidate microRNAs based on previous data (Chapter 1, Section 1.5.3-4)(Figure 5.10). Bioinformatic predictions highlighted several candidate genes involved in epithelial barrier maintenance/repair and innate

immune responses that have predicted binding sites for the microRNAs of interest in their 3'UTRs. What can be concluded from this data is that miR-200b, -429 and -23a significantly decrease in response to HRV-16 infection compared to UV-RV at 48-72 hours in both the healthy and asthmatic cohorts. Though miR-200b, miR-200c and miR-429 belong to the same family (miR-200 family)—miR-200c was not significantly altered in response to HRV-16 infection under any measured condition. Though miRNAs in the same family target the same 3'UTRs generally, each microRNA has its own predicted binding affinity and differential mirSVR score, highlighting a predicted differential biological response to each member of a family (Betel, Koppal et al. 2010). In addition to this, it is known that each microRNA—even those in families—have differential microRNA expression patterns dependent on cellular context. This could suggest that whilst miR-200b and miR-429 are responsive to HRV-16 infection, miR-200c is not and thus levels do not significantly change. Comparison of the microRNA changes between healthy and asthmatic individuals showed no significant difference in miRNA responses in disease—though it seemed though there was a trend for a greater percentage reduction in the asthmatic group. Once again the lack of classification of this asthmatic cohort based on characteristics beyond disease severity may have impeded the results from becoming significant and thus greater sample numbers with greater sub-classifications would be required.

To confirm whether the bioinformatic predictions held any validity, putative target mRNA expression was measured in response to HRV-16 to determine whether these were coexpressed in the cells or whether levels changed in-line with their predicted microRNA regulators (Figure 5.11).

ZEB1 mRNA—the most likely candidate for modulation by the miR-200 family—was not significantly altered in response to HRV-16 in any condition. The lack of ZEB1 mRNA change suggests that the miR-200 family does not modulate the effect of ZEB1 via mRNA degradation but are much more likely to cause translational repression. It is suggested that if a 3'UTR has multiple predicted binding sites for the same microRNA—it is a likely candidate for translational suppression (Valencia-Sanchez, Liu et al. 2006). This suppression is achieved through impeding translational initiation through interference either with the 5'cap structure or through preventing association of the eIF4F cap-binding complex (Eulalio, Huntzinger et al. 2008). As ZEB1 has 5 predicted binding sites

for miR-200b and miR-429 this makes it highly likely candidate for translational repression.

As a transcriptional repressor of E-cadherin expression, it was postulated that alterations to ZEB1 expression through miR-mediated means would impact upon E-cadherin expression and thus E-cadherin mRNA was measured. E-cadherin mRNA was significantly decreased in response to HRV-16 at 24 hours in healthy individuals. However it was not significantly altered at any other time or condition. As it has already been shown that ZEB1 represses E-cadherin mRNA expression (Gregory, Bert et al. 2008), it would be helpful to do Western blotting to confirm that protein is also reduced. However the significant difference in E-cadherin mRNA at 24 hours in healthy donor cells coincides with the time when most infected cells are undergoing apoptosis and shedding (Turner, Hendley et al. 1982)(Wilkinson Collins, unpublished) Therefore this decrease in mRNA could be part of the response of infected cells to trigger apoptosis and shed. Loss of E-cadherin correlates with induction of apoptosis in some circumstances (Steinhusen, Weiske et al. 2001). Where the changes in E-cadherin mRNA are not significant, it may be a reflection of most shedding occuring at 24 hours and residual cells may be trying to repair the barrier at later time points. Also the lack of significant change in E-cadherin mRNA asthmatic cells may reflect a delayed apoptotic response (REF). The lack of mRNA decrease at the majority of time points could mean that either the miRNA changes have no impact on ZEB1 expression or are not significantly decreased enough to elevate ZEB1 and effect E-cadherin. Additionally it could mean that in this specific circumstance, ZEB1 may act to prevent significant changes to E-cadherin expression in response to HRV-16 infection and thus this maintains a steady level.

TNFAIP3/A20 has a stable predicted binding site for miR-23a in its 3'UTR in addition to a predicted binding site with a low mirSVR score for members of the miR-200 family. In response to HRV-16, TNFAIP3/A20 mRNA is increased significantly in asthmatics at 48 hours. As there is this elevation in response to viral infection at significantly decreased miRNA-23a, -200b and -429 levels, it suggests that these microRNAs might be exerting an effect via mRNA degradation (Chapter 1, Section1.5.2). It has been suggested the miRNAs with only 1 predicted binding site in the 3'UTR of a target mRNA are more likely to trigger a mRNA degradation event (Valencia-Sanchez, Liu et al. 2006) via either endonucleolytic cleavage, RISC-associated cleavage or SLICER independent degradation

(Ameres and Zamore 2013). Examination of the 3'UTR of TNFAIP3/A20 shows only one binding site for both miR-23a and miR-200 family members, thus indicating it a likely target for mRNA degradation.

Alterations to TNFAIP3/A20 have previously been shown to have impacts on NF-κB signalling (Parvatiyar and Harhaj 2011) as well as potentially enhancing epithelial barrier integrity through stabilisation of occludin in TJs through deubiquitination (Kolodziej, Lodolce et al. 2011). In addition, the 3'UTR of occludin has a predicted seed sequence for miR-200b, -200c and -429 which is why occludin mRNA response to HRV-16 was assessed. Occludin mRNA was significantly elevated in response to HRV-16 and significantly decreased miRNAs at 48 and 72 hours in both healthy and asthmatic ALI cultures. This suggests that miR-200 family members may act at the level of mRNA degradation to regulate occludin expression which, as previously discussed, aligns with what is currently proposed regarding microRNA regulation as there is only 1 target site for the microRNAs of interest in the 3'UTR of occludin (Valencia-Sanchez, Liu et al. 2006). In addition to this, it may provide further evidence for TNFAIP3/A20 stabilising occludin and limiting' proteosomal degradation—as increased TNFAIP3/A20 is correlated to increased occludin in this experimental set up—though this would warrant further investigation before a solid conclusion could be drawn.

The microRNA and mRNA responses observed here occur at the later time points of 48 and 72 hours post-infection in both healthy and asthmatic donors. At these later times not only are the ALI cultures supporting HRV-16 replication and particle release, but they are additionally significantly upregulating the expression of IFN-β and IFN-λ mRNA and responding to IFN-β and IFN-λ. These events—though linked—have two opposing outcomes and thus give rise to two distinct cellular populations. The first population of cells is the infected cells which respond to the HRV-16 infection by upregulating levels of ICAM-1 expression on the cell surface (Papi and Johnston 1999), elevating expression of cytokines/chemokines involved in the innate immune response (Subauste, Jacoby et al. 1995) and increasing cellular apoptosis and shedding (Turner, Hendley et al. 1982). The second population of cells are the uninfected cells which are responding to the innate immune mediators that have been released from neighbouring infected cells—primarily the type I and III IFNs to cause the upregulation of genes involved in antiviral state adoption to decrease the potential infectivity of these cells (Goodbourn, Didcock et al.

2000, Levy and Garcia-Sastre 2001, Durbin, Kotenko et al. 2013). This means the current experimental set-up is showing amalgamated results from distinct cell populations—the virally infected and the antivirally adoptive state cells.

It has previously been shown that microRNA levels can alter in response to infection—miR-155 is elevated in response to *Helicobacter pylori* infections (Ma, Becker Buscaglia et al. 2011). Epstein Barr virus has been shown to elevate miR-155 and miR-146 in B-cells (Imig, Motsch et al. 2011). MiR-128 and miR-155 are able to regulate HRV-1B infection through inhibiting viral replication and, interestingly, both have been shown to be under-expressed in bronchial cells from asthmatics (Bondanese, Francisco-Garcia et al. 2014). Therefore the differential microRNA expression observed during infection could be directly related to HRV-16 replication. It has also been shown that microRNAs can be directly modulated by IFNs. Treating Huh7 cells with exogenous IFN-β has been shown to cause upregulation of a number of miRNAs including miR-1 and miR-196 and downregulate expression of others such as miR-122. MiR-26a expression has been shown to increase in response to exogenous IFN-α treatment in hepatocellular carcinoma cells (Wang, Sun et al. 2015) whilst IFN-γ treatment can upregulate miR-29b expression in colorectal cancer cells (Yuan, Zhou et al. 2015). Therefore the differential microRNA expression observed here could be in response to IFN release and subsequent signalling.

Therefore it is hypothesised that the microRNA changes observed in the ALI cultures are caused by viral replication or by IFNs or even both. This could go some way to further explain why the monolayers do not have a similar microRNA response during infection as they have lower HRV-16 infection and have lower IFN mRNA induction compared to ALI cultures, even though monolayers have been infected with a higher MOI of 2. Currently it is impossible to elucidate which of these responses are leading to the microRNA changes—or whether it is perhaps a combinatorial effect—which warrants further investigation. Chen et al. have previously shown that in infection of HBECs with HRV-16 at MOI=10, only ~5% cells become infected (Chen, Hamati et al. 2006). It has additionally been shown that these infected cells appear as discrete patches (~10% of surface area), surrounded by regions of uninfected cells (Mosser, Brockman-Schneider et al. 2002). This suggests that >90% of cells are uninfected and thus are liable to be responding to the innate immune mediators. The response of ALI differentiated primary human cultures will be the subject of my next chapter of experimental study.

CHAPTER SIX: Changes to MicroRNAs and other Epithelial Barrier Characteristics in Response to IFN Treatment in ALI Cultures

6.1: Introduction

As discussed in the previous chapter, HRV-16 infection of the upper airway epithelium results in a sub population of infected cells surrounded by uninfected cells (Mosser, Brockman-Schneider et al. 2002, Mosser, Vrtis et al. 2005). Though both these cell populations are responding to the presence of virus—the manner in which they respond is different.

Infected epithelial cells are the site at which HRV-16 particles have bound to ICAM-1 receptors on the epithelial surface and internalised, subsequently leading to viral uncoating, replication and translation—culminating in the production of infectious progeny (Fuchs and Blaas 2010, Fuchs and Blaas 2012, Jacobs, Lamson et al. 2013). During this process of viral internalisation and genome replication, PAMPs and dsRNA are detected by RIG-I and MDA5, activating a number of signalling cascades which trigger a cellular response to the virus, culminating in the activation of the proinflammatory immune response through upregulation of cytokines/chemokines—leading to innate immune cell recruitment/activation (Tosi 2005, Parker and Prince 2011). Importantly, type I and III IFNs are also produced in infected cells upon activation of the TLR-3 and TLR-7 signalling cascades, by dsRNA/PAMPs, which lead to the expression and release of IFN-β and IFN-λ and the upregulation of IFNs act protectively on neighbouring cells in the airway as antiviral immune mediators (Goodbourn, Didcock et al. 2000, Levy and Garcia-Sastre 2001, Durbin, Kotenko et al. 2013).

Therefore uninfected epithelial cells are not responding directly to viral binding, entry and replication, but instead are responding to signals at the epithelial surface some of which are being released by the neighbouring infected cells (Goodbourn, Didcock et al. 2000, Levy and Garcia-Sastre 2001, Durbin, Kotenko et al. 2013). Thus IFNs act in both autocrine and paracrine manners, binding to their specific IFN receptors which are

expressed on a number of cellular surfaces, including the airway epithelium (de Weerd and Nguyen 2012). The binding of IFNs to receptors triggers a conformational change in the receptor, allowing for activation of the JAK-STAT mediated signalling pathways which culminate in upregulation of ISG expression leading to cells adopting an antiviral state: thus these neighbouring uninfected cells are less permissible to viral infection (Yoneyama, Suhara et al. 1998, Levy and Garcia-Sastre 2001, Takaoka and Yanai 2006, de Weerd, Samarajiwa et al. 2007, Uze and Monneron 2007, Iversen and Paludan 2010).

Data obtained in Chapter 5, Part II indicated that the microRNAs of interest significantly decreased during HRV-16 infection in ALI cultures derived from both healthy and asthmatic donors. However these significant changes were not seen until 48-72 hours post-infection. At these later points, in addition to elevated levels of HRV-16 vRNA and viral particle release, there were also significant increases in the expression of IFN-β and IFN-λ mRNA. This data suggests that in the experimental setup, cells are responding to both stimuli and thus the miRNA changes represent an amalgamation of both infected and uninfected cell populations. Chen et al. have previously conducted studies that suggest that when HBEC monolayers are infected with HRV at MOI=10, only 5% of the cells in the monolayer become virally infected (Chen, Hamati et al. 2006). Similarly inoculation of epithelium with HRV shows that only a small proportion of cells at the site of inoculation become infected (Mosser, Brockman-Schneider et al. 2002, Mosser, Vrtis et al. 2005) and these infected cells are removed by 24-48 hours (Turner, Hendley et al. 1982). As this experimental setup only uses HRV-16 at MOI=1, it is likely that <5% of cells in ALI cultures become infected, suggesting that >95% of epithelial cells in this model are uninfected cells and thus are likely to be responding to the presence of antiviral acting IFNs. I therefore propose to investigate the effect of exogenous IFN on microRNA expression in uninfected ALI differentiated primary bronchial epithelial cells. As previous data from Chapter 4, Section II showed that miR-200b and miR-429 were both significantly decreased in response to HRV-16, it was decided to focus on assaying one of these microRNAs. As miR-429 showed more significant reductions in response to virus it was chosen as the 'representative' miRNA from the miR-200 family alongside miR-23a for assaying in this experimental series.

Type I IFNs have been shown to be expressed in response to various RNA viruses in a number of tissues. Close examination of the specific cell phenotypes that express and

release the type I IFNs during viral infection show that IFN-α/β are released by a large number of cell types (Trinchieri 2010). Comparatively, the Type III IFNs have a far more limited tissue expression in response to RNA viruses—with strongest expression noted in the stomach, intestine and lungs (de Weerd and Nguyen 2012, Huayllazo 2012). Examination of IFN-λ expression from different cell types suggested highest induction and release in epithelial cells (Sommereyns, Paul et al. 2008). Examination of the distribution of IFN receptor subunits has further supported a more restricted repertoire of cellular targets for IFN-λ compared to IFN-α/β (Sommereyns, Paul et al. 2008, de Weerd and Nguyen 2012, Huayllazo 2012). Co-expression of IFNAR1 and IFNAR2 subunits is found on a large number of cell surfaces including, but not limited to, T-cells, B-cells, endothelial cells and epithelial cells (Huayllazo 2012). Co-expression of IFNLR1 and IL10R subunits is more restrictive and found on fewer cell surfaces limited to eosinophils, keratinocytes, hepatocytes, dendritic cells and epithelial cells (Huayllazo 2012). Of these cell types, IFN-λ receptor expression is highest on epithelial cell surfaces (Sommereyns, Paul et al. 2008, Donnelly and Kotenko 2010). Together this suggests that IFN-λ is primarily promoting antiviral responses at epithelial cell surfaces including lung. Therefore it was of interest to investigate the release of IFN-λ from infected ALI differentiated primary airway epithelial cells and to explore whether microRNA levels are affected by exogenous IFN stimulation in the absence of virus infection.

In the context of IFN effects on airway epithelium, I decided to explore the effect of IFN-λ in both an intact epithelial barrier and a damaged/repairing epithelial barrier. A fully differentiated ALI culture has a tight, intact epithelial barrier (Stewart, Torr et al. 2012) and thus treating these cultures for 72 hours with IFN-λ aims to examine the effect of IFN in the absence of the virus; allowing for determination of whether miRNA change can be directly attributable to IFN-λ responses. A differentiating ALI culture is actively elaborating a new epithelial barrier, which mimics the barrier repair process observed in response to HRV-16-mediated cell shedding (Erjefalt and Persson 1997); allowing for determination of the effect IFN-λ has on barrier homeostasis and whether this correlates with changes in the expression of specific miRNAs. Additionally it has been noted that epithelial barrier integrity (de Boer, Sharma et al. 2008, Yeo and Jang 2010, Xiao, Puddicombe et al. 2011) and repair (Holgate 2007) is impaired in asthmatics—allowing for further exploration of whether asthmatics have a differential response to IFNs.

Numerous microRNAs have been shown to alter in response to the presence of IFN, which leads to the alteration of cellular characteristics. MiR-26a expression is enhanced in hepatocellular carcinoma cells in response to exogenous IFN-α treatment which in turn leads to decreased expression of EZH2, causing inhibition of cellular proliferation (Wang, Sun et al. 2015). IFN-γ treatment of colorectal cancer cells causes upregulation of miR-29b expression which leads to decreased cell growth mediated by the miR-29b target, IRF-1 (Yuan, Zhou et al. 2015). MiRNAs can also alter the IFN-induced signalling cascade and impact upon the antiviral state adoption. MiR-1231 has a predicted binding site on the 3'UTR of IFNAR1 which may indicate its' role in IFN-α/β immune signalling. Polymorphisms in the miR-1231 binding region has been shown to be linked to hepatitis B pathogenesis and hepatocellular carcinoma (Sedger 2013). MiR-155 can target STAT-1 which in turn can affect a number of STAT-1 mediated signalling cascades, including type I and III IFNs and impact upon antiviral gene expression—such as MxA (Sedger 2013). Another miRNA family implicated in modulation of antiviral gene expression is the miR-29 family. Increased miR-29 expression has been shown to downregulate RNAse-L both independently (non-stress) and via antagonistic effects via HuR (stress)(Lee, Ezelle et al. 2013).

6.2: Hypothesis, Aims and Objectives

Exogenous IFN-λ causes changes in the expression level of miR-23a and miR-429 in (a) differentiated and (b) differentiating ALI primary bronchial epithelial cultures leading to altered expression of predicted targets ZEB1, TNFAIP3/A20, occludin and E-cadherin, correlating with altered epithelial barrier characteristics.

Aim: To confirm IFN-λ protein release in response to HRV-16 to then subsequently treat HBECs during and after culture differentiation to determine if selected miRNAs alter in response. To assess whether miRNA changes are correlated with changes in mRNA/protein levels of bioinformatically predicted targets and alterations in epithelial barrier.

Objective(s):

- To confirm IFN-λ protein release from HRV-16 infected ALI cultures (via ELISA)
- To assess changed in miR-429 and miR-23a levels in response to exogenous IFN-λ treatment:

(a) Every 24 hours for 72 hours in fully differentiated HBEC ALI cultures

(b) Every 7 days during 21 day differentiation of HBEC ALI cultures

- To assess changes in mRNA (via RT-qPCR) and protein (via western blotting) changes of miRNA predicted targets in both (a) and (b)
- To assess the effect of exogenous IFN-λ on epithelial barrier integrity in both (a) and (b) and assess whether there is a correlation with miRNA expression.

6.3: Results

6.3.1: IFN-λ Protein Responses during HRV-16 Infection in ALI Cultures

In Chapter 4, Part II IFN-λ mRNA was shown to be significantly elevated in response to HRV-16 infection compared to UV-RV control at 24, 48 and 72 hours in both healthy and asthmatic ALI cultures. Media supernatants from these cultures were assessed to assay release of IFN-λ protein in response to viral infection (Figure 6.1). In healthy individuals, IFN-λ protein was significantly elevated in response to HRV-16 at both 24 and 48 hours ($p=0.0156$). Peak IFN-λ protein was detected at 48 hours with a median of approximately of 1000 pg/ml present in supernatants (Figure 6.1a). In asthmatic individuals, IFN-λ protein was once again significantly increased in response to HRV-16 at 24 and 48 hours ($p=0.0313$) with a median release of ~500pg/ml detected. As with healthy donor cells, peak IFN-λ protein release in supernatant was detected at 48 hours post-infection. Levels of IFN-λ protein were generally lower in culture supernatants from asthmatic donor cells at 24 hours compared with cell supernatants from healthy donor cultures, with the exception of high readings in two asthma donor supernatants (Figure 6.1b). These differences between protein release in supernatant between healthy and asthmatic donor cultures were not statistically significant.

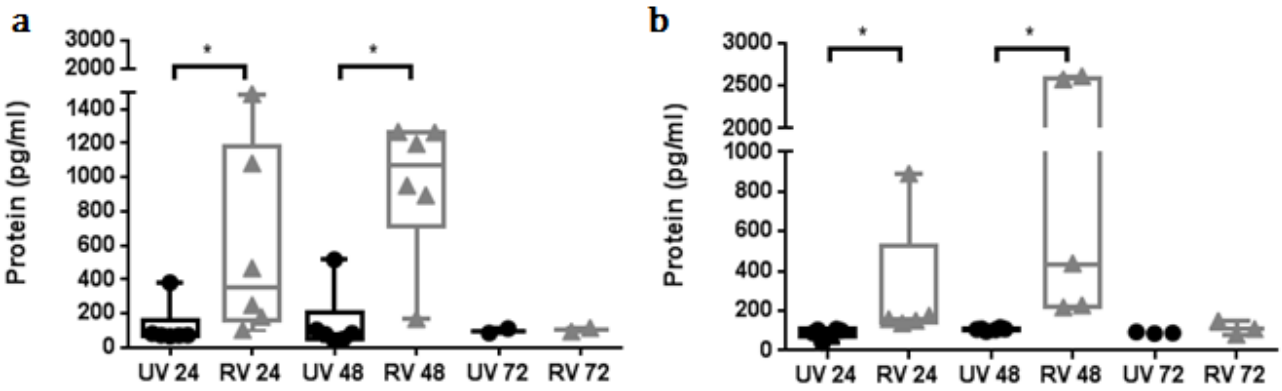

Figure 6.3: ELISA quantification of IFN-λ from supernatants of UV-RV (UV) and HRV-16 (RV) infected ALI cultures from healthy (a) and asthmatic (b) donors. Graphs represent n=6 (except 72 hours where n=2 (a) and n=3 (b), p=*≤0.05calculated via Wilcoxon matched pairs, signed rank test). Expressed as interquartile range and mean with 95% confidence intervals shown

6.3.2: Effect of Exogenous IFN-λ on 21 day ALI Differentiated Bronchial Airway Epithelial Cultures

IFN-λ protein assays from HRV-16 infected ALI cultures confirmed levels of ~1000pg/ml (therefore 1ng/ml) in response to viral infection. To ensure the exogenous treatment model remained physiologically relevant, it was decided to treat uninfected cells with a concentration of 1ng/ml of IFN-λ which was replaced every 24 hours over the experimental duration. In the 21 day differentiated ALI model (intact epithelial barrier checked with TER assays), this was exogenous treatment of 1ng/ml IFN-λ for 72 hours to reflect timings of miRNA expression assayed during HRV-16 infection experiments.

To confirm ALI cultures were responding to exogenous IFN-λ, mRNA levels of the ISG MxA GTPase was measured via RT-qPCR (Figure 6.2). Previous experiments have confirmed significant induction of MxA expression in response to exogenous IFN treatment (9.94 fold induction)(Rusinova 2013) and HRV-16 infection (9.01 fold induction)(Chen, Hamati et al. 2006). MxA mRNA was significantly induced in response to exogenous IFN-λ treatment at 24, 48 and 72 hours when compared to an untreated control in healthy ALI cultures. MxA mRNA was most significantly induced in healthy cultures after 24 hours of IFN-λ treatment (Figure 6.2a). In asthmatic cultures, MxA mRNA was elevated in IFN-λ treated cells compared to untreated cells but this was not significant. One sample showed greatly induced levels at 48 hours in cells from an asthmatic donors at ~150 fold compared to untreated cells, however of n=3, it appears 2 samples had a much lower fold-induction of MxA mRNA, suggesting that the asthmatic donor cells might be less responsive to IFN-λ (Figure 6.2b). Statistically a comparison of mean MxA fold-change showed no significant differences between MxA mRNA induction in asthmatic and healthy individuals.

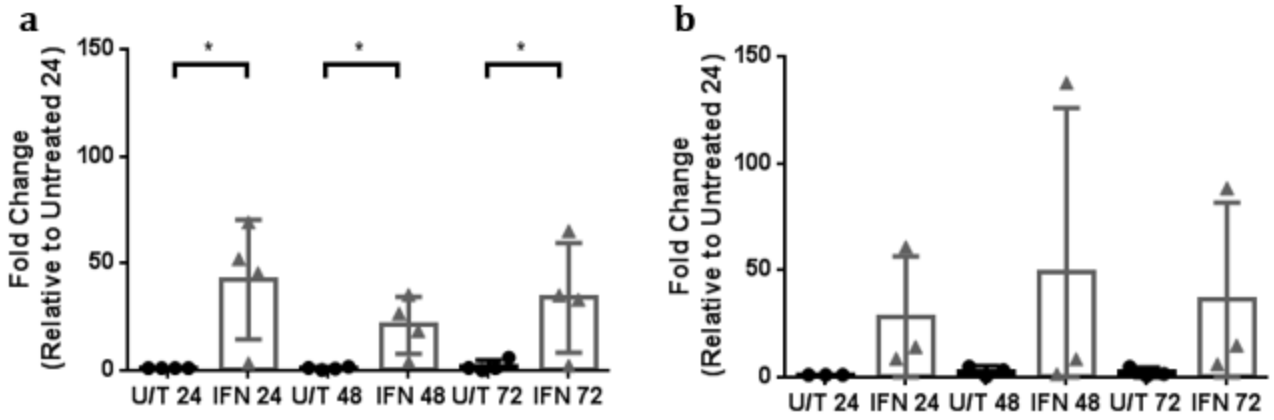

Figure 6.2: RT-qPCR quantification of MxA GTPase mRNA in untreated (U/T) and IFN-λ treated (IFN) differentiated ALI cultures from healthy (a) and asthmatic (b) donors. Graphs represent n=4 (healthy) and n=3 (asthmatic), p=*≤0.05calculated via two-tailed Paired T-test. Error bars= SD.

6.3.3: IFN-λ Treatment and MicroRNA Expression in 21 day Differentiated ALI Bronchial Airway Epithelial Cultures

After confirming that the ALI cultures were responding to exogenous IFN-λ treatment, miR-23a and miR-429 levels were assessed using RT-mediated qPCR assays as previously described (Figure 6.3). MiR-23a was significantly decreased in response to IFN-λ treatment at 24 ($p=0.0091$), 48 ($p=0.0313$) and 72 ($p=0.0105$) hours in cultures from healthy donors. MiR-23a was significantly decreased at 24 ($p=0.0286$) and 48 hours ($p=0.0484$), in response to IFN treatment, in cultures from asthmatics—with levels changing at 72 hours, but not significantly ($p=0.1043$) (Figure 6.3a-b).

MiR-429 was significantly decreased in response to IFN-λ treatment at 24 ($p=0.0297$), 48 ($p=0.0397$) and 72 ($p=0.0383$) hours in ALI cultures from healthy donors. Whereas MiR-429 levels were not significantly decreased in response to IFN-λ at any time in cultures from asthmatic donors (Figure 6.3c-d).

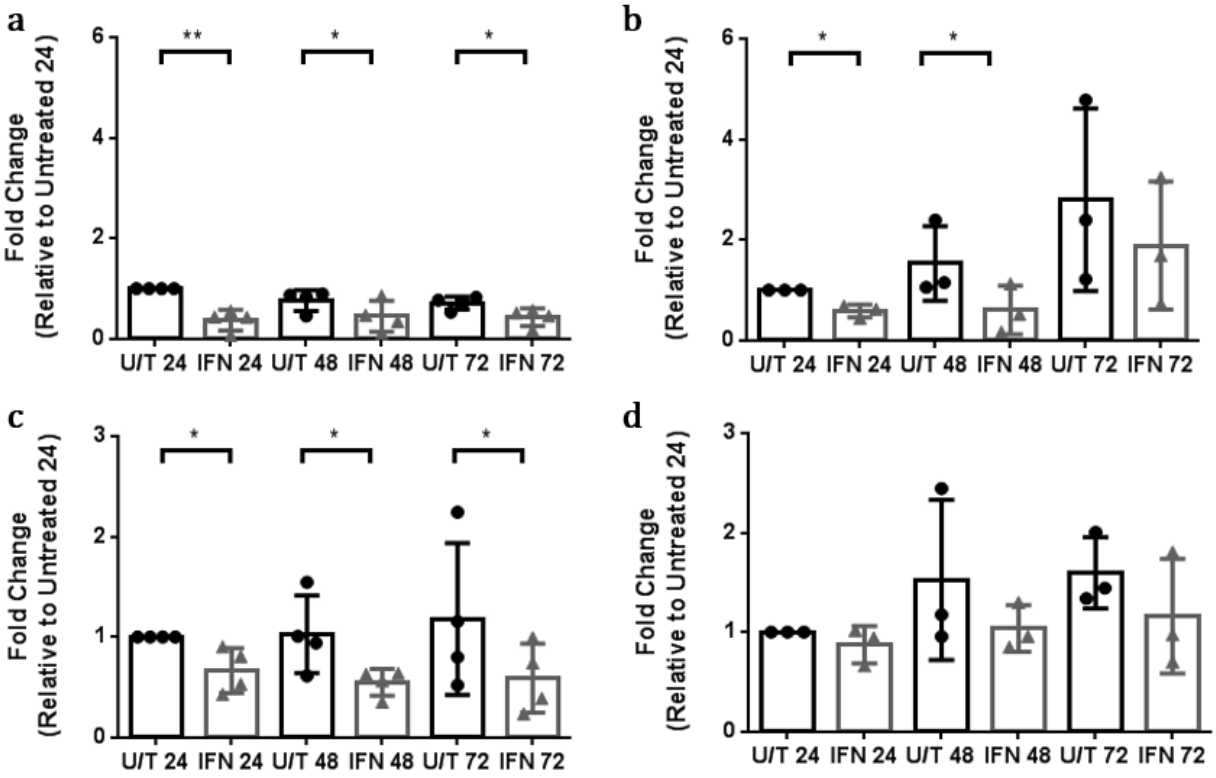

Figure 6.3: RT-qPCR quantification of miR-23a (a-b) and miR-429 (c-d) in untreated (U/T) and IFN-λ treated (IFN) differentiated ALI cultures from healthy (a-c) and asthmatic (b-d) donors.. Graphs represent n=4 (healthy) and n=3 (asthmatic), p=*≤0.05; p=**≤0.01 calculated via two-tailed Paired T-test. Error bars= SD

6.3.4: Effect of IFN-λ Treatment of Differentiated ALI Cultures on Expression of Predicted mRNA Targets of miRNAs

Bioinformatic predictions in Chapter 3 highlighted four potential miR-23a/429 messenger RNA targets that could encode proteins that play a role in epithelial barrier maintenance and innate immune responses: ZEB1 (miR-23a, -429 target), E-cadherin (miR-23a target), TNFAIP3 (miR-23a, -429 target) and occludin (miR-429 target). These mRNAs were assayed to determine their relative expression levels, in response to IFN-λ treatment, in order to assess whether the timing of significant reductions in miR-23a and -429 expression could be correlated to changes in target mRNAs (Figure 6.4).

In ALI cultures from healthy and asthmatic donors, mRNA for ZEB1 was expressed but levels of ZEB1 mRNA did not significantly change in response to IFN-λ treatment at any time point (Figure 6.4a-b). E-cadherin mRNA was expressed, though not statistically significantly changed at any time point, in cultures from healthy or asthmatic donors in response to 24 to 72 hours of exogenous IFN-λ treatment when compared to untreated controls. However, the expression level of E-cadherin mRNA appeared to be lower at 48 and 72 hours of IFN-λ treatment, approaching significance at 72 hours ($p=0.072$) and suggesting that more donor samples would be informative (Figure 6.4c-d). TNFAIP3 mRNA was coexpressed in all cultures and levels from healthy individuals showed a significant elevation in response to IFN treatment at 48 hours ($p=0.0138$) and approaching significance at 72 hours ($p=0.067$). TNFAIP3 mRNA levels in ALI cultures from asthmatic donors also showed a significant elevation in response to exogenous IFN-λ treatment at 48 hours ($p=0.0147$)(Figure 6.4e-f). In cultures from healthy and asthmatic donors occludin mRNA was expressed. In healthy donor cultures, IFN-λ treatment caused an increase that approached significance at 24 hours ($p=0.0863$) and was significant at 48 hours ($p=0.0427$). In asthmatic cultures, occludin mRNA was not significantly altered in response to IFN-λ treatment at any time-point (Figure 6.4g-h).

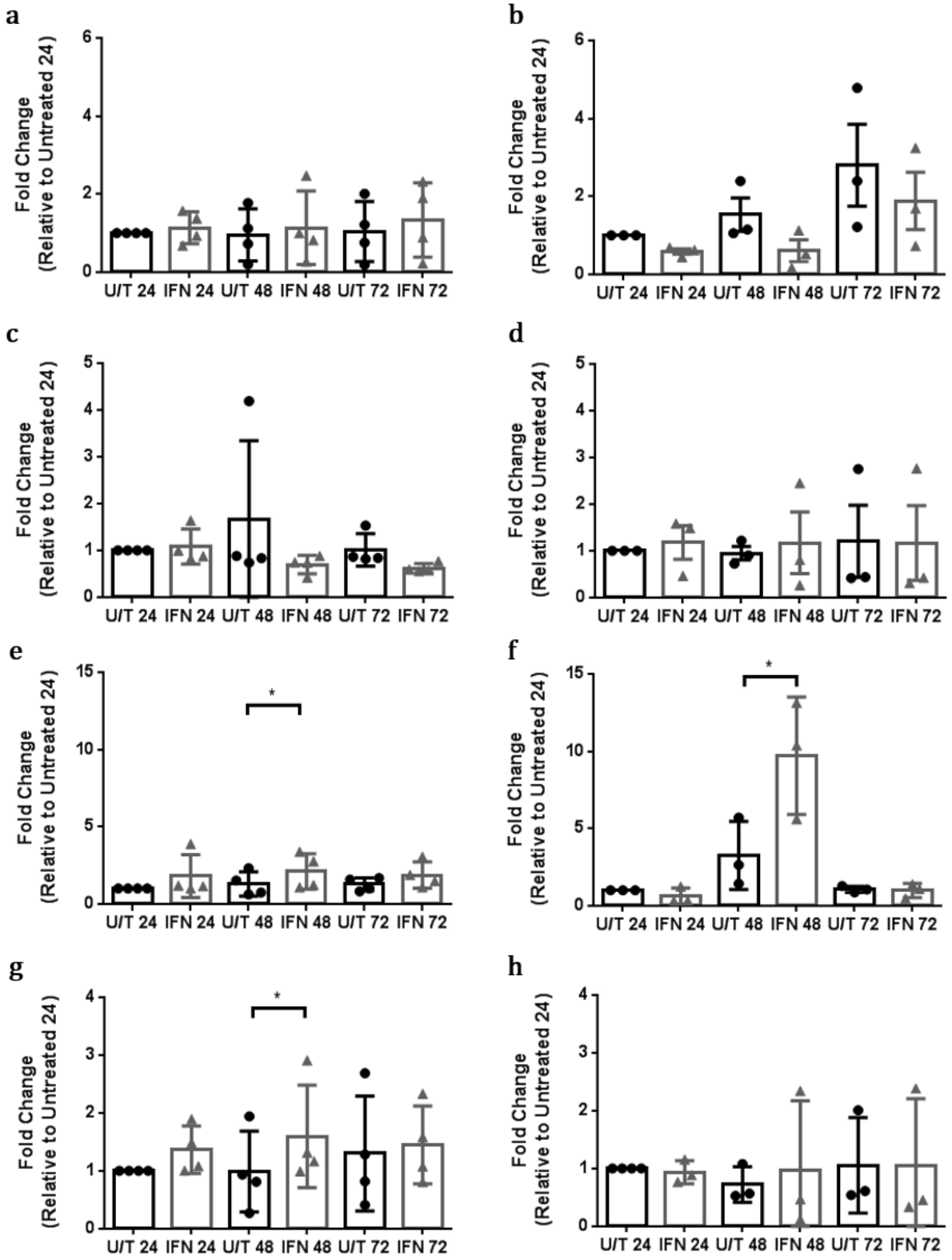

Figure 6.4: RT-qPCR quantification of ZEB1 (a-b), E-cadherin (c-d), TNFAIP3 (e-f) and occludin (g-h) in untreated (U/T) and IFN-λ treated (IFN) differentiated ALI cultures from healthy (a, c, e, g) and asthmatic (b, d, f, h) donors. Graphs represent n=4 (healthy) and n=3 (asthmatic), p=*≤0.05-calculated via two-tailed Paired T-test. Error bars= SD.

6.3.5: Effect of IFN-λ Treatment of Differentiated ALI Cultures on Expression of Proteins encoded by Predicted mRNA Targets of miRNAs

Whilst significant changes in mRNA level might determine altered expression of some predicted miR-23a and miR-429 targets (TNFAIP3/A20, occludin and E-cadherin), this did not confirm altered protein expression of targets. As such, protein lysates from differentiated ALI cultures (treated/untreated) were probed for TNFAIP3/A20, ZEB1 and actin (control) via western blotting to allow quantification and determination of whether miRNA and mRNA changes correlated to differential protein expression (Figure 6.5).

Actin was going to be used as an internal loading and transfer control as well as to provide a protein that ZEB1/A20 could be normalised against for relative sample quantification to determine changes in protein level in response to IFN-λ treatment. However, actin levels were shown to alter in response to exogenous IFN treatment by 72 hours in both healthy and asthmatic samples. This prevented actin from being used as a control. Cytokeratin-18 was also tried as a control, but levels of this protein were below detection thus unable to be to be utilised either. As such ZEB1 and A20 protein were subjected to a 'relative normalisation' process in which:

- The same sample area size was utilised for protein quantification of untreated and treated bands on blot
- Background was subtracted from quantified protein
- Untreated samples were normalised to 1. Treated samples were normalised relative to untreated at the same time point.

ZEB1 could only be detected in n=2 healthy and n=2 asthmatic ALI cultures. In healthy individuals, ZEB1 protein expression increased in response to exogenous IFN-λ treatment relative to untreated controls across all time points. In asthmatic individuals, ZEB1 protein expression was increased in response to exogenous IFN-λ at 24 and 48 hours, with a slight decline in expression relative to untreated control at 72 hours. In both asthma and healthy ALI cultures, ZEB1 protein was most strongly induced relative to control at 24 hours with the relative fold change becoming less pronounced over the subsequent 48 hours.

TNAIP3/A20 protein could not be detected in any patient at any time point despite alterations to primary and secondary antibody concentrations and incubation times.

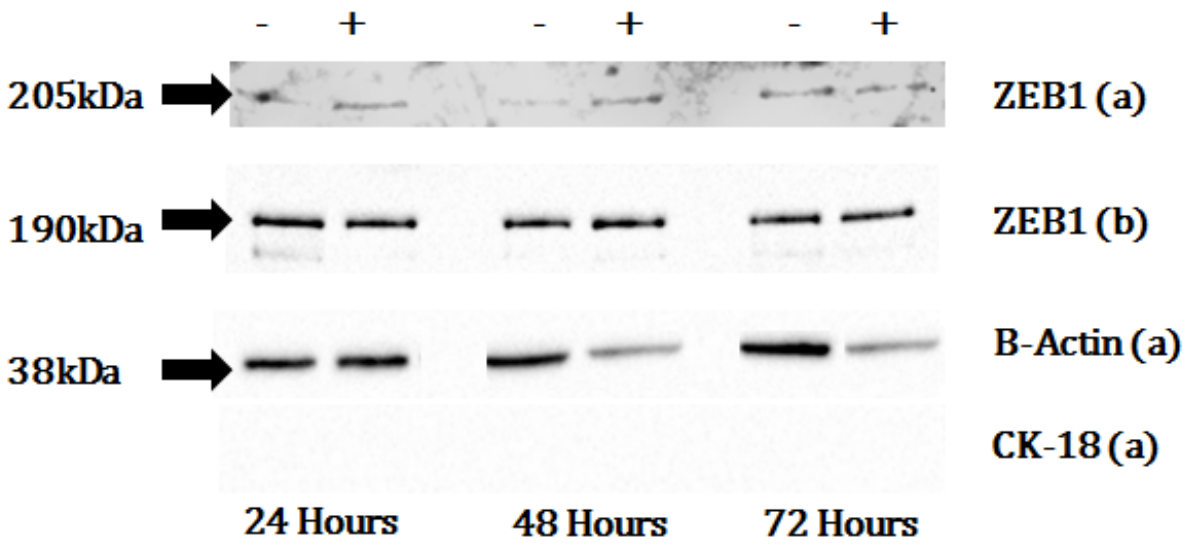

	24: Relative Fold Change	48: Relative Fold Change	72: Relative Fold Change
Healthy	+2.321	+1.457	+1.074
Asthmatic	+2.801	+1.111	-0.993

Figure 6.5: Relative ZEB1 protein changes in Untreated (-) and IFN-λ (+) differentiated ALI cultures from healthy (a) and asthmatic (b) donors with 24-72 hours of treatment. Blots representative of n=2 healthy, n=2 asthmatics. Relative fold change calculated from quantification of intensity of IFN treated against Untreated in BioRad Image Lab Plus.

6.3.6: Characterising the Effect of IFN-λ Treatment of Differentiated ALI Cultures on Epithelial Barrier Permeability and Localisation of E-cadherin and Occludin

6.3.6.a: Epithelial Barrier Integrity

TER measurement was utilised to assess the ionic permeability of ALI cultures during 21 day differentiation. As cells differentiate and an epithelial barrier forms—TER measurements increased. For healthy ALI cultures, TER >1000Ω was normal at 21 days with good barrier formation and cellular differentiation. TER measurements in asthmatic ALI cultures were more variable with some cultures providing TER >1000Ω and other samples <500Ω, however this was considered normal for severe asthmatic ALI cultures due to previous experiments showing reduced barrier in ALI cultures from asthmatic donors (Xiao et al., 2011)(Figure 6.6).

In ALI cultures, from healthy donors, TER appeared lower in response to exogenous IFN-λ treatment across all time points, however these differences were not statistically significant. At 24 hours mean TER measurements decreased by ~200Ω in response to IFN. At 48 hours the response to IFN-λ treatment was less pronounced with only an ~80Ω decrease in mean readings. At 72 hours there was once again a large difference in TER between treated and untreated ALI cultures with a ~300Ω difference. These differences were not significant, although larger sample numbers may have given significant changes (Figure 6.6a). In asthmatic ALI cultures, TER did not decrease significantly in response to exogenous IFN-λ treatment after 24-48 hours. There was a decrease in mean TER after in response to treatment at 72 hours with a decrease of ~200Ω however this difference was not significant (Figure 6.6b).

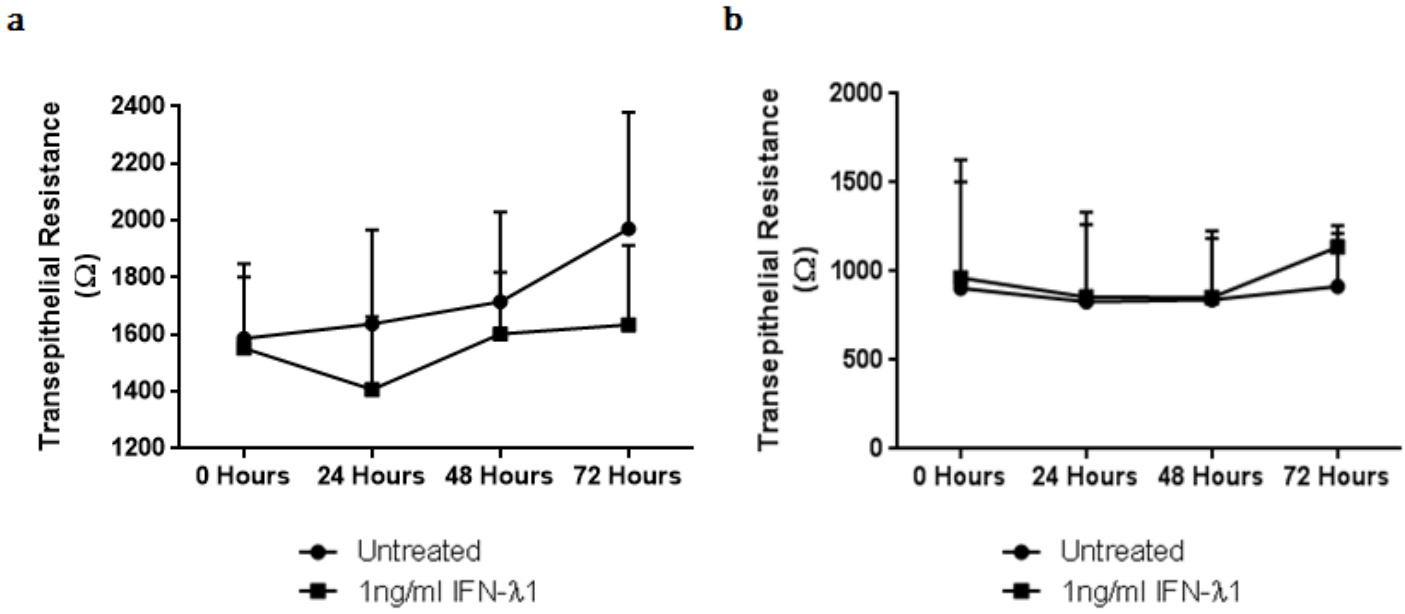

Figure 6.6: Transepithelial Resistance of differentiated ALI cultures from healthy (a) and asthmatic (b) patients over 72 hours of IFN-λ treatment. n=4. Error bars= SD.

5.3.6.b: Morphology of Cultures and Epithelial Barrier Protein Localisation

To further investigate morphological changes and subsequent potential impacts upon epithelial barrier integrity, confocal microscopy was utilised to determine localisation and distribution of two key epithelial barrier proteins E-cadherin and occludin (Figure 6.7-8).

In untreated ALI cultures from healthy donors, cells appeared with a regular 'cobblestone' morphology in which cells formed a continuous, uninterrupted epithelial layer. E-cadherin and occludin protein were shown to be localised to the epithelial junctions with small quantities in cytoplasm. After 72 hours of IFN-λ treatment, there were not large, noticeable changes in cell morphology. However there appeared to be interruption of the epithelial layer as DAPI staining showed regions in which nuclei were absent , giving rise to 'holes' in the culture. Analysis of E-cadherin protein showed isolated regions of increased E-cadherin density/accumulation which correlated with decreased nuclear staining (Figure 6.7a). Analysis of occludin protein showed no significant difference in protein localisation, distribution or intensity in response to IFN-λ treatment (Figure 6.7b).

In untreated cultures from asthmatic donors there was once again uniform 'cobblestone' morphology across the epithelial surface with no apparent disruptions to the layer. Cells appeared to be larger in asthmatic cultures compared to healthy cultures, thus there were fewer cells in each sample section. E-cadherin and occludin protein were localised to epithelial junctions with some distribution in the cell cytoplasm. There appeared to be more cytoplasmic localisation of protein in asthmatic cultures compared to healthy cultures. After 72 hours of IFN-λ treatment, there were no apparent changes in morphology though absence of nuclear staining was once again observed. These were not as widespread in asthmatic cultures. Unlike healthy cultures, these holes did not correlate with altered E-cadherin staining intensity/accumulation (Figure 6.8a). Occludin intensity/localisation did not alter in response to treatment (Figure 6.8b).

a
Untreated
IFN-λ
DAPI
E-Cadherin
Merge
30 µm

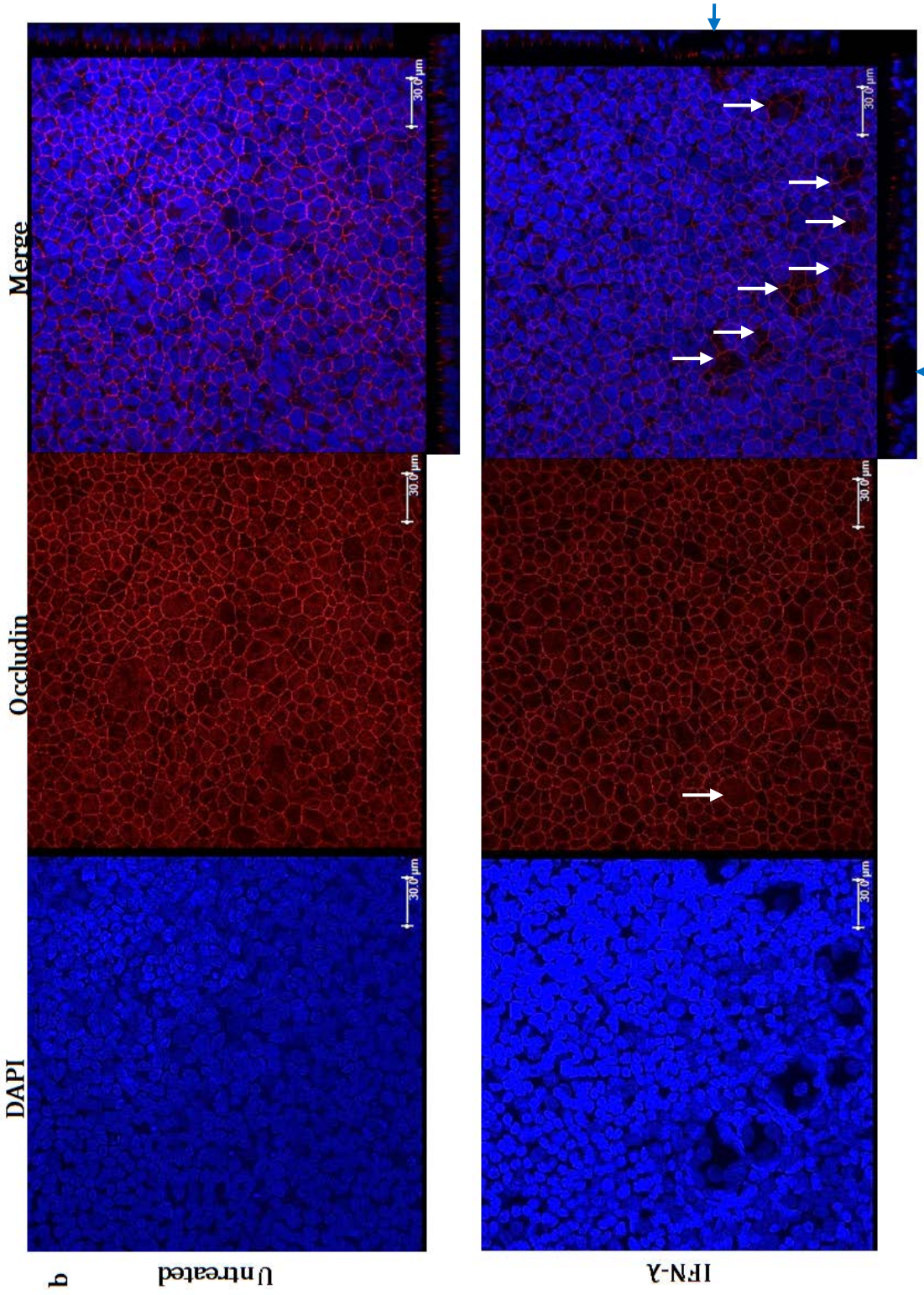

Figure 6.7: Immunofluorescent staining of E-cadherin (a) and occludin (b) in healthy differentiated ALI cultures. Images show localisation and intensity of junctional proteins in control (untreated) and 72 hour IFN-λ treated cultures. Images representative of n=4 experiments.

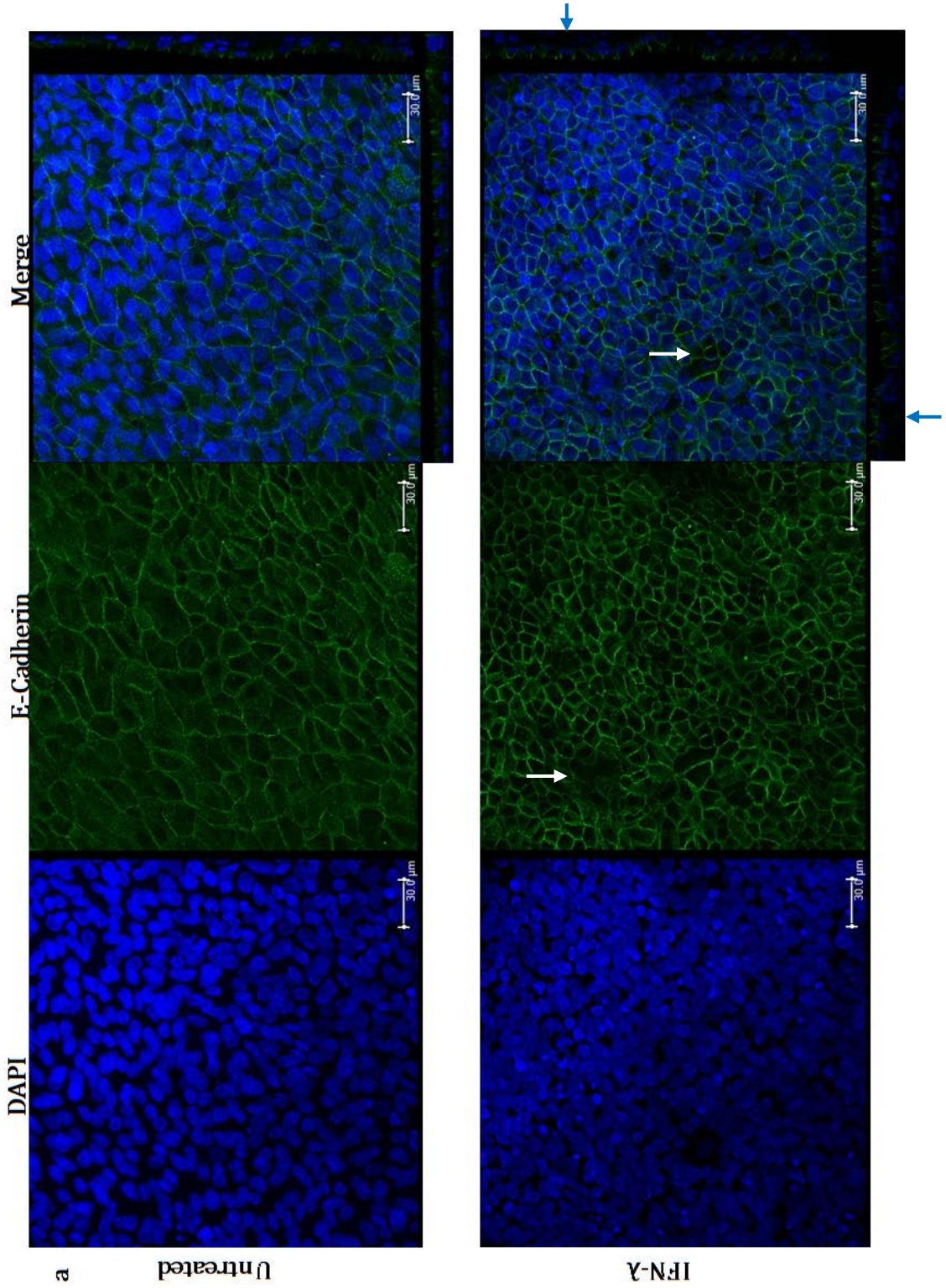
a
Untreated
IFN-λ
DAPI
E-Cadherin
Merge
30.0 µm

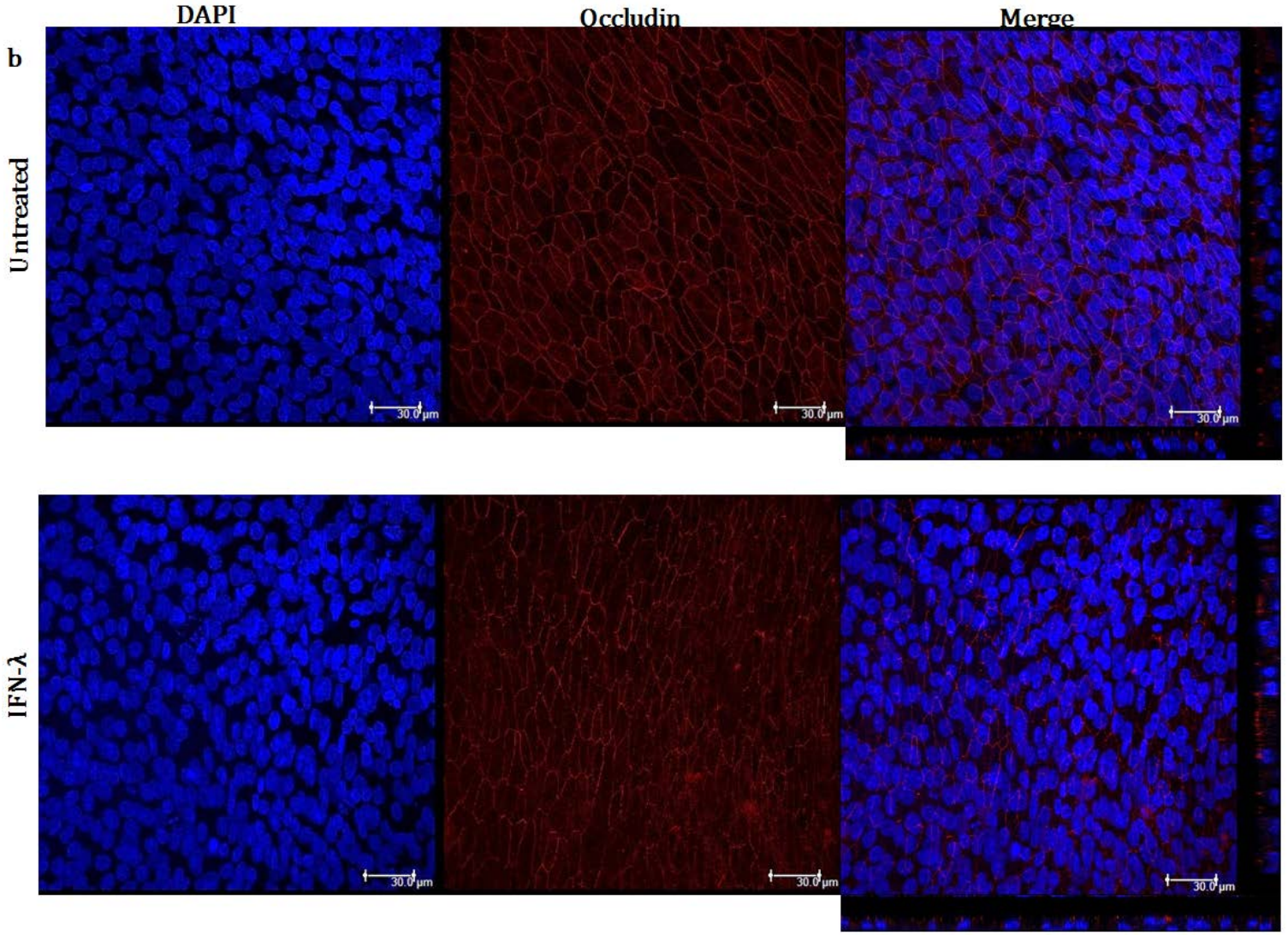

Figure 6.8: Immunofluorescent staining of E-cadherin (a) and occludin (b) in asthmatic differentiated ALI cultures. Images show localisation and intensity of junctional proteins in control (untreated) and 72 hour IFN-λ treated cultures. Images representative of n=4 experiments.

6.3.7: Effect of Exogenous IFN-λ on Primary Bronchial Epithelial cells Undergoing Differentiation for 21 days at ALI

IFN-λ protein was confirmed to be 1ng/ml in response to HRV-16 infection in differentiated ALI cultures; the same concentration was used to treat HBECs during differentiation to determine the effect of 'physiological' IFN levels on barrier development and cellular differentiation over 21 days.

MxA mRNA was significantly elevated at day 7 (p=0.0477), 14 (p=0.0308) and approaching significance at day 21 (p=0.067) in response to exogenous IFN-λ treatment when compared to untreated controls in cultures from healthy donors. MxA mRNA was strongly induced compared to an untreated control at day 7 (~38 fold induction)(Figure 6.9a). In cultures from asthmatic individuals, MxA mRNA was induced in response to IFN treatment across all time points—however this was not significant. Significance was approached at day 7 (p=0.0919) and day 21 (p=0.0515), suggesting this may be achieved with increased sample size. MxA mRNA expression was most strongly induced in response to IFN at day 7 (~59 fold induction)(Figure 6.9b).

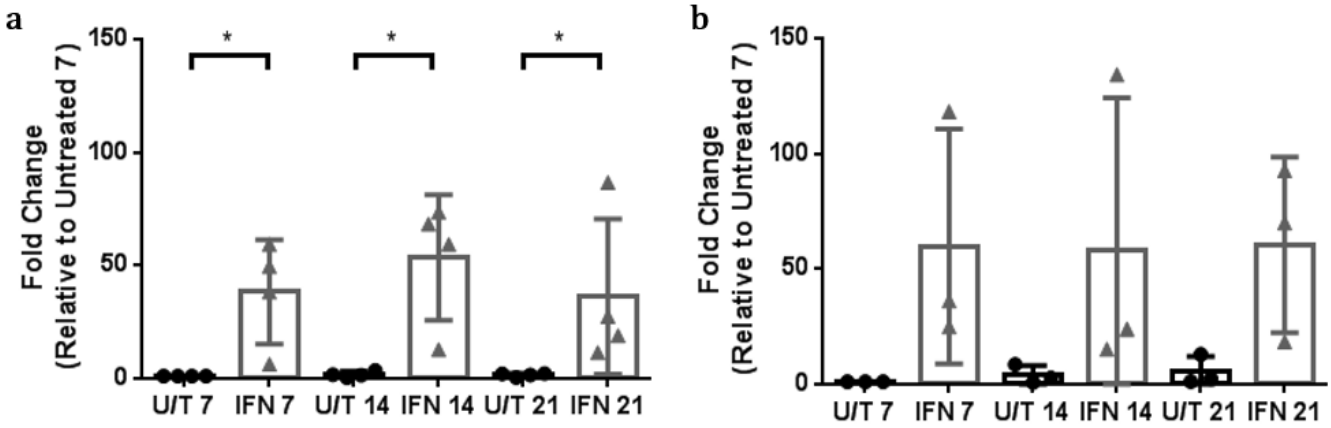

Figure 6.9: RT-qPCR quantification of MxA GTPase mRNA in untreated (U/T) and IFN-λ treated (IFN) differentiating ALI cultures from healthy (a) and asthmatic (b) donors. Graphs represent n=4 (healthy) and n=3 (asthmatic), p=*≤0.05calculated via two-tailed Paired T-test. Error bars= SD.

6.3.8: IFN-λ Treatment and MicroRNA Responses in Differentiating ALI Cultures

After confirming differentiating ALI cultures responded to exogenous IFN-λ, levels of miR-23a and miR-429 were quantified via RT-mediated qPCR assays as previously described (Figure 5.11). MiR-23a was significantly decreased in response to IFN-λ at day 7 (p=0.0006), day 14 (p=0.061) and day 21 (p=0.0373) in healthy ALI cultures. In differentiating asthmatic ALIs, miR-23a decreased in response to exogenous IFN treatment, but this was not significant at any time (Figure 6.10a-b).

MiR-429 levels were significantly decreased at day 7 (p=0.0131), 14 (p=0.0219) and 21 (p=0.0152) in response to exogenous IFN when compared to control in healthy samples. MiR-429 levels were most greatly declined in response to IFN-λ treatment (relative to control) at day 21—with a decrease of ~52% in microRNA level. MiR-429 levels were decreased in response to IFN-λ in asthmatic ALI cultures but once again this was not significant (Figure 6.10c-d).

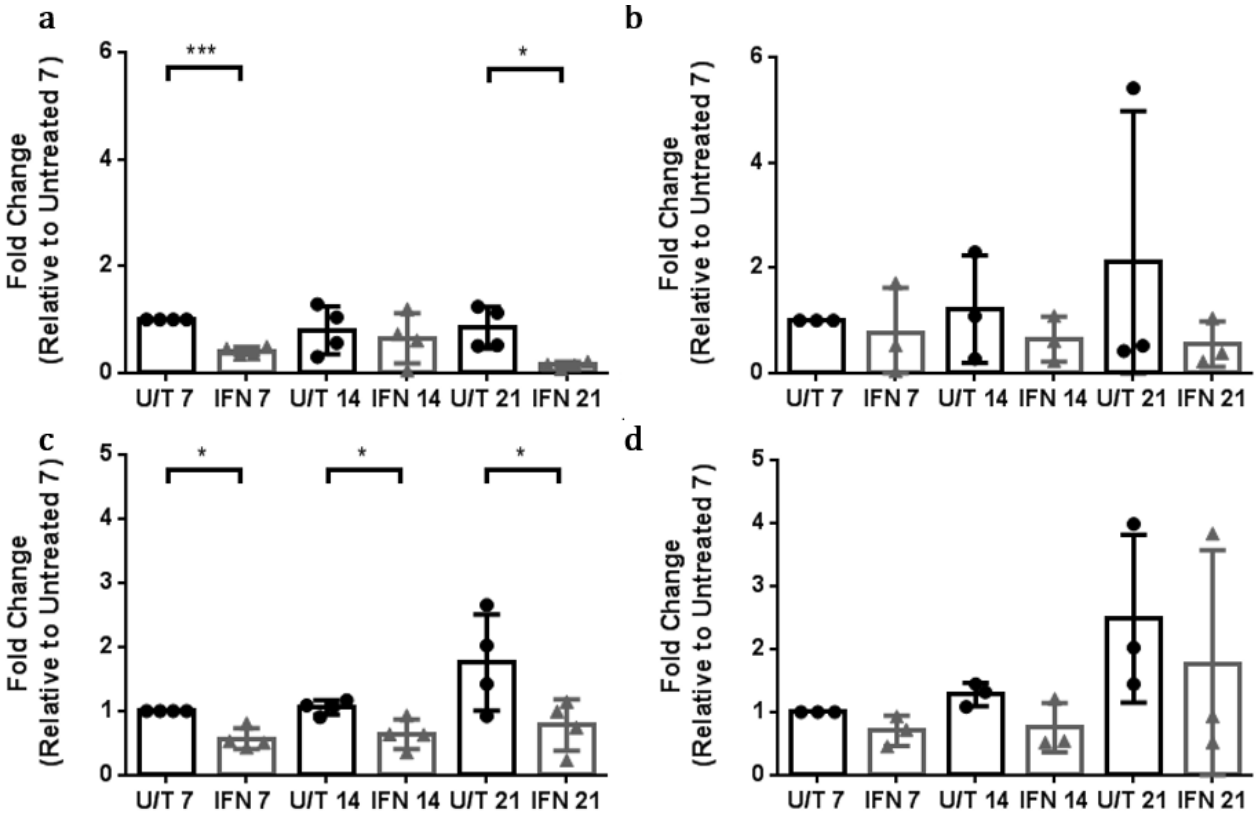

Figure 6.10: RT-qPCR quantification of miR-23a (a-b) and miR-429 (c-d) in untreated (U/T) and IFN-λ treated (IFN) differentiated ALI cultures from healthy (a-c) and asthmatic (b-d) donors. Graphs represent n=4 (healthy) and n=3 (asthmatic), p=*≤0.05; p=***≤0.001 calculated via two-tailed Paired T-test. Error bars= SD

6.3.9: Effect of IFN-λ Treatment of Differentiating ALI Cultures on Expression of Predicted mRNA Targets of miRNAs

As previously discussed, mRNA levels of miR-23a and miR-429 targets TNFAIP3, occludin, ZEB1 and E-cadherin were quantified utilising RT-qPCR to determine if significant changes in mRNA expression could be correlated to significant alterations in microRNAs in response to IFN-λ treatment (Figure 6.11).

ZEB1 mRNA levels were elevated in response to IFN-λ treatment at all time points in healthy ALI cultures but this was only significant at day 7 ($p=0.0202$). ZEB1 mRNA levels were also elevated in response to IFN treatment in asthmatic differentiating ALI cultures—however this was not significant (Figure 6.11a-b). E-cadherin mRNA levels were significantly decreased in response to IFN-λ at both day 14 ($p=0.0435$) and day 21 ($p=0.0491$) in differentiating healthy ALI cultures. IFN-λ treatment slightly decreased E-cadherin mRNA levels at day 7 but this was not significant. In differentiating cultures from asthmatic donors, E-cadherin mRNA was significantly decreased in response to IFN at both day 14 ($p=0.0227$) and day 21 ($p=0.0411$). E-cadherin mRNA was also decreased in response to IFN-λ at day 7 but this was not significant (Figure 6.11c-d). TNFAIP3 mRNA was elevated in response to IFN-λ in differentiating healthy cultures at all time points, though this was significant only on day 14 ($p=0.0275$). In asthmatic differentiating ALI cultures, IFN-λ decreased TNFAIP3 mRNA expression on both day 7 and 21, but significantly increased TNFAIP3 mRNA expression at day 14 ($p=0.0294$)(Figure 6.11e-f). In differentiating ALI cultures from healthy donors, occludin mRNA was elevated in response to exogenous IFN-λ across all time points which approached significance at day 7 ($p=0.0770$) and was significant at day 21 ($p=0.0481$). Occludin mRNA was also elevated in response to IFN treatment in differentiating ALIs from asthmatic donors—but this did not approach significance (Figure 6.11g-h).

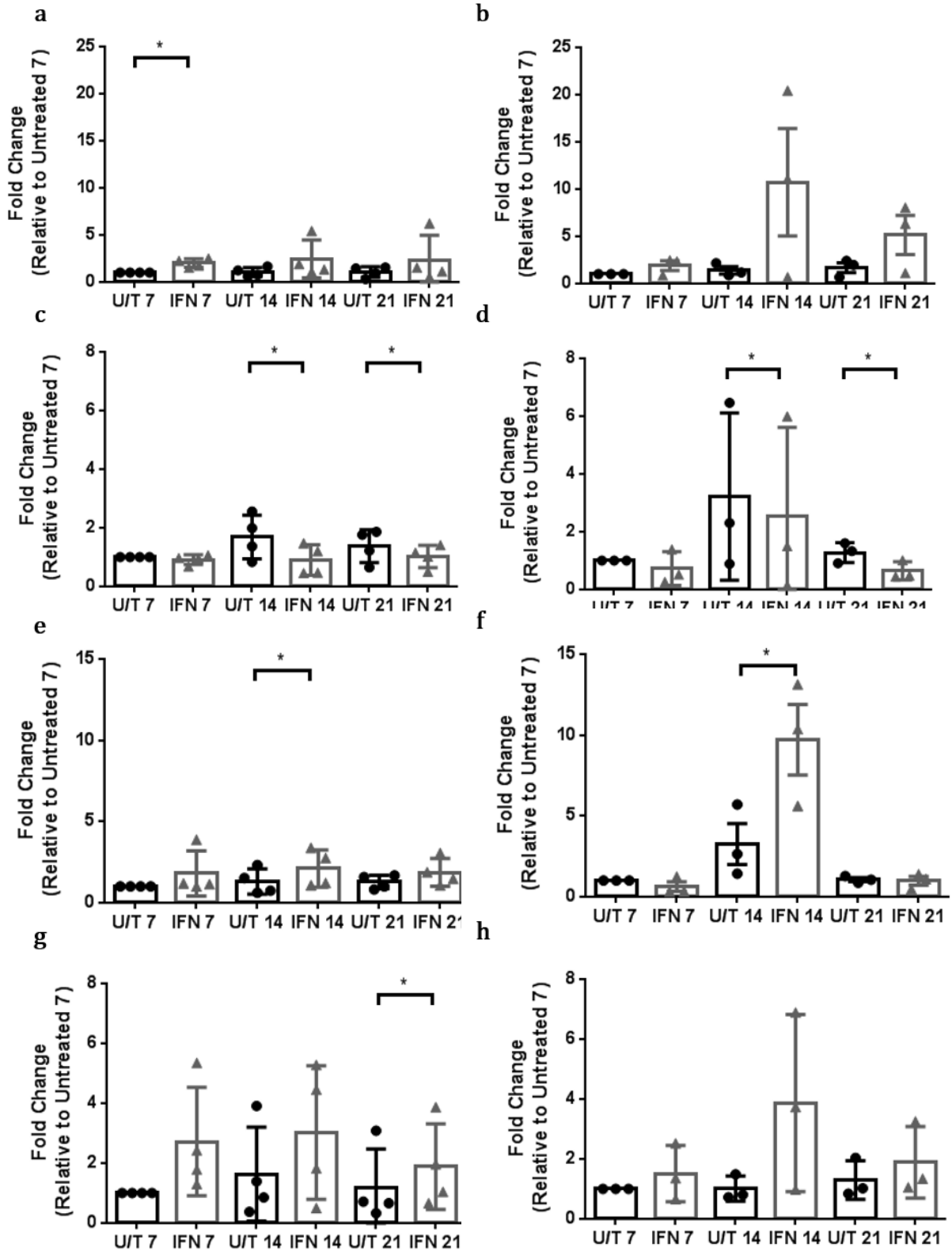

Figure 6.11: RT-qPCR quantification of ZEB1 (a-b), E-cadherin (c-d), TNFAIP3 (e-f) and occludin (g-h) in untreated (U/T) and IFN-λ treated (IFN) differentiating ALI cultures from healthy (a, c, e, g) and asthmatic (b, d, f, h) donors. Graphs represent n=4 (healthy) and n=3 (asthmatic), p=*≤0.05calculated via two-tailed Paired T-test. Error bars= SD.

6.3.10: Effect of IFN-λ Treatment of Differentiating ALI Cultures on Expression of Proteins encoded by Predicted mRNA Targets of miRNAs

As with Section 5.3.5, protein levels of ZEB1 and TNFAIP3/A20 were quantified using western blotting detection methods with actin as the proposed protein control/normaliser. As with Section 5.3.5 western blotting, levels of actin protein were shown to alter in response to IFN-λ treatment by 21 days of treatment and thus could not be used as a control. Cytokeratin-18 was once again tested as a proposed alternative control but could not be detected in differentiating ALI cultures thus proteins could only be relatively quantified as described previously (Figure 6.12-3).

ZEB1 could only be detected in n=2 healthy and n=1 asthmatic ALI cultures. ZEB1 protein expression was marginally increased in response to IFN-λ treatment at both day

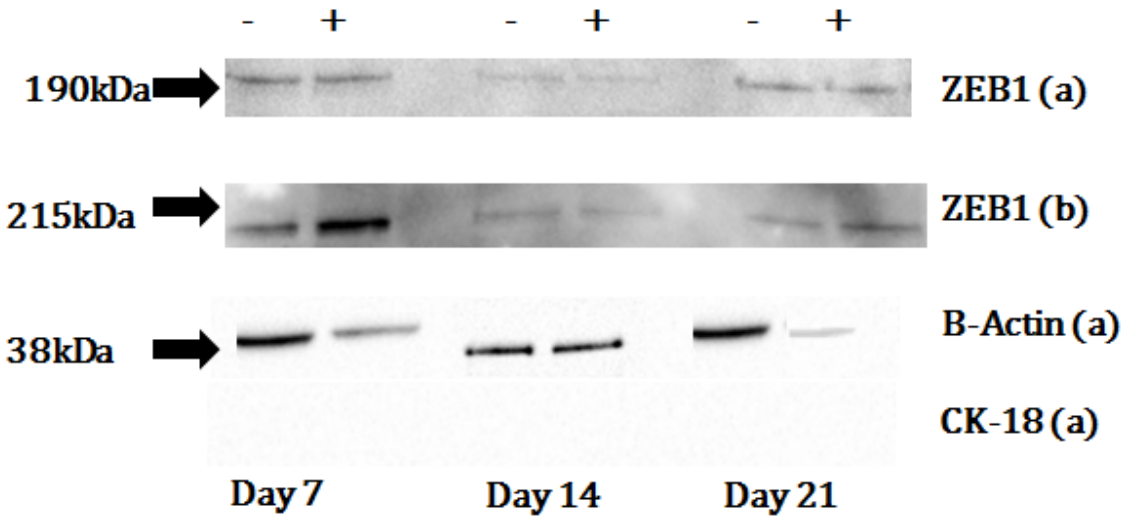

	7: Relative Fold Change	14: Relative Fold Change	21: Relative Fold Change
Healthy	+1.105	+1.554	-0.763
Asthmatic	-0.612	-0.842	-0.867

Figure 6.12: Relative ZEB1 protein changes in Untreated (-) and IFN-λ (+) differentiating ALI cultures from healthy (a) and asthmatic (b) donors with 24-72 hours of treatment. Blots representative of n=2 healthy, n=2 asthmatics. Relative fold change calculated from quantification of intensity of IFN treated against Untreated in BioRad Image Lab Plus.

7 and 14 in healthy samples, with levels decreased at day 21. Asthmatic individuals had decreased ZEB1 protein expression in response to IFN across all time points (Figure 6.12).

A20 protein was detected in n=3 healthy and n=2 asthmatic differentiating ALI cultures. Levels of A20 protein were decreased in response to IFN-λ treatment at day 7 and 14 in healthy cultures—but became slightly elevated by Day 21. A20 protein in asthmatic ALIs was elevated in response to exogenous IFN treatment across all time points (Figure 6.13).

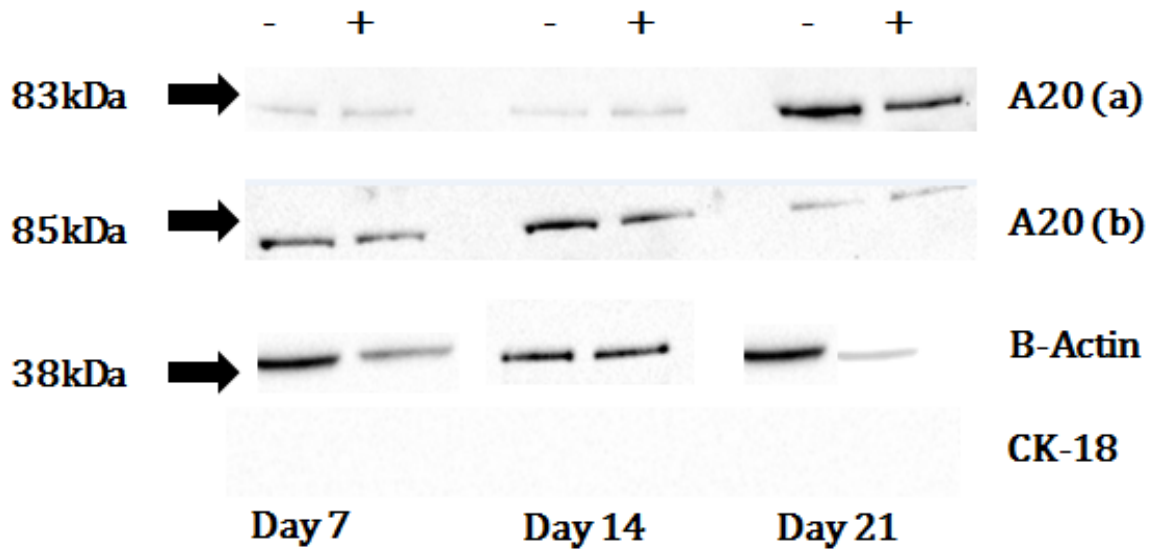

	7: Relative Fold Change	14: Relative Fold Change	21: Relative Fold Change
Healthy	-0.861	-0.811	+1.104
Asthmatic	+1.471	+1.567	+1.593

Figure 6.13: Relative A20 protein changes in Untreated (-) and IFN-λ (+) differentiating ALI cultures from healthy (a) and asthmatic (b) donors with 24-72 hours of treatment. Blots representative of n=2 healthy, n=2 asthmatics. Relative fold change calculated from quantification of intensity of IFN treated against Untreated in BioRad Image Lab Plus.

6.3.11: Characterising Further Changes in Epithelial Barrier Characteristics /Innate Immune Responses During IFN-λ Treatment in Differentiating ALI Cultures

6.3.11.a: Epithelial Barrier Integrity

TER measurement was utilised to track epithelial barrier formation and cellular differentiation over experiment duration. Measurements were taken every ~2 days to see epithelial barrier development in differentiating cultures from healthy and asthmatic donors in untreated and IFN-treated conditions (Figure 6.14a-b). In differentiating cultures from healthy donors, TER began to increase after 5 days of ALI culturing, indicating barrier formation. By day 7, differences in TER in response to exogenous IFN-λ were visible, with a decrease of ~100Ω in TER in treated cultures. By day 14 this IFN-associated TER decrease was at ~600Ω and approached significance ($p=0.0625$). By 21 days ALI differentiation—TER in IFN-λ treated ALI cultures was ~400Ω lower than the untreated controls (Figure 6.14a). In differentiating asthmatic samples, TER began to increase after 7 days of ALI culturing. There were minimal differences in TER between untreated and treated differentiating cultures. A slight decrease in TER values in response to IFN-λ was observed at day 10 with (100Ω). At 21 days of ALI differentiation, TER in IFN-λ treated cultures was ~300Ω lower than untreated controls (Figure 6.14b).

Macromolecular permeability of the epithelial barrier was assessed through determining relative passage of FITC-labelled 4kD Dextran from apical to basolateral compartments of the ALI culture model (Figure 6.14c-d). In differentiating ALI cultures from healthy donors, FITC-labelled 4kD Dextran passage was significantly elevated in cultures treated with exogenous IFN-λ at day 7 ($p=0.0261$), 14 ($p=0.0439$) and 21 ($p=0.0478$). Highest relative FITC 4kD passage in IFN treatment compared to control was observed at day 14, with a ~13-fold elevation (Figure 5.15c). In differentiating ALI cultures from asthmatic donors, FITC passage was elevated in response to IFN-λ treatment at day 7, 14 and 21—with significance being approached at both day 14 ($p=0.0738$) and 21 ($p=0.0542$). Highest relative FITC-labelled 4kD passage in IFN-λ treated cultures was observed at day 21 with a ~6-fold elevation compared to the untreated controls (Figure 6.14d).

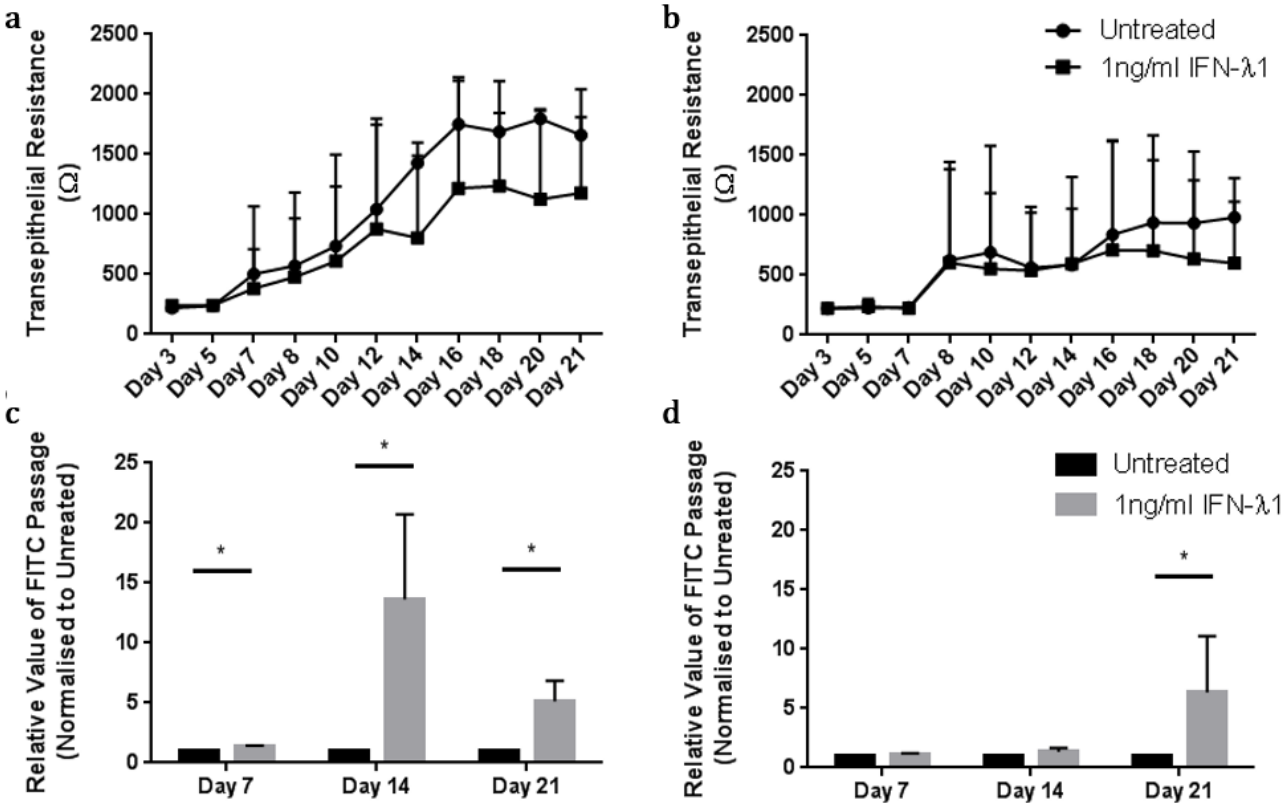

Figure 6.14: Epithelial barrier integrity in untreated and IFN-λ treated differentiating healthy (a, c) and asthmatic (b, d) ALI cultures over 21 days. Transepithelial resistance (a-b) was measured every ~48 hours. FITC 4kD Dextran (c-d) passage was measured every 7 days. n=4 p=*≤0.05calculated via two-tailed Paired T-test. Error bars= SD.

5.3.11.b: Cell Counts of Cultures

Impact of IFN-λ treatment upon cell number was assessed through counts of cells numbers on transwell filters at day 7, 14 and 21 (Figure 6.15). In both healthy and asthmatic differentiating cultures, cell numbers increased over 21 days. In differentiating cultures from healthy donors, IFN-λ treated transwells had significantly less cells in at day 7 ($p=0.0184$), 14 ($p=0.0059$) and 21 ($p=0.0086$) when compared to untreated controls. This was most pronounced at day 21, in which mean cell counts indicated a ~35% reduction in cell number. In differentiating asthmatic cultures, transwell cell counts between treated and untreated samples indicated no significant difference in cell number in response to exogenous IFN-λ. Cell number at day 7 showed alteration to cell number in response to IFN-λ treatment. At day 14 there was a slight elevation cell number in treated cultures (~7%). The most pronounced effect was observed at day 21, with a ~18% reduction in cell number in response to IFN-λ treatment.

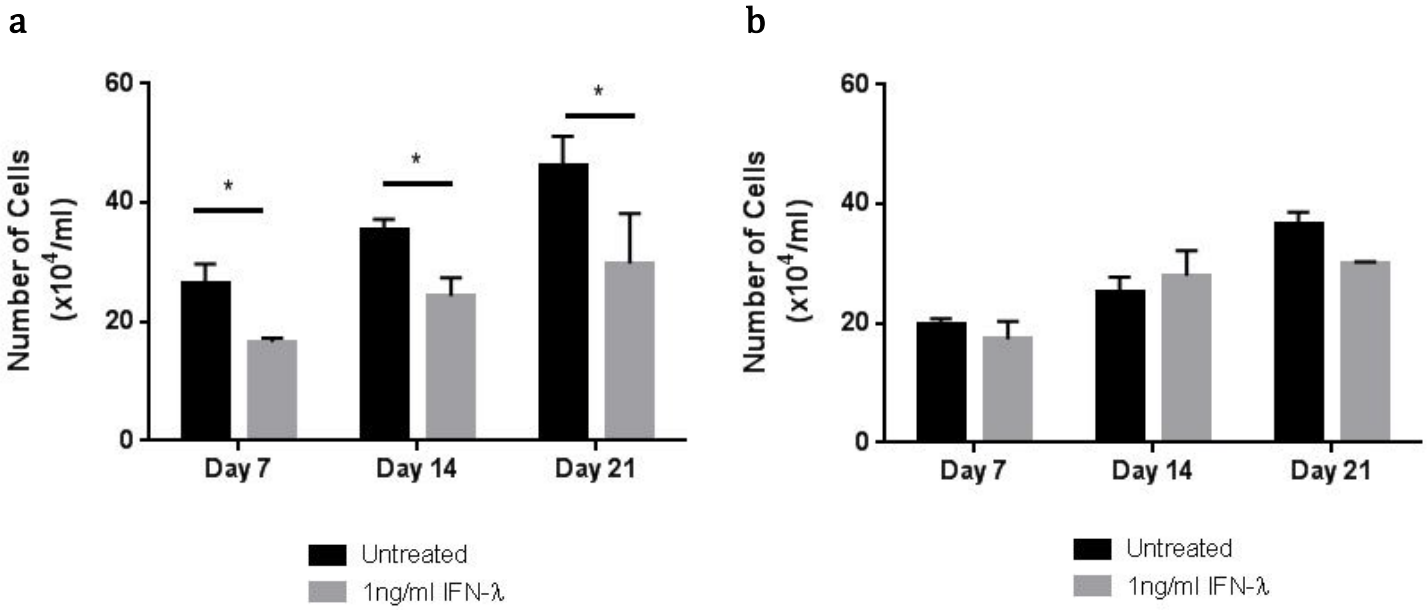

Figure 6.15: Cell counts of untreated and IFN-λ treated differentiating healthy (a) and asthmatic (b) ALI cultures on transwells over 21 days. n=4 p=*≤0.05calculated via two-tailed Paired T-test. Error bars= SD.

6.3.11.c: Morphology of Cultures and Epithelial Protein localisation

In addition to assessing morphological changes, visualisation and quantification of two epithelial barrier proteins—E-cadherin and occludin—was conducted (Figure 6.16-21).

In differentiating ALI cultures from healthy individuals at day 7, there are limited differences in the cell morphology and protein localisation between treated and untreated cultures (Figure 6.16). There was a mixture of larger cells with isolated regions of smaller, more compact 'cobblestone' cells present. In both conditions, small quantities of E-cadherin protein was localised within the junction with a larger proportion localised within the cytoplasm. E-cadherin was additionally not consistently present around cellular edge with slight 'fractures' in staining (Figure 6.16a). Occludin had a similar localisation junctional regions and within the cytoplasm in both treated and untreated ALI cultures with slight fractures in protein staining (Figure 6.16b). Comparison of staining intensity in untreated and IFN-λ treated ALI cultures, suggested more intense E-cadherin and occludin staining in response to treatment.

At day 14, there were more prominent differences between the untreated and treated differentiating healthy ALI cultures (Figure 6.17). Distinctive 'cobblestone' cell morphology had developed in both conditions. IFN-λ treated cultures had regions where cells were larger and appeared to have an elongated and stretched morphology. This was not present in untreated cultures. Treated differentiating ALIs also had regions in which DAPI nuclei staining was absent—giving rise to 'holes' (as observed in the 72 hour treated samples). E-cadherin protein was localised within the junction in both untreated and IFN-treated samples. Staining of E-cadherin within the junctional region appeared more discrete in untreated differentiating healthy cultures. In IFN-λ treated differentiating cultures, junctional staining was less distinct and there was a larger quantity of E-cadherin staining in the cytoplasm. In IFN-λ treated cultures, there were regions in which there were spaces between staining E-cadherin (Figure 6.17a). Occludin protein was localised mainly to junctional regions with a small proportion in the cytoplasm in untreated cells. In treated differentiating cultures, occludin protein was less discretely localised across the subapical region with some cytoplasmic localisation. In IFN-λ treated cultures, there were large numbers of cells which appeared to have no occludin protein (Figure 6.17b). Comparison of staining intensity between untreated and treated ALIs

showed more intense E-cadherin staining in IFN-λ treated cultures and more intense occludin staining in untreated cells.

By day 21 of IFN-λ treatment in differentiating healthy ALI cultures there were vast differences (Figure 6.18). Morphologically, cells in the IFN-λ treated cultures appeared larger and elongated compared to untreated cells with their 'cobblestone' appearance. Treated cultures had comparatively fewer cells per section than untreated cultures indicated by decreased DAPI staining. E-cadherin localisation was primarily junctional in both untreated and treated cultures— but localisation was more restricted and discrete in untreated cultures whilst IFN-treatment showed more distribution along the apicolateral surface (Figure 6.18a). Similarly occludin was localised more focally in untreated differentiating cultures with increased distribution in response to IFN treatment (Figure 6.18b). There were regions in which no E-cadherin and occludin staining was present in cell borders of IFN-λ treated differentiating cultures. Comparison of staining intensity showed more intense E-cadherin staining and less intense occludin staining in response to exogenous IFN-λ treatment. Examination of Z-stack indicated that there was less pseudostratification of the culture in response to exogenous IFN-λ treatment as there were regions in which Z-stack only showed a single cell layer.

After 7 days of exogenous IFN-λ treatment—differentiating ALI cultures from asthmatic donors had limited differences in cell morphology and protein localisation between untreated and treated cells (Figure 6.19). Comparisons to healthy differentiating cultures at the day 7 indicated that asthmatic cultures had a higher proportion of larger cells with less 'cobblestone' regions. E-cadherin protein was localised both to the epithelial junctions and the cytoplasm in both untreated and treated differentiating cultures. Occludin protein was localised primarily to the epithelial junctions in untreated and treated cells, with a small level of staining in the cytoplasm. In response to IFN-λ treatment, there was less occludin and E-cadherin present in epithelial junctions of differentiating cells leading to large regions of multiple cells with no distinguished boundaries. Comparison of staining intensity showed increased E-cadherin staining intensity and decreased occludin staining intensity in response to IFN-λ.

At day 14, differentiating asthmatic ALI cultures began to show differences in response to IFN-λ treatment (Figure 6.20). Distinctive cobblestone morphology of the ALI culture

had begun to develop in the asthmatics by this time point—but appeared to be less compact/tight when compared to observed at day 14 in healthy differentiating cultures. In IFN-treated cultures, there were regions in which larger, morphologically stretched HBEC cells were present, and thus decreased cell numbers per section. These morphological differences appeared less frequently in asthmatic cultures compared the same conditions in healthy cultures. E-cadherin protein was mainly localised to the junction in untreated asthmatic cultures whilst E-cadherin was less distinctly localised in treated cultures, with still a large proportion of E-cadherin present in cytoplasm. There were no apparent differences between occludin localisation in response to IFN-λ treatment in asthmatic cultures. Comparison of staining intensity showed more intense staining of E-cadherin and decreased intensity of occludin staining in response to treatment.

By day 21 of treatment, untreated cultures retained the 'cobblestone' appearance but as noted at day 14—cells were comparatively larger and less compact than observed in healthy cultures (Figure 6.21). In the IFN-λ treated cells, morphological changes noted above were more widespread by day 21. E-cadherin localisation was primarily junctional, with discrete focal points of staining in untreated differentiating cultures. Treated cultures had less distinct E-cadherin staining across the apicolateral edges of cells and additionally having increased staining present in the cytoplasm. Occludin was also less discretely localised in response to IFN-λ treated. Additionally there were junctions in which occludin staining was not present in treated cultures. Staining intensity showed the same results as in day 7 and 14. As observed in the Z-stacks from healthy differentiating cultures, IFN-λ treated differentiating asthmatic cultures appeared to have higher incidences of single cell layers compared to untreated controls.

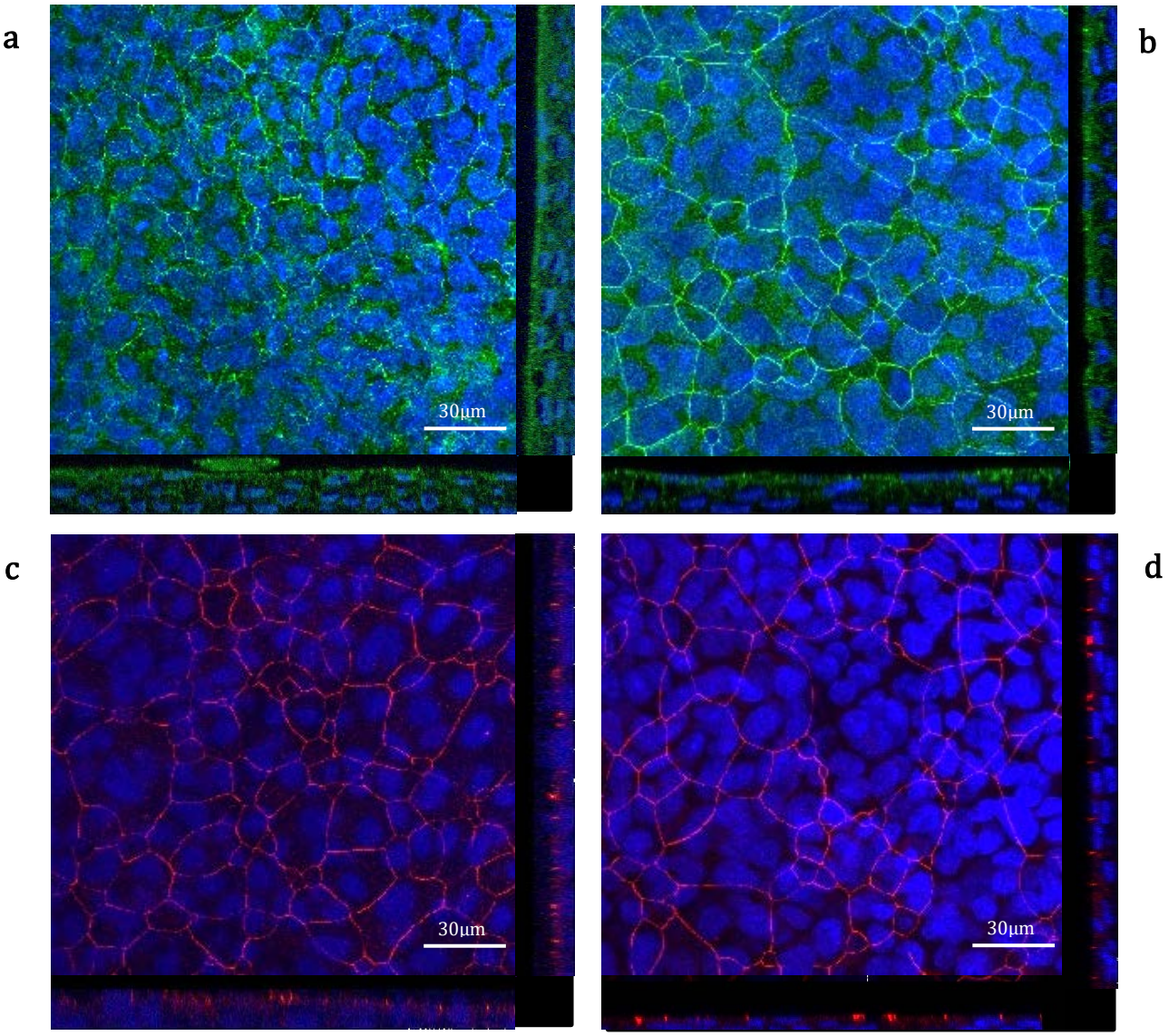

Figure 6.16: Immunofluorescent staining of E-cadherin (a-b) and occludin (c-d) in healthy differentiating ALI cultures. Images show localisation and intensity of junctional proteins in untreated control (a, c) and 7 days IFN-λ treated (b, d) cultures. Images representative of n=4 experiments.

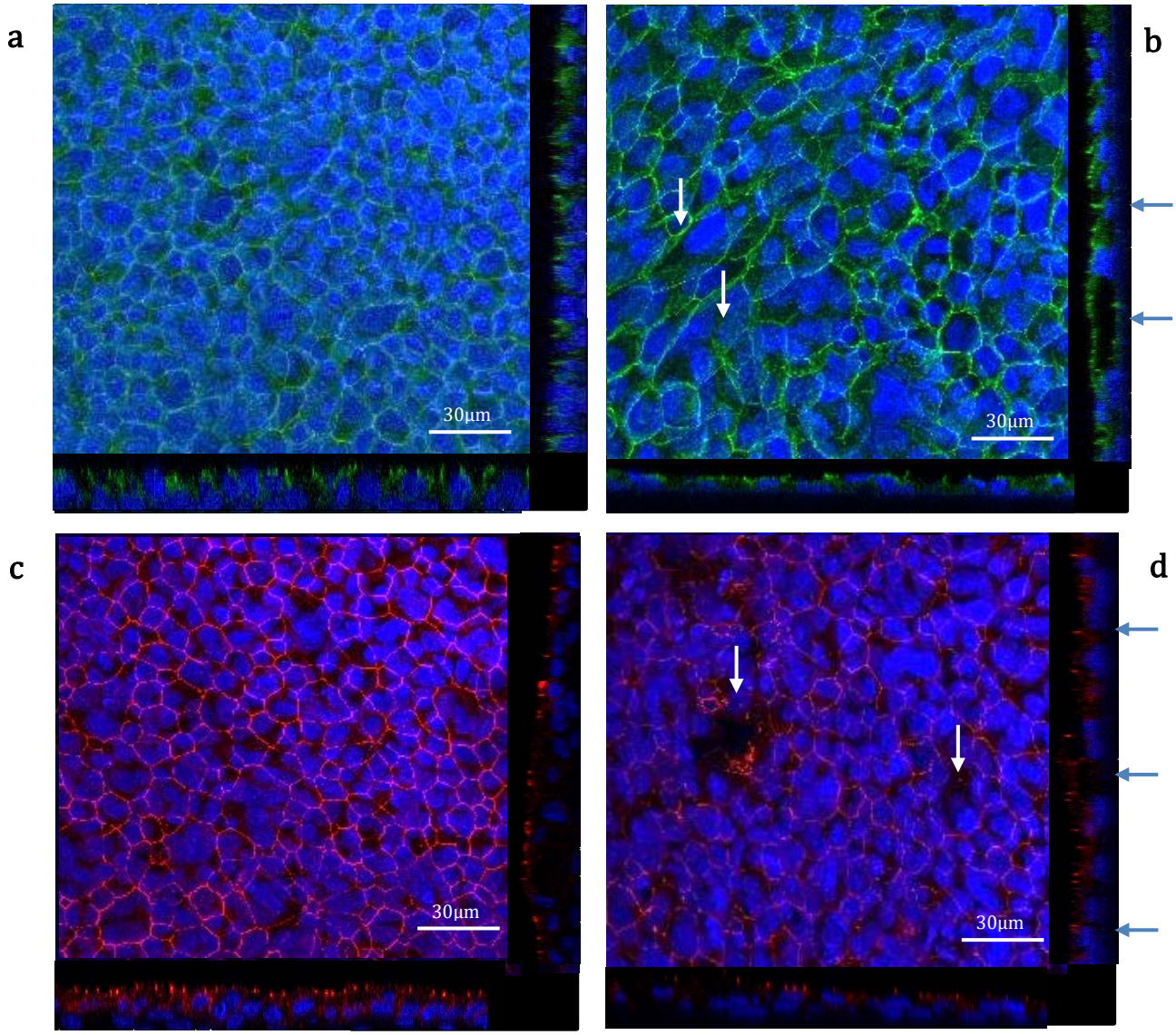

Figure 6.17: Immunofluorescent staining of E-cadherin (a-b) and occludin (c-d) in healthy differentiated ALI cultures. Images show localisation and intensity of junctional proteins in untreated control (a, c) and 14 days IFN-λ treated (b, d) cultures. Images representative of n=4 experiments.

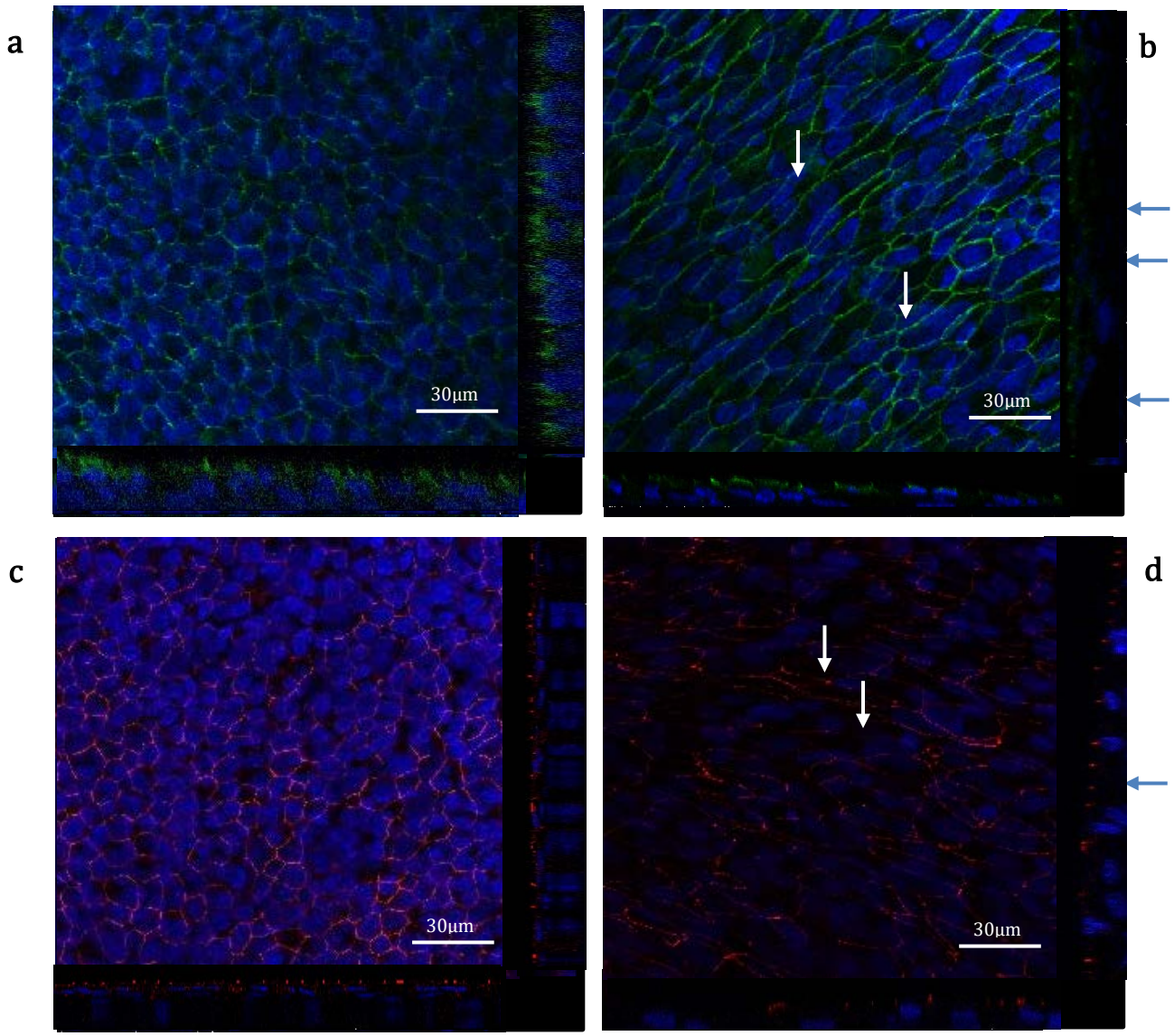

Figure 6.18: Immunofluorescent staining of E-cadherin (a-b) and occludin (c-d) in healthy differentiating ALI cultures. Images show localisation and intensity of junctional proteins in untreated control (a, c) and 21 days IFN-λ treated (b, d) cultures. Images representative of n=4 experiments.

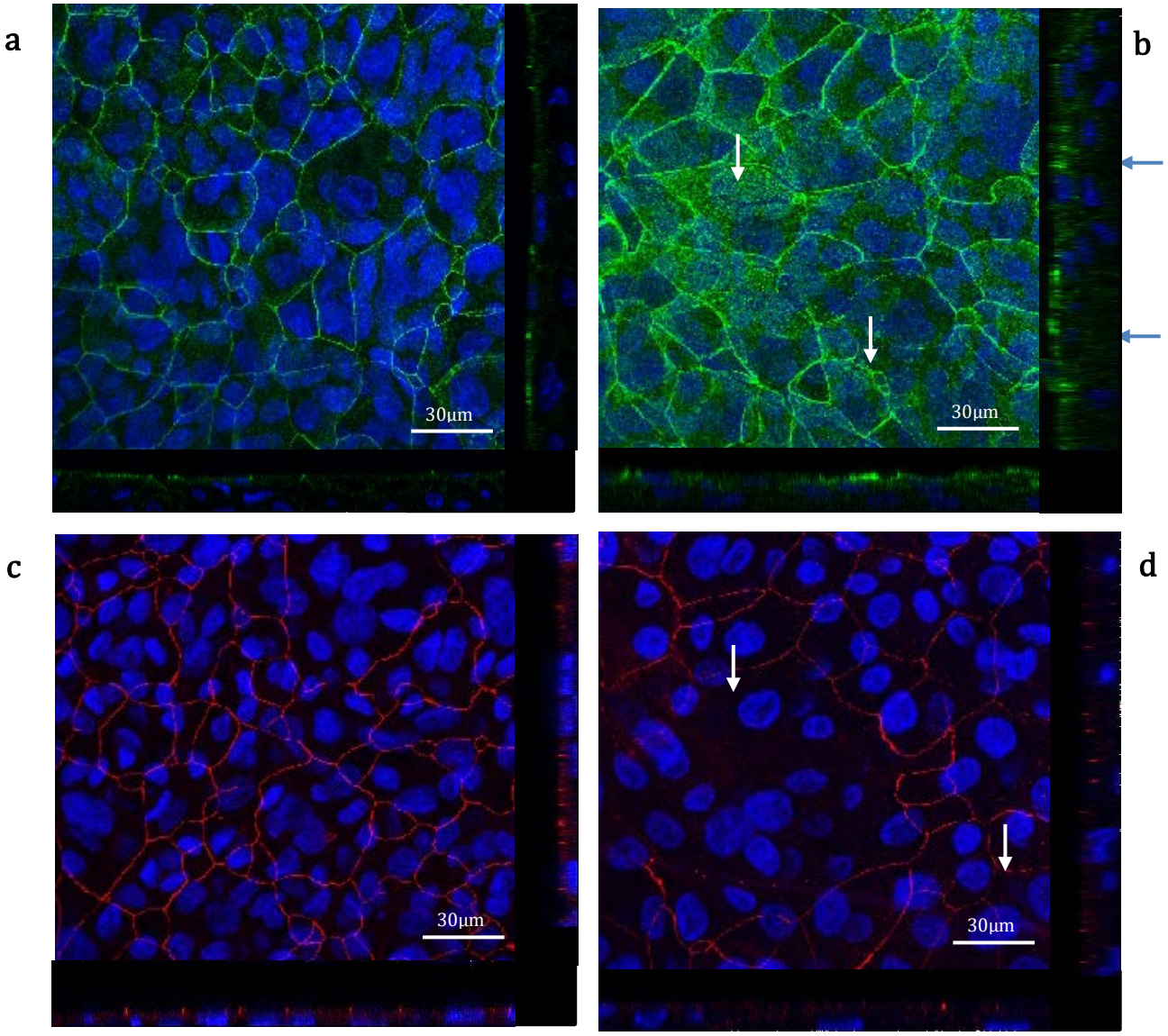

Figure 6.19: Immunofluorescent staining of E-cadherin (a-b) and occludin (c-d) in asthmatic differentiating ALI cultures. Images show localisation and intensity of junctional proteins in untreated control (a, c) and 7 days IFN-λ treated (b, d) cultures. Images representative of n=4 experiments.

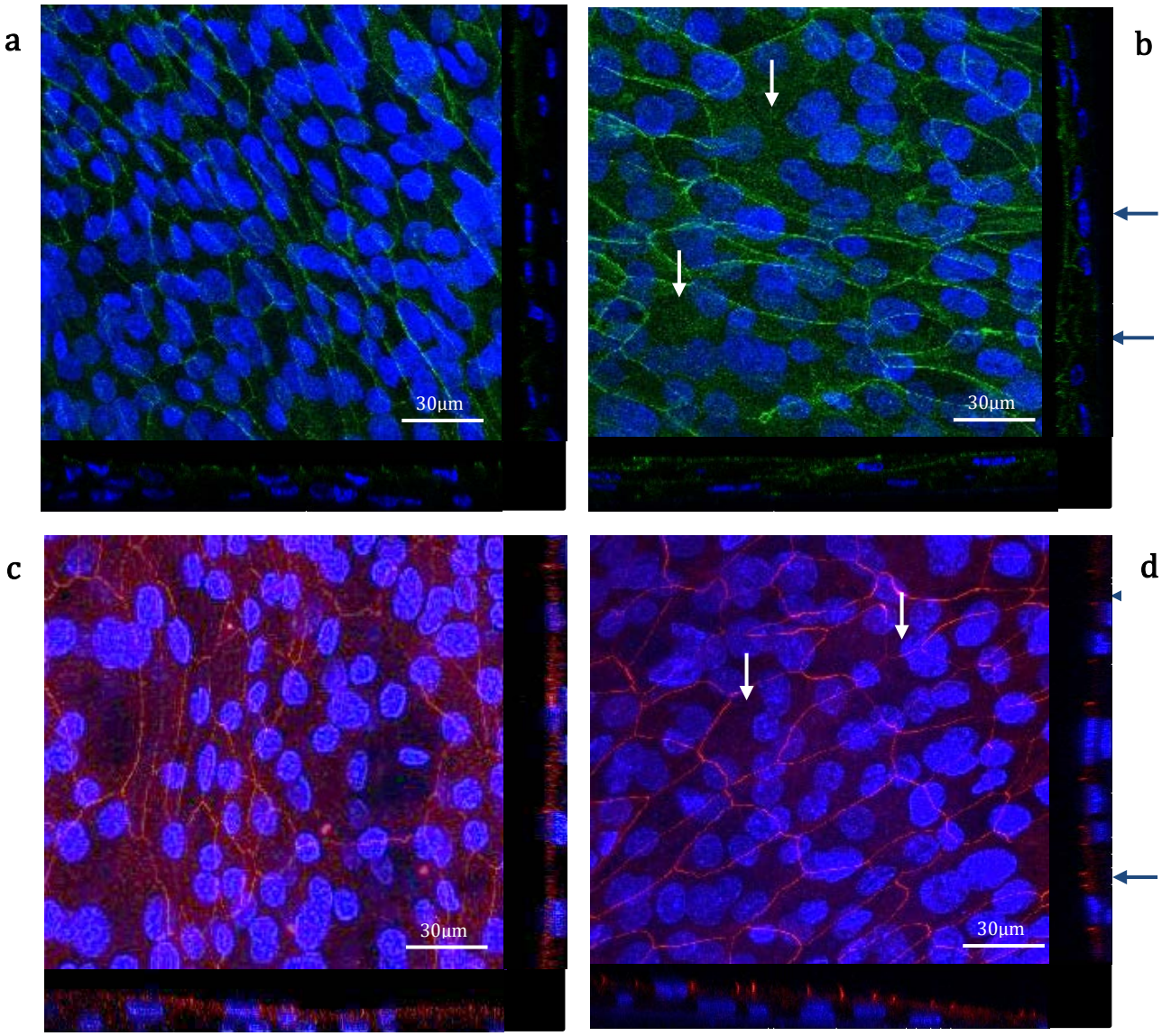

Figure 6.20: Immunofluorescent staining of E-cadherin (a-b) and occludin (c-d) in asthmatic differentiating ALI cultures. Images show localisation and intensity of junctional proteins in untreated control (a, c) and 14 days IFN-λ treated (b, d) cultures. Images representative of n=4 experiments.

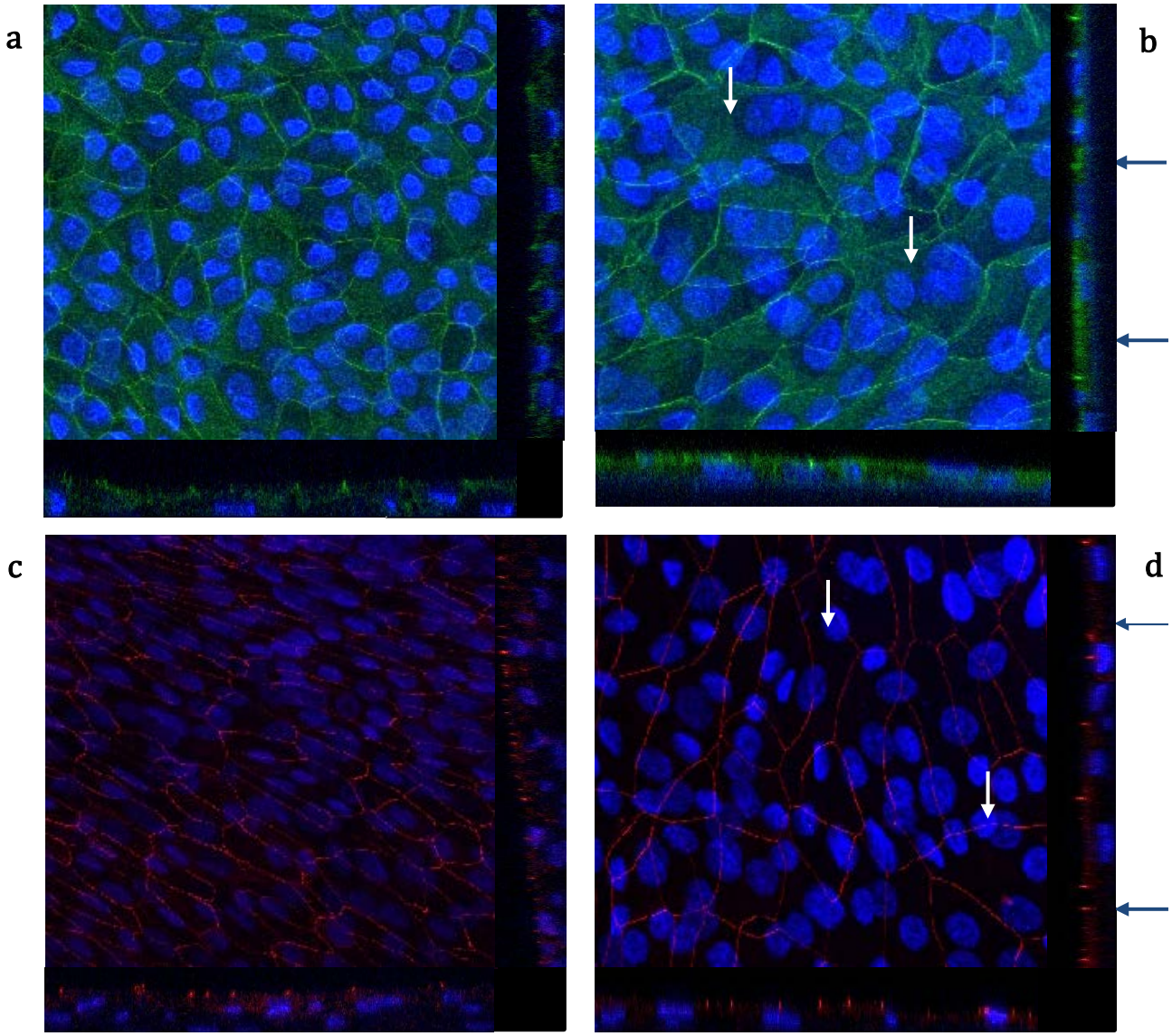

Figure 6.21: Immunofluorescent staining of E-cadherin (a-b) and occludin (c-d) in asthmatic differentiating ALI cultures. Images show localisation and intensity of junctional proteins in untreated control (a, c) and 21 days IFN-λ treated (b, d) cultures. Images representative of n=4 experiments.

6.4: Discussion

During both *in vivo* and *in vitro* HRV-16 infections it has been shown that only a small proportion of epithelial cells become virally infected (Mosser, Brockman-Schneider et al. 2002, Mosser, Vrtis et al. 2005, Chen, Hamati et al. 2006). These infected cells release a large quantity of interferons which act as antiviral mediators on the neighbouring uninfected cells, causing the upregulation in the expression of a variety of ISGs—ultimately cumulating in these cells becoming less permissible to infection (Goodbourn, Didcock et al. 2000, Levy and Garcia-Sastre 2001, Durbin, Kotenko et al. 2013). From the data obtained in Chapter 4, it was apparent that *in vitro* HBEC ALI cultures from both healthy and asthmatic donors were permissible to HRV-16 infection and, at the same time, significantly upregulated expression of both IFN-β and IFN-λ mRNA. This meant that decreases in miRNA expression and subsequent alterations to predicted target mRNA expression could be attributed to both infected and uninfected cell populations. As it has previously been shown in *in vitro* HBEC models of HRV-16 infection that only a small percentage of cells become virally infected (<10%)(Mosser, Brockman-Schneider et al. 2002), it was decided to focus on the uninfected cells and their response to released IFNs—specifically looking at IFN-λ due to its' mainly epithelial receptor distribution (Sommereyns, Paul et al. 2008) and increased prominence of release in the lung in response to infection (Huayllazo 2012).

Firstly it had to be confirmed that the significant increase in IFN-λ mRNA expression correlated to significant increase in IFN-λ protein release in response to HRV-16 infection. IFN-λ protein was significantly elevated in supernatants from HRV-16 infected cells compared to UV-RV controls at both 24 and 48 hours in healthy and asthmatic ALI cultures—with peak release at 48 hours in both cohorts. Due to the limited supernatant samples for 72 hours (n=2 for healthy; n=3 for asthmatics) it was not possible to assess whether IFN-λ protein release was elevated in response to viral replication at this time point, though from the limited data points it appears as though by 72 hours IFN-λ protein concentration is not greatly different in HRV-16 compared to UV-RV controls. As in Sykes et al., there were no significant differences in IFN-λ protein release in healthy and asthmatic cohorts and thus the asthmatic cohort were not considered to have an impaired IFN response of less protein release (Sykes, Macintyre et al. 2014), contrary to other studies (Wark, Johnston et al. 2005, Contoli, Message et al. 2006). Instead the data

suggests that whilst IFN-λ protein release is not significantly altered between the two cohorts, the timing of release appears to be different. Though both groups have peak IFN-λ protein release at 48 hours, healthy ALI cultures seem to produce and release IFN-λ faster with a ~2-fold higher level at 24 hours compared to asthmatics. Previous investigations have shown the existence of a delayed asthmatic response during allergen challenges which was linked to T_H1:T_H2 ratios (Pelikan 2011). As IFN-λ has been previously shown to have immunomodulatory effects with the T_H1:T_H2 system (Jordan, Eskdale et al. 2007, Edwards and Johnston 2011), it can be suggested that this delayed asthmatic response could be linked to delayed IFN-λ release and delayed subsequent polarisation of T_H1 system. Additionally, previous studies within the Epithelial Barrier and Inflammation group have confirmed that asthmatic patients present with delayed apoptotic responses during HRV-16 infection (Wilkinson, Unpublished). As signalling through the IFNλR1 receptor subunit has been previously been linked to cell cycle arrest and apoptosis (Li, Lewis-Antes et al. 2008), it can be suggested once again that this delayed asthmatic response could be linked to delayed IFN-λ release and signalling.

In the first experimental series—treating fully differentiated ALI cultures with IFN-λ for 72 hours—the aim was to have a similar experimental setup as in Chapter 4, Part II (minus cell shedding) to examine the effect of released IFN-λ upon uninfected cells. ALI cultures response to exogenous IFN-λ at a physiologically relevant concentration (1ng/ml) was confirmed through quantifying mRNA induction of the key interferon stimulated gene, MxA GTPase. MxA GTPase mRNA induction has previously been confirmed to be significantly induced in response to HRV-16 infection and has been shown to be significantly induced in response to exogenous IFN treatment (Chen, Hamati et al. 2006, Rusinova 2013). HBEC ALI cultures had higher MxA GTPase fold induction in IFN-λ treated cells compared to untreated controls at all time points—this confirmed all subsequent experimental observations could be attributed as an effect of IFN-λ. Though there was no statistical significance difference between the mRNA induction in healthy and asthmatics—it appears though n=2 asthmatics are less responsive to IFN-λ treatment as their mRNA levels are not much higher than untreated controls.

In healthy, differentiated ALI cultures, there were reductions in miR-23a and miR-429 at 24, 48 and 72 hours in response to exogenous IFN-λ treatment when compared to controls—these reductions were significant at both 24 and 72 hours. As cells were shown

to be responding to the exogenous IFN-λ treatment, it can be postulated that a consequence of IFN signalling was to significantly decrease the microRNAs of interest. As these microRNAs have predicted roles in epithelial barrier maintenance and repair (via ZEB1, E-cadherin and occludin (Vareille, Kieninger et al. 2011)) and innate immune responses (via TNFAIP3/A20 (Parvatiyar and Harhaj 2011)) this suggests that IFN-λ plays a role in modulating these characteristics during viral infection. As in healthy cultures, miR-23a and miR-429 were decreased in response to IFN-λ in differentiated ALI cultures from asthmatics. However, it was only miR-23a that showed significant decreases (at 24 and 48 hours) whilst miR-429 was not significantly decreased at any time point. The lack of significance in miR-429 response in these asthmatic cultures may be indicative of a differential microRNA response to IFN-λ stimulus in asthmatic individuals. However due to the limited sample number (n=3) this is purely speculation and would have to be confirmed through increasing sample size for both patient cohorts. If this postulation is indeed correct, it suggests that as a consequence of differential microRNA responses to IFN, asthmatic patients may show differential responses in the predicted targets ZEB1, E-cadherin, TNFAIP3/A20 and occludin, culminating in differential epithelial barrier modulation and innate immune response—a characteristic often noted in viral infection responses in asthmatic patients compared to healthy individuals (Wark, Johnston et al. 2005, Xiao, Puddicombe et al. 2011).

As with Chapter 5, mRNA of the microRNA's predicted targets was assessed to determine whether these changed in response to IFN-induced microRNA alterations. To further corroborate changes in miRNA and targets—protein levels were also assessed via western blotting and immunofluorescent staining/confocal microscopy.

ZEB1 mRNA was not significantly altered in response to IFN-λ treatment in any experimental condition. In healthy individuals ZEB1 mRNA was slightly elevated in response to IFN-λ which correlated with significantly decreased miR-429 and miR-23a expression. In asthmatic individuals there was slight elevation of ZEB1 mRNA at 24 and 48 hours in response to IFN-λ which once again correlated with significantly decreased miR-23a. The lack of significant changes to ZEB1 mRNA in response to microRNA changes could indicate that miR-23a and miR-429 cause translational repression of ZEB1 protein opposed to causing mRNA degradation. As the 3'UTR of ZEB1 has multiple predicted miR-

429 binding sites current dogma would suggest miR-429 is likely to cause translational suppression opposed to degradation (Valencia-Sanchez, Liu et al. 2006).

ZEB1 protein was shown to be elevated in response to IFN-λ treatment relative to untreated controls at all times in healthy individuals and at 24 and 48 hours in asthmatic samples. It is difficult to draw a solid conclusion from this protein data due to the difficulties that occurred during ZEB1 blotting. For both healthy and asthmatic samples, ZEB1 was only detectable in n=2 patients which makes the result less conclusive due to lack of repeatability. In addition, the protein result is a relative quantitation comparison between untreated and treated without any normalisation—caused by being unable to use actin or cytokeratin-18 as a control. Alteration in the detectable protein concentration of actin in response to IFN-λ either suggests uneven transfer or, more likely, indicates that IFN-λ treatment may affect other cytoskeletal properties in HBEC cultures. As exogenous IFN-γ has previously been shown to increase the abundance and alter the distribution of actin filaments in HeLa cells (Wang, Pfeffer et al. 1981) and the type I IFNs have been shown to downregulate the expression of β-actin mRNA in hepatocytes (Rusinova 2013), it is likely that exogenous IFN-λ could alter β-actin protein expression. To increase the validity of this result, I would advise the use of a larger number of samples and the use of a suitable, unchanged control protein for a more accurate quantitation of ZEB1 protein.

If the protein result is a true result, it can be suggested that IFN-λ causes significant decreases in miR-23a and miR-429 levels which, in turn, causes the levels of ZEB1 protein increase due to decreased microRNA-mediated translational repression. Consequently increased ZEB1 protein may impact upon epithelial barrier integrity through increased transcriptional repression of E-cadherin as has been previously described (Bolos, Peinado et al. 2003).

E-cadherin mRNA was decreased in response to IFN-λ at 48 and 72 hours in healthy ALI cultures, though this was not a significant change. This slight decrease of E-cadherin expression correlated to decreased miRNA expression and increased ZEB1 protein expression. This may suggest that in response to IFN-λ treatment there is very slight elevation ZEB1 mediated transcriptional repression of E-cadherin mRNA. Alternatively, this may suggest that ZEB1 is elevated to prevent significant changes to E-cadherin level

in response to IFN-λ stimulus. In asthmatic cultures E-cadherin mRNA was again not significantly altered in response to IFN-λ treatment. Conversely to observations in asthmatic samples, there was elevation of E-cadherin mRNA at 24 and 48 hours suggesting that IFN-λ may increase E-cadherin expression. Previous data has shown that in some contexts and cell types IFN-α can upregulate E-cadherin (Masuda, Saito et al. 2000). By 72 hours, E-cadherin mRNA is slightly reduced in response to IFN-λ which correlated to decreased miR-23a levels and increased ZEB1 protein expression. This further suggests that ZEB1 is elevated to prevent significant changes to E-cadherin mRNA in response to IFN-λ—but this response is delayed in asthmatics, hence the elevated mRNA observed at 24 and 48 hours. As it has previously been noted that asthmatic individuals have a number of delayed processes when compared to healthy individuals (i.e. delayed cell shedding (Wilkinson, Unpublished), delayed viral clearance (Kim and Gern 2012)), it is feasible that asthmatics could have delayed responses to miRNA changes (and subsequent miR-mediated changes). As previously pointed out, it is difficult to draw solid conclusions from this data due to only having an n=4 of healthy samples and an n=3 of asthmatic samples and no significance and thus would require further investigation with larger sample sizes to ascertain whether this is merely a coincidental observation or a true result.

To further corroborate the observations of E-cadherin mRNA, E-cadherin protein was measured via immunofluorescent staining. Direct comparison of staining intensity (measured at 650v) suggested no difference in protein concentration in response to IFN-λ treatment in both healthy and asthmatic individuals. This methodology of quantifying protein via immunofluorescence presumes that staining efficiency was consistent across all filters, which may not be the case. It also has limitations in terms of sensitivity—subtle differences may not be detectable by the laser/computer software and could be lost during the scanning process. Additionally, these judgements have been made by eye, which inherently comes with limitations. To confirm the results obtained from the confocal microscopy, total E-cadherin concentration would need to be assessed via western blotting. Immunofluorescent staining does show a difference in E-cadherin distribution in response to IFN-λ treatment in both healthy and asthmatic samples—regions in which there were higher concentrations of E-cadherin in the cellular junctions which correlated with decreased DAPI staining—though this was less pronounced in

asthmatic samples. This particular pattern of staining has previously been associated with cellular shedding and subsequent reorganisation/redistribution of junctional proteins (Guan, Watson et al. 2011)—which suggests that IFN-λ is triggering the shedding of epithelial cells. As mentioned above, there were less of these regions in asthmatic samples and as previously discussed, asthmatic individuals have been shown to have impaired/delayed cell shedding in response to viral infection (Wilkinson, Unpublished).

TNFAIP3/A20 mRNA was elevated in response to IFN-λ treatment at 24, 48 and 72 hours in healthy individuals but once again this was not significant. This increase in mRNA levels correlated with significant decreases in miR-23a and miR-429 in response to interferon—once again suggesting that these events could be associated. In asthmatic individuals, TNFAIP3/A20 mRNA levels were very similar in response to IFN-λ treatment at 24 and 72 hours—but significantly decreased at 48 hours. At 48 hours, there was also significant reduction in the level of miR-23a. As per bioinformatic predictions, it would be expected that a significant decrease in miR-23a would lead to increased TNFAIP3/A20 mRNA/protein if this microRNA regulated expression. As this is not the case it may suggest that despite there being predicted binding sites in the 3'UTR, miR-23a does not target TNFAIP3 and consequently the correlation observed in healthy samples is coincidence. Alternatively, it suggests in there is a differential response to IFN-λ in asthmatics and whilst miR-23a significantly decreases, another miRNA—with a stronger binding affinity—may be significantly induced, thus counteracting the miR-23a response.

To further assess whether significant decreases in the chosen miRNAs lead to significant changes in TNFAIP3/A20 protein was measured via western blotting. This would allow for the elucidation as to whether the miRNAs have a potential targeting effect (via translational modulation (Doench and Sharp 2004)). However, across the n=3 of healthy and n=3 asthmatic samples, TNFAIP3/A20 protein could not be detected using conditions from the H1 HeLa antibody optimisation trials and the conditions which allowed for detection of TNFAIP3/A20 protein in the differentiating ALI cultures (see below). The lack of detection suggests that the protein concentration of TNFAIP3/A20 in differentiated ALI cultures is below the level of detection. As TNFAIP3/A20 is a crucial negative regulator of NF-κB activation (Parvatiyar and Harhaj 2011) it is feasible that cellular concentration of TNFAIP3/A20 is low at baseline to allow for immediate

increases in NF-κB action. Subsequently the level of TNFAIP3/A20 elevates upon activation of the NF-κB-dependent inhibitory feedback loop to ensure no aberrant inflammation occurs (Shembade, Ma et al. 2010, Ruland 2011). Whilst type I IFNs have been shown to be able to activate NF-κB in a non-conventional signal transduction pathway (Du, Wei et al. 2007) the subsequent NF-κB-dependent inhibitory feedback loop may not be activated within the 72 hour sampling window, thus TNFAIP3/A20 protein remains undetectable.

In addition to TNFAIP3/A20 having effects on NF-κB activation, it is proposed to have effects on epithelial barrier integrity through increasing stabilisation of occludin within TJs (Kolodziej, Lodolce et al. 2011). Additionally, miR-429 has a bioinformatically predicted binding site in the 3'UTR of occludin. Occludin mRNA was elevated in response to IFN-λ treatment across times in healthy individuals—though this was not significant. This elevated occludin mRNA correlated with decreased miR-429 and elevated TNFAIP3/A20 mRNA which suggests these events may be linked. In asthmatic ALI cultures, occludin mRNA remained largely unchanged at 24 and 72 hours, with slight elevation at 48 hours though again this was not significant. The lack of changes at 24 and 72 hours correlated with no significant changes in miR-429 and TNFAIP3/A20. As previously highlighted, there are difficulties drawing solid conclusions from the data due to the limited sample size and its' biological relevance cannot be said with certainty due to a lack of statistical significance.

As with E-cadherin, occludin protein concentration and distribution was studied using immunofluorescent staining and confocal microscopy. There were no visible differences in occludin protein concentration or localisation in response to 72 hours of IFN-λ treatment in either healthy or asthmatic ALI cultures. The only visible differences between untreated and treated cultures were the 'holes' in which DAPI staining was reduced—suggesting a loss of nuclei—which may indicate cellular shedding. Once again this effect was less visible in asthmatic samples, suggesting an impaired IFN-λ induced cell shedding in asthmatics when compared to healthy cultures. As discussed in the E-cadherin results, occludin results obtained from the immunofluorescence have limitations in terms of sensitivity, staining efficiency and judgements made by eye. To confirm the total concentration of occludin protein in the HBEC samples in untreated and treated samples a whole protein lysate would have to be assessed via western blotting.

In addition to characterising the response of microRNAs and the proposed targets to 72 hours of exogenous IFN-λ—other characteristics of the ALI cultures were observed. TER indicated an increased ionic permeability in response to IFN-λ treatment in healthy individuals across all times. This suggests a decrease in epithelial barrier integrity, specifically highlighting a potential disruption of the epithelial tight junctions (Anderson and Van Itallie 2009) in response to IFN-λ in healthy ALI cultures. This correlates with previous data showing a number of cytokines can promote epithelial barrier dysregulation (Bruewer, Luegering et al. 2003); though there is no published data to suggest type I or III IFNs have this effect. As previously observed in viral infection (Sajjan, Wang et al. 2008)—the TER was most greatly decreased at 24 hours of treatment and appeared to begin to recover over subsequent time points, suggesting a short-lived epithelial barrier disruption with epithelial barrier repair occurring over subsequent 48 hours as has been observed in *in vitro* wound repair of epithelium (Herard, Zahm et al. 1996). This proposed barrier repair may also be reasoning why there were no observable differences in E-cadherin/occludin protein concentration at 72 hours in the confocal imaging. Therefore, it would be extremely useful to examine the immunofluorescent staining at 24 and 48 hours to further examine IFN-λ effect on protein concentration/distribution. Asthmatic differentiated cultures did not have a TER decrease in response to exogenous IFN-λ treatment—suggesting that there was no change to ionic permeability and thus no decrease in epithelial barrier integrity or disruption to tight junctions (Anderson and Van Itallie 1995). As previously discussed, asthmatic individuals are shown to have impaired epithelial shedding during viral infections (Wilkinson, unpublished) and have impaired healing (Davies, Wicks et al. 2003) which could, in part, be indicative of a decreased, or lack, of responsiveness of these cells to viral stimuli—including a lack of responsiveness to released IFN-λ. This decreased/lack of responsiveness could be the reasoning in which asthmatic individuals have differential responses in miRNA, mRNA and protein compared to healthy samples, plus have no altered epithelial barrier integrity to IFN-λ.

Phase contrast images were used to study the morphology of the whole ALI culture. In response to 72 hours of IFN-λ treatment, there were regions of morphological changes in both healthy and asthmatic samples. In these regions of morphological change, cells adopted a more ‘elongated’ and ‘stretched’ shape—having a more mesenchymal

appearance compared to the rest of the 'cobblestone', epithelial cells within the culture. This potentially could indicate that exogenous IFN-λ treatment may trigger EMT in isolated regions of culture. However this seems unlikely as current literature suggests IFN-α promotes MET in tumour cells (Kudryavets, Bezdenezhnykh et al. 2011), thus type III IFNs are likely to have a similar effect. Alternatively this morphological change could suggest that IFN-λ causes unjamming of cells—leading to the differences in cell shape and motility (Park, Kim et al. 2015). As EMT has been linked to differences in adhesive contacts (Ikenouchi, Matsuda et al. 2003, Gregory, Bert et al. 2008, Korpal, Lee et al. 2008) and there are no apparent differences between E-cadherin and occludin within the junctions in untreated and treated cultures—it is more likely to indicate an unjamming event is occurring as cell jamming/unjamming has been shown not to be associated with cell-to-cell adhesion (Park, Kim et al. 2015).

In addition to exploring the effect on the IFN-λ on differentiated cells that mimic the intact, uninfected cell population during a HRV-16 infection—the second experimental setup explored the response of a damaged and repairing epithelial barrier to IFN-λ. This was an important condition to explore as during viral infection the epithelial barrier becomes damaged (Sajjan, Wang et al. 2008) as cells are shed (Turner, Hendley et al. 1982) and repairs under the presence of virally induced mediators such as IFN-λ (Vareille, Kieninger et al. 2011)—therefore IFNs may play a role in barrier homeostasis.

As with the experiments with differentiated cells, MxA mRNA levels were measured to confirm that IFN-λ treated cells were responding to the exogenous interferon through upregulation of key ISGs. MxA mRNA was significantly upregulated in IFN-λ treated cells compared to untreated controls across all experimental conditions—therefore confirming differentiating ALIs responded to exogenous IFN treatment. As discussed before, subsequent differences observed between untreated and treated ALI cultures could be attributed as a response to the IFN-λ stimulus.

MiR-23a and miR-429 were significantly decreased in treated, healthy ALI cultures at day 7, 14 and 21 when compared to untreated ALI controls. As these treated cultures have been shown to be responding to exogenous IFN-λ through the upregulation of ISGs—it can be postulated that these microRNAs are also being affected by IFN-λ which causes a significant reduction. As these microRNAs have predicted targets that play a role in

epithelial barrier modulation (ZEB1, E-cadherin and occludin) and innate immune responses (TNFAIP3/A20), this suggests that IFN-λ could play a role in modulating these responses in the repairing/differentiating epithelium. In asthmatic ALI cultures, miR-23a and miR-429 were decreased in response to exogenous IFN-λ treatment—but this was not significant at any time point. This data, along with the MxA mRNA data, suggests that whilst asthmatic ALI cultures are responding to IFN-λ, there is a differential cellular response of these specific microRNAs in asthmatics when compared to healthy cultures. However as with the experiments on differentiated cultures, there are difficulties drawing solid conclusions from the data due to the limited sample size (n=4 healthy; n=3 asthmatic) and thus to draw more solid conclusions a larger number of samples would have to be used in addition to increasing stratification of asthmatic sample characterisation.

ZEB1 mRNA was elevated in response to IFN-λ treatment in both asthmatic and healthy ALI cultures. The only significant elevation in ZEB1 mRNA levels in response to IFN-λ was observed at day 7 in healthy differentiating ALI cultures ($p=0.0202$). In all instances, the increase in ZEB1 mRNA was correlated to decreased levels of miR-23a (*in silico* predicted target of ZEB1) and miR-429 (target of ZEB1 (Gregory, Bert et al. 2008, Korpal, Lee et al. 2008)). Together this suggests that the specific miRNAs do target the 3'UTR of ZEB1 mRNA and alter expression. Though the levels of ZEB1 mRNA increase in response to IFN-λ treatment/miRNA reduction this is not significant (aside from at day 7 in healthy cultures) which once again suggests that the miRNAs may exert their regulatory effect through translational repression opposed to mRNA degradation (Doench and Sharp 2004). To further examine the plausibility of this postulated mechanism of miRNA action, levels of ZEB1 protein was assessed. At day 7 and 14 ZEB1 protein was seen to be higher in IFN-λ treated cells relative to untreated cells in healthy individuals—correlating with decreased miRNAs, thus further supporting the proposed miRNA:ZEB1 mRNA interaction and subsequent modulation of protein expression. Despite the specific microRNAs still being significantly decreased at day 21 and increased mRNA—ZEB1 protein was seen to be decreased in response to IFN-λ treated cells at this time. Decreased ZEB1 protein was also observed in treated cells at all times in asthmatic samples. This could suggest that previous correlated microRNA and ZEB1 activities were purely coincidental and not causational. Alternatively it may suggest that whilst miRNA levels

have been significantly reduced in response to IFN-λ treatment at this time point, there may have been increased level of microRNA association with polysomes hence impacting upon the miRNA's ability to alter protein translation (Molotski and Soen 2012). This highlights the need for further assessment of miR-23a/-429's concentrations/locations within polysomes to investigate whether these microRNA changes are occurring in a manner that could affect the translational pool within the cells. Limitations of the ZEB1 protein data also would also have to be addressed to allow for more reliable conclusions to be drawn—the data obtained here only represent n=2 healthy and n=1 asthmatic and thus larger sample numbers are required with repeatability. And, as addressed above, there is the need for a suitable protein control within the western blot.

Altered levels of ZEB1 have previously been shown to alter E-cadherin expression, as ZEB1 is a known transcriptional repressor of CDH1 (Bolos, Peinado et al. 2003). E-cadherin mRNA was shown to be decreased in response to treatment at all times in both healthy and asthmatic cultures—with significance at both day 14 and 21. This E-cadherin mRNA decrease correlated with increased ZEB1 mRNA which may suggest ZEB1 is regulating E-cadherin expression as has been postulated and previously shown. Given the unreliability of ZEB1 protein data, the proposed interaction and action cannot be confirmed with certainty and thus remains purely speculative.

To further assess E-cadherin expression and localisation in response to IFN-λ treatment, immunofluorescent staining was utilised. There were limited differences in assumed protein concentration on day 7 between the IFN-λ treated and untreated control differentiating cells in both healthy and asthmatic individuals, with localisation both at epithelial junctions and cytoplasmically, indicating the beginning of AJ formation and barrier maturation. Staining at day 14 showed higher intensity staining for E-cadherin in response to IFN-λ treatment in both asthmatic and healthy cultures. Examination of Z-stack localisation suggests that E-cadherin protein appears to be apicolateral in both conditions; however it is more dispersed and less focal than the untreated cells suggesting it that IFN-λ prevents E-cadherin focussing in AJs. The same observations were made at day 21. Though staining intensity appeared higher in response to IFN-λ at day 14 and 21, overall each treated section has decreased cell number which may indicate that total E-cadherin protein concentration has decreased. Previous exogenous IFN-α

treatment of hepatocytes have shown that IFNs can cause downregulation of E-cadherin mRNA expression(-1.74 fold)(Rusinova 2013).

TNFAIP3/A20 mRNA was higher in IFN-λ treated cells than untreated controls across all time points in healthy, differentiating cultures. The elevated mRNA correlates with significantly decreased miR-23a and miR-429 which suggests that these microRNAs do bind and target the 3'UTR of TNFAIP3/A20 mRNA as predicted and alter expression. It is postulated that this increased TNFAIP3/A20 expression will decrease NF-κB activation (Parvatiyar and Harhaj 2011) and additionally alter TJ characteristics via enhancing occludin localisation within junctions (Kolodziej, Lodolce et al. 2011). In asthmatic individuals, TNFAIP3/A20 mRNA was decreased at day 7 and 21—and significantly increased at day 14. These mRNA changes do not appear to correlate with changes in microRNA—as both miR-23a and -429 were decreased (albeit not significantly) and thus should lead to elevated TNFAIP3/A20 if the miRNAs do target TNFAIP3/A20. As discussed above, it has previously been noted that in addition to miRNA's requiring sequence specificity to a target 3'UTR and exert an effect, there is a need to be associated with the 'translational pool' within polysomes (Molotski and Soen 2012). Thus in healthy differentiating cells, when there is a decrease in miRNAs and a correlating increase in mRNA this occurs has effect on polysomal microRNAs (which effects translation) but in the asthmatic differentiating cells, the miR-23a and -429 alterations do not occur in polysomes and instead a different miRNA may be responsible for the observed changes in TNFAIP3/A20 in these cells. As with the differentiated cells, there appears to be a differential response to interferon treatment in asthmatic differentiating cells verses healthy cultures.

Unlike in differentiated cultures, A20 protein was detectable in n=3 healthy and n=2 asthmatic differentiating cultures. Once again there are limitations of this protein data due to the small sample size and repeatability issues and the lack of a relevant control. A20 protein was not elevated in response to IFN-λ treatment at day 7 or 14—despite elevated mRNA levels—but it was elevated by day 21. It has previously been shown that changes in mRNA do not necessarily correlate to protein quantity as there are a number of other processes to consider such as relative mRNA abundance, free ribosomal units for translation and protein turnover (Maier, Guell et al. 2009). Thus the observed increase in mRNA at day 7 and 14 may not lead to changes in protein expression immediately and

consequently the chosen times of sampling wouldn't show this effect. The inverse may also explain why, despite mRNA decreases in response to interferon, A20 protein was higher in asthmatics. The A20 protein data does however further reinforce the concept that asthmatic and healthy HBECs respond differently to exogenous IFN-λ treatment—suggesting that these cells may respond differently to IFN-λ *in vivo* during rhinovirus infection.

Occludin mRNA was elevated in response to IFN-λ treated differentiating cells across all experimental conditions—correlating to decreased microRNAs and elevated TNFAIP3/A20 mRNA. Conversely examination of occludin protein via immunofluorescent staining showed less intense occludin staining in treated cells—suggesting a lower concentration of occludin in these cells. Once again the lack of alignment between mRNA and protein data shows that changes in transcription and translation do not necessarily correlate and a number of other biological processes have to be taken in to account (Maier, Guell et al. 2009). Additionally, as discussed several times above, there are limitations with drawing conclusions on protein concentration based purely off confocal data. As for differential protein localisation, it appeared that IFN-λ treatment had an effect on localisation with less continuous localisation to epithelial cell junctions at both day 7, 14 and 21 in both healthy and asthmatic cultures. Given that at day 21 there was a relative increase of A20 protein in treated cells, it was postulated that this should increase occludin stability within TJs (Kolodziej, Lodolce et al. 2011), however the lack of occludin staining at some cell edges suggests that occludin is less stable/junctionally localised. This could suggest that either A20 does not have this stabilising effect in airway epithelium (unlike what has been observed in intestinal epithelial cells)(Kolodziej, Lodolce et al. 2011) or that though occludin appears less continuously, it has increased stability in the junctions.

In addition to characterising the response of microRNAs and the proposed targets to 21 days of exogenous IFN-λ—other characteristics of the ALI cultures were observed. TER was measured every ~48 hours to monitor epithelial barrier development in response to treatment—helping to elucidate the role of IFN-λ on epithelial barrier repair that occurs during rhinovirus infection. In healthy samples, IFN-λ treatment led to decreased TER which approached significance by day 14. As TER is a measure of epithelial barrier integrity mainly associated with epithelial tight junctions (Anderson and Van Itallie

1995), it suggests that IFN-λ impedes barrier formation and strengthening in damaged/repairing epithelium. It appears IFN-λ may promote epithelial dysregulation in damaged barrier possibly to promote the unjamming of cells to increase motility during repair/differentiation (Park, Kim et al. 2015) in addition to facilitating cell shedding during infection (Turner, Hendley et al. 1982). In asthmatic samples, TER was lower in untreated cultures and there was less of a pronounced decrease of TER in response to exogenous IFN-λ compared to healthy, differentiating cells. The decreased TER in untreated cells suggests that epithelial barrier development and strength is impaired at baseline in the asthmatic cohort when compared to healthy individuals (Georas and Rezaee 2014). The decreased impact of IFN-λ treatment to TER therefore could have two potential explanations—either that as the epithelial barrier is already impaired and weaker and thus IFN-λ has less of an effect or that asthmatic cells themselves are less responsive to IFN-λ. Both of these postulations could go some way to explaining why asthmatic individuals have impaired responses to rhinovirus infections.

The passage of FITC-labelled 4kD Dextran from apical to basolateral compartment was measured to assess macromolecular permeability of cultures in response to exogenous IFN-λ—allowing for potential assessment of tight junction integrity (specifically occludin). Macromolecular permeability was significantly increased in response to IFN-λ treatment across all days in healthy individuals. This suggests that IFN-λ is able to elevate macromolecular permeability thus likely to be affecting the adherens junctions, though the precise mechanism of action is unknown. As discussed above with reference to TER, it suggests that IFN-λ may promote cellular unjamming and motility which (Park, Kim et al. 2015), during rhinovirus infection, may play a role in cell shedding and damage repair processes. In asthmatic individuals once again macromolecular permeability was higher at baseline than healthy cultures—further supporting the notion that asthmatic individuals have impaired epithelial barrier integrity (Xiao, Puddicombe et al. 2011)—and though macromolecular permeability increased in response to IFN-λ treatment, this was not significant. The lack of significance could either be further evidence of a lack of responsiveness of these cells to IFN-λ, or could be in part due to the limited cohort size (n=4) as significance was approached at day 14 and 21.

Further to observations made in the immunofluorescent staining regarding apparent decreased cell numbers in imaged sections, total cell counts were conducted to determine

the impact of IFN-λ. In untreated cultures, cell numbers increased over 21 days of differentiation in both patient cohorts. However, in response to IFN-λ treatment in healthy cultures there was a significant reduction in cell number compared to untreated cells. As IFN-λ has previously been shown to be able to induce cellular apoptosis (Sangfelt, Erickson et al. 2000, Dumoutier, Tounsi et al. 2004) and have anti-proliferative effects (Brand, Beigel et al. 2005) —it is plausible to suggest these effects are occurring in airway epithelial cells. In addition to this it is well known that during HRV infection cells are shed from the epithelial layer (Turner, Hendley et al. 1982); but it is not yet clear whether this is a consequence of viral replication or the increased released IFNs and thus IFN-λ may also be causing cell loss via shedding. In addition to this, examination of Z-Stacks taken from immunofluorescent staining suggest the decreased cell number could be linked to the decreased pseudostratification of epithelial cells in IFN-λ treated cultures. In IFN-λ treated cultures, cells appear to remain as a monolayer and do not appear to differentiate—suggesting IFN-λ may impede differentiation processes in epithelial cells. Though no current data exists as to the role of IFN-λ in differentiation, other IFNs have been shown to play a role in defining differentiation in a dose and cell dependent manner (Moritz and Kirchner 1986). Further experimentation would be required to determine which of these proposed mechanisms are occurring in response to exogenous IFN treatment.

Drawing together the data from the response of differentiated and differentiating cells to exogenous IFN-λ treatment suggests that in addition to establishing the antiviral state in response to HRV-16 infection, IFN-λ plays a role in modulating the epithelial barrier. It also appears that this modulatory effect on the epithelial barrier is different according to the integrity of the barrier itself—as results obtained from differentiated cells (mimicking intact barrier) and differentiating cells (mimicking damaged and repairing barrier) are different.

In an intact barrier, IFN-λ appears to be sufficient to cause a short-term reduction in epithelial barrier integrity, isolated areas of cellular shedding (Guan, Watson et al. 2011) and trigger cellular unjamming (Park, Kim et al. 2015). This process may be linked to the significant decreases in miR-23a and miR-429 that were observed in response to IFN-λ treatment which subsequently led to elevated ZEB1 protein expression and decreased E-cadherin mRNA expression—a process that has previously been confirmed to alter

epithelial barrier characteristics. This suggests that changes in miRNAs—caused by IFN-λ could underpin the barrier modulation effect. Due to the difficulty detecting A20 protein, there is no evidence to suggest IFN-λ/miRNAs could affect NF-κB activation. Similarly there is no evidence to suggest TNFAIP3/A20 altered occludin expression/stability in junctions—thus the effect of IFN-λ influenced miR-23a/429 changes on intact TJs is still speculative.

In damaged/repairing barrier, the presence of IFN-λ leads to decreased epithelial barrier integrity, decreased cell numbers—either by decreased proliferation (Brand, Beigel et al. 2005), impeded differentiation (Moritz and Kirchner 1986), increased apoptosis (Sangfelt, Erickson et al. 2000, Dumoutier, Tounsi et al. 2004), increased cell shedding (Turner, Hendley et al. 1982) or a combination of these—and trigger more widespread cell unjamming (Park, Kim et al. 2015). Though reductions of miR-23 and miR-429 are observed at the same time which correlates with changes in the predicted mRNA targets (occludin, ZEB1, TNFAIP3/A20 and E-cadherin) it did not appear to affect the translational pool as protein changes were not correlated and thus it appears in differentiating cells—these miRNAs changes do not influence junctional formation—instead some other interferon stimulated pathway underpins the changes.

Despite IFN-λ exerting different modulatory effects on epithelial barrier according to barrier 'state', one observation remained consistent: asthmatic epithelial cells responded differently—and to a lesser extent—than healthy epithelial cells. It has previously been speculated that asthmatic individuals present with more severe, persisting symptoms of HRV infection (Grunberg and Sterk 1999, Gavala, Bertics et al. 2011, Kim and Gern 2012) due to impaired epithelial barrier (Xiao, Puddicombe et al. 2011) and impaired innate immune responses. Though some studies have highlighted significant differences in interferon release to HRV-16 infection (Wark, Johnston et al. 2005, Contoli, Message et al. 2006), there was no difference in IFN-λ release to HRV-16 within this cohort. In this experimental series, treating asthmatic cultures with exogenous IFN-λ at a concentration similar to that released in response to viral infection, provided different responses in miRNAs/mRNAs/proteins and less pronounced changes in epithelial barrier when compared to healthy cultures. This may suggest that rather than deficient IFN release, it's deficient response to IFN stimulus which contributes to the asthmatic response to HRV infection.

CHAPTER SEVEN: Final Discussion

7.1: Summary of Key Findings

HRV16 effects on 21 day differentiated ALI bronchial epithelial cultures

- MiR-23a, miR-200b and miR-429 expression was significantly decreased in response to HRV-16 infection in 21 day differentiated, ALI cultured bronchial epithelial cells from both healthy and asthmatic donors. Interferon-β, -λ mRNAs were increased in response to HRV16 infection.
- Significant changes in MiR-23a, miR-200b and miR-429 expression correlated with significant changes in the mRNA levels of bioinformatically predicted targets occludin, TNFAIP3 and E-cadherin with no significant difference in detection levels of ZEB1 mRNA in cultures from both healthy and asthmatic donors.
- Interferon-λ protein release was significantly increased in assays of culture supernatants from 21 day differentiated, ALI cultured bronchial epithelial cells from both healthy and asthmatic donors in response to HRV16 infection.

Interferon-λ effects on post 21 day differentiated ALI bronchial epithelial cultures

- The effect of 24 – 72 hours exogenous treatment of IFN-λ on 21 day differentiated cultures from healthy donor cells showed significant reduction in MiR-23a and miR-429 with significant increases in MxA GTPase mRNA (an anti-viral response gene). In asthmatic donor cultures, MiR-23a was significantly decreased at 24 and 48 hours of treatment, whereas miR-429 was not significantly reduced. There was no corresponding significant increase in MxA mRNA.
- In cultures from healthy donors, predicted mRNA targets of miR-23a and -429 were significantly increased in expression at 48 hours of treatment for TNFAIP3 and occludin, but unchanged for ZEB1 and E-cadherin, with Western Blots showing a trend for increased expression of ZEB1 at 24 and 48 hours. In cultures from asthmatic donors, TNFAIP3 mRNA was significantly increased in expression at 48 hours of treatment, but unchanged for occludin, ZEB1 and E-cadherin. Western Blots suggested an increase at 24 hours in ZEB1.

- Exogenous IFN-λ treatment caused no significant changes in transepithelial resistance (TER), however there was a trend for reduction of TER in healthy donor cultures and changes in cell morphology and an apparent reduction in cell number in cultures from both healthy and asthmatic donors—however the effects were less pronounced in asthmatic individuals.

Interferon-λ effects on 7, 14 and 21 day differentiating ALI bronchial epithelial cultures

- In response to exogenous IFN-λ treatment of 7, 14 and 21 day differentiating ALI cultures from healthy donors, there were significant reductions in miR-23a and miR-429 and significant increases in MxA GTPase mRNA. In differentiating ALI cultures from asthmatic donors, reductions in miR-23a and miR-429 were not significant and there was no significant increase in MxA mRNA. The data suggested that the asthmatic cultures were less responsive to IFN-λ.
- In cultures from healthy donors, the predicted mRNA targets of miR-23a and -429 were significantly increased in expression at 14 days of treatment for TNFAIP3 and at 21 days for occludin mRNA. ZEB1 mRNA was significantly increased at 7 days and showed a trend upwards at 14 and 21 days. E-cadherin mRNA (transcriptionally repressed by ZEB1) was reduced at 14 and 21 days of treatment, with Western Blots showing limited changes to ZEB1 protein. In cultures from asthmatic donors, the predicted mRNA target of miR-23a and miR-429, TNFAIP3, was increased at 14 days of IFN-λ treatment. Thus miRNA decreases correlated with small but significant changes in the detection of mRNA for TNFAIP3/A20 and occludin and alterations in TNFAIP3/A20 and ZEB1 protein detection on Western Blots.
- Exogenous IFN-λ treatment caused no significant changes in transepithelial resistance, however the macromolecular permeability increased significantly in cultures from healthy donors at all three time points and cultures from asthmatic donors showed a delayed increase at 21 days. Cell morphology and cell number were changed in ALI cultures from healthy and asthmatic donors, however the effects were again less pronounced in asthmatic individuals.

Luciferase reporter assays in Hela cells

- These studies suggested that MiR-23a binds to the 3'UTR of TNFAIP3/A20 and reduces expression, increasing NF-κB activity.

7.2: Discussion

At the beginning of this project it was postulated that HRV-16 infection in culture differentiated airway epithelia would lead to alterations of the miRNAs of interest (miR-23a and the miR-200 family) and that the miRNA responses would be different in cultures from healthy and asthmatic patients.

These miRNAs of interest were chosen due to previous data obtained by the Epithelial Barrier and Inflammation group. MiR-200 family members had been shown to be decreased in a TNF-α treated colonic cell line which correlated with barrier dysregulation. MiR-23a was shown be elevated in renal epithelial cells in response to TNF-α and TGF-β treatment which correlated with reduced expression of TNFAIP3/A20 protein expression and enhanced NF-κB activation within cells. Bioinformatic predictions highlighted several potential targets of these miRNAs which could be associated with altered innate immunity and epithelial barrier maintenance including ZEB1, E-cadherin, occludin and TNFAIP3/A20.

Initial use of HBECs that were grown as submerged monolayer cultures showed limited miRNA responses to HRV-16 infection. Given that this model is less reflective of the *in vivo* environment (Technologies 2016) and showed fairly erratic responses to infection and infection controls (UV-RV) it was decided to move the investigation to a more physiologically relevant model. HBECs that were differentiated at ALI had a more repeatable response to HRV-16 and had architecture more reflective of the *in vivo* environment (Inc 2013). Upon viral infection, significant decreases in miR-23a and some miR-200 family members (miR-200b and miR-429, but not miR-200c) were observed. These significant decreases correlated with significant changes in mRNA of TNFAIP3/A20, occludin and E-cadherin. MiRNA or mRNA changes were similar in healthy and asthmatic samples and there appeared to be were no significant differences in the response to virus

During HRV-16 infection in ALI cultures, only a small proportion of cells are actively infected (Mosser, Vrtis et al. 2005, Chen, Hamati et al. 2006), while many other cells are exposed to mediators released from infected cells. As such investigation of HRV-16-induced immune modulators was conducted—specifically focussing on the epithelial interferon, IFN-λ (Sommereyns, Paul et al. 2008). IFN-λ mRNA and protein was significantly elevated in response to HRV-16 infection and the amount released was not significantly different in healthy compared to asthmatic samples. Using an IFN-λ concentration equivalent to that observed in supernatant from infected cultures; differentiated and differentiating ALI cultures were exogenously treated.

Differentiated ALI cultures were treated for 72 hours to reflect an experimental setup similar to that of the HRV-16 infections. It was proposed that treating this culture allowed for determination of how non-infected cells of the epithelial layer—which present with an intact epithelial barrier—respond to IFN-λ. Along with significant reductions in miR-23a and miR-429 in healthy cultures there were significant changes to TNFAIP3/A20 and occludin mRNA and increased ZEB1 protein. However, there were a number of observations that suggested that cultures from asthmatic donors responded differently to ones from healthy donors. There were no significant changes to miR-429 or occludin mRNA. Additionally there was a significant increase in the macromolecular permeability to FITC-labelled dextran indicating disruption of epithelial barrier in response to IFN-λ treatment in cultures from healthy donors, but not in asthmatic donor cultures. In the phase contrast micrographs, asthmatic donor cultures did not show 'gaps' in the cell layer with loss of nuclear staining and potential cell shedding/reorganisation (Guan, Watson et al. 2011) to the same extent as in healthy cells. This suggests that asthmatic cells did not respond to exogenous IFN-λ to the same extent—or indeed the same manner—as healthy cells. This interpretation is supported by the observation that mRNA for the anti-viral GTPase protein, MxA, was significantly elevated in response to IFN-λ in cultures from healthy donors but not from asthmatic donors.

Differentiating ALI cultures were treated over 21 days with IFN-λ to determine the effect of IFN-λ on differentiating cells in barrier formation/repair after damage (Vareille, Kieninger et al. 2011) which occurs in regions where cells have been shed due to infection (Turner, Hendley et al. 1982). Once again significant reductions in miR-23a and miR-429 were observed in healthy individuals—but not in asthmatics. Healthy cells also showed

significant alterations in ZEB1, E-cadherin, occludin and TNFAIP3/A20 mRNA in response to IFN-λ treatment however results from protein data suggested that these changes may have been more global and may not have impacted upon the translational pool (Molotski and Soen 2012). The response in asthmatics was once again observed to be different. Other characteristics observed to change in response to IFN-λ treatment in healthy differentiating cells include decreased cell numbers (measured via cell counts) and significant morphological changes that indicate enhanced cell motility/unjamming (Park, Kim et al. 2015). These changes were less pronounced in asthmatics, indicating a decreased responsiveness of asthmatics to IFN-λ.

Previously some of the binding of miR-23a/-429 to the 3'UTR of predicted targets had been confirmed (ZEB1 and miR-429). Utilising *in vitro* binding experiments, miR-23a was confirmed to bind to the 3'UTR of TNFAIP3/A20 which, in turn, correlated with differential NF-κB activation. Whilst designing constructs for to confirm miR-429 binding to the 3'UTR of occludin—Yu et al. published data to confirm this interaction utilising the same experimental strategy/design (Yu, Lu et al. 2016). This confirmed that alterations in miR-23a and miR-429 would impact expression of ZEB1 (and subsequently E-cadherin)(Korpal, Lee et al. 2008), TNFAIP3/A20 (and subsequently NF-κB activation) and occludin(Yu, Lu et al. 2016)—thus modulating epithelial barrier integrity and innate immune responses.

7.3: Proposed Model of the Effect of HRV-16 Infection on Barrier Integrity and Innate Immune Responses

Overall the data presented within this project may highlight a potential new conceptual model for how HRV-16 infection impacts upon epithelial barrier integrity and innate immune responses—and how these may be associated with changes in the two specific microRNAs of interest: miR-23a and miR-429.

After the initial inhalation, binding and cellular uptake of HRV-16 viral particles, the virus begins to replicate within bronchial epithelial cells. This viral replication is 'sensed' by a number of PRRs causing subsequent activation of intracellular signalling cascades. The outcome of these signalling cascades are altered cellular processes through differential expression patterns—which includes significant reduction of miR-23a and miR-429 levels. The significant reduction of miR-23a allows for increased TNFAIP3/A20

expression. Elevated levels of TNFAIP3/A20 will lead to increased negative regulation of NF-κB signalling ensuring that inflammation and innate immune responses are carefully maintained and 'dampened down' when necessary to prevent excessive/aberrant immune activity. Significant reductions in miR-429 levels will lead to enhanced ZEB1 protein translation. Elevated levels of ZEB1 allows for increased transcriptional repression of E-cadherin—a key protein in AJ assembly and maintenance. Lower levels of E-cadherin expression could lead to short-term weakening of the epithelial barrier between infected cells and non-infected neighbours allowing for shedding of the infected cell from the epithelial layer.

In addition to HRV-16 mediated downregulation of miR-429 and miR-23a expression, significant increases in IFN-β and IFN-λ transcription and IFN-λ protein release were also observed. As well as the released IFN-λ acting in an autocrine manner to reinforce the activation of ISGs involved with cellular arrest/apoptosis, IFN-λ can act in a paracrine manner to cause differential expression in neighbouring uninfected cells with an aim to create an antiviral state in the epithelial layer. As with infected cells, one of the outcomes of the differential expression is a significant reduction in miR-23a and miR-429 levels.

In uninfected cells with an intact barrier, the reduction of miR-23a leads to significant upregulation of TNFAIP3/A20 expression. As discussed above, increased TNFAIP3/A20 expression leads to enhanced negative regulation of NF-κB which causes reduced activation of proinflammatory processes and other innate immune responses within uninfected cells. This once again functions to ensure that excessive inflammation is not present across the whole epithelial layer and that immune responses are more targeted to cells that are infected—preventing damage to uninfected cells that are providing intact epithelial barrier defence. Additionally significant reductions in miR-429 may play a role in modulation of epithelial barrier integrity. As discussed above, reduction in miR-429 leads to increased levels of ZEB1 which subsequently decreases E-cadherin expression levels. Within uninfected cells, this reduction of E-cadherin allows for short-term weakening of the epithelial barrier to help facilitate cellular shedding events and additionally allows for the passage of innate immune cells across the barrier to help combat infection. MiR-429 downregulation also allows for significant upregulation of occludin mRNA. As epithelial barrier weakening is only short-term, it seems likely that

after the initial weakening event facilitated by ZEB1/E-cadherin, occludin expression is enhanced to facilitate epithelial barrier resealing and repair.

In uninfected cells with a damaged/impaired barrier, the reductions in miR-23a and miR-429 may not affect the translational protein pool, thus the microRNAs may not exert the same effect as noted for cells above. However, it appears as though IFN-λ facilitates cellular unjamming, increases cellular movement/motility and decreases cell number (by decreasing cell division and/or enhancing apoptosis) to impact upon the reorganisation of the epithelial layer though the exact mechanisms underpinning these characteristic changes is currently unknown.

Whilst this model is proposed to occur in both healthy and asthmatic individuals, there is evidence to suggest that these processes may be impaired in asthmatics (delayed cell shedding in response to HRV-16, decreases responsiveness to IFN-λ in both differentiated and differentiating cells). This may underpin why individuals with asthma present with more persistent rhinovirus infections with increased symptom severity and duration. This may also suggest that current strategies to use inhaled, exogenous IFN-λ as a therapeutic for asthma (Synairgen, 2016) may have limited practical applications.

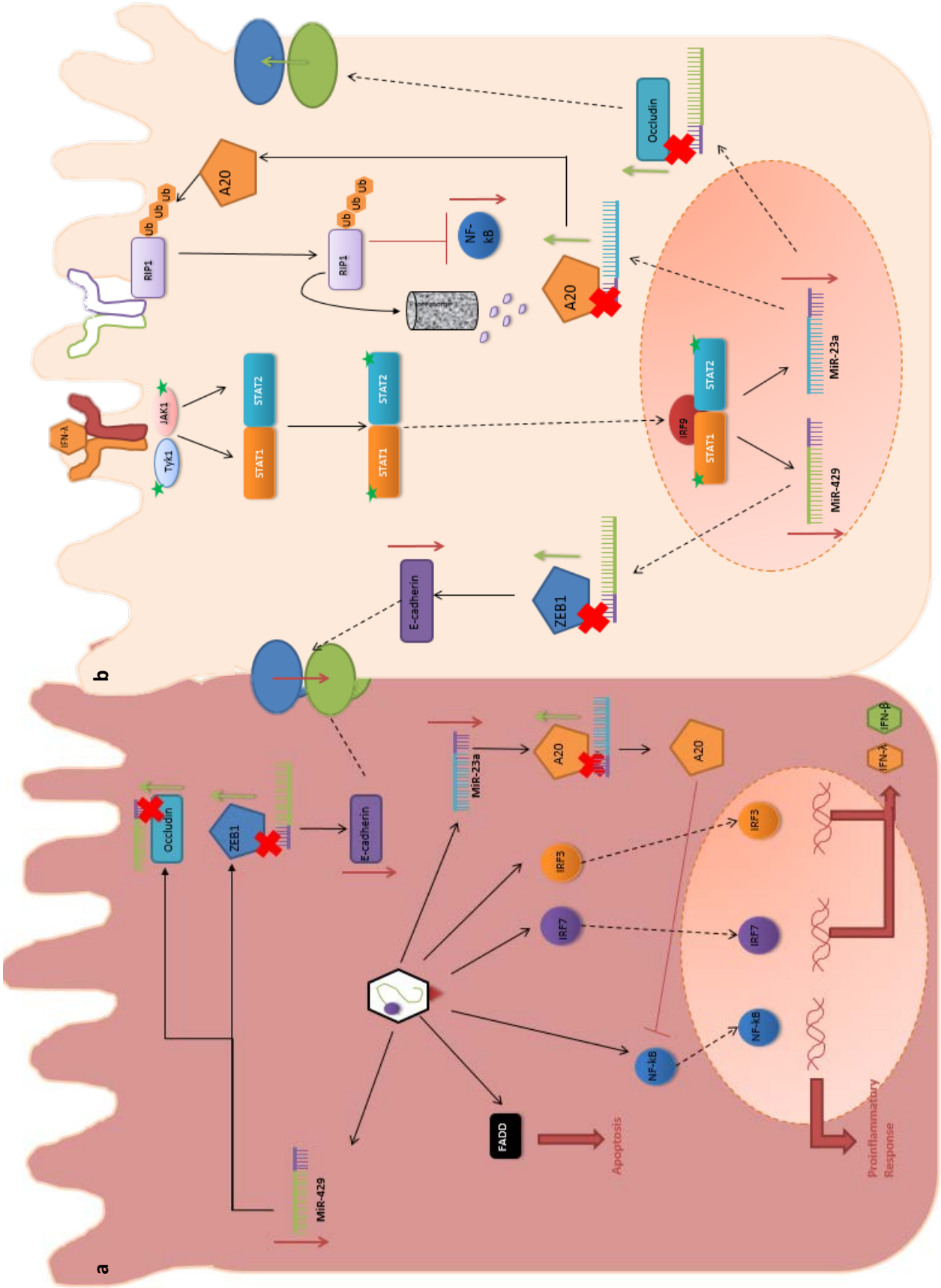

Figure 7.1: Proposed model of the effect of HRV-16 infection on Barrier Integrity and Innate Immune Responses via changes to miRNA expression. (a) Indicates proposed effect in direct consequence to viral infection within cell. (b) Indicates proposed effect in response to IFN-λ released in response to HRV-16 infection

7.4: Future Directions

This project has addressed some of the key questions originally posed as to the effect that HRV-16 infection may have on specific microRNAs involved in epithelial barrier integrity and innate immune responses. However, to help draw more robust conclusions, there are further studies that should be considered in future.

Firstly, with regard to the HRV-16 infection series, it would be useful to study the concentration of ZEB1, E-cadherin, A20 and occludin protein to further confirm the miRNA and mRNA changes effect the translational pool. Other studies have previously shown decreased levels of E-cadherin in HRV-16 infection and very tightly regulated activation of NF-κB (suggesting TNFAIP3/A20 regulation) which makes the postulated effect highly likely—however it would be interesting to link all of these changes occurring at the same time in the same patient samples.

It is this same need for further protein data that would help draw more robust conclusions about the IFN-λ treated miRNA/mRNA changes. Additionally, it would be extremely useful to have time-lapse data of IFN-λ treated cells to support the notion of enhanced cell motility. Additionally it would be useful to determine whether IFN-λ treatment is predisposing cells to apoptose (via monitoring markers of apoptosis such as caspases), arrest cell cycle (via proliferation assays) or shed (via shed cell supernatant counts).

The data has also turned up several new, interesting research questions that could be addressed in future:

Are asthmatic cells truly less responsive to IFN-λ? And if so, why?

- Using exogenous IFN-λ dose response experiments to assess characteristics of asthmatic ALIs to 72 hours of treatment—utilising cell counts, transepithelial resistance, FITC-labelled 4kD passage, time lapse microscopy, RT-qPCR, apoptosis assays, proliferation assays, immunofluorescent staining and western blotting.
- Examination of IFN-λ receptor distribution/expression on ALI cultures
    - If these appear to be downregulated—whether overexpression via an expression construct can restore functionality.

- Using current clinical classifications of asthmatics to test whether this is a feature that is 'universal' across asthmatics or whether this apparent lack of responsiveness to IFN-λ is a feature of an asthmatic subset.

Does IFN-β have the same effects on miRNAs (and targets) and epithelial barrier characteristics as IFN-λ?

- Utilising the same experimental designs as above but utilising exogenous IFN-β treatment with an appropriate concentration of IFN-β determined through quantification of protein release in supernatants from MOI=1 HRV-16 infected ALI cultures.

APPENDIX A: Patient Characteristics

Subjects	Total	Brushing/Biopsy	Male/Female	Age (Years)	FEV1 (% predicted)	Never/Ex/ Smokers
Healthy	5	5/0	3/2	31.8	115	5/0/0

Patient Characteristics for Chapter Five, Part I (Monolayer) experiments

Subjects	Total	Brushing/ Biopsy	Male/ Female	Age (Years)	FEV1 (% predicted)	ICS (mcg /day)	BTS	Never/Ex/ Smokers
Healthy	6	4/2	4/2	41.6	96.5			4/2/0
Asthma	6	5/1	2/4	39.1	78.1	1758	4.2	5/1/0

Patient Characteristics for Chapter Five, Part II (HRV-16 ALI) experiments

Subjects	Total	Brushing/ Biopsy	Male/ Female	Age (Years)	FEV1 (% predicted)	ICS (mcg /day)	BTS	Never/Ex/ Smokers
Healthy	4	4/0	2/2	36	112.5			3/1/0
Asthma	4	4/0	2/2	42.7	76.15	2800	4.5	2/1/1

Patient Characteristics for Chapter Six (IFN ALI) experiments

APPENDIX B: Composition of Reagents

1% Agarose Gel

	Weight (g)
Agarose Powder (Sigma Aldrich)	0.5
	Volume (ml)
1x TBE (Sigma Aldrich)	50

LB Agar

	Weight (g)
LB Agar Powder (Fisher Scientific)	10.5
	Volume (ml)
ddH_2O	300

LB Broth

	Weight (g)
LB Broth Powder (Fisher Scientific)	8
	Volume (ml)
ddH_2O	400

3mg/ml Retinoic Acid Stock

	Weight (mg)
Retinoic Acid (Sigma Aldrich)	50
	Volume (ml)
DMSO (Sigma Aldrich)	16.67
20ul of 50mg/ml Retinoic Acid further diluted in 4ml DMSO to give 50uM stock utilised in 1x ALI media (Table 2.5)	

1x TBE (pH 8.3)

	1x 1L ddH_2O
Boric Acid (Sigma Aldrich)	5.5g
0.5M EDTA (Thermo Fisher Scientific)	5ml
0.020M Tris Base (Thermo Fisher Scientific)	10.8g

APPENDIX C: Ct Ranges for MiRNA Data

24 Hours	MiR-200b	MiR-200c	MiR-429	MiR-23a
Healthy	20-22	21-22	23-24	23-24
Asthmatic	20-22	21-22	21-23	24-25

48 Hours	MiR-200b	MiR-200c	MiR-429	MiR-23a
Healthy	20-22	21-22	23-25	24-26
Asthmatic	20-22	21-22	21-23	24-26

72 Hours	MiR-200b	MiR-200c	MiR-429	MiR-23a
Healthy	21-22	21-22	24-27	25-28
Asthmatic	20-22	21-22	23-28	26-28

Raw Ct Ranges for miRNAs in Chapter 4, Part II (HRV-16 ALIs)

24 Hours	MiR-429	MiR-23a
Healthy	23-24	23-24
Asthmatic	21-23	24-25

48 Hours	MiR-429	MiR-23a
Healthy	23-24	23-24
Asthmatic	21-23	24-25

72 Hours	MiR-429	MiR-23a
Healthy	23-24	23-24
Asthmatic	21-23	24-25

Raw Ct Ranges for miRNAs in Chapter 5 (IFN-λ ALIs)

APPENDIX

APPENDIX D: Product List & Materials

Product	Supplier	Product Code
1Kb Plus DNA Ladder	ThermoFisher, UK	10787-018
10% Mini-Protean TGX Gel, 10 Well	BioRad, UK	456-1033
A20/TNFAIP3 Rabbit Antibody	New England Biosciences, UK	4625
Acetone	Sigma-Aldrich, USA	48358
Amersham ECL anti-Rabbit IgG HRP-linked whole antibody from Donkey	GE Healthcare, UK	NA934
Amersham ECL Select Western Blotting Detection Reagent	GE Healthcare, UK	RPN2235
Amersham ECL Prime Blocking Reagent	GE Healthcare, UK	RPN418
Anti-beta Actin Antibody HRP-linked Loading Control	Abcam, UK	Ab20272
BCA Protein Assay Kit	Pierce/ThermoFisher, UK	23227
Beta-mercaptoethanol	Sigma-Aldrich, USA	M6250
Bovine Serum Albumin, lyophilized powder, >96%	Sigma-Aldrich, USA	A8806
Bronchial Epithelial Cell Growth Media (BEGM)	Lonza, Switzerland	CC-3171
BEGM Bullet Kit	Lonza, Switzerland	CC-4175
CDH1 Human Primer FAM-MGB	Life Technologies/ThermoFisher, UK	4331182-hs01023894
Collagen I Bovine Protein	Life Technologies/ThermoFisher, UK	A1064401
Chloroform	Sigma-Aldrich, USA	C2434
Crystal Violet Solution	Sigma-Aldrich, USA	HT90132
DAPI for Nucleic Acid Staining	Sigma-Aldrich, USA	D9542
Dimethyl Sulfoxide (DMSO)	Sigma-Aldrich, USA	D5879
DTT	Sigma-Aldrich, USA	43815
Dulbecco's Modified Eagle's Medium (DMEM) with 4.5g/L glucose, Phenol Red and L-Glutamine	Lonza, Switzerland	12-604F
E-cadherin Antibody (5h6L18) Abfinitiy Rabbit Monoclonal	ThermoFisher, UK	701134
E-cadherin/CDH1 Antibody (4A2C7)	ThermoFisher, UK	33-4000
Fetal Bovine Serum	Life Technologies/ThermoFisher, UK	1600-044
Fluorescein Isocynate-dextran 4kDa	Sigma-Aldrich, USA	FD4
GAPDH Primer (Taqman Style assay)	Primer Design, UK	DD-hu-300-GAPDH

GeneAmp dNTP Blend (100nM)	Invitrogen/ThermoFisher, UK	N8080261
Glycerol	Sigma-Aldrich, USA	49781
Glycine	Fisherr Scientific, UK	BP381
Goat Serum 10%	Invitrogen/ThermoFisher, UK	50-1972
H1 HeLa Cells	ATCC, USA	ATCCRL-1958
Hams-F12 with L-Glutamine, Phenol Red and Sodium Pyruvate	PAA, GE- Healthcare	E15-817
HRV-1B Ideal Accompanying Reagent: oasign lyophilised one-step qRT-PCR mastermix	Primer Design, UK	OneStep-oasig-150-HRV1B
HRV-16 Ideal Accompanying Reagent: oasign lyophilised one-step qRT-PCR mastermix	Primer Design, UK	OneStep-oasig-150-HRV16
hsa-miR-1275 Taqman MicroRNA Assay	Life Technologies/ThermoFisher, UK	4427975-002840
hsa-miR-200b Taqman MicroRNA Assay	Life Technologies/ThermoFisher, UK	4427975-
hsa-miR-200c Taqman MicroRNA Assay	Life Technologies/ThermoFisher, UK	4427975-002300
hsa-miR-21 Taqman MicroRNA Assay	Life Technologies/ThermoFisher, UK	4427975-000397
hsa-miR-23a Taqman MicroRNA Assay	Life Technologies/ThermoFisher, UK	4427975-001024
hsa-miR-429 Taqman MicroRNA Assay	Life Technologies/ThermoFisher, UK	4427975-000399
Human Rhinovirus Subtype 16 Standard Kit	Primer Design, UK	Path-HRV16-Par-HRV16-standard
IL6 Human Primer FAM-MGB	Life Technologies/ThermoFisher, UK	4331182-hs00174131
IL8 Human Primer FAM-MGB	Life Technologies/ThermoFisher, UK	4331182-hs00174103
IFN-λ1 (IL-29) DuoSet ELISA	R&D Systems, USA	DY7246
IFN-λ1 Primer (Taqman Style assay)	Primer Design, UK	DD-hu-300-IFN-L1
IFN-λ2/3 Primer (Taqman Style assay)	Primer Design, UK	DD-hu-300-IFN-L2/3
KpnI 4000 units, 10,000 units/ml	New England Biosciences	R0142S
LB Agar Solution	Fisher Scientific, UK	BP1425
LB Broth Solution	Fisher Scientific, UK	BP1426
Methanol	Sigma-Aldrich, USA	494437
Minimum Essential Media (MEM) with Earle's Salts, L-Glutamine and Phenol Red	PAA/GE Healthcare, UK	E15-825
miRNeasy Mini Kit	QIAgen, Germany	217004
Multiscribe Reverse Transcriptase (50 units/ul)	Invitrogen/ThermoFisher, UK	4311235

MX1Human Primer FAM-MGB	Life Technologies/ThermoFisher, UK	4331182-hs00895608
Natural Protease XIV (from Streptomyces griseus)	Sigma-Aldrich, USA	P5147
NEB 5-alpha High Efficiency Competent E.coli cells	New England Biosciences, UK	CS987H
Non Essential Amino Acids x100 (NEAA)	Life Technologies/ThermoFisher, UK	1140-035
Occludin Antibody (6H10L9) Abfinity Rabbit Monoclonal	ThermoFisher, UK	71161
Occludin Antibody (OC-3F10)	ThermoFisher, UK	33-1500
OCLN Human Primer FAM-MGB	Life Technologies/ThermoFisher, UK	4331182-hs00170162
Phosphate Buffered Saline (PBS) without Ca or Mg	Lonza, Switzerland	17-516F
Protease Inhibitor Cocktail	Sigma-Aldrich, USA	P8340
QIAgen Plasmid Maxi Kit	QIAgen, German	12162
QIAprep Spin Miniprep Kit	QIAgen, Germany	27104
QIAzol Lysis Reagent	QIAgen, Germany	79306
Random Hexamers (50uM)	Invitrogen/ThermoFisher, UK	N8080127
Recombinant Human IFN-β 20ug	PeproTech, USA	300-02B
Recombinant Human IFN-λ 20ug	PeproTech, USA	300-02L
Reverse Transcriptase Buffer (x10)	Invitrogen/ThermoFisher, UK	18090050B
Retinoic Acid (50mg)	Sigma-Aldrich, USA	R2625
RNase Inhibitor (20 units/ul)	Applied Biosystems/ThermoFisher UK	N8080119
RNeasy Mini Kit	QIAgen, Germany	74104
RNU44 Taqman MicroRNA Assay—control miRNA	Life Technologies/ThermoFisher, UK	4427975-001094
Spectra Multicolor High Range Protein Ladder	ThermoFisher, UK	26625
Sodium Chloride	Fisher Scientific, UK	BP358
Sodium Dodecyl Sulphate	Fisher Scientific, UK	BP166
Sodium Pyruvate (100mM)	Life Technologies/ThermoFisher, UK	11360-070
Stop Solution (for ELISA)	R&D Systems, USA	DY994
Substrate Reagent Pack (for ELISA)	R&D Systems, USA	DY999
TaqMan Control Genomic DNA (human)	Life Technologies/ThermoFisher, UK	4312660
TaqMan MicroRNA Reverse Transcription Kit	Applied Biosystems/ThermoFisher, UK	4366597
TaqMan Universal PCR Mastermix (x2) no AmpErase UNG	Applied Biosystems/ThermoFisher, UK	4324018
TCF8/ZEB1 Rabbit mAb	New England Biosciences, UK	3396
TNFAIP3 Human Primer FAM-MGB	Life Technologies/ThermoFisher, UK	4331182-hs00234713

TOPO TA Cloning Kit (for subcloning) without competent cells	ThermoFisher, UK	450641
Trans-Blot Turbo Mini PDVF Transfer Packs	BioRad, UK	170-4156
Tris-Base	Fisher Scientific, UK	BP152
Tris Hydrochloride	Fisher Scientific, UK	BP1758
Trypsin-EDTA	Sigma-Aldrich, USA	T3924
Tryptose Phosphate Broth Solution	Sigma-Aldrich, USA	T8159
Tween-20	Fisher Scientific, UK	BP337
XbaI 3000 units, 20,000 units/ml	New Englan Biosciences	R0145S
ZEB1 Human Primer FAM-MGB	Life Technologies/ThermoFisher, UK	4331182-hs00232783

LIST OF REFERENCES

Ameres, S. L. and P. D. Zamore (2013). "Diversifying microRNA sequence and function." Nat Rev Mol Cell Biol **14**(8): 475-488.

Anderson, J. M. and C. M. Van Itallie (1995). "Tight junctions and the molecular basis for regulation of paracellular permeability." Am J Physiol **269**(4 Pt 1): G467-475.

Anderson, J. M. and C. M. Van Itallie (2009). "Physiology and function of the tight junction." Cold Spring Harb Perspect Biol **1**(2): a002584.

Ank, N., H. West, C. Bartholdy, K. Eriksson, A. R. Thomsen and S. R. Paludan (2006). "Lambda interferon (IFN-lambda), a type III IFN, is induced by viruses and IFNs and displays potent antiviral activity against select virus infections in vivo." J Virol **80**(9): 4501-4509.

Arden, K. E. and I. M. Mackay (2009). "Human rhinoviruses: coming in from the cold." Genome Med **1**(4): 44.

Asthma-UK. (2015). "Asthma UK | Asthma facts and FAQs." Retrieved 6th November, 2015, from https://www.asthma.org.uk/asthma-facts-and-statistics.

Atmar, R. L., E. Guy, K. K. Guntupalli, J. L. Zimmerman, V. D. Bandi, B. D. Baxter and S. B. Greenberg (1998). "Respiratory tract viral infections in inner-city asthmatic adults." Arch Intern Med **158**(22): 2453-2459.

Avraham, R. and Y. Yarden (2012). "Regulation of signalling by microRNAs." Biochem Soc Trans **40**(1): 26-30.

Bai, T. R., J. M. Vonk, D. S. Postma and H. M. Boezen (2007). "Severe exacerbations predict excess lung function decline in asthma." Eur Respir J **30**(3): 452-456.

Bals, R. and P. S. Hiemstra (2004). "Innate immunity in the lung: how epithelial cells fight against respiratory pathogens." Eur Respir J **23**(2): 327-333.

Barnes, K. C. (1999). "Gene-environment and gene-gene interaction studies in the molecular genetic analysis of asthma and atopy." Clin Exp Allergy **29 Suppl 4**: 47-51.

Barnes, P. J. (1998). "Efficacy of inhaled corticosteroids in asthma." J Allergy Clin Immunol **102**(4 Pt 1): 531-538.

Barnes, P. J. (2008). "Immunology of asthma and chronic obstructive pulmonary disease." Nat Rev Immunol **8**(3): 183-192.

Bazzoni, G. (2003). "The JAM family of junctional adhesion molecules." Curr Opin Cell Biol **15**(5): 525-530.

Becker, T. M., S. R. Durrani, Y. A. Bochkov, M. K. Devries, V. Rajamanickam and D. J. Jackson (2013). "Effect of exogenous interferons on rhinovirus replication and airway inflammatory responses." Ann Allergy Asthma Immunol **111**(5): 397-401.

Berube, K., Z. Prytherch, C. Job and T. Hughes (2010). "Human primary bronchial lung cell constructs: the new respiratory models." Toxicology **278**(3): 311-318.

Betel, D., A. Koppal, P. Agius, C. Sander and C. Leslie (2010). "Comprehensive modeling of microRNA targets predicts functional non-conserved and non-canonical sites." Genome Biol **11**(8): R90.

Betel, D., M. Wilson, A. Gabow, D. S. Marks and C. Sander (2008). "The microRNA.org resource: targets and expression." Nucleic Acids Res **36**(Database issue): D149-153.

Bochkov, Y. A., K. M. Hanson, S. Keles, R. A. Brockman-Schneider, N. N. Jarjour and J. E. Gern (2010). "Rhinovirus-induced modulation of gene expression in bronchial epithelial cells from subjects with asthma." Mucosal Immunol **3**(1): 69-80.

Bochkov, Y. A., K. Watters, S. Ashraf, T. F. Griggs, M. K. Devries, D. J. Jackson, A. C. Palmenberg and J. E. Gern (2015). "Cadherin-related family member 3, a childhood asthma susceptibility gene product, mediates rhinovirus C binding and replication." Proc Natl Acad Sci U S A **112**(17): 5485-5490.

Boller, K., D. Vestweber and R. Kemler (1985). "Cell-adhesion molecule uvomorulin is localized in the intermediate junctions of adult intestinal epithelial cells." J Cell Biol **100**(1): 327-332.

Bolos, V., H. Peinado, M. A. Perez-Moreno, M. F. Fraga, M. Esteller and A. Cano (2003). "The transcription factor Slug represses E-cadherin expression and induces epithelial to mesenchymal transitions: a comparison with Snail and E47 repressors." J Cell Sci **116**(Pt 3): 499-511.

Bondanese, V. P., A. Francisco-Garcia, N. Bedke, D. E. Davies and T. Sanchez-Elsner (2014). "Identification of host miRNAs that may limit human rhinovirus replication." World J Biol Chem **5**(4): 437-456.

Bonnelykke, K., P. Sleiman, K. Nielsen, E. Kreiner-Moller, J. M. Mercader, D. Belgrave, H. T. den Dekker, A. Husby, A. Sevelsted, G. Faura-Tellez, L. J. Mortensen, L. Paternoster, R. Flaaten, A. Molgaard, D. E. Smart, P. F. Thomsen, M. A. Rasmussen, S. Bonas-Guarch, C. Holst, E. A. Nohr, R. Yadav, M. E. March, T. Blicher, P. M. Lackie, V. W. Jaddoe, A. Simpson, J. W. Holloway, L. Duijts, A. Custovic, D. E. Davies, D. Torrents, R. Gupta, M. V. Hollegaard, D. M. Hougaard, H. Hakonarson and H. Bisgaard (2014). "A genome-wide association study identifies CDHR3 as a susceptibility locus for early childhood asthma with severe exacerbations." Nat Genet **46**(1): 51-55.

Bossios, A., S. Psarras, D. Gourgiotis, C. L. Skevaki, A. G. Constantopoulos, P. Saxoni-Papageorgiou and N. G. Papadopoulos (2005). "Rhinovirus infection induces cytotoxicity and delays wound healing in bronchial epithelial cells." Respir Res **6**: 114.

Bracken, C. P., P. A. Gregory, N. Kolesnikoff, A. G. Bert, J. Wang, M. F. Shannon and G. J. Goodall (2008). "A double-negative feedback loop between ZEB1-SIP1 and the microRNA-200 family regulates epithelial-mesenchymal transition." Cancer Res **68**(19): 7846-7854.

Braman, S. S. (2006). "The global burden of asthma." Chest **130**(1 Suppl): 4S-12S.

Brand, S., F. Beigel, T. Olszak, K. Zitzmann, S. T. Eichhorst, J. M. Otte, J. Diebold, H. Diepolder, B. Adler, C. J. Auernhammer, B. Goke and J. Dambacher (2005). "IL-28A and IL-29 mediate antiproliferative and antiviral signals in intestinal epithelial cells and murine CMV infection increases colonic IL-28A expression." Am J Physiol Gastrointest Liver Physiol **289**(5): G960-968.

Broide, D. H., M. Lotz, A. J. Cuomo, D. A. Coburn, E. C. Federman and S. I. Wasserman (1992). "Cytokines in symptomatic asthma airways." J Allergy Clin Immunol **89**(5): 958-967.

Bruewer, M., A. Luegering, T. Kucharzik, C. A. Parkos, J. L. Madara, A. M. Hopkins and A. Nusrat (2003). "Proinflammatory cytokines disrupt epithelial barrier function by apoptosis-independent mechanisms." J Immunol **171**(11): 6164-6172.

BTS (2014). British guideline on the management of asthma. B. T. Society, British Thoracic Society & Scottish Intercollegiate Guidelines Network. **1:** 192.

Buggele, W. A., K. E. Johnson and C. M. Horvath (2012). "Influenza A virus infection of human respiratory cells induces primary microRNA expression." J Biol Chem **287**(37): 31027-31040.

Bullens, D. M., A. Decraene, E. Dilissen, I. Meyts, K. De Boeck, L. J. Dupont and J. L. Ceuppens (2008). "Type III IFN-lambda mRNA expression in sputum of adult and school-aged asthmatics." Clin Exp Allergy **38**(9): 1459-1467.

Caamano, J. and C. A. Hunter (2002). "NF-kappaB family of transcription factors: central regulators of innate and adaptive immune functions." Clin Microbiol Rev **15**(3): 414-429.

Cano, A., M. A. Perez-Moreno, I. Rodrigo, A. Locascio, M. J. Blanco, M. G. del Barrio, F. Portillo and M. A. Nieto (2000). "The transcription factor snail controls epithelial-mesenchymal transitions by repressing E-cadherin expression." Nat Cell Biol **2**(2): 76-83.

Cao, M., M. Seike, C. Soeno, H. Mizutani, K. Kitamura, Y. Minegishi, R. Noro, A. Yoshimura, L. Cai and A. Gemma (2012). "MiR-23a regulates TGF-beta-induced epithelial-mesenchymal transition by targeting E-cadherin in lung cancer cells." Int J Oncol **41**(3): 869-875.

Chen, Y., E. Hamati, P. K. Lee, W. M. Lee, S. Wachi, D. Schnurr, S. Yagi, G. Dolganov, H. Boushey, P. Avila and R. Wu (2006). "Rhinovirus induces airway epithelial gene expression through double-stranded RNA and IFN-dependent pathways." Am J Respir Cell Mol Biol **34**(2): 192-203.

Cho, J. H., R. Gelinas, K. Wang, A. Etheridge, M. G. Piper, K. Batte, D. Dakhallah, J. Price, D. Bornman, S. Zhang, C. Marsh and D. Galas (2011). "Systems biology of interstitial lung diseases: integration of mRNA and microRNA expression changes." BMC Med Genomics **4**: 8.

Collison, A., C. Herbert, J. S. Siegle, J. Mattes, P. S. Foster and R. K. Kumar (2011). "Altered expression of microRNA in the airway wall in chronic asthma: miR-126 as a potential therapeutic target." BMC Pulm Med **11**: 29.

Contoli, M., G. Caramori, P. Mallia, S. Johnston and A. Papi (2005). "Mechanisms of respiratory virus-induced asthma exacerbations." Clin Exp Allergy **35**(2): 137-145.

Contoli, M., S. D. Message, V. Laza-Stanca, M. R. Edwards, P. A. Wark, N. W. Bartlett, T. Kebadze, P. Mallia, L. A. Stanciu, H. L. Parker, L. Slater, A. Lewis-Antes, O. M. Kon, S. T. Holgate, D. E. Davies, S. V. Kotenko, A. Papi and S. L. Johnston (2006). "Role of deficient type III interferon-lambda production in asthma exacerbations." Nat Med **12**(9): 1023-1026.

Corne, J., S. Smith, J. Schreiber and S. T. Holgate (1994). "Prevalence of atopy in asthma." Lancet **344**(8918): 344-345.

Corne, J. M., C. Marshall, S. Smith, J. Schreiber, G. Sanderson, S. T. Holgate and S. L. Johnston (2002). "Frequency, severity, and duration of rhinovirus infections in asthmatic and non-asthmatic individuals: a longitudinal cohort study." Lancet **359**(9309): 831-834.

Corren, J. (2013). "Asthma phenotypes and endotypes: an evolving paradigm for classification." Discov Med **15**(83): 243-249.

Costa, C., M. Bergallo, F. Sidoti, M. E. Terlizzi, S. Astegiano, S. Botto, M. Elia and R. Cavallo (2009). "What role for human rhinoviruses in the lower respiratory tract?" New Microbiol **32**(1): 115-117.

Crystal, R. G., S. H. Randell, J. F. Engelhardt, J. Voynow and M. E. Sunday (2008). "Airway epithelial cells: current concepts and challenges." Proc Am Thorac Soc **5**(7): 772-777.

Davies, D. E. (2009). "The role of the epithelium in airway remodeling in asthma." Proc Am Thorac Soc **6**(8): 678-682.

Davies, D. E. and S. T. Holgate (2002). "Asthma: the importance of epithelial mesenchymal communication in pathogenesis. Inflammation and the airway epithelium in asthma." Int J Biochem Cell Biol **34**(12): 1520-1526.

Davies, D. E., J. Wicks, R. M. Powell, S. M. Puddicombe and S. T. Holgate (2003). "Airway remodeling in asthma: new insights." J Allergy Clin Immunol **111**(2): 215-225; quiz 226.

de Arruda, E., 3rd, T. E. Mifflin, J. M. Gwaltney, Jr., B. Winther and F. G. Hayden (1991). "Localization of rhinovirus replication in vitro with in situ hybridization." J Med Virol **34**(1): 38-44.

de Boer, W. I., H. S. Sharma, S. M. Baelemans, H. C. Hoogsteden, B. N. Lambrecht and G. J. Braunstahl (2008). "Altered expression of epithelial junctional proteins in atopic asthma: possible role in inflammation." Can J Physiol Pharmacol **86**(3): 105-112.

de Veer, M. J., M. Holko, M. Frevel, E. Walker, S. Der, J. M. Paranjape, R. H. Silverman and B. R. Williams (2001). "Functional classification of interferon-stimulated genes identified using microarrays." J Leukoc Biol **69**(6): 912-920.

de Weerd, N. A. and T. Nguyen (2012). "The interferons and their receptors--distribution and regulation." Immunol Cell Biol **90**(5): 483-491.

de Weerd, N. A., S. A. Samarajiwa and P. J. Hertzog (2007). "Type I interferon receptors: biochemistry and biological functions." J Biol Chem **282**(28): 20053-20057.

Diamond, M. S. and M. Farzan (2013). "The broad-spectrum antiviral functions of IFIT and IFITM proteins." Nat Rev Immunol **13**(1): 46-57.

Dickensheets, H., F. Sheikh, R. Shepard, P. Hillyer, R. L. Rabin and R. P. Donnelly (2013). "69 : Interferon-lambda is produced by and induces autocrine expression of interferon-stimulated genes in human bronchial epithelial cells." Cytokine **63**(3): 259.

Ding, X., M. Ma, J. Teng, F. Shao, R. K. Teng, S. Zhou, Y. Zhang, E. Wu and X. Wang (2015). "Numb induces E-cadherin adhesion dissolution, cytoskeleton reorganization, and migration in tubular epithelial cells contributing to renal fibrosis." Curr Mol Med.

Doench, J. G. and P. A. Sharp (2004). "Specificity of microRNA target selection in translational repression." Genes Dev **18**(5): 504-511.

Donnelly, R. P. and S. V. Kotenko (2010). "Interferon-lambda: a new addition to an old family." J Interferon Cytokine Res **30**(8): 555-564.

Dotzauer, A. and L. Kraemer (2012). "Innate and adaptive immune responses against picornaviruses and their counteractions: An overview." World J Virol **1**(3): 91-107.

Du, Z., L. Wei, A. Murti, S. R. Pfeffer, M. Fan, C. H. Yang and L. M. Pfeffer (2007). "Non-conventional signal transduction by type 1 interferons: the NF-kappaB pathway." J Cell Biochem **102**(5): 1087-1094.

Dumoutier, L., A. Tounsi, T. Michiels, C. Sommereyns, S. V. Kotenko and J. C. Renauld (2004). "Role of the interleukin (IL)-28 receptor tyrosine residues for antiviral and antiproliferative activity of IL-29/interferon-lambda 1: similarities with type I interferon signaling." J Biol Chem **279**(31): 32269-32274.

Durbin, R. K., S. V. Kotenko and J. E. Durbin (2013). "Interferon induction and function at the mucosal surface." Immunol Rev **255**(1): 25-39.

E.K Wagner, M. J. H., D.C Bloom and D. Camerini (2008). Part IV: Replication Patterns of Specific Viruses. Basic Virology. E. K. Wagner. Oxford, UK, Blackwell Publishin. **1:** 249-251.

Edwards, M. R. and S. L. Johnston (2011). "Interferon-lambda as a new approach for treatment of allergic asthma?" EMBO Mol Med **3**(6): 306-308.

Erjefalt, J. S. and C. G. Persson (1997). "Airway epithelial repair: breathtakingly quick and multipotentially pathogenic." Thorax **52**(11): 1010-1012.

Eulalio, A., E. Huntzinger and E. Izaurralde (2008). "Getting to the root of miRNA-mediated gene silencing." Cell **132**(1): 9-14.

Evans, M. J., L. S. Van Winkle, M. V. Fanucchi and C. G. Plopper (2001). "Cellular and molecular characteristics of basal cells in airway epithelium." Exp Lung Res **27**(5): 401-415.

Fensterl, V. and G. C. Sen (2011). "The ISG56/IFIT1 gene family." J Interferon Cytokine Res **31**(1): 71-78.

Festjens, N., T. Vanden Berghe, S. Cornelis and P. Vandenabeele (2007). "RIP1, a kinase on the crossroads of a cell's decision to live or die." Cell Death Differ **14**(3): 400-410.

Finkelman, F. D., I. M. Katona, J. F. Urban, Jr., J. Holmes, J. Ohara, A. S. Tung, J. V. Sample and W. E. Paul (1988). "IL-4 is required to generate and sustain in vivo IgE responses." J Immunol **141**(7): 2335-2341.

Fitzgerald, K. A. (2011). "The interferon inducible gene: Viperin." J Interferon Cytokine Res **31**(1): 131-135.

Fuchs, R. and D. Blaas (2010). "Uncoating of human rhinoviruses." Rev Med Virol **20**(5): 281-297.

Fuchs, R. and D. Blaas (2012). "Productive entry pathways of human rhinoviruses." Adv Virol **2012**: 826301.

Fulcher, M. L., S. Gabriel, K. A. Burns, J. R. Yankaskas and S. H. Randell (2005). "Well-differentiated human airway epithelial cell cultures." Methods Mol Med **107**: 183-206.

Furuse, M., T. Hirase, M. Itoh, A. Nagafuchi, S. Yonemura, S. Tsukita and S. Tsukita (1993). "Occludin: a novel integral membrane protein localizing at tight junctions." J Cell Biol **123**(6 Pt 2): 1777-1788.

Gaajetaan, G. R., T. H. Geelen, J. H. Vernooy, M. A. Dentener, N. L. Reynaert, G. G. Rohde, E. V. Beuken, G. E. Grauls, C. A. Bruggeman and F. R. Stassen (2013). "Interferon-beta induces a long-lasting antiviral state in human respiratory epithelial cells." J Infect **66**(2): 163-169.

Ganesan, S., A. T. Comstock and U. S. Sajjan (2013). "Barrier function of airway tract epithelium." Tissue Barriers **1**(4): e24997.

Ganz, T. (2002). "Antimicrobial polypeptides in host defense of the respiratory tract." J Clin Invest **109**(6): 693-697.

Garrod, D. and M. Chidgey (2008). "Desmosome structure, composition and function." Biochim Biophys Acta **1778**(3): 572-587.

Gavala, M. L., P. J. Bertics and J. E. Gern (2011). "Rhinoviruses, allergic inflammation, and asthma." Immunol Rev **242**(1): 69-90.

Georas, S. N. and F. Rezaee (2014). "Epithelial barrier function: at the front line of asthma immunology and allergic airway inflammation." J Allergy Clin Immunol **134**(3): 509-520.

Giembycz, M. A., M. Kaur, R. Leigh and R. Newton (2008). "A Holy Grail of asthma management: toward understanding how long-acting beta(2)-adrenoceptor agonists enhance the clinical efficacy of inhaled corticosteroids." Br J Pharmacol **153**(6): 1090-1104.

Goodbourn, S., L. Didcock and R. E. Randall (2000). "Interferons: cell signalling, immune modulation, antiviral response and virus countermeasures." J Gen Virol **81**(Pt 10): 2341-2364.

Green, R. H., C. E. Brightling and P. Bradding (2007). "The reclassification of asthma based on subphenotypes." Curr Opin Allergy Clin Immunol **7**(1): 43-50.

Gregory, P. A., A. G. Bert, E. L. Paterson, S. C. Barry, A. Tsykin, G. Farshid, M. A. Vadas, Y. Khew-Goodall and G. J. Goodall (2008). "The miR-200 family and miR-205 regulate epithelial to mesenchymal transition by targeting ZEB1 and SIP1." Nat Cell Biol **10**(5): 593-601.

Grunberg, K. and P. J. Sterk (1999). "Rhinovirus infections: induction and modulation of airways inflammation in asthma." Clin Exp Allergy **29 Suppl 2**: 65-73.

Guan, Y., A. J. Watson, A. M. Marchiando, E. Bradford, L. Shen, J. R. Turner and M. H. Montrose (2011). "Redistribution of the tight junction protein ZO-1 during physiological shedding of mouse intestinal epithelial cells." Am J Physiol Cell Physiol **300**(6): C1404-1414.

Gulino, A., L. Di Marcotullio and I. Screpanti (2010). "The multiple functions of Numb." Exp Cell Res **316**(6): 900-906.

Haller, O., P. Staeheli and G. Kochs (2007). "Interferon-induced Mx proteins in antiviral host defense." Biochimie **89**(6-7): 812-818.

Haller, O., S. Stertz and G. Kochs (2007). "The Mx GTPase family of interferon-induced antiviral proteins." Microbes Infect **9**(14-15): 1636-1643.

Harada, H., T. Fujita, M. Miyamoto, Y. Kimura, M. Maruyama, A. Furia, T. Miyata and T. Taniguchi (1989). "Structurally similar but functionally distinct factors, IRF-1 and IRF-2, bind to the same regulatory elements of IFN and IFN-inducible genes." Cell **58**(4): 729-739.

Hardyman, M. A., E. Wilkinson, E. Martin, N. P. Jayasekera, C. Blume, E. J. Swindle, N. Gozzard, S. T. Holgate, P. H. Howarth, D. E. Davies and J. E. Collins (2013). "TNF-alpha-mediated bronchial barrier disruption and regulation by src-family kinase activation." J Allergy Clin Immunol **132**(3): 665-675 e668.

Hartsock, A. and W. J. Nelson (2008). "Adherens and tight junctions: structure, function and connections to the actin cytoskeleton." Biochim Biophys Acta **1778**(3): 660-669.

Herard, A. L., J. M. Zahm, D. Pierrot, J. Hinnrasky, C. Fuchey and E. Puchelle (1996). "Epithelial barrier integrity during in vitro wound repair of the airway epithelium." Am J Respir Cell Mol Biol **15**(5): 624-632.

Hofer, F., M. Gruenberger, H. Kowalski, H. Machat, M. Huettinger, E. Kuechler and D. Blaas (1994). "Members of the low density lipoprotein receptor family mediate cell entry of a minor-group common cold virus." Proc Natl Acad Sci U S A **91**(5): 1839-1842.

Holgate, S. T. (2007). "Epithelium dysfunction in asthma." J Allergy Clin Immunol **120**(6): 1233-1244; quiz 1245-1236.

Holgate, S. T. (2010). "A brief history of asthma and its mechanisms to modern concepts of disease pathogenesis." Allergy Asthma Immunol Res **2**(3): 165-171.

Holgate, S. T., H. S. Arshad, G. C. Roberts, P. H. Howarth, P. Thurner and D. E. Davies (2010). "A new look at the pathogenesis of asthma." Clin Sci (Lond) **118**(7): 439-450.

Holgate, S. T., D. E. Davies, P. M. Lackie, S. J. Wilson, S. M. Puddicombe and J. L. Lordan (2000). "Epithelial-mesenchymal interactions in the pathogenesis of asthma." J Allergy Clin Immunol **105**(2 Pt 1): 193-204.

Holgate, S. T. and R. Polosa (2006). "The mechanisms, diagnosis, and management of severe asthma in adults." Lancet **368**(9537): 780-793.

Huayllazo, K. G. (2012). "Interferons and Their Receptors: Distribution and Regulation." Retrieved 13/11/2016, 2016, from http://www.slideshare.net/kelvin2112/the-interferons-and-their-receptors-distribution-and.

Huber, O. (2003). "Structure and function of desmosomal proteins and their role in development and disease." Cell Mol Life Sci **60**(9): 1872-1890.

Huntzinger, E. and E. Izaurralde (2011). "Gene silencing by microRNAs: contributions of translational repression and mRNA decay." Nat Rev Genet **12**(2): 99-110.

Ikenouchi, J., M. Matsuda, M. Furuse and S. Tsukita (2003). "Regulation of tight junctions during the epithelium-mesenchyme transition: direct repression of the gene expression of claudins/occludin by Snail." J Cell Sci **116**(Pt 10): 1959-1967.

Imig, J., N. Motsch, J. Y. Zhu, S. Barth, M. Okoniewski, T. Reineke, M. Tinguely, A. Faggioni, P. Trivedi, G. Meister, C. Renner and F. A. Grasser (2011). "microRNA profiling in Epstein-Barr virus-associated B-cell lymphoma." Nucleic Acids Res **39**(5): 1880-1893.

Stem Cell Technologies Inc (a) (2013, January 2013). "Air-Liquid Interface Culture For Respiratory Research." Document #29885 Retrieved 14/07, 2016, from https://cdn.stemcell.com/media/files/techbulletin/TB29885-Air_Liquid_Interface_Culture_Respiratory_Research.pdf.

Stem Cell Technologies Inc (b). (2013, 2013). "Webinar: PneumaCult-ALI: An Improved Medium Formulation for the Differentiation of Human Bronchial Epithelial Cells." Retrieved 11/09/2013, 2013, from https://www.stemcell.com/pneumacult-ali-an-improved-medium-formulation-for-the-differentiation-of-human-bronchial-epithelial-cells.html.

Inoue, Y. and N. Shimojo (2013). "Epidemiology of virus-induced wheezing/asthma in children." Front Microbiol **4**: 391.

Ivanov, D. B., M. P. Philippova and V. A. Tkachuk (2001). "Structure and functions of classical cadherins." Biochemistry (Mosc) **66**(10): 1174-1186.

Iversen, M. B. and S. R. Paludan (2010). "Mechanisms of type III interferon expression." J Interferon Cytokine Res **30**(8): 573-578.

Jackson, D. J. and S. L. Johnston (2010). "The role of viruses in acute exacerbations of asthma." J Allergy Clin Immunol **125**(6): 1178-1187; quiz 1188-1179.

Jacobs, S. E., D. M. Lamson, K. St George and T. J. Walsh (2013). "Human rhinoviruses." Clin Microbiol Rev **26**(1): 135-162.

Jakiela, B., R. Brockman-Schneider, S. Amineva, W. M. Lee and J. E. Gern (2008). "Basal cells of differentiated bronchial epithelium are more susceptible to rhinovirus infection." Am J Respir Cell Mol Biol **38**(5): 517-523.

Jansson, M. D. and A. H. Lund (2012). "MicroRNA and cancer." Mol Oncol **6**(6): 590-610.

Jin, Y., Z. Chen, X. Liu and X. Zhou (2013). "Evaluating the microRNA targeting sites by luciferase reporter gene assay." Methods Mol Biol **936**: 117-127.

Johnston, S. L., P. K. Pattemore, G. Sanderson, S. Smith, M. J. Campbell, L. K. Josephs, A. Cunningham, B. S. Robinson, S. H. Myint, M. E. Ward, D. A. Tyrrell and S. T. Holgate (1996). "The relationship between upper respiratory infections and hospital admissions for asthma: a time-trend analysis." Am J Respir Crit Care Med **154**(3 Pt 1): 654-660.

Jordan, W. J., J. Eskdale, S. Srinivas, V. Pekarek, D. Kelner, M. Rodia and G. Gallagher (2007). "Human interferon lambda-1 (IFN-lambda1/IL-29) modulates the Th1/Th2 response." Genes Immun **8**(3): 254-261.

Judson, R. L., T. S. Greve, R. J. Parchem and R. Blelloch (2013). "MicroRNA-based discovery of barriers to dedifferentiation of fibroblasts to pluripotent stem cells." Nat Struct Mol Biol **20**(10): 1227-1235.

Kelly, J. T. and W. W. Busse (2008). "Host immune responses to rhinovirus: mechanisms in asthma." J Allergy Clin Immunol **122**(4): 671-682; quiz 683-674.

Kemler, R. (1992). "Classical cadherins." Semin Cell Biol **3**(3): 149-155.

Kemler, R. and M. Ozawa (1989). "Uvomorulin-catenin complex: cytoplasmic anchorage of a Ca2+-dependent cell adhesion molecule." Bioessays **11**(4): 88-91.

Kim, H. Y., R. H. DeKruyff and D. T. Umetsu (2010). "The many paths to asthma: phenotype shaped by innate and adaptive immunity." Nat Immunol **11**(7): 577-584.

Kim, W. K. and J. E. Gern (2012). "Updates in the relationship between human rhinovirus and asthma." Allergy Asthma Immunol Res **4**(3): 116-121.

Klezovitch, O. and V. Vasioukhin (2015). "Cadherin signaling: keeping cells in touch." F1000Res **4**(F1000 Faculty Rev): 550.

Knight, D. A. and S. T. Holgate (2003). "The airway epithelium: structural and functional properties in health and disease." Respirology **8**(4): 432-446.

Koliais, S. I. and N. J. Dimmock (1973). "Replication of rhinovirus RNA." J Gen Virol **20**(1): 1-15.

Kolodziej, L. E., J. P. Lodolce, J. E. Chang, J. R. Schneider, W. A. Grimm, S. J. Bartulis, X. Zhu, J. S. Messer, S. F. Murphy, N. Reddy, J. R. Turner and D. L. Boone (2011). "TNFAIP3 maintains intestinal barrier function and supports epithelial cell tight junctions." PLoS One **6**(10): e26352.

Korpal, M., E. S. Lee, G. Hu and Y. Kang (2008). "The miR-200 family inhibits epithelial-mesenchymal transition and cancer cell migration by direct targeting of E-cadherin transcriptional repressors ZEB1 and ZEB2." J Biol Chem **283**(22): 14910-14914.

Kotla, S., T. Peng, R. E. Bumgarner and K. E. Gustin (2008). "Attenuation of the type I interferon response in cells infected with human rhinovirus." Virology **374**(2): 399-410.

Kovalenko, A., C. Chable-Bessia, G. Cantarella, A. Israel, D. Wallach and G. Courtois (2003). "The tumour suppressor CYLD negatively regulates NF-kappaB signalling by deubiquitination." Nature **424**(6950): 801-805.

Krol, J., I. Loedige and W. Filipowicz (2010). "The widespread regulation of microRNA biogenesis, function and decay." Nat Rev Genet **11**(9): 597-610.

Kudryavets, Y. I., N. O. Bezdenezhnykh, O. O. Lykhova, N. I. Semesiuk and A. L. Vorontsova (2011). "The role of interferon as a modifier of epithelial-mesenchymal transition in tumor cells." Exp Oncol **33**(3): 178-181.

Kumar, A., Y. Takada, A. M. Boriek and B. B. Aggarwal (2004). "Nuclear factor-kappaB: its role in health and disease." J Mol Med (Berl) **82**(7): 434-448.

Lambrecht, B. N. and H. Hammad (2012). "The airway epithelium in asthma." Nat Med **18**(5): 684-692.

Lawrence, T. (2009). "The nuclear factor NF-kappaB pathway in inflammation." Cold Spring Harb Perspect Biol **1**(6): a001651.

Lee, T. Y., H. J. Ezelle, T. Venkataraman, R. G. Lapidus, K. A. Scheibner and B. A. Hassel (2013). "Regulation of human RNase-L by the miR-29 family reveals a novel oncogenic role in chronic myelogenous leukemia." J Interferon Cytokine Res **33**(1): 34-42.

Lee, W. M., W. Wang and R. R. Rueckert (1995). "Complete sequence of the RNA genome of human rhinovirus 16, a clinically useful common cold virus belonging to the ICAM-1 receptor group." Virus Genes **9**(2): 177-181.

Lessler, J., N. G. Reich, R. Brookmeyer, T. M. Perl, K. E. Nelson and D. A. Cummings (2009). "Incubation periods of acute respiratory viral infections: a systematic review." Lancet Infect Dis **9**(5): 291-300.

Levy, D. E. and A. Garcia-Sastre (2001). "The virus battles: IFN induction of the antiviral state and mechanisms of viral evasion." Cytokine Growth Factor Rev **12**(2-3): 143-156.

Li, W., A. Lewis-Antes, J. Huang, M. Balan and S. V. Kotenko (2008). "Regulation of apoptosis by type III interferons." Cell Prolif **41**(6): 960-979.

Lu, Q. (2010). "delta-Catenin dysregulation in cancer: interactions with E-cadherin and beyond." J Pathol **222**(2): 119-123.

Lu, T. X., A. Munitz and M. E. Rothenberg (2009). "MicroRNA-21 is up-regulated in allergic airway inflammation and regulates IL-12p35 expression." J Immunol **182**(8): 4994-5002.

Ma, X., L. E. Becker Buscaglia, J. R. Barker and Y. Li (2011). "MicroRNAs in NF-kappaB signaling." J Mol Cell Biol **3**(3): 159-166.

Maes, T., F. A. Cobos, F. Schleich, V. Sorbello, M. Henket, K. De Preter, K. R. Bracke, G. Conickx, C. Mesnil, J. Vandesompele, L. Lahousse, F. Bureau, P. Mestdagh, G. F. Joos, F. L. Ricciardolo, G. G. Brusselle and R. Louis (2016). "Asthma inflammatory phenotypes show differential microRNA expression in sputum." J Allergy Clin Immunol **137**(5): 1433-1446.

Maier, T., M. Guell and L. Serrano (2009). "Correlation of mRNA and protein in complex biological samples." FEBS Lett **583**(24): 3966-3973.

Martin-Padura, I., S. Lostaglio, M. Schneemann, L. Williams, M. Romano, P. Fruscella, C. Panzeri, A. Stoppacciaro, L. Ruco, A. Villa, D. Simmons and E. Dejana (1998). "Junctional adhesion molecule, a novel member of the immunoglobulin superfamily that distributes at intercellular junctions and modulates monocyte transmigration." J Cell Biol **142**(1): 117-127.

Martinez-Nunez, R. T., V. P. Bondanese, F. Louafi, A. S. Francisco-Garcia, H. Rupani, N. Bedke, S. Holgate, P. H. Howarth, D. E. Davies and T. Sanchez-Elsner (2014). "A microRNA network dysregulated in asthma controls IL-6 production in bronchial epithelial cells." PLoS One **9**(10): e111659.

Masuda, T., H. Saito, F. Kaneko, K. Atsukawa, M. Morita, H. Inagaki, N. Kumagai, K. Tsuchimoto and A. H. Ishii (2000). "Up-regulation of E-cadherin and I-catenin in human hepatocellular carcinoma cell lines by sodium butyrate and interferon-alpha." In Vitro Cell Dev Biol Anim **36**(6): 387-394.

Matter, K. and M. S. Balda (2003). "Signalling to and from tight junctions." Nat Rev Mol Cell Biol **4**(3): 225-236.

Mattijssen, S. and G. J. Pruijn (2012). "Viperin, a key player in the antiviral response." Microbes Infect **14**(5): 419-426.

McIntyre, C. L., N. J. Knowles and P. Simmonds (2013). "Proposals for the classification of human rhinovirus species A, B and C into genotypically assigned types." J Gen Virol **94**(Pt 8): 1791-1806.

Meng, W. and M. Takeichi (2009). "Adherens junction: molecular architecture and regulation." Cold Spring Harb Perspect Biol **1**(6): a002899.

Miller, E. K., J. Z. Hernandez, V. Wimmenauer, B. E. Shepherd, D. Hijano, R. Libster, M. E. Serra, N. Bhat, J. P. Batalle, Y. Mohamed, A. Reynaldi, A. Rodriguez, M. Otello, N. Pisapia, J. Bugna, M. Bellabarba, D. Kraft, S. Coviello, F. M. Ferolla, A. Chen, S. J. London, G. K. Siberry, J. V. Williams and F. P. Polack (2012). "A mechanistic role for type III IFN-lambda1 in asthma exacerbations mediated by human rhinoviruses." Am J Respir Crit Care Med **185**(5): 508-516.

Molotski, N. and Y. Soen (2012). "Differential association of microRNAs with polysomes reflects distinct strengths of interactions with their mRNA targets." RNA **18**(9): 1612-1623.

Mordstein, M., E. Neugebauer, V. Ditt, B. Jessen, T. Rieger, V. Falcone, F. Sorgeloos, S. Ehl, D. Mayer, G. Kochs, M. Schwemmle, S. Gunther, C. Drosten, T. Michiels and P. Staeheli (2010). "Lambda interferon renders epithelial cells of the respiratory and gastrointestinal tracts resistant to viral infections." J Virol **84**(11): 5670-5677.

Moreno-Moya, J. M., F. Vilella and C. Simon (2014). "MicroRNA: key gene expression regulators." Fertil Steril **101**(6): 1516-1523.

Moritz, T. and H. Kirchner (1986). "The effect of interferons on cellular differentiation." Blut **53**(5): 361-370.

Mosser, A. G., R. Brockman-Schneider, S. Amineva, L. Burchell, J. B. Sedgwick, W. W. Busse and J. E. Gern (2002). "Similar frequency of rhinovirus-infectible cells in upper and lower airway epithelium." J Infect Dis **185**(6): 734-743.

Mosser, A. G., R. Vrtis, L. Burchell, W. M. Lee, C. R. Dick, E. Weisshaar, D. Bock, C. A. Swenson, R. D. Cornwell, K. C. Meyer, N. N. Jarjour, W. W. Busse and J. E. Gern (2005). "Quantitative and qualitative analysis of rhinovirus infection in bronchial tissues." Am J Respir Crit Care Med **171**(6): 645-651.

Murdoch, J. R. and C. M. Lloyd (2010). "Chronic inflammation and asthma." Mutat Res **690**(1-2): 24-39.

Nata, T., M. Fujiya, N. Ueno, K. Moriichi, H. Konishi, H. Tanabe, T. Ohtake, K. Ikuta and Y. Kohgo (2013). "MicroRNA-146b improves intestinal injury in mouse colitis by activating nuclear factor-kappaB and improving epithelial barrier function." J Gene Med **15**(6-7): 249-260.

Nawijn, M. C., T. L. Hackett, D. S. Postma, A. J. van Oosterhout and I. H. Heijink (2011). "E-cadherin: gatekeeper of airway mucosa and allergic sensitization." Trends Immunol **32**(6): 248-255.

Ngoc, P. L., D. R. Gold, A. O. Tzianabos, S. T. Weiss and J. C. Celedon (2005). "Cytokines, allergy, and asthma." Curr Opin Allergy Clin Immunol **5**(2): 161-166.

O'Brien, T. R., L. Prokunina-Olsson and R. P. Donnelly (2014). "IFN-lambda4: the paradoxical new member of the interferon lambda family." J Interferon Cytokine Res **34**(11): 829-838.

O'Byrne, P. M. (2011). "Therapeutic strategies to reduce asthma exacerbations." J Allergy Clin Immunol **128**(2): 257-263; quiz 264-255.

O'Byrne, P. M., S. Pedersen, C. J. Lamm, W. C. Tan, W. W. Busse and S. I. Group (2009). "Severe exacerbations and decline in lung function in asthma." Am J Respir Crit Care Med **179**(1): 19-24.

Oeckinghaus, A. and S. Ghosh (2009). "The NF-kappaB family of transcription factors and its regulation." Cold Spring Harb Perspect Biol **1**(4): a000034.

Ordonez, C. L. and J. V. Fahy (2001). "Epithelial desquamation in asthma." Am J Respir Crit Care Med **164**(10 Pt 1): 1997.

Ordonez, C. L., R. Khashayar, H. H. Wong, R. Ferrando, R. Wu, D. M. Hyde, J. A. Hotchkiss, Y. Zhang, A. Novikov, G. Dolganov and J. V. Fahy (2001). "Mild and moderate asthma is associated with airway goblet cell hyperplasia and abnormalities in mucin gene expression." Am J Respir Crit Care Med **163**(2): 517-523.

Ordonez, C. L., T. E. Shaughnessy, M. A. Matthay and J. V. Fahy (2000). "Increased neutrophil numbers and IL-8 levels in airway secretions in acute severe asthma: Clinical and biologic significance." Am J Respir Crit Care Med **161**(4 Pt 1): 1185-1190.

Ozawa, M., M. Ringwald and R. Kemler (1990). "Uvomorulin-catenin complex formation is regulated by a specific domain in the cytoplasmic region of the cell adhesion molecule." Proc Natl Acad Sci U S A **87**(11): 4246-4250.

Papadopoulos, N. G., P. J. Bates, P. G. Bardin, A. Papi, S. H. Leir, D. J. Fraenkel, J. Meyer, P. M. Lackie, G. Sanderson, S. T. Holgate and S. L. Johnston (2000). "Rhinoviruses infect the lower airways." J Infect Dis **181**(6): 1875-1884.

Papi, A. and S. L. Johnston (1999). "Rhinovirus infection induces expression of its own receptor intercellular adhesion molecule 1 (ICAM-1) via increased NF-kappaB-mediated transcription." J Biol Chem **274**(14): 9707-9720.

Park, J. A., J. H. Kim, D. Bi, J. A. Mitchel, N. T. Qazvini, K. Tantisira, C. Y. Park, M. McGill, S. H. Kim, B. Gweon, J. Notbohm, R. Steward, Jr., S. Burger, S. H. Randell, A. T. Kho, D. T. Tambe, C. Hardin, S. A. Shore, E. Israel, D. A. Weitz, D. J. Tschumperlin, E. P. Henske, S. T. Weiss, M. L. Manning, J. P. Butler, J. M. Drazen and J. J. Fredberg (2015). "Unjamming and cell shape in the asthmatic airway epithelium." Nat Mater **14**(10): 1040-1048.

Parker, D. and A. Prince (2011). "Innate immunity in the respiratory epithelium." Am J Respir Cell Mol Biol **45**(2): 189-201.

Parvatiyar, K. and E. W. Harhaj (2011). "Regulation of inflammatory and antiviral signaling by A20." Microbes Infect **13**(3): 209-215.

Paterson, E. L., N. Kolesnikoff, P. A. Gregory, A. G. Bert, Y. Khew-Goodall and G. J. Goodall (2008). "The microRNA-200 family regulates epithelial to mesenchymal transition." ScientificWorldJournal **8**: 901-904.

Pearce, N., J. Pekkanen and R. Beasley (1999). "How much asthma is really attributable to atopy?" Thorax **54**(3): 268-272.

Pelikan, Z. (2011). "Delayed asthmatic response to bronchial challenge with allergen-mediators, eicosanoids, eosinophil and neutrophil constituents in the blood and urine." Respiration **82**(3): 225-236.

Perez, T. D. and W. J. Nelson (2004). "Cadherin adhesion: mechanisms and molecular interactions." Handb Exp Pharmacol(165): 3-21.

Peterson, S. M., J. A. Thompson, M. L. Ufkin, P. Sathyanarayana, L. Liaw and C. B. Congdon (2014). "Common features of microRNA target prediction tools." Front Genet **5**: 23.

Pezzulo, A. A., T. D. Starner, T. E. Scheetz, G. L. Traver, A. E. Tilley, B. G. Harvey, R. G. Crystal, P. B. McCray, Jr. and J. Zabner (2011). "The air-liquid interface and use of primary cell cultures are

important to recapitulate the transcriptional profile of in vivo airway epithelia." Am J Physiol Lung Cell Mol Physiol **300**(1): L25-31.

Prytherch, Z., C. Job, H. Marshall, V. Oreffo, M. Foster and K. BeruBe (2011). "Tissue-Specific stem cell differentiation in an in vitro airway model." Macromol Biosci **11**(11): 1467-1477.

Rao, R. (2009). "Occludin phosphorylation in regulation of epithelial tight junctions." Ann N Y Acad Sci **1165**: 62-68.

Reynolds, A. B. (2007). "p120-catenin: Past and present." Biochim Biophys Acta **1773**(1): 2-7.

Reynolds, A. B., J. M. Daniel, Y. Y. Mo, J. Wu and Z. Zhang (1996). "The novel catenin p120cas binds classical cadherins and induces an unusual morphological phenotype in NIH3T3 fibroblasts." Exp Cell Res **225**(2): 328-337.

Rincon, M. and C. G. Irvin (2012). "Role of IL-6 in asthma and other inflammatory pulmonary diseases." Int J Biol Sci **8**(9): 1281-1290.

Rodriguez, A., E. Vigorito, S. Clare, M. V. Warren, P. Couttet, D. R. Soond, S. van Dongen, R. J. Grocock, P. P. Das, E. A. Miska, D. Vetrie, K. Okkenhaug, A. J. Enright, G. Dougan, M. Turner and A. Bradley (2007). "Requirement of bic/microRNA-155 for normal immune function." Science **316**(5824): 608-611.

Rogers, D. F. (1994). "Airway goblet cells: responsive and adaptable front-line defenders." Eur Respir J **7**(9): 1690-1706.

Ru, J., H. Sun, H. Fan, C. Wang, Y. Li, M. Liu and H. Tang (2014). "MiR-23a facilitates the replication of HSV-1 through the suppression of interferon regulatory factor 1." PLoS One **9**(12): e114021.

Ruland, J. (2011). "Return to homeostasis: downregulation of NF-kappaB responses." Nat Immunol **12**(8): 709-714.

Rusinova, I. F. S. Y., S.; Kannan, A.; Cumming, H.; Chapman, R.; Hertzog, P.J (2013). "INTERFEROME v2.0: an updated database of annotate interferon-regulated genes." Nucleic Acids Res (database issue): D1040-1046.

Sadler, A. J. and B. R. Williams (2008). "Interferon-inducible antiviral effectors." Nat Rev Immunol **8**(7): 559-568.

Saha, S. K., M. A. Berry, D. Parker, S. Siddiqui, A. Morgan, R. May, P. Monk, P. Bradding, A. J. Wardlaw, I. D. Pavord and C. E. Brightling (2008). "Increased sputum and bronchial biopsy IL-13 expression in severe asthma." J Allergy Clin Immunol **121**(3): 685-691.

Sajjan, U., Q. Wang, Y. Zhao, D. C. Gruenert and M. B. Hershenson (2008). "Rhinovirus disrupts the barrier function of polarized airway epithelial cells." Am J Respir Crit Care Med **178**(12): 1271-1281.

Sangfelt, O., S. Erickson and D. Grander (2000). "Mechanisms of interferon-induced cell cycle arrest." Front Biosci **5**: D479-487.

Sato, K., T. Watanabe, S. Wang, M. Kakeno, K. Matsuzawa, T. Matsui, K. Yokoi, K. Murase, I. Sugiyama, M. Ozawa and K. Kaibuchi (2011). "Numb controls E-cadherin endocytosis through p120 catenin with aPKC." Mol Biol Cell **22**(17): 3103-3119.

Sato, M., H. Suemori, N. Hata, M. Asagiri, K. Ogasawara, K. Nakao, T. Nakaya, M. Katsuki, S. Noguchi, N. Tanaka and T. Taniguchi (2000). "Distinct and essential roles of transcription factors IRF-3 and IRF-7 in response to viruses for IFN-alpha/beta gene induction." Immunity **13**(4): 539-548.

Savolainen, C., S. Blomqvist and T. Hovi (2003). "Human rhinoviruses." Paediatr Respir Rev **4**(2): 91-98.

Schleimer, R. P., A. Kato, R. Kern, D. Kuperman and P. C. Avila (2007). "Epithelium: at the interface of innate and adaptive immune responses." J Allergy Clin Immunol **120**(6): 1279-1284.

Schneeberger, E. E. and R. D. Lynch (2004). "The tight junction: a multifunctional complex." Am J Physiol Cell Physiol **286**(6): C1213-1228.

Sedger, L. M. (2013). "microRNA control of interferons and interferon induced anti-viral activity." Mol Immunol **56**(4): 781-793.

Shahana, S., E. Bjornsson, D. Ludviksdottir, C. Janson, O. Nettelbladt, P. Venge, G. M. Roomans and B. H. R. group (2005). "Ultrastructure of bronchial biopsies from patients with allergic and non-allergic asthma." Respir Med **99**(4): 429-443.

Shapiro, L., A. M. Fannon, P. D. Kwong, A. Thompson, M. S. Lehmann, G. Grubel, J. F. Legrand, J. Als-Nielsen, D. R. Colman and W. A. Hendrickson (1995). "Structural basis of cell-cell adhesion by cadherins." Nature **374**(6520): 327-337.

Shapiro, L. and W. I. Weis (2009). "Structure and biochemistry of cadherins and catenins." Cold Spring Harb Perspect Biol **1**(3): a003053.

Shembade, N. and E. Harhaj (2010). "A20 inhibition of NFkappaB and inflammation: targeting E2:E3 ubiquitin enzyme complexes." Cell Cycle **9**(13): 2481-2482.

Shembade, N., A. Ma and E. W. Harhaj (2010). "Inhibition of NF-kappaB signaling by A20 through disruption of ubiquitin enzyme complexes." Science **327**(5969): 1135-1139.

Simpson, J. L., R. Scott, M. J. Boyle and P. G. Gibson (2006). "Inflammatory subtypes in asthma: assessment and identification using induced sputum." Respirology **11**(1): 54-61.

Skalsky, R. L. and B. R. Cullen (2010). "Viruses, microRNAs, and host interactions." Annu Rev Microbiol **64**: 123-141.

Skalsky, R. L., K. E. Olson, C. D. Blair, M. A. Garcia-Blanco and B. R. Cullen (2014). "A "microRNA-like" small RNA expressed by Dengue virus?" Proc Natl Acad Sci U S A **111**(23): E2359.

Snapper, C. M., F. D. Finkelman, D. Stefany, D. H. Conrad and W. E. Paul (1988). "IL-4 induces co-expression of intrinsic membrane IgG1 and IgE by murine B cells stimulated with lipopolysaccharide." J Immunol **141**(2): 489-498.

Solberg, O. D., E. J. Ostrin, M. I. Love, J. C. Peng, N. R. Bhakta, L. Hou, C. Nguyen, M. Solon, C. Nguyen, A. J. Barczak, L. T. Zlock, D. P. Blagev, W. E. Finkbeiner, K. M. Ansel, J. R. Arron, D. J. Erle and P. G. Woodruff (2012). "Airway epithelial miRNA expression is altered in asthma." Am J Respir Crit Care Med **186**(10): 965-974.

Sommereyns, C., S. Paul, P. Staeheli and T. Michiels (2008). "IFN-lambda (IFN-lambda) is expressed in a tissue-dependent fashion and primarily acts on epithelial cells in vivo." PLoS Pathog **4**(3): e1000017.

Steinhusen, U., J. Weiske, V. Badock, R. Tauber, K. Bommert and O. Huber (2001). "Cleavage and shedding of E-cadherin after induction of apoptosis." J Biol Chem **276**(7): 4972-4980.

Stevenson, B. R., J. D. Siliciano, M. S. Mooseker and D. A. Goodenough (1986). "Identification of ZO-1: a high molecular weight polypeptide associated with the tight junction (zonula occludens) in a variety of epithelia." J Cell Biol **103**(3): 755-766.

Stewart, C. E., E. E. Torr, N. H. Mohd Jamili, C. Bosquillon and I. Sayers (2012). "Evaluation of differentiated human bronchial epithelial cell culture systems for asthma research." J Allergy (Cairo) **2012**: 943982.

Subauste, M. C., D. B. Jacoby, S. M. Richards and D. Proud (1995). "Infection of a human respiratory epithelial cell line with rhinovirus. Induction of cytokine release and modulation of susceptibility to infection by cytokine exposure." J Clin Invest **96**(1): 549-557.

Sykes, A., M. R. Edwards, J. Macintyre, A. del Rosario, E. Bakhsoliani, M. B. Trujillo-Torralbo, O. M. Kon, P. Mallia, M. McHale and S. L. Johnston (2012). "Rhinovirus 16-induced IFN-alpha and IFN-beta are deficient in bronchoalveolar lavage cells in asthmatic patients." J Allergy Clin Immunol **129**(6): 1506-1514 e1506.

Sykes, A., J. Macintyre, M. R. Edwards, A. Del Rosario, J. Haas, V. Gielen, O. M. Kon, M. McHale and S. L. Johnston (2014). "Rhinovirus-induced interferon production is not deficient in well controlled asthma." Thorax **69**(3): 240-246.

Synairgen PLC (2016) 'Press Release: Interferon Lambda Intellectual Property Licensed from Imperial Innovations' Accessed 19 November 2016.

Tak, P. P. and G. S. Firestein (2001). "NF-kappaB: a key role in inflammatory diseases." J Clin Invest **107**(1): 7-11.

Takaoka, A. and H. Yanai (2006). "Interferon signalling network in innate defence." Cell Microbiol **8**(6): 907-922.

Takegami, T., R. J. Kuhn, C. W. Anderson and E. Wimmer (1983). "Membrane-dependent uridylylation of the genome-linked protein VPg of poliovirus." Proc Natl Acad Sci U S A **80**(24): 7447-7451.

Tang, Y., A. Banan, C. B. Forsyth, J. Z. Fields, C. K. Lau, L. J. Zhang and A. Keshavarzian (2008). "Effect of alcohol on miR-212 expression in intestinal epithelial cells and its potential role in alcoholic liver disease." Alcohol Clin Exp Res **32**(2): 355-364.

Technologies, S. (2016). "Technical Bulletin: Air-Liquid Interface Culture For Respiratory Research." Retrieved 13/11/2016, from https://cdn.stemcell.com/media/files/techbulletin/TB29885-Air_Liquid_Interface_Culture_Respiratory_Research.pdf?_ga=1.228742495.2131830894.1479037026.

Tian, X., Z. Liu, B. Niu, J. Zhang, T. K. Tan, S. R. Lee, Y. Zhao, D. C. Harris and G. Zheng (2011). "E-cadherin/beta-catenin complex and the epithelial barrier." J Biomed Biotechnol **2011**: 567305.

Tosi, M. F. (2005). "Innate immune responses to infection." J Allergy Clin Immunol **116**(2): 241-249; quiz 250.

Tran, N. and G. Hutvagner (2013). "Biogenesis and the regulation of the maturation of miRNAs." Essays Biochem **54**: 17-28.

Trinchieri, G. (2010). "Type I interferon: friend or foe?" J Exp Med **207**(10): 2053-2063.

Tsukita, S. and M. Furuse (2000). "The structure and function of claudins, cell adhesion molecules at tight junctions." Ann N Y Acad Sci **915**: 129-135.

Turner, R. B., J. O. Hendley and J. M. Gwaltney, Jr. (1982). "Shedding of infected ciliated epithelial cells in rhinovirus colds." J Infect Dis **145**(6): 849-853.

Uze, G. and D. Monneron (2007). "IL-28 and IL-29: newcomers to the interferon family." Biochimie **89**(6-7): 729-734.

Valencia-Sanchez, M. A., J. Liu, G. J. Hannon and R. Parker (2006). "Control of translation and mRNA degradation by miRNAs and siRNAs." Genes Dev **20**(5): 515-524.

Van Itallie, C. M. and J. M. Anderson (2014). "Architecture of tight junctions and principles of molecular composition." Semin Cell Dev Biol **36**: 157-165.

Vareille, M., E. Kieninger, M. R. Edwards and N. Regamey (2011). "The airway epithelium: soldier in the fight against respiratory viruses." Clin Microbiol Rev **24**(1): 210-229.

Vaz, C., A. S. Mer, A. Bhattacharya and R. Ramaswamy (2011). "MicroRNAs modulate the dynamics of the NF-kappaB signaling pathway." PLoS One **6**(11): e27774.

Wahid, F., A. Shehzad, T. Khan and Y. Y. Kim (2010). "MicroRNAs: synthesis, mechanism, function, and recent clinical trials." Biochim Biophys Acta **1803**(11): 1231-1243.

Wang, E., L. M. Pfeffer and I. Tamm (1981). "Interferon increases the abundance of submembranous microfilaments in HeLa-S3 cells in suspension culture." Proc Natl Acad Sci U S A **78**(10): 6281-6285.

Wang, G., Y. Sun, Y. He, C. Ji, B. Hu and Y. Sun (2015). "miR-26a promoted by interferon-alpha inhibits hepatocellular carcinoma proliferation and migration by blocking EZH2." Genet Test Mol Biomarkers **19**(1): 30-36.

Wang, Y. L., A. B. Malik, Y. Sun, S. Hu, A. B. Reynolds, R. D. Minshall and G. Hu (2011). "Innate immune function of the adherens junction protein p120-catenin in endothelial response to endotoxin." J Immunol **186**(5): 3180-3187.

Wark, P. A., S. L. Johnston, F. Bucchieri, R. Powell, S. Puddicombe, V. Laza-Stanca, S. T. Holgate and D. E. Davies (2005). "Asthmatic bronchial epithelial cells have a deficient innate immune response to infection with rhinovirus." J Exp Med **201**(6): 937-947.

Watanabe, Y., A. Kishi, N. Yachie, A. Kanai and M. Tomita (2007). "Computational analysis of microRNA-mediated antiviral defense in humans." FEBS Lett **581**(24): 4603-4610.

Wertz, I. and V. Dixit (2014). "A20--a bipartite ubiquitin editing enzyme with immunoregulatory potential." Adv Exp Med Biol **809**: 1-12.

Wertz, I. E., K. Newton, D. Seshasayee, S. Kusam, C. Lam, J. Zhang, N. Popovych, E. Helgason, A. Schoeffler, S. Jeet, N. Ramamoorthi, L. Kategaya, R. J. Newman, K. Horikawa, D. Dugger, W. Sandoval, S. Mukund, A. Zindal, F. Martin, C. Quan, J. Tom, W. J. Fairbrother, M. Townsend, S. Warming, J. DeVoss, J. Liu, E. Dueber, P. Caplazi, W. P. Lee, C. C. Goodnow, M. Balazs, K. Yu, G. Kolumam and V. M. Dixit (2015). "Phosphorylation and linear ubiquitin direct A20 inhibition of inflammation." Nature **528**(7582): 370-375.

WHO (2007). Asthma. Global surveillance, prevention and control of Chronic Respiratory Diseases: A comprehensive approach. J. B. a. N. Khaltaev, World Health Organisation. **1:** 15-20.

Wilczynska, A. and M. Bushell (2015). "The complexity of miRNA-mediated repression." Cell Death Differ **22**(1): 22-33.

Wills-Karp, M. (2004). "Interleukin-13 in asthma pathogenesis." Immunol Rev **202**: 175-190.

Winter, J., S. Jung, S. Keller, R. I. Gregory and S. Diederichs (2009). "Many roads to maturity: microRNA biogenesis pathways and their regulation." Nat Cell Biol **11**(3): 228-234.

Wu, S., S. Huang, J. Ding, Y. Zhao, L. Liang, T. Liu, R. Zhan and X. He (2010). "Multiple microRNAs modulate p21Cip1/Waf1 expression by directly targeting its 3' untranslated region." Oncogene **29**(15): 2302-2308.

Wu, X. B., M. Y. Wang, H. Y. Zhu, S. Q. Tang, Y. D. You and Y. Q. Xie (2014). "Overexpression of microRNA-21 and microRNA-126 in the patients of bronchial asthma." Int J Clin Exp Med **7**(5): 1307-1312.

Xiao, B., Z. Liu, B. S. Li, B. Tang, W. Li, G. Guo, Y. Shi, F. Wang, Y. Wu, W. D. Tong, H. Guo, X. H. Mao and Q. M. Zou (2009). "Induction of microRNA-155 during Helicobacter pylori infection and its negative regulatory role in the inflammatory response." J Infect Dis **200**(6): 916-925.

Xiao, C., S. M. Puddicombe, S. Field, J. Haywood, V. Broughton-Head, I. Puxeddu, H. M. Haitchi, E. Vernon-Wilson, D. Sammut, N. Bedke, C. Cremin, J. Sones, R. Djukanovic, P. H. Howarth, J. E. Collins, S. T. Holgate, P. Monk and D. E. Davies (2011). "Defective epithelial barrier function in asthma." J Allergy Clin Immunol **128**(3): 549-556 e541-512.

Ye, D., S. Guo, R. Al-Sadi and T. Y. Ma (2011). "MicroRNA regulation of intestinal epithelial tight junction permeability." Gastroenterology **141**(4): 1323-1333.

Yeo, N. K. and Y. J. Jang (2010). "Rhinovirus infection-induced alteration of tight junction and adherens junction components in human nasal epithelial cells." Laryngoscope **120**(2): 346-352.

Yoneyama, M., W. Suhara, Y. Fukuhara, M. Fukuda, E. Nishida and T. Fujita (1998). "Direct triggering of the type I interferon system by virus infection: activation of a transcription factor complex containing IRF-3 and CBP/p300." EMBO J **17**(4): 1087-1095.

Yu, T., X. J. Lu, J. Y. Li, T. D. Shan, C. Z. Huang, H. Ouyang, H. S. Yang, J. H. Xu, W. Zhong, Z. S. Xia and Q. K. Chen (2016). "Overexpression of miR-429 impairs intestinal barrier function in diabetic mice by down-regulating occludin expression." Cell Tissue Res **366**(2): 341-352.

Yuan, L., C. Zhou, Y. Lu, M. Hong, Z. Zhang, Z. Zhang, Y. Chang, C. Zhang and X. Li (2015). "IFN-gamma-mediated IRF1/miR-29b feedback loop suppresses colorectal cancer cell growth and metastasis by repressing IGF1." Cancer Lett **359**(1): 136-147.

Zaheer, R. S., S. Wiehler, M. H. Hudy, S. L. Traves, J. B. Pelikan, R. Leigh and D. Proud (2014). "Human rhinovirus-induced ISG15 selectively modulates epithelial antiviral immunity." Mucosal Immunol **7**(5): 1127-1138.

Zhang, L., M. E. Peeples, R. C. Boucher, P. L. Collins and R. J. Pickles (2002). "Respiratory syncytial virus infection of human airway epithelial cells is polarized, specific to ciliated cells, and without obvious cytopathology." J Virol **76**(11): 5654-5666.

Zhang, Q., X. K. Guo, L. Gao, C. Huang, N. Li, X. Jia, W. Liu and W. H. Feng (2014). "MicroRNA-23 inhibits PRRSV replication by directly targeting PRRSV RNA and possibly by upregulating type I interferons." Virology **450-451**: 182-195.

Zhu, Z., W. Tang, A. Ray, Y. Wu, O. Einarsson, M. L. Landry, J. Gwaltney, Jr. and J. A. Elias (1996). "Rhinovirus stimulation of interleukin-6 in vivo and in vitro. Evidence for nuclear factor kappa B-dependent transcriptional activation." J Clin Invest **97**(2): 421-430.